THE
PHYSICAL REVIEW
*A Journal of Experimental and Theoretical Physics Established by E. L. Nichols in 1893*

VOL. 52, NO. 2 JULY 15, 1937 SECOND SERIES

# Scattering of Fast Electrons in Hydrogen

A. L. HUGHES* AND S. S. WEST
*Wayman Crow Laboratory of Physics, Washington University, St. Louis, Missouri*
(Received May 10, 1937)

Electrons of 2000-volt energy scattered by hydrogen molecules are found to be divided into two distinct groups, those scattered elastically and those scattered inelastically. The former have been scattered by the nuclei, while the latter have been scattered by the atomic electrons. The theoretical ratio of the number inelastically scattered to the number elastically scattered differs according to whether one adopts the classical theory of scattering or the wave mechanical. The difference comes in through the fact that when particles are scattered by similar particles, such as electrons by electrons, the two theories lead to different expressions. The experimental results are in much closer agreement with the predictions of the wave mechanical theory than with those of the classical theory. A slight difference between the results obtained with helium and those obtained with hydrogen may be attributed to diffraction effects which are present when scattering is due to diatomic molecules.

IN a former paper[1] the authors investigated the ratio of the number of inelastically scattered electrons to the number of elastically scattered electrons, when a beam of electrons is directed into helium, as a function of the angle of scattering in order to test whether the classical or the wave-mechanical description of the scattering of like particles by like particles is supported by experiment. The principle of the method may be summarized as follows. In order that a 2000-volt electron may be deflected by a helium nucleus or by an atomic electron through an appreciable angle (say 20° or more), classical orbit theory shows that it must pass by the deflecting center within a distance which is considerably smaller than the average distance between the atomic electrons and the nucleus in the helium atom. Consequently if we find fast electrons scattered through an appreciable angle by atoms of helium, it is legitimate to assume that the electron has been scattered either by a nucleus or by one of the atomic electrons, and not by the cooperation of two or more scattering centers. This allows us to regard helium as providing a mixture of electrons and nuclei acting independently of each other. Among the electrons scattered at a definite angle by such a gas, there will be two groups, those scattered by the nuclei and those scattered by the atomic electrons. They will be clearly distinguished from each other by the fact that those scattered (elastically) by the nuclei lose no energy, while those scattered (inelastically) by the atomic electrons lose a finite amount of energy which is greater the larger the angle of scattering.

The probability that an electron of velocity $v$ and mass $m$ will be scattered into unit solid angle at an angle $\phi$ with the original direction by another electron, initially at rest, is, according to the classical theory, as given by Darwin[2]

$$\alpha_1 = (e^4/m^2v^4)4\cos\phi\,(\mathrm{cosec}^4\,\phi+\sec^4\,\phi). \quad (1)$$

* The senior author was aided in part by a grant from the Rockefeller Foundation to Washington University for research in science.

[1] A. L. Hughes and S. S. West, Phys. Rev. **50**, 320 (1936).

[2] C. G. Darwin, Phil. Mag. **27**, 499 (1914).

A different formula

$$\alpha_2=(e^4/m^2v^4)4\cos\phi\,(\operatorname{cosec}^4\phi + \sec^4\phi-\Phi\operatorname{cosec}^2\phi\sec^4\phi) \quad (2)$$

is given by wave mechanics.[3] (For angles over 20° and electron energies of 2000 volts or more, $\Phi$ is very close to 1.) When an electron is scattered by a nucleus (i.e., by an unlike particle) both the classical method and the wave-mechanical method lead to the same formula

$$\alpha=(Z^2e^4/4m^2v^4)\operatorname{cosec}^4(\phi/2), \quad (3)$$

where $Ze$ is the charge on the nucleus.

Experimentally we measure $\alpha'/\alpha$, the number of inelastically scattered electrons divided by the number of elastically scattered electrons, and compare this with $\alpha_1'/\alpha(=Z\alpha_1/\alpha)$ or with $\alpha_2'/\alpha=(Z\alpha_2/\alpha)$, to decide whether the classical or the wave-mechanical description is supported experimentally.

In the paper cited, it was shown that the results obtained with helium were decisively in favor of the wave-mechanical theory. This paper gives an account of a repetition of the experiment using hydrogen in place of helium. Since the apparatus and mode of obtaining results are precisely the same as before, all description of the apparatus and methods of measurement are here omitted and the reader is referred to the previous paper.

The results for scattering of electrons by hydrogen are summarized in Table I. These are plotted in Fig. 1, which shows the classical theoretical curve, the wave-mechanical theoretical curve, and the experimental points. The estimated uncertainties in the experimental values are given numerically in Table I, and are shown by vertical lines on Fig. 1. It may be concluded definitely that the results for hydrogen are much closer to the values predicted by the wave-mechanical theory than to those predicted by the classical theory. We may conclude, therefore, that the collision of one electron with another can be described satisfactorily by the wave-mechanical theory but not by the classical theory. The experimental values for 24.5° and 29.5° show a slight, but apparently definite, deviation from the wave-mechanical curve by amounts somewhat greater than the estimated experimental uncertainty. On the other hand, the experimental values for the larger angles (on which we are inclined to put less reliance because the scattered currents are smaller and more difficult to measure) show no definite deviation from the curve.[4]

For purposes of comparison the values obtained previously for the scattering of 2000-v electrons in helium are plotted in the diagram. (These values have each been multiplied by two,

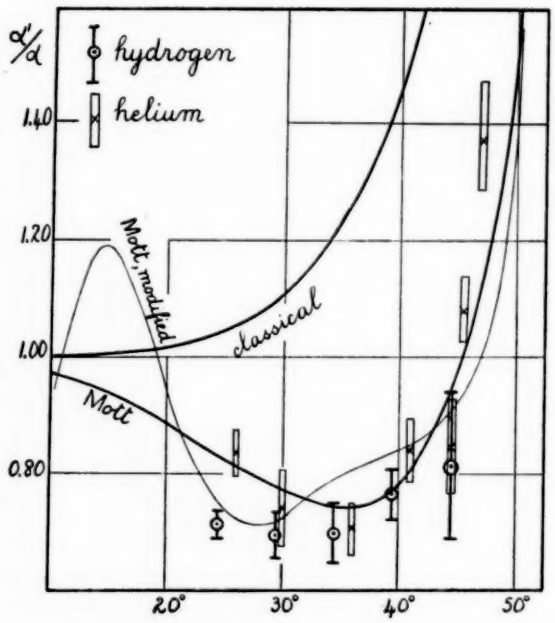


FIG. 1. Ratio of inelastically scattered to elastically scattered electrons.

TABLE I. *Ratio of inelastic scattering to elastic scattering in hydrogen, for 2000-v electrons.*

| ANGLE | EXPERIMENTAL $\alpha'/\alpha$ | THEORETICAL | |
|---|---|---|---|
| | | $\alpha_1'/\alpha$ | $\alpha_2'/\alpha$ |
| 24.5° | 0.715±0.022 | 1.043 | 0.833 |
| 29.5° | 0.695±0.040 | 1.098 | 0.773 |
| 34.5° | 0.698±0.049 | 1.214 | 0.745 |
| 39.5° | 0.765±0.042 | 1.432 | 0.768 |
| 44.5° | 0.812±0.126 | 1.870 | 0.943 |

[3] N. F. Mott and H. S. W. Massey, *The Theory of Atomic Collisions* (Oxford University Press, 1933), p. 76.

[4] A careful independent determination of the experimental ratios at 24.5° and 29.5° was made by Mr. R. F. Moody. He obtained the values 0.711 and 0.697 which check very well with the values given in Table I, and so give us considerable confidence in the results at these two angles. Unfortunately circumstances did not permit a check at other angles. It should be stated that the readings as taken by an observer give no hint whatever of the final ratio which is obtained only after a considerable calculation involving many readings. The method is outlined in the previous paper.

since the ordinates for the theoretical curve for hydrogen are just twice those for helium.)

A possible explanation of the slight difference between the fit of the hydrogen and the helium points and the theoretical curve at 24.5° and 29.5° may be found in the fact that in hydrogen the scattering is done by diatomic molecules while that in helium is due to monatomic molecules. We know from experiments on the *elastic* scattering of fast electrons (5000 to 50,000 volts) by polyatomic molecules, that well marked diffraction effects occur, which for the case of diatomic molecules can be described by $\alpha(1+\sin x/x)$, where $\alpha$ is the elastic scattering due to a single atom and $x=2\pi d \sin(\phi/2)/\lambda$, in which $\phi$ is the angle of scattering, $\lambda$ the electron wave-length and $d$ the distance apart of the atoms in the diatomic molecule.[5] Following the usual procedure we shall assume that the diffraction factor $(1+\sin x/x)$ applies only to the coherent scattering (i.e., the elastic scattering), while the incoherent, or inelastic, scattering is not modified by diffraction effects. Consequently this consideration leads to replacing $\alpha_2'/\alpha$ by $\alpha_2'/\alpha(1+\sin x/x)$. In computing $x$ we assume $d=0.74$A for the interatomic distance in the hydrogen molecule.[6] The modified curve, $\alpha_2'/\alpha(1+\sin x/x)$, is shown as a light line in Fig. 1. It is clear that the two experimental points on which we place most reliance are closer to the modified curve than to the unmodified curve. On the other hand the other points are possibly closer to the unmodified curve, but the accuracy with which they were determined does not permit a clear cut decision as to which of the two alternative curves they fit better. It is perhaps well to mention that the *maximum* scattered electron currents were of the order of $10^{-15}$ amp. and that Fig. 1 is drawn on a very open scale.

Objection may be raised, with some justification, to the procedure of superposing the diffraction concept which implies that the two nuclei in each molecule cooperate, on a viewpoint in which the essential feature is that in deriving the (inelastic/elastic) ratios we postulate that the scattering centers are wholly independent of each other and act individually. Closer analysis indicates that the diffraction concept is added only to the elastic scattering whose function in this investigation is merely to afford a standard with which to compare the inelastic scattering. There is no attempt to apply a diffraction "correction" to the inelastic scattering; our picture of *this* loses nothing of its original simplicity and directness. We may infer that our conclusion that the scattering of electrons by electrons is best described by a wave-mechanical theory still holds; experiments with hydrogen instead of helium introduce an additional problem of just how to handle the diffraction effects in the elastic scattering which may be present in the diatomic molecule.

Inasmuch as various circumstances have compelled us to discontinue this investigation for the present, it was deemed advisable to publish the results as they stand, even though they have raised, but left unanswered, the intriguing question whether or not the diffraction factor $(1+\sin x/x)$ must be included in a complete theory. Should the answer be in the affirmative, these measurements may give us, in principle at any rate, a new method of determining the interatomic distance in the hydrogen molecule. We wish to acknowledge the assistance given to us by Mr. R. F. Moody.

[5] Mott and Massey give a more exact formula for hydrogen, but since, in it, the dominating term is $(1+\sin x/x)$, it will be sufficient for our purpose to consider it alone.

[6] R. S. Mulliken, Rev. Mod. Phys. **4**, 1 (1932).

# The Range of the $\alpha$-Particles from Thorium

G. H. HENDERSON AND G. C. LAURENCE
*Dalhousie University, Halifax and National Research Council Laboratory, Ottawa*

(Received September 21, 1936)

Recent values of this range are discussed. It is pointed out that the value found by Kurie and Knopf may be too high and that the treatment of data on a probability paper plot is unjustified in such measurements.

THE range of the $\alpha$-particles from Th has just been determined from pleochroic halo experiments[1] to be $2.40\pm0.07$ cm at 0°C and 760 mm. This may be compared with two recent values, $2.46\pm0.05$ due to Henderson and Nickerson[2] and $2.72\pm0.03$ due to Kurie and Knopf.[3] Both these were found by the Wilson chamber method first introduced by one of us[4] (for U I and U II) for dealing with weak sources. Since two values of this important radioactive constant obtained by independent methods are in reasonable agreement, it appears opportune to point out what appear to us to be two sources of error in the work of Kurie and Knopf, which may account for the divergence of their value.

The first is the use of an apparently unjustifiable method of treating data on a probability paper plot,[5] and the second is the use of a very thick (1 cm) source. The following analysis is made as brief as possible consistent with showing the possible significance of these points.

A parallel beam of $\alpha$-particle tracks should theoretically be distributed about a mean range $l$ in such a way that the fraction whose lengths lie between $x$ and $x+dx$ is $(1/\rho(\pi)^{\frac{1}{2}})\exp -(x-l)^2/\rho^2\,dx$, where $\rho$ is the straggling coefficient.

The percentage $N$ of the tracks whose lengths exceed $x$ is given by the integral of the above expression, $N=50$ percent $\cdot(I-\mathrm{erf}(x-l/\rho))$. The range of the $\alpha$-particles is obtained by extrapolating the sharply descending linear portion of the number-distance curve, to meet the $x$-axis (and adding a small correction).

On probability paper the scale of percentages is distorted by the transformation $\mathrm{erf}-y=(N-50\text{ percent})/50$ percent, so that the number distance curve reduces to the straight line

$$y=(x-l)/\rho.$$

In practice the distribution is affected by experimental conditions. If the source of $\alpha$-particles has a thickness equivalent in absorption to an air thickness $m$, the number distance curve is expressed[4] by $N=f(m,\rho,l,x)$, where

$$f(m,\rho,l,x)=50\%\cdot\left[1-\frac{m+x-l}{m}\,\mathrm{erf}\,\frac{m+x-l}{\rho}+\frac{x-l}{m}\,\mathrm{erf}\,\frac{x-l}{\rho}+\frac{\rho}{m(\pi)^{\frac{1}{2}}}\left\{\exp-\frac{(x-l)^2}{\rho^2}-\exp-\frac{(m+x-l)^2}{\rho^2}\right\}\right],$$

which on probability paper does not approximate to a straight line unless $m\ll\rho$.[6]

When there are two $\alpha$-particle groups (e.g., due to isotopes) we have

$$N=(1-p)f(m,\rho_1,l_1,x)+pf(m,\rho_2,l_2,x),$$

where $p$ is the fraction of the total included in the longer group.

Examples of such curves are shown in Fig. 1 $A$, $B$ and $C$ which are drawn with $m=0$, 0.5 cm and 1.0 cm, with $p$ taken as 0.25. We have taken $\rho_1=\rho_2=0.058$ cm, $l_1=2.53$ cm, $l_2=3.06$ cm. For the purpose of illustration here attempted these values correspond sufficiently well to the case of U I and U II, these substances being chosen because there is no disagreement about the ranges.

[1] G. H. Henderson, C. M. Muskat and D. P. Crawford, Proc. Roy. Soc. **A158**, 199 (1937).
[2] G. H. Henderson and J. L. Nickerson, Phys. Rev. **36**, 1344 (1930).
[3] F. N. D. Kurie and G. D. Knopf, Phys. Rev. **43**, 311 (1933).
[4] G. C. Laurence, Phil Mag. **5**, 1027 (1928).
[5] F. N. D. Kurie, Phys. Rev. **41**, 701 (1932).
[6] This curve is further distorted, particularly for thick sources, by the fact that a smaller solid angle is available in the Wilson chamber for the longer range particles.

The case of Th is not greatly different. It will be seen that the usual method[7] of determining the range of the shorter component from the break in the curve is satisfactory in all three cases, although the break becomes less pronounced with increasing thickness of source, which is therefore to be avoided.

In Kurie's method the percentage of tracks in the longer group is first found from the number-distance curve plotted on probability paper. He states without proof that "this curve has reduced to three straight lines. The conclusion at once suggests itself that the midpoint of the short connecting line gives the fraction of the U II [longer component] tracks." He goes on to state that he tested this idea by constructing several two component curves whose proportions were known and that the fractions of the two curves as got from the mid-point were all within 1 percent of the known values. Having found the percentage in the longer group he draws through this percentage a line parallel to the $x$ axis on the Cartesian number distance curve. He then finds the range by extrapolating the upper portion of this curve to meet this line, which he calls the "no particle line" for the shorter group.

The practical effectiveness of this method, particularly with thick sources, may be judged from the lower part of Fig. 1, where the curves $A$, $B$, and $C$ are replotted on probability paper as $A'$, $B'$ and $C'$. The curve $A'$, for an infinitely thin source, has two asymptotic arms joined by an inflection so flat that the middle portion is approximately a straight line. For thick sources the arms are not asymptotic and the middle part of the curve may have several inflections, the number depending on the values of $\rho_1$, $\rho_2$, $m$, $pl_1 - l_2$. It is difficult to see how Kurie's method is to be used with curves of the type of $B'$ and $C'$. It appears that there is a wide latitude of choice in drawing straight lines on such a probability paper plot and that the mid-point of the connecting line has little meaning either theoretically or empirically.

Moreover it must be remembered that in practice the theoretical curves are replaced by a curve passing through experimental points which

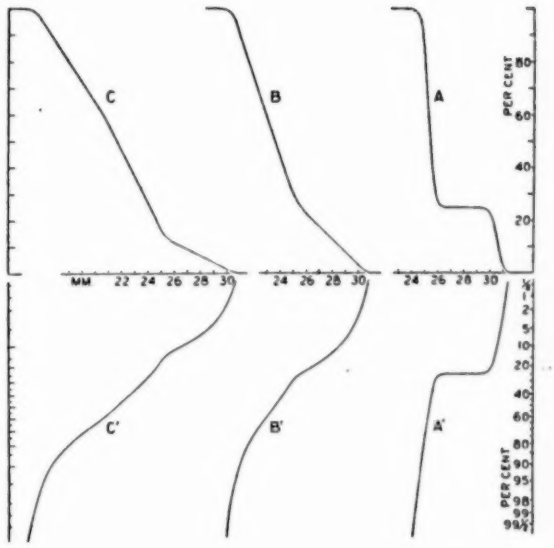


FIG. 1.

are subject to statistical errors associated with the small number of tracks obtainable under the difficult experimental conditions. Furthermore, making use of the asymptotes lays undue weight on the regions at very high and very low values of $N$, which on the Gaussian distribution represent the smallest number of tracks and the greatest statistical errors.

These practical difficulties render the use of the probability plot method uncertain even for thin sources. Even if we ignore statistical errors in the ideal case $A'$ (Fig. 1), where the source is sufficiently thin to separate clearly the effects of the two isotopes, this method is in no way superior to the use of the ordinary Cartesian plot $A$ and we find it difficult to see any advantage in using the method in such measurements.

Kurie and Knopf used an unusually thick source of 1 cm air equivalent. Since the results from the probability paper plot seem doubtful, recourse may be had to their original data, plotted in Cartesians (their Fig. 2). The slope of their curve as drawn is too steep to do justice to the data but from the break in the curve it would appear that they have been led to estimate the range of thorium somewhat too high. The effect of a thick source may be seen by comparing this curve with that published by one of us using a thin layer of thorium, when the break is much more pronounced.

[7] See reference 4 for the correction which must be applied for finite thickness of source.

# Effects of Long Range Forces on Neutron-Proton Scattering

S. S. SHARE AND J. R. STEHN
*University of Wisconsin, Madison, Wisconsin*
(Received May 18, 1937)

Experiments on the angular distribution of fast neutrons scattered by protons have yielded conflicting results. Some indicate spherically symmetric scattering in the center-of-gravity coordinate system; this is consistent with the ordinarily assumed short range interaction (radius $<3\times10^{-13}$ cm). Others indicate a greater amount of scattering in the backward direction. It is here shown that this asymmetry could be explained by assuming an additional long range interaction which is *attractive* for $p$ particles. If of the Majorana type, this interaction is consequently repulsive for $s$ particles. Such an interaction, of depth 1 $mc^2$, extending out to a radius of $11\times10^{-13}$ cm, is roughly sufficient for the purpose.

DIRECT determination of neutron-proton interaction forces is at present possible only through experiments on the scattering of neutrons by protons combined with the binding energy of the deuteron. The spin dependence of these forces is determined by the total elastic scattering cross section, and by the cross section for absorption (with the formation of deuterons).[1] The range of these forces can be estimated from the angular dependence of the elastic cross section, especially for high energy particles. The present note is concerned with this latter point.

The experiments consist in bombarding some hydrogen-containing material with neutrons and observing the angular distribution of recoil protons. The results of different observers are summarized in Table I.

There is genuine disagreement among the various observers, although the preponderant opinion favors spherical symmetry. In spite of this it was thought advisable to publish the present calculations in order to show more clearly what a deviation from spherical symmetry can imply about the interaction.

## TYPES OF INTERACTION

It is well known that a very short range interaction between neutron and proton (of radius much less than the wave-length of the neutron) gives spherically symmetric scattering, for here only the zero-order phase shift, $K_0$, is appreciable. Even for a simple potential well of width $0.7\ e^2/mc^2$ ($2\times10^{-13}$ cm), Bethe and Peierls[2] showed that deviations from spherical symmetry would be negligible for neutrons with energies $<20$ Mev. By assuming a broader potential well of the Morse curve type, with depth $2\ mc^2$ even at so large a separation as $r=2.0\ e^2/mc^2$, Morse, Fisk, and Schiff[3] found appreciable deviation from spherical symmetry at neutron energies as low as 4 Mev. This deviation was of the wrong sign, however, to agree with the data of Harkins *et al.*; neutron energies of about 20 Mev were necessary to make the deviation have the proper sign and magnitude. Such high energies are quite out of the question. Even in the experiments of Harkins *et al.*, data given by other investigators[4] indicate that most of the neutrons had energies below 5 Mev. Therefore the interaction assumed by Morse, Fisk, and Schiff does not agree with the asymmetry found by Harkins *et al.* and by Lampson *et al.* Various other types of interaction are discussed below so as to see how the data of these observers can be accounted for.

Morse, Fisk, and Schiff obtained much larger asymmetries than Bethe and Peierls. As they pointed out, this was due to their use of a potential well which may be thought of as a narrow deep central portion plus a broad shallow "tail." Only the tail will have an appreciable effect on particles of relative angular momentum $L$ greater than zero. The phase shifts for $L>0$ are affected mainly by the tail, whereas the phase shift for $L=0$ and the deuteron binding energy are determined by the potential energy curve as a

[1] Cf. for example, H. A. Bethe and R. F. Bacher, Rev. Mod. Phys. **8**, 117 (1936).
[2] H. A. Bethe and R. Peierls, Proc. Roy. Soc. **A149**, 176 (1935).
[3] P. M. Morse, J. B. Fisk and L. I. Schiff, Phys. Rev. **51**, 706 (1937).
[4] J. Chadwick, reference 2 of Table I; J. R. Dunning, Phys. Rev. **45**, 586 (1934); T. W. Bonner and L. M. Mott-Smith, Phys. Rev. **46**, 258 (1934).

TABLE I. *Experimental results.*

| Observer | Recoil protons from | Energy of neutrons | No. of collisions observed | Deviation from spherically symmetric scattering in c.g. system |
|---|---|---|---|---|
| Monod-Herzen[1] | Hydrogen gas | several Mev | 84 | None |
| Monod-Herzen[1] | Hydrogen gas | <0.5 Mev | 93 | More forward |
| Chadwick[2] | Paraffin | ? | ? | None |
| Kurie[3] | Paraffin | >2.5 Mev | 160 | None |
| Meitner and Phillipp[4] | Hydrogenous gases | 0.2–14.0 Mev | 100 | None |
| Harkins, Kamen, Newson and Gans[5] | Hydrogenous gases | 0.4–? Mev | 730 | More backward |
| Lampson, Mueller, and Barton[6] | Photographic emulsion | 2.55 Mev | ? | More backward |
| Kruger, Shoupp, and Stallmann[7] | Hydrogenous gases | 2.55 Mev | 810 | None |

[1] G. Monod-Herzen, J. de phys. **5**, 96 (1934).
[2] J. Chadwick, Proc. Roy. Soc. **A142**, 1 (1933).
[3] F. N. D. Kurie, Phys. Rev. **44**, 463 (1933). Kurie concluded that there was more scattering backward (more recoil protons forward) than would be the case in spherically symmetric scattering. He made no correction, however, for the fact that a proton recoiling at a larger angle has been given less of the incident neutron's energy and is on that account less likely to emerge from the paraffin. This correction involves multiplying the data by a factor $(26\cos^4\Theta - 8\cos\Theta)^{-1}$, or effectively by $1/\cos^4\Theta$. (In deriving this correction factor, the range $-$ (energy)$^4$ proportionality law has been assumed, the maximum range of the recoil protons has been taken as 26 cm in air, and the minimum observable range has been taken as 8 cm.) When corrected in this manner, the data are consistent with spherically symmetric scattering.
[4] L. Meitner and K. Phillipp, Zeits. f. Physik **87**, 484 (1934).
[5] W. D. Harkins, M. D. Kamen, H. W. Newson and D. M. Gans, Phys. Rev. **50**, 980 (1936).
[6] C. W. Lampson, D. W. Mueller and H. A. Barton, Phys. Rev. **51**, 1021 (1937).
[7] P. G. Kruger, W. E. Shoupp and F. W. Stallmann, Phys. Rev. **51**, 1021 (1937).

whole. This suggests that the essential requirements of the deuteron binding energy and of proper phase shifts can be satisfied by using an approximation to the true potential in the form of a double rectangular well, of the type illustrated in Fig. 1. The central portion of the well must be deep and relatively narrow, in order to account for the binding energies of $H^2$, $H^3$, and $He^4$. The tail portion can be adjusted to yield the observed scattering. A tail of depth 1 or $2mc^2$, extending out to $r=3$ or $4e^2/mc^2$, is sufficient to explain asymmetries of the magnitude observed. As will be shown later (see Fig. 1), a Majorana potential of this type gives the experimental asymmetry with neutron energies as low as 10 Mev. Yet this is still too high. For neutron energies such as have been used in the recent experiments, this potential gives asymmetry of the wrong sign (i.e., too few recoils forward).

The formula for the recoil cross section in the laboratory reference system is given by:[5]

$$d\sigma = \{\sum_L (2L+1)^2 \sin^2 K_L [P_L(\theta)]^2 + \sum_{L>L'} 2(2L+1)(2L'+1) \sin K_L \sin K_{L'} \times \cos(K_L - K_{L'}) P_L(\theta) P_{L'}(\theta)\} k^{-2} \cos\Theta d\Omega.$$

Here $d\sigma$ is the cross section for recoils into solid angle $d\Omega$,
$k^2 = ME'/\hbar^2$,
$E'$ is the energy in the c. g. system,
$E$ $(=2E')$ is the energy in the laboratory system (note that $E$ (in Mev) $= 1.020\,E'$ (in $mc^2$)),
$K_L$ is the phase shift for the radial function of angular momentum $L$,
$P_L(\theta)$ is the Legendre polynomial of order $L$ in $\cos\theta$,
$\Theta$ is the angle of recoil in the laboratory system,
$\theta$ $(=\pi - 2\Theta)$ is the angle of scattering in the c. g. system.

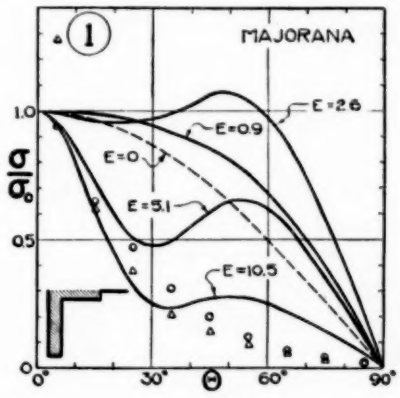


FIG. 1. Customarily assumed type of interaction (depths not drawn to scale) and scattering angular distributions for this interaction for various values of the neutron energy $E$, in Mev. The curves for the highest energies have roughly the proper asymmetry to fit the experimental points because the $d$ wave scattering counteracts the adverse $p$ wave scattering. The energies are, however, too high to fit experiment. The points are the data of Harkins *et al.*

[5] This can be obtained from the formula given on p. 24 of Mott and Massey, *Theory of Atomic Collisions* (Oxford 1933), by reasoning similar to that used in reference 5 of Table I.

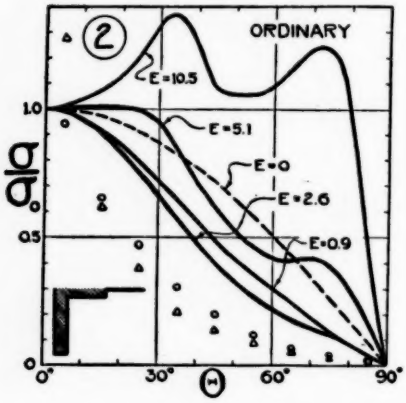


FIG. 2. A possible type of interaction (depths not to scale) and scattering angular distributions from it for various values of the neutron energy $E$, in Mev. The $d$ wave scattering here spoils agreement at the higher energies. The points are the data of Harkins *et al.*

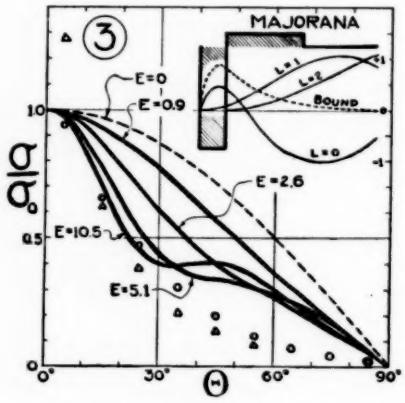


FIG. 3. A probable type of interaction (depths not to scale) and scattering angular distributions from it for various values of the neutron energy $E$, in Mev. Wave functions, properly normalized, are sketched in for the bound state of the deuteron, and for the $s$, $p$, and $d$ radial functions for free neutrons of energy 2.62 Mev. All these are for a simple square potential hole of width 1 $e^2/mc^2$, *not* for the potential illustrated. The points are the data of Harkins *et al.*

For low energies, when $K_1$ is small and $K_2$, $K_3$, $\cdots$ are negligible, the expression simplifies to $d\sigma \cong \{1-6K_1 \cot K_0 \cos 2\Theta\} k^{-2} \sin^2 K_0 \cos \Theta d\Omega$. The observed asymmetry requires that $K_1 \cot K_0$ be positive. As Bethe and Peierls[2] have pointed out, this indicates for the triplet interaction (for which $K_0$ lies between $\pi/2$ and $\pi$) a positive $K_1$, or an *attractive* potential acting on $p$ particles. For the singlet interaction (for which $K_0$ lies between 0 and $\pi/2$) a negative $K_1$, or a repulsive potential acting on $p$ particles, would be indicated. However, scattering by the singlet state turns out to be of subordinate—though not negligible—importance for the cases here in question; this can be seen in Table II.

With an "ordinary" potential of the type illustrated in Fig. 2, then, it is possible roughly to fit the data, as is seen in the figure. Equally good is a Majorana potential of the type shown in Fig. 3; for it, too, is attractive for $p$ particles. A potential of this latter type has already been proposed by Mamasachlisov[6] in order to explain data on capture and total scattering cross sections for slow neutrons. The proposed tail was 4.5 $mc^2$ high and extended out to 9.3 $e^2/mc^2$. Dmitrieff,[7] however, has pointed out the unsatisfactory nature of a potential of these dimensions —in particular the extremely asymmetric scattering it would involve.

Figs. 1, 2, and 3 show the angular distributions of recoil protons calculated by use of potentials of the three types illustrated. In each case the central well is of radius 1 $e^2/mc^2$ ($=2.81\times10^{-13}$ cm) and the tail extends out to $r=4\ e^2/mc^2$. The depth of the tail was taken to be 1 $mc^2$ for the triplet interaction. The triplet central well depth was then adjusted to make the binding energy of the deuteron 4.35 $mc^2$. The depth of the singlet interaction was taken to be a constant fraction of the triplet interaction (so that the ratio of tail depth to central well depth is the same for both the singlet and the triplet interactions), and that fraction was chosen to make the total cross section for slow neutrons approach 178 $(e^2/mc^2)^2$ $=14.0\times10^{-24}$ cm$^2$ in the limit of zero energy.[8] The depth of singlet interaction used corresponds to a "virtual" singlet level.

Inasmuch as $K_1$ was found to be quite large in some cases, the $d$ phase shift $K_2$ was also calculated for those cases and was found to have appreciable influence on the shape of the scattering angular distribution curves. The effect of $K_3$ is inappreciable except in the $E=10.5$ curves; these would be lowered about 40 percent if the $f$ wave phase shifts were included, and our

[6] V. I. Mamasachlisov, Physik. Zeits. Sowjetunion **9**, 198 (1936).

[7] N. N. Dmitrieff, Physik. Zeits. Sowjetunion **11**, 225 (1937).

[8] E. Fermi, Ricerca Scient. **7**, 37 (1936). The value used here is the cross section for neutrons of groups $A$ and $D$ (energies just over 1 volt), *not* that for thermal neutrons. The latter is about 3 times too large on account of the effects of the chemical binding of the protons.

conclusions would be unchanged thereby. Table II gives the constants found for the curves. The energy dependence of $K_0$ and $K_1$ is similar to that shown in the tables of Morse, Fisk, and Schiff.[3] For comparison, the depths of well appropriate to a simple potential hole 1 $e^2/mc^2$ wide, without a tail are: triplet—41.4 $mc^2$, singlet—22.6 $mc^2$.

In the course of the calculation it was found convenient to check the values of $K_0$ and $K_1$ found by exact solution of the radial boundary value problem, with those determined by the approximate value:[9]

$$K_L \leqq -\int (V/E') F_L^2 d\rho.$$

Here $V$ is the value of the potential energy, $\rho = kr$, and $F_L$ is $\rho$ times the radial wave function, normalized to unit amplitude at $r = \infty$.

For central wells of radii from 0.5 to 1.5 $e^2/mc^2$, the results were practically identical with those of radius 1 $e^2/mc^2$ shown in Table II. For a radius of 2 $e^2/mc^2$, however, the central well makes a large contribution to $K_1$, such that in Fig. 1 the proper asymmetry could be obtained with yet lower energies ($\sim$5 Mev). Such a broad central well, however, is considered unlikely to fit with the binding energies of the light nuclei. The size of the tail has been kept limited here, so that $K_1$, $K_2$, $\cdots$ are quite small. This is consistent with the hypothesis that proton-proton forces differ from neutron-proton forces only by the electrostatic repulsion, for evidence from proton-proton scattering indicates that $K_1$, $K_2$, $\cdots$ are negligible at 0.9 Mev energies. Other ranges and depths of tail could have been chosen to fit the data with even better success than the sample chosen here; but the approximate nature of the potential well assumed, as well as the uncertainty of the experimental results, makes closer fitting of the observed asymmetry unnecessary at present.

TABLE II. *Constants for the interactions.*

| Interaction | | (1) Majorana | | (2) Ordinary | | (3) Majorana | |
|---|---|---|---|---|---|---|---|
| | | Triplet | Singlet | Triplet | Singlet | Triplet | Singlet |
| Central well depth | | 40.2 | 17.5 | 40.2 | 17.5 | 42.5 | 27.0 |
| Tail depth | | 1.0 | 0.435 | 1.0 | 0.435 | −1.0 | −0.635 |
| $E=0.94$ Mev | $K_0$ | 149.9° | 46.5° | 149.9° | 46.5° | 143.0° | 73.5° |
| | $K_1$ | −2.4 | −1.1 | 3.9 | 1.3 | 3.4 | 2.1 |
| | $K_2$ | 0.0 | 0.0 | 0.0 | 0.0 | 0.0 | 0.0 |
| | $\sigma_0$ | 1.73 | 6.76 | 5.15 | 5.40 | 6.19 | 9.48 |
| $E=2.62$ Mev | $K_0$ | 134.3 | 45.6 | 134.3 | 45.6 | 121.4 | 78.0 |
| | $K_1$ | −7.5 | −3.7 | 11.8 | 4.1 | 9.7 | 5.7 |
| | $K_2$ | 1.1 | 0.5 | 1.1 | 0.5 | −1.1 | −0.7 |
| | $\sigma_0$ | 0.85 | 3.18 | 4.64 | 1.40 | 5.99 | 3.57 |
| $E=5.14$ Mev | $K_0$ | 119.8 | 43.5 | 119.8 | 43.5 | 103.9 | 72.3 |
| | $K_1$ | −13.0 | −6.1 | 19.2 | 7.3 | 13.2 | 7.9 |
| | $K_2$ | 4.6 | 1.9 | 4.6 | 1.9 | −4.0 | −2.4 |
| | $\sigma_0$ | 1.67 | 2.36 | 2.34 | 0.57 | 4.52 | 1.75 |
| $E=10.5$ Mev | $K_0$ | 100.2 | 43.3 | 100.2 | 43.3 | 86.0 | 61.1 |
| | $K_1$ | −14.8 | −8.0 | 19.8 | 7.4 | 7.8 | 5.5 |
| | $K_2$ | 9.9 | 4.3 | 9.9 | 4.3 | −8.3 | −5.2 |
| | $\sigma_0$ | 2.84 | 1.84 | 0.68 | 0.44 | 2.19 | 0.80 |

All well depths are in $mc^2$. Each central well radius is equal to 1 $e^2/mc^2$. $\sigma_0$ is the absolute recoil cross section per unit solid angle at 0° in units of $(e^2/mc^2)^2$.

## Conclusion

We have seen that, for interaction wells narrow enough to keep $K_1$ and higher order phase-shifts reasonably small, the explanation of the asymmetric data requires a shallow long range interaction which is *attractive* for $p$ particles. Such an interaction can be attained by the assumption, either of ordinary forces which are attractive for all values of $L$, or of Majorana forces which are repulsive for even values of $L$. Since Majorana forces seem better suited to account for the structure of heavy nuclei[10] and of light ones,[11] they are preferable to ordinary forces; nevertheless the long range repulsive effect on $s$ particles is rather novel. There seems to be as yet no theoretical explanation of such an interaction as this.

It should be emphasized that the asymmetric scattering discussed here is contradicted by many experiments. The purpose of this work is merely to indicate that a potential of type (3) would be needed should this asymmetry prove real.

We are deeply grateful to Professor Breit for his many helpful suggestions on this problem.

*Note added in proof:* J. H. Bartlett (Phys. Rev. **51**, 889 (1937) has suggested that the asymmetric scattering could also be explained by using different width wells for $s$ and $p$-interactions. He finds as we do that a positive $K_1$ is necessary (and thus presumably that the $p$ interaction must involve an attractive force); but it is not clear that such single-well interactions will fit simultaneously the scattering experiments and the mass defects of both light and heavy nuclei.

[9] H. M. Taylor, Proc. Roy. Soc. **A136**, 605 (1932), Eq. (11). Cf. also G. Breit, E. U. Condon, and R. D. Present, Phys. Rev. **50**, 825 (1936), Eq. (8.1), for form used here.

[10] E. Majorana, Zeits. f. Physik **82**, 137 (1933); G. Breit and E. Feenberg, Phys. Rev. **50**, 850 (1936); E. Wigner, Nat. Acad. Sci. Proc. **22**, 662 (1936).

[11] E. Feenberg and E. Wigner, Phys. Rev. **51**, 95 (1937); E. Feenberg and M. Phillips, Phys. Rev. **51**, 597 (1937); E. Wigner, Phys. Rev. **51**, 947 (1937).

# Magnetic Scattering of Slow Neutrons

O. HALPERN AND M. H. JOHNSON, JR.
*Department of Physics, New York University, University Heights, New York, N. Y.*
(Received May 3, 1937)

According to well-known theoretical results, atomic or ionic magnetic moments should *per se* contribute to the cross section for the scattering of slow neutrons. It is suggested that this contribution may be separated from that due to nuclear scattering by a comparison of the scattering of a metal with the scattering from the corresponding ions of different valence. This magnetic scattering should occur in unmagnetized paramagnetic bodies and, in favorable cases, should be several times as great as the nuclear scattering. Accepting the present value for the magnetic moment of the neutron such experiments will yield information concerning the velocity distribution of the incident neutrons.

AS first pointed out by Bloch,[1] the magnetic moments of atoms or ions should contribute appreciably to the scattering cross section of slow neutrons. To separate the magnetic from the nuclear scattering, he suggested magnetic polarization experiments on saturated ferromagnetic bodies. These experiments would allow the production of beams of neutrons whose spins were preferentially oriented; this partially "polarized" state could be detected by a second scattering or absorption in a ferromagnetic body with a properly chosen direction of magnetization.

The principle of Bloch's suggestion can be mathematically expressed as follows: Denoting by $\psi_n$ and $\psi_m$ the wave functions of a neutron scattered by nuclear or magnetic forces respectively, the total cross section is proportional to $|\psi_n \pm \psi_m|^2$, where the sign depends on the relative orientation of atomic and neutron magnetic moments. For an unpolarized beam of neutrons or an unmagnetized body one obtains by averaging an expression proportional to $|\psi_n|^2 + |\psi_m|^2$ for the total scattering cross section. Whereas for a magnetized body the cross term $2\psi_n\psi_m$ will not disappear in the average, leading to the polarization effects mentioned above.

Bloch's suggestion has been given a more detailed mathematical treatment by Schwinger.[2] His result for the scattering cross section of an unpolarized beam in an unmagnetized body agrees with the expression of Bloch and can be written

$$\sigma = \sigma_n + \sigma_m = (\sigma_n + 0.67 \times 10^{-24} B^2) \text{ cm}^2, \quad (1)$$

where $B$ denotes the number of Bohr magnetons of the scattering atom (ion). According to the derivation the expression is valid only if $\lambda/2\pi$ ($\lambda$ = wave-length of incident neutron) is large compared to the linear dimensions of the atomic domain which gives rise to the magnetic moment. The second term of (1) is multiplied by a "magnetic form factor" which decreases rapidly from the value 1 when $\lambda/2\pi$ becomes smaller than the linear dimensions of the relevant atomic domain. It is further assumed in (1) that the magnetic moment of the neutron is equal to 2 nuclear Bohr magnetons.

Instead of experimenting with ferromagnetic bodies and producing "polarized" neutron beams, the magnetic scattering could also be detected and separated in nonmagnetized bodies as follows. Successive scattering observations with a metal and its salts will lead to different cross sections for the metal if the metallic salts show a varying paramagnetism depending on the valence with which the metal enters into the chemical combination. Since the nuclear cross sections are usually several times $10^{-24}$ cm$^2$, it is clear from (1) that the magnetic cross section is in general comparable to and may even be a multiple of the nuclear cross section.

Since (1) is only valid for sufficiently large values of $\lambda/2\pi$, discussion should be centered on substances with incomplete inner shells. Table I of the ions of the iron group shows the dependence of $B$ on the valence. In Table I we have replaced the values for the "effective Bohr magneton numbers" given by Van Vleck[3] by the

[1] Bloch, Phys. Rev. **50**, 259 (1936).
[2] Schwinger, Phys. Rev. **51**, 544 (1937).
[3] J. H. Van Vleck, *Electric and Magnetic Susceptibilities* (Oxford University Press, 1932), Par. 72, 73.

actual Bohr magneton numbers which are of importance for the neutron scattering. With the exception of the ferromagnetic substances Fe, Co and Ni, the metals show comparatively small paramagnetism. But even in the last mentioned cases the difference between the magneton numbers of the ions in metallic and salt form are very appreciable, the maximum magneton number for the ferromagnetic metals being about 2.

It deserves mentioning that the magneton numbers given in Table I are very nearly the same for solid salts and solutions so that they can be ascribed with certainty to the metallic ion and not to any molecular complex. Under this same assumption the experimental paramagnetism may be theoretically understood (cf. Van Vleck, reference 3).

The elements of the Pd, Pt and Ur group, except $Mo^{+++}$, do not seem to show sufficiently large values of $B$ to be of interest. Among the trivalent ions of the rare earths, however, the elements Tb, Er, Ds, Ho, seem to be most promising. The first two having $B=9$, the last two $B=10$. For this group, on the other hand, Gd shows a *capture* cross section of the order $2\times10^{-20}$ cm². Hence any possibility of using these elements rests on a quite complete chemical separation of the rare earths. Assuming that any one of these elements has a capture cross section less than $50\times10^{-24}$ cm² and that it is free of Gd to a tenth of a percent, the capture and magnetic scattering cross section should become of equal order of magnitude and thus the magnetic effect easily demonstrable.

The principal difficulty, in our opinion in obtaining a result of the estimated magnitude in these experiments will lie in the wave-length of the so-called thermal neutrons. The wave-length of neutrons in thermal equilibrium at room temperature is approximately 1.5A. Since the average velocity of a beam of thermal neutrons in our opinion will lie considerably above the so-called thermal velocity, it will in general be impossible to satisfy the condition that $\lambda/2\pi$ is larger than the relevant atomic domain. Rough considerations have led us to believe that this atomic domain is not much smaller than a Bohr radius ($0.53\times10^{-8}$ cm) for the elements of the iron group. For this reason the rare earths would be preferable if the above-mentioned obstacles can be overcome. This should lead to a pronounced effect from the form factor and in particular, should result in preferential forward scattering as well as a decrease in the total scattering cross sections.

TABLE I. *Number of Bohr magnetons.*

| Ion | True Magnetic Number | Ion | True Magnetic Number |
|---|---|---|---|
| $V^{++++}$ | 1 | $Mn^{++}$ | 5 |
| $V^{+++}$ | 2 | $Fe^{+++}$ | 5 |
| $V^{++}$ | 3 | $Fe^{++}$ | >4 |
| $Cr^{+++}$ | 3 | $Co^{++}$ | 4 |
| $Mn^{++++}$ | >3 | $Ni^{++}$ | >2 |
| $Cr^{++}$ | 4 | $Cu^{++}$ | 1 |
| $Mn^{+++}$ | >4 | | |

The polarization experiments so far carried out have led to results only a small fraction of the anticipated effect. This might be due either to high velocities (small wave-length) of the neutrons, as seems likely, or due to a smaller magnetic moment of the neutron. The scattering experiments here suggested should show an increase in the cross section by many hundred percent. If the observation should not agree with this theoretical prediction, then further experiments on the angular distribution of scattering should distinguish between the two possible causes for the discrepency. Since for scattering under small angles, the influence of the form factor (shortness of wave-length) can be neglected, too small an effect in such experiments would have to be ascribed to an incorrect assumption as to the magnitude of the neutron's magnetic moment. On the other hand if the small angle scattering is large, these experiments would present some information about the velocity distribution of the incoming neutrons.

Our colleague, Dr. M. D. Whitaker, has begun experiments of the kind suggested in this note.*

* *Footnote added in proof:* For scattering in paramagnetic media the second term of (1) should be multiplied by $(j+1)/j$ where $j$ is the angular momentum of the scattering ion in units $\hbar$. See Phys. Rev. **51**, 992 (1937).

# Note on the Radiation Field of the Electron

F. BLOCH AND A. NORDSIECK*
*Stanford University, California*

(Received May 14, 1937)

Previous methods of treating radiative corrections in non-stationary processes such as the scattering of an electron in an atomic field or the emission of a $\beta$-ray, by an expansion in powers of $e^2/\hbar c$, are defective in that they predict infinite low frequency corrections to the transition probabilities. This difficulty can be avoided by a method developed here which is based on the alternative assumption that $e^2\omega/mc^3$, $\hbar\omega/mc^2$ and $\hbar\omega/c\Delta p$ ($\omega$=angular frequency of radiation, $\Delta p$=change in momentum of electron) are small compared to unity. In contrast to the expansion in powers of $e^2/\hbar c$, this permits the transition to the classical limit $\hbar=0$. External perturbations on the electron are treated in the Born approximation. It is shown that for frequencies such that the above three parameters are negligible the quantum mechanical calculation yields just the directly reinterpreted results of the classical formulae, namely that the total probability of a given change in the motion of the electron is unaffected by the interaction with radiation, and that the mean number of emitted quanta is infinite in such a way that the mean radiated energy is equal to the energy radiated classically in the corresponding trajectory.

## I. INTRODUCTION

THE quantum theory of radiation has been successfully applied to radiative emission and absorption processes. If the methods which lead to these results are used to obtain more general radiative corrections, a characteristic difficulty arises. This difficulty is clearly visible in the formulae given by Mott, Sommerfeld[1] and Bethe and Heitler[2] for the probability of scattering of an electron in a Coulomb field accompanied by the emission of a single light quantum. If the emitted quantum lies in a frequency range $\omega$ to $\omega+d\omega$, this probability is for small frequencies proportional to $d\omega/\omega$ independently of the angle of scattering. Taking these formulae literally and asking for the total probability of scattering with the emission of any light quantum, one therefore gets by integration over $\omega$ a result which diverges logarithmically in the low frequencies. The same difficulty appears in the radiative correction to the probability of $\beta$-decay,[3] and to that of other nonstationary processes.

This "infrared catastrophe" is obviously unrelated to the fundamental "ultraviolet" difficulties of quantum electrodynamics, exemplified by the divergent result for the self-energy of the electron. While the latter is already inherent in the classical theory, the former has no counterpart there. There is, however, a feature in the classical theory which indicates the cause of the difficulty: If for simplicity one considers only frequencies which are small compared to the reciprocal of the collision time, the mechanism of emission may be described as follows. The amplitude of each Fourier component of the proper field of the electron before the impact retains its value after the impact.[4] The difference between the new field and the field proper to the electron in its new motion is the emitted radiation. The significant point is now that $I_\omega$, the radiated intensity per unit frequency interval, does not approach zero[5] as $\omega\to 0$. Hence $I_\omega/\hbar\omega$, which may be taken as an estimate of the mean number of light quanta emitted per unit frequency range, tends to infinity as $\omega\to 0$. Since the same result has to be expected in a rigorous quantum-theoretical treatment, one has to anticipate that only the probability for the simultaneous emission of infinitely many quanta can be finite; the probability of emission of any finite number of quanta must vanish.

* National Research Fellow.

[1] N. F. Mott., Proc. Camb. Phil. Soc. **27**, 255 (1931); A. Sommerfeld, Ann. d. Physik **11**, 257 (1931).

[2] H. Bethe and W. Heitler, Proc. Roy Soc. **A146**, 83 (1934).

[3] J. K. Knipp and G. E. Uhlenbeck, Physica **3**, 425 (1936); F. Bloch, Phys. Rev. **50**, 272 (1936); see pp. 276–7 in the latter.

[4] This is in strict analogy to the mechanical model of an oscillator initially held away from its equilibrium position by a constant force, the value of which suddenly changes. We shall see later that the same analogy holds in quantum mechanics, where it finds its mathematical expression in the expansion of the wave function of an oscillator with one equilibrium position in terms of the wave functions corresponding to a new equilibrium position.

[5] For a charged particle moving in a pure Coulomb field, $I_\omega\sim\log 1/\omega\tau$ as $\omega\to 0$, where $\tau$ is the collision time; in a field which falls off more rapidly than $1/r^2$ for large $r$, $I_\omega$ approaches a finite value.

In these circumstances the ordinary treatment of the interaction between electron and field by a consistent expansion in powers of $e$, the charge of the electron, is clearly inadequate, for such a procedure is based on the physical assumption that the probability of multiple light quantum emission decreases with increasing number of emitted quanta. In fact, however, if one considers only frequencies above a certain minimum frequency $\omega_0$, the expansion parameter of such a treatment is $e^2/\hbar c\cdot(v/c)^2 \log E/\hbar\omega_0$ ($E$, $v$ the kinetic energy resp. velocity of the electron),[6] which in the limit $\omega_0\to 0$ violates the original assumption that it is small.

In order to avoid this expansion, a method is developed below in which the coupling between the electron and the electromagnetic waves of low frequency is not considered as a small perturbation. The method is analogous to the classical expansion in powers of $e^2\omega/mc^3$, the ratio of the electron radius to the wave-length considered, in which in first approximation the motion of the electron is treated as given and the reaction of the field on the electron is taken into account in higher orders. We shall show how this can be formulated in quantum mechanics as the solution in successive approximations of a system of two simultaneous differential equations; of these approximations only the one of lowest order is here needed and investigated. After thus having treated the system electron plus electromagnetic field, transitions of this system due to external forces on the electron can be treated by the ordinary method of small perturbations.[7]

## II. Formulation of the Method

The Hamilton operator of the total system electron plus electromagnetic field, after elimination of the longitudinal parts of the electric field, is[8]

$$\mathcal{H}=c\{(\boldsymbol{\alpha},\ \mathbf{p}-(e/c)\mathbf{A})+\beta mc\}+(1/8\pi)\int((\mathbf{E}^{tr})^2+\mathbf{H}^2)dV.$$

We expand the vector potential $\mathbf{A}$ in the form

$$\mathbf{A}=2c(\pi\hbar/\Omega)^{\frac{1}{2}}\sum_{s\lambda}\omega_s^{-\frac{1}{2}}\boldsymbol{\varepsilon}_{s\lambda}(P_{s\lambda}\cos(\mathbf{k}_s,\mathbf{r})+Q_{s\lambda}\sin(\mathbf{k}_s,\mathbf{r})),$$

where $\Omega$ is the volume within which the cyclical boundary conditions are applied, the summation index $s$ characterizes the direction and circular frequency $\omega_s$ of the various waves with propagation vector $\mathbf{k}_s$, $\lambda$ their state of polarization; and $\boldsymbol{\varepsilon}_{s\lambda}$ is a unit vector in the direction of polarization. The dynamical variables $P_{s\lambda}$ and $Q_{s\lambda}$ are related to the quantized amplitudes $a(\lambda,\mathbf{k})$ and $a^+(\lambda,\mathbf{k})$[9] according to

$$2^{-\frac{1}{2}}(P_{s\lambda}+iQ_{s\lambda})=a(\lambda,\mathbf{k}_s),$$
$$2^{-\frac{1}{2}}(P_{s\lambda}-iQ_{s\lambda})=a^+(\lambda,\mathbf{k}_s),$$

and obey the commutation laws

$$[P_{s\lambda},Q_{s'\lambda'}]=-i\delta_{ss'}\delta_{\lambda\lambda'};\qquad [P_{s\lambda},P_{s'\lambda'}]=[Q_{s\lambda},Q_{s'\lambda'}]=0.$$

We then obtain

$$\mathcal{H}=c\{(\boldsymbol{\alpha},\ \mathbf{p}-\sum_{s\lambda}\mathbf{a}_{s\lambda}[P_{s\lambda}\cos(\mathbf{k}_s,\mathbf{r})+Q_{s\lambda}\sin(\mathbf{k}_s,\mathbf{r})])+\beta mc\}+\tfrac{1}{2}\sum_{s\lambda}(P_{s\lambda}^2+Q_{s\lambda}^2)\hbar\omega_s, \quad (1)$$

where
$$\mathbf{a}_{s\lambda}=2e(\pi\hbar/\Omega\omega_s)^{\frac{1}{2}}\boldsymbol{\varepsilon}_{s\lambda}. \quad (2)$$

The matrix vector $\boldsymbol{\alpha}$ of Dirac is to be interpreted physically as the velocity of the electron divided by $c$. If following the procedure in classical theory, we should in first approximation neglect the reaction of the electromagnetic field on the electron, we should be led to replace $\boldsymbol{\alpha}$ in (1) by the $c$ number

$$\boldsymbol{\mu}=\mathbf{v}/c, \quad (3)$$

where $\mathbf{v}$ stands for the (constant) velocity of the electron in its undisturbed motion. The operator $\beta$ has then at the same time to be replaced by $(1-\mu^2)^{\frac{1}{2}}$. But with $c$ numbers substituted for $\boldsymbol{\alpha}$ and $\beta$ in (1) the dynamical problem can immediately be solved. Indeed, the presence of the interaction energy in (1) then causes no mathe-

[6] This is the order of magnitude of the ratio of the probabilities of single quantum emission and radiationless process.

[7] A case in which the action of a scattering field on the electron is not considered as a small perturbation, is treated in the following paper by A. Nordsieck.

[8] W. Pauli, *Handbuch der Physik*, Vol. 24, p. 266.

[9] W. Pauli, *Handbuch der Physik* Vol. 24, p. 250 ff.; the notation used in the present paper is essentially the same as that of G. Wentzel, *Handbuch der Physik* Vol. 24, p. 740 ff.

matical difficulty, since being closely analogous to the potential of a given constant force on each field oscillator, it can be taken into account by merely adding functions of $\mathbf{r}$ to the $P_{s\lambda}$ and $Q_{s\lambda}$.

Of course, the above replacement is not rigorously justified. In order to enable one to take into account the error thus committed by successive approximations, we proceed as follows. The solution $\psi(\mathbf{r}, Q_{s\lambda})$ of the wave equation

$$\mathfrak{H}\psi = E\psi \tag{4}$$

can be uniquely separated into two parts

$$\psi = \psi^+ + \psi^- \tag{5}$$

by the help of the operator

$$\Lambda = (\boldsymbol{\alpha}, \boldsymbol{\mu}) + \beta(1-\mu^2)^{\frac{1}{2}} \tag{6}$$

and the conditions

$$\Lambda\psi^+ = \psi^+; \quad \Lambda\psi^- = -\psi^-. \tag{7}$$

Using further the relations

$$\Lambda\boldsymbol{\alpha} = 2\boldsymbol{\mu} - \boldsymbol{\alpha}\Lambda; \quad \Lambda\beta = 2(1-\mu^2)^{\frac{1}{2}} - \beta\Lambda \tag{8}$$

and adding and subtracting Eqs. (4) and

$$\Lambda\mathfrak{H}\psi = E\Lambda\psi \tag{4a}$$

we get

$$\begin{aligned}&\{c(\boldsymbol{\mu}, \mathbf{p} - \sum_{s\lambda}\mathbf{a}_{s\lambda}[P_{s\lambda}\cos(\mathbf{k}_s, \mathbf{r}) + Q_{s\lambda}\sin(\mathbf{k}_s, \mathbf{r})]) \\ &+ mc^2(1-\mu^2)^{\frac{1}{2}} \pm \tfrac{1}{2}\sum_{s\lambda}(P_{s\lambda}^2 + Q_{s\lambda}^2)\hbar\omega_s \mp E\}\psi^{+,-} \\ &= -c(\boldsymbol{\mu} \pm \boldsymbol{\alpha}, \mathbf{p} - mc(1-\mu^2)^{-\frac{1}{2}}\boldsymbol{\mu} \\ &- \sum_{s\lambda}\mathbf{a}_{s\lambda}[P_{s\lambda}\cos(\mathbf{k}_s, \mathbf{r}) + Q_{s\lambda}\sin(\mathbf{k}_s, \mathbf{r})])\psi^{-,+}\end{aligned} \tag{9}$$

where the upper sign goes with the first superscript and the lower with the second.

The two functions $\psi^+$ and $\psi^-$ in Eqs. (9) correspond in the limit as the interaction between the electron and the field tends to zero, to motions of the electron in states with momentum $mc(1-\mu^2)^{-\frac{1}{2}}\boldsymbol{\mu}$ and with energies $\pm mc^2(1-\mu^2)^{-\frac{1}{2}}$, respectively. The approximation mentioned before of first assuming the velocity of the electron to be a given $c$ number $\boldsymbol{\mu}c$ is equivalent to an approximate solution of the equations (9) in which the right-hand sides are neglected and $\psi^-$ is assumed to be zero. The latter assumption is made to obtain a state in which the energy of the electron is positive.

We accordingly solve the equation

$$\begin{aligned}&\{c(\boldsymbol{\mu}, \mathbf{p} - \sum_{s\lambda}\mathbf{a}_{s\lambda}[P_{s\lambda}\cos(\mathbf{k}_s, \mathbf{r}) \\ &+ Q_{s\lambda}\sin(\mathbf{k}_s, \mathbf{r})]) + mc^2(1-\mu^2)^{\frac{1}{2}} \\ &+ \tfrac{1}{2}\sum_{s\lambda}(P_{s\lambda}^2 + Q_{s\lambda}^2)\hbar\omega_s - E\}u = 0.\end{aligned} \tag{10}$$

This can best be done by first making the canonical transformation

$$\begin{aligned}&P_{s\lambda} = P'_{s\lambda} + \sigma_{s\lambda}\cos(\mathbf{k}_s, \mathbf{r}); \\ &Q_{s\lambda} = Q'_{s\lambda} + \sigma_{s\lambda}\sin(\mathbf{k}_s, \mathbf{r}); \quad \mathbf{r} = \mathbf{r}'; \\ &\mathbf{p} = \mathbf{p}' - \sum_{s\lambda}\hbar\mathbf{k}_s\sigma_{s\lambda}[P'_{s\lambda}\cos(\mathbf{k}_s, \mathbf{r}) \\ &+ Q'_{s\lambda}\sin(\mathbf{k}_s, \mathbf{r}) + \tfrac{1}{2}\sigma_{s\lambda}].\end{aligned} \tag{11}$$

The corresponding transformation of the wave function is

$$\begin{aligned}u(\mathbf{r}, Q_{s\lambda}) = \exp\{&i\sum_{s\lambda}\sigma_{s\lambda}\cos(\mathbf{k}_s, \mathbf{r}) \\ &\times[Q'_{s\lambda} + \tfrac{1}{2}\sigma_{s\lambda}\sin(\mathbf{k}_s, \mathbf{r})]\} \cdot u'(\mathbf{r}, Q'_{s\lambda}).\end{aligned} \tag{12}$$

Choosing

$$\sigma_{s\lambda} = (\boldsymbol{\mu}, \mathbf{a}_{s\lambda})/\hbar(k_s - (\boldsymbol{\mu}, \mathbf{k}_s)) \tag{13}$$

one obtains for $u'$ the simple equation

$$\begin{aligned}&\{c(\boldsymbol{\mu}, \mathbf{p}') + mc^2(1-\mu^2)^{-\frac{1}{2}} + \tfrac{1}{2}\sum_{s\lambda}(P'^2_{s\lambda} + Q'^2_{s\lambda})\hbar\omega_s \\ &- (c/2\hbar)\sum_{s\lambda}(\boldsymbol{\mu}, \mathbf{a}_{s\lambda})^2/(k_s - (\boldsymbol{\mu}, \mathbf{k}_s)) - E\}u' = 0\end{aligned} \tag{14}$$

with the general solution

$$\begin{aligned}u' = \gamma(\boldsymbol{\mu})\Omega^{-\frac{1}{2}}\exp\{&i/\hbar(mc(1-u^2)^{-\frac{1}{2}}\boldsymbol{\mu} + \mathbf{g}, \mathbf{r})\} \\ &\times \prod_{s\lambda}h_{m_{s\lambda}}(Q'_{s\lambda}),\end{aligned} \tag{15}$$

$$\begin{aligned}E(\boldsymbol{\mu}, m_{s\lambda}, \mathbf{g}) &= mc^2(1-\mu^2)^{-\frac{1}{2}} + c(\boldsymbol{\mu}, \mathbf{g}) \\ &+ \sum_{s\lambda}(m_{s\lambda} + \tfrac{1}{2})\hbar\omega_s - (c/2\hbar)\sum_{s\lambda}(\boldsymbol{\mu}, \mathbf{a}_{s\lambda})^2/(k_s - (\boldsymbol{\mu}, \mathbf{k}_s)).\end{aligned} \tag{16}$$

Here $\gamma(\boldsymbol{\mu})$ is a normalized four-component amplitude satisfying the relation $\Lambda\gamma = \gamma$.[10] $\mathbf{g}$ is an arbitrary vector introduced so that for a fixed value of $\boldsymbol{\mu}$ the functions (15) form a complete orthogonal set. We shall below use only such functions $u'$ for which $\mathbf{g} = 0$, so that for vanishing interaction between electron and field we have to deal with an electron of momentum $mc(1-\mu^2)^{-\frac{1}{2}}\boldsymbol{\mu}$.

[10] $\gamma$ may be taken to be proportional to any linear combination of the columns of $(1+\Lambda)$.

$h_m(x)$ is the normalized solution of the oscillator equation

$$h_m''-x^2h_m+(2m+1)h_m=0.$$

Going back to the original function $u$ and the original variables $Q_{s\lambda}$, we have from (11), (12), and (15)

$$u(\mathfrak{y}, m_{s\lambda})=\gamma(\mathfrak{y})\Omega^{-\frac{1}{2}}\exp\{i/\hbar(mc(1-\mu^2)^{-\frac{1}{2}}\mathfrak{y}, \mathfrak{r}) +i\sum_{s\lambda}\sigma_{s\lambda}\cos(\mathfrak{k}_s, \mathfrak{r})[Q_{s\lambda}-\tfrac{1}{2}\sigma_{s\lambda}\sin(\mathfrak{k}_s, \mathfrak{r})]\} \cdot\prod_{s\lambda}h_{m_{s\lambda}}(Q_{s\lambda}-\sigma_{s\lambda}\sin(\mathfrak{k}_s, \mathfrak{r})). \quad (17)$$

It is to be noted that the approximate validity of this solution is not conditioned by the smallness of the fine structure constant $e^2/\hbar c$, since we have neglected only the recoil of the electron and can therefore make the solution (17) the more accurate the larger a mass we assign to the electron. In order to obtain the number which must be supposed to be small in order to have (17) valid, one may calculate $\psi^-$ in first approximation and compare its norm with the norm of $\psi^+$, which is unity. An estimate of norm $(\psi^-)$ gives

$$\text{norm}\,(\psi^-)\sim e^2\omega_1/mc^3[f(\mu)(\hbar\omega_1/mc^2) +g(\mu)(e^2\omega_1/mc^3)],$$

where $\omega_1$ is the highest frequency taken into account, and $f$ and $g$ are functions of $\mu$ alone such that for small $\mu$, $f\sim 1/3\pi$, $g\sim(4/9\pi^2)\mu^2$ and for large $(1-\mu^2)^{-\frac{1}{2}}$, $f\sim(1/4\pi)(1-\mu^2)$, $g\sim(1/4\pi^2)(1-\mu^2)^2\log(1/(1-\mu^2))$. That the expansion parameter is not $e^2/\hbar c$ may also be seen by considering the classical limit, in which $\hbar$ is assumed to be zero; in this limit the shifts $\sigma_{s\lambda}\cos(\mathfrak{k}_s, \mathfrak{r})$ and $\sigma_{s\lambda}\sin(\mathfrak{k}_s, \mathfrak{r})$ of $P_{s\lambda}$ and $Q_{s\lambda}$ expressed in (17) correctly describe the superposition of the transverse part of the field produced by the uniformly moving electron, on the field of the external light waves.[11]

## III. Application to Small Perturbations on the Electron; Transition Probabilities and Mean Radiated Energy

The solution (17) can be used to calculate transition probabilities due to small external perturbations acting on the electron. Consider a transition of the system between two states characterized by the velocities $\mathfrak{v}=\mathfrak{y}c$ and $\mathfrak{w}=\mathfrak{v}c$ of the electron and the quantum numbers $m_{s\lambda}$ and $n_{s\lambda}$, respectively. The matrix element of a perturbation $V$ operating on the coordinate and spin variables of the electron is given by

$$V(\mathfrak{y}, m_{s\lambda}; \mathfrak{v}, n_{s\lambda}) =\frac{1}{\Omega}\int d\mathfrak{r}\exp\{-i/\hbar(mc(1-\mu^2)^{-\frac{1}{2}}\mathfrak{y}, \mathfrak{r})\} \cdot\gamma^*(\mathfrak{y})\,V\delta(\mathfrak{v})\exp\{i/\hbar(mc(1-\nu^2)^{-\frac{1}{2}}\mathfrak{v}, \mathfrak{r}\} \cdot\prod_{s\lambda}I(\mathfrak{k}_s; \sigma_{s\lambda}, m_{s\lambda}; \tau_{s\lambda}, n_{s\lambda}), \quad (18)$$

where $\tau_{s\lambda}$ is the same function of $\mathfrak{v}$ as $\sigma_{s\lambda}$ is of $\mathfrak{y}$ (see (13)), $\delta(\mathfrak{v})$ is a four-component amplitude for the state $\mathfrak{v}$ corresponding to $\gamma(\mathfrak{y})$ for the state $\mathfrak{y}$, and

$$I(\mathfrak{k}; \sigma, m; \tau, n)=\int dQh_m(Q-\sigma\sin(\mathfrak{k}, \mathfrak{r})) \times\exp\{-i(\sigma-\tau)\cos(\mathfrak{k}, \mathfrak{r})Q+\tfrac{1}{2}i(\sigma^2-\tau^2) \times\sin(\mathfrak{k}, \mathfrak{r})\cos(\mathfrak{k}, \mathfrak{r})\}h_n(Q-\tau\sin(\mathfrak{k}, \mathfrak{r})) \quad (19)$$
$$=\exp\{-i(m-n)(\mathfrak{k}, \mathfrak{r})\}\cdot K$$

with

$$K(\sigma, m; \tau, n)=\exp\{-\tfrac{1}{4}(\sigma-\tau)^2\} \times(m!n!)^{\frac{1}{2}}[-i2^{-\frac{1}{2}}(\sigma-\tau)]^{|m-n|} \sum_{\zeta=0}^{l}\frac{[-\frac{1}{2}(\sigma-\tau)^2]^\zeta}{(l-\zeta)!\zeta!(|m-n|+\zeta)!}, \quad (20)$$

where $l=m$ if $m\leq n$ and $l=n$ otherwise.[12] Putting the value (19) of $I$ into (18), we can write the matrix elemeht in the form

$$V(\mathfrak{y}, m_{s\lambda}; \mathfrak{v}, n_{s\lambda})=\frac{1}{\Omega}F(\mathfrak{q})\prod_{s\lambda}K(\sigma_{s\lambda}, m_{s\lambda}; \tau_{s\lambda}, n_{s\lambda}), \quad (21)$$

where

$$F(\mathfrak{q})=\int d\mathfrak{r}\exp\{-i(\mathfrak{q}, \mathfrak{r})\}\gamma^*(\mathfrak{y})\,V\delta(\mathfrak{v}) \quad (22)$$

and $$\mathfrak{q}=(mc/\hbar)[(1-\mu^2)^{-\frac{1}{2}}\mathfrak{y}-(1-\nu^2)^{-\frac{1}{2}}\mathfrak{v}] +\sum_{s\lambda}(m_{s\lambda}-n_{s\lambda})\mathfrak{k}_s. \quad (23)$$

[11] In fact, the quantities $\sigma_{s\lambda}$ can be obtained exactly by Fourier analysis of the transverse part of the classical vector potential of a uniformly moving electron.

[12] The integral over $Q$ is best evaluated by using the generating function for the Hermitian polynomials.

From (21) follows the probability per unit time of the transition $\mathfrak{y}$, $m_{s\lambda}\to\mathfrak{v}$, $n_{s\lambda}$ in the form

$$T(\mathfrak{y}, m_{s\lambda}; \mathfrak{v}, n_{s\lambda}) = (2\pi/\hbar\Omega^2) \times D[mc^2(1-\mu^2)^{-\frac{1}{2}} - mc^2(1-\nu^2)^{-\frac{1}{2}} + \sum_{s\lambda}(m_{s\lambda}-n_{s\lambda})\hbar\omega_s] \, |F(\mathfrak{q})|^2 \times \prod_{s\lambda} |K(\sigma_{s\lambda}, m_{s\lambda}; \tau_{s\lambda}, n_{s\lambda})|^2, \quad (24)$$

where $D$ is Dirac's $\delta$-function.[13]

To simplify the discussion we shall from now on neglect the last (electromagnetic) terms in (23) and in the argument of $D$ in (24). We thus consider the changes in energy and momentum of the electromagnetic field to be small compared to the energy and the change in momentum of the electron, an assumption which is clearly justified for the treatment of the low frequencies.[14] Furthermore, we consider the state $\mathfrak{y}$, $m_{s\lambda}$ for which all $m_{s\lambda}=0$; this means that initially no free quanta are present. The probability per unit time for a transition in which $n_{s\lambda}$ quanta of the kind $s, \lambda$ are emitted and the electron after the transition moves in a direction within the element of solid angle $\sin\vartheta d\vartheta d\varphi$ is by (24) and (20)

$$U(\mathfrak{y}; \mathfrak{v}, n_{s\lambda}) \sin\vartheta d\vartheta d\varphi = (1/4\pi^2\hbar^4\Omega) \sin\vartheta d\vartheta d\varphi (m^2 v c/(1-v^2)) \times |F(\mathfrak{q})|^2 \prod_{s\lambda} |K(\sigma_{s\lambda}, 0; \tau_{s\lambda}, n_{s\lambda})|^2 \quad (25)$$

$$= (1/4\pi^2\hbar^4\Omega) \sin\vartheta d\vartheta d\varphi (m^2 v c/(1-v^2)) \, |F(\mathfrak{q})|^2 \times \prod_{s\lambda} \exp\{-\tfrac{1}{2}(\sigma_{s\lambda}-\tau_{s\lambda})^2\} \frac{[\frac{1}{2}(\sigma_{s\lambda}-\tau_{s\lambda})^2]^{n_{s\lambda}}}{n_{s\lambda}!}. \quad (26)$$

The result confirms what has been anticipated in the introduction, namely, that the probability of the emission of any finite number of quanta is zero. In order to show this, consider first the case in which no light quanta are emitted, i.e., where every $n_{s\lambda}=0$. We have then from (13) and (2)

$$\prod_{s\lambda} \exp\{-\tfrac{1}{2}(\sigma_{s\lambda}-\tau_{s\lambda})^2\} = \exp\left\{-(2\pi e^2/\hbar\Omega) \times \sum_{s\lambda} \omega_s^{-1} \left[\frac{(\mathfrak{y}, \mathfrak{e}_{s\lambda})}{k_s - (\mathfrak{y}, \mathbf{k}_s)} - \frac{(\mathfrak{v}, \mathfrak{e}_{s\lambda})}{k_s - (\mathfrak{v}, \mathbf{k}_s)}\right]^2\right\}. \quad (27)$$

The exponent becomes, after introducing the number of modes of vibration $\Omega/(2\pi)^3 \cdot d\mathbf{k}_s$ in the interval $d\mathbf{k}_s$ and carrying out the sum over $\lambda$,

$$-(e^2/4\pi^2\hbar c) \lim_{\omega_0\to 0} \int_{\omega_0}^{\omega_1} \frac{d\omega_s}{\omega_s} \int_0^{\pi} \sin\vartheta_s d\vartheta_s \int_0^{2\pi} d\varphi_s \times \left[\left(\frac{\mathfrak{y}}{1-\mu_s} - \frac{\mathfrak{v}}{1-\nu_s}\right)^2 - \left(\frac{\mu_s}{1-\mu_s} - \frac{\nu_s}{1-\nu_s}\right)^2\right], \quad (28)$$

where $\vartheta_s$, $\varphi_s$ are the polar angles of $\mathbf{k}_s$ and $\mu_s$, $\nu_s$ are the components of $\mathfrak{y}$, $\mathfrak{v}$ along $\mathbf{k}_s$ and where we have cut off the frequency spectrum at an upper limit $\omega_1$. The integration over the angles gives a finite positive factor; the integration over $\omega_s$, however, gives a result which is logarithmically infinite in the limit $\omega_0\to 0$. Hence (27) vanishes. If a finite number of the $n_{s\lambda}$ in (26) are different from zero, (26) differs from (27) in only a finite number of factors, thus remaining zero.

However, the total probability of a transition $\mathfrak{y}\to\mathfrak{v}$ of the electron independently of the number of quanta emitted, which is given by the sum of (26) over all values of every $n_{s\lambda}$, is just

$$(1/4\pi^2\hbar^4\Omega) \sin\vartheta d\vartheta d\varphi (m^2 v c/(1-v^2)) \, |F(\mathfrak{q})|^2, \quad (29)$$

which is the result which one would have obtained by neglecting entirely the interaction with the electromagnetic field. This result had physically to be expected since the change in momentum of the electromagnetic field has been neglected compared to that of the electron.

From the facts that the probability of the transition $\mathfrak{y}\to\mathfrak{v}$ accompanied by the emission of a finite number of light quanta is zero and that the total transition probability is finite, it follows that the mean total number of quanta emitted is infinite.

The mean radiated energy in the frequency interval $d\omega_s$ and in the angular range $d\vartheta_s$, $d\varphi_s$

[13] In the argument of the $\delta$-function there should stand, rigorously speaking, $E(\mathfrak{y}, m_{s\lambda}, 0) - E(\mathfrak{v}, n_{s\lambda}, 0)$ where the values of $E$ are given by (16). We have neglected the term $-(c/2h)\sum_{s\lambda}(\mathfrak{y}, a_{s\lambda})^2/(k_s-(\mathfrak{y}, \mathbf{k}_s))$ in (16), representing the kinetic electromagnetic self-energy of the electron, compared to the mass term $mc^2(1-\mu^2)^{-\frac{1}{2}}$. One may, in order to be consistent, imagine the frequency spectrum to be broken off at an upper limit $\omega_1$ such that $e^2\omega_1/mc^3 \ll 1$. Since we are here concerned with difficulties arising from the low frequencies, this procedure, although connected with the fundamental difficulties of electrodynamics, does not affect our conclusions.

[14] For the treatment of higher frequencies one may use an expansion in powers of $e^2/\hbar c$.

when the electron is deflected into the element of solid angle $\sin\vartheta d\vartheta d\varphi$ is given by

$$(\Omega/(2\pi c)^3)\omega_s^2 d\omega_s \sin\vartheta_s d\vartheta_s d\varphi_s \times \sum_\lambda \sum_{n_{s\lambda}=0}^{\infty} n_{s\lambda}\hbar\omega_s U \sin\vartheta d\vartheta d\varphi \quad (30)$$

$$= (1/4\pi^2\hbar^4\Omega)\sin\vartheta d\vartheta d\varphi (m^2 vc/(1-v^2))\,|F(\mathbf{q})|^2 \cdot (e^2/4\pi^2 c)\left[\left(\frac{\mathfrak{v}}{1-\mu_s}-\frac{\mathfrak{v}}{1-\nu_s}\right)^2 - \left(\frac{\mu_s}{1-\mu_s}-\frac{\nu_s}{1-\nu_s}\right)^2\right] d\omega_s \sin\vartheta_s d\vartheta_s d\varphi_s. \quad (31)$$

This has been obtained by making use of (26), (13) and (2) and of the formula

$$\sum_{n=0}^{\infty} n e^{-x} x^n/n! = x.$$

On account of the extra factor $\omega_s$ in (30), the mean total energy, unlike the mean total number of quanta, is finite. Formula (31) is just the total probability that the electron be scattered into the element of solid angle $\sin\vartheta d\vartheta d\varphi$ multiplied by the amount of energy which it would radiate classically in such a deflection. The expansion in powers of $e^2/hc$ in the limit of small frequencies, where alone Formula (31) may be supposed to be valid, leads to the same result for the mean energy radiated, though its results are entirely misleading so far as transition probabilities are concerned.[15]

The above considerations can be applied almost literally also to cases such as the theory of $\beta$-decay, in which the external perturbation does not act on the electron coordinates, but creates an electron. The only difference, so far as the electromagnetic field is concerned, consists in replacing $\mathfrak{v}c$ by the velocity of the nucleus and $vc$ by the velocity with which the electron is created. Here again the total probability of $\beta$-decay is unaltered by the interaction of the electron with the low frequency radiation and the mean radiated energy is in agreement with that calculated by expanding in powers of $e^2/hc$.

[15] This remark does not affect the cross section for the emission of a high frequency quantum as calculated by Bethe and Heitler, and experimentally verified. However, the cross section so derived has to be interpreted, not as the probability that the high frequency quantum alone be emitted, but as the probability that this happens no matter how many other light quanta are emitted.

JULY 15, 1937 PHYSICAL REVIEW VOLUME 52

# The Low Frequency Radiation of a Scattered Electron

A. NORDSIECK*
*Stanford University, California*

(Received May 24, 1937)

The radiative scattering of a nonrelativistic electron is treated by an approximate method which neglects the reaction of the radiation field on the motion of the electron. In this approximation the different modes of oscillation of the radiation field are independent of one another, and can therefore be treated individually. For frequencies of the radiation small compared to the inverse impact time of the electron, it is shown that the probability of emitting any finite number of quanta is zero, and that the mean radiated energy depends only on the total change in velocity of the electron, the amount of energy radiated being given by the same formula as in classical theory.

## 1. INTRODUCTION

IN a previous paper[1] Bloch and the author have treated the interaction of a relativistic electron and the radiation field by a method which consists essentially of an expansion in powers of the parameters $e^2\omega/mc^3$, $\hbar\omega/E$, $\hbar\omega/c\Delta p$ ($\omega$ = angular frequency of radiation; $E$ = kinetic energy, $\Delta p$ = change in momentum, of electron). Applications of the method to actual physical processes were made in an approximate way by regarding external influences on the electron, such as atomic

* National Research Fellow.
[1] F. Bloch and A. Nordsieck, Phys. Rev. **52**, 54 (1937); subsequently referred to as I.

fields or the interactions responsible for $\beta$-ray processes, as small perturbations. It was shown that, to the extent to which these approximations are legitimate, the classical prediction concerning the radiation emitted is valid in the mean, and the motion of the electron is unaffected by the radiation field.

In this paper the radiative scattering of a non-relativistic electron in a potential field $V(\mathbf{r})$ is considered from the same point of view, but without regarding $V(\mathbf{r})$ as a small perturbation. A treatment of this problem with no restrictions except that the above mentioned parameters shall be small is possible in principle but complicated and dependent on the detailed form of $V(\mathbf{r})$. Since all frequencies except the extremely low ones may be treated adequately by the ordinary expansion in powers of $e^2/\hbar c$, as was shown in I, we shall have offset the additional complication of treating the scattering field exactly by imposing a further restriction on the frequency.

We may again guide our considerations just as was done in I, by reference to the corresponding classical problem. If the potential energy of the electron at a distance $\mathbf{r}$ from the center of the scattering field is $V(\mathbf{r})$ and if $V(\mathbf{r})$ tends to zero faster than $1/r$ as $r\to\infty$, as we shall for simplicity assume throughout this paper, the classical orbit of the electron has the form $\mathbf{r}=\mathbf{r}(t)$ with

$$\begin{aligned}\mathbf{r}(t)&\sim\mathbf{v}t+\mathbf{a}; \quad t<-T/2,\\ &\sim\mathbf{w}t+\mathbf{b}; \quad t>T/2,\end{aligned}$$

where $\mathbf{v}$ and $\mathbf{w}$ are the initial and final velocities, $\mathbf{a}$ and $\mathbf{b}$ are constants and $T$ is the collision time. For $-T/2<t<T/2$, $\mathbf{r}(t)$ will be a more complicated function, which, however, does not affect the radiation of sufficiently low frequencies. The amount of energy radiated with angular frequency $\omega$ in a direction within the element of solid angle $d\Sigma$ is given by

$$(e^2/4\pi^2c^3)\,|\ddot{r}_{\perp,\,\omega}|^2 d\omega d\Sigma, \tag{1}$$

where $\ddot{r}_{\perp,\,\omega}$ is the Fourier component of the component of the acceleration perpendicular to the direction of propagation of the radiation:

$$\ddot{r}_{\perp,\,\omega}=\int_{-\infty}^{\infty}dt\ddot{r}_{\perp}(t)e^{-i\omega t}=-\omega^2\int_{-\infty}^{\infty}dtr_{\perp}(t)e^{-i\omega t}.$$

For frequencies such that $\omega T\ll 1$, this expression depends essentially only on the initial and final velocities $\mathbf{v}$ and $\mathbf{w}$, and may be evaluated without knowledge of the detailed motion of the electron during the collision:

$$\ddot{r}_{\perp,\,\omega}=(v_{\perp}-w_{\perp})(1+O(\omega T)).$$

Hence the amount of low frequency radiation is

$$(e^2/4\pi^2c^3)(v_{\perp}-w_{\perp})^2 d\omega d\Sigma. \tag{2}$$

The simplicity of this result depends physically on the fact that the deflection of the electron takes place suddenly with respect to the periods of the radiation considered, so that the simple methods of sudden impulse dynamics apply.

These considerations indicate that if in the quantum theoretical treatment of the problem we limit ourselves to frequencies small compared to the reciprocal of the impact time, we shall get a correspondingly simple treatment. In fact, when we neglect the additional parameters $\hbar\omega/E$ and $\hbar\omega/c\Delta p$, which are a measure of the effect of the quantum mechanical fluctuations of the radiation field on the electron, we may expect to get exactly the classical formula (2). The motion of the electron itself in the scattering field need not, of course, be describable in classical terms.

## 2. Radiative Scattering

We shall keep the notation of I except where further symbols are explicitly defined. The Hamilton function is

$$\mathcal{H}=(1/2m)(\mathbf{p}-(e/c)\mathbf{A})^2+V(\mathbf{r})+\tfrac{1}{2}\sum_{s\lambda}\hbar\omega_s(P_{s\lambda}^2+Q_{s\lambda}^2),$$

where

$$(e/c)\mathbf{A}=\sum_{s\lambda}\mathbf{a}_{s\lambda}[P_{s\lambda}\cos(\mathbf{k}_s,\mathbf{r})+Q_{s\lambda}\sin(\mathbf{k}_s,\mathbf{r})].$$

Let $\psi(\mathbf{r})$ describe the motion of the electron without interaction with the radiation:

$$\{p^2/2m+V(\mathbf{r})-\tfrac{1}{2}mv^2\}\psi(\mathbf{r})=0$$

and suppose $\psi$ to have the asymptotic form for large $r$ appropriate to a scattering experiment:

$$\psi(\mathbf{r})\sim\exp(im(\mathbf{v},\mathbf{r})/\hbar)+f(\theta,\varphi)/r\cdot\exp(imvr/\hbar). \tag{3}$$

If we now write for the solution $\Psi(\mathbf{r}, Q_{s\lambda})$ of the

equation $\{\mathcal{H}-E\}\Psi=0$,

$$\Psi(\mathbf{r}, Q_{s\lambda})=\psi(\mathbf{r})U(\mathbf{r}, Q_{s\lambda}) \tag{4}$$

we get for $U$ the equation

$$(\psi/2m)(\mathbf{p}-(e/c)\mathbf{A})^2U+(\mathbf{p}\psi/m)(\mathbf{p}-(e/c)\mathbf{A})U +(\psi/2)\sum_{s\lambda}\hbar\omega_s(P_{s\lambda}^2+Q_{s\lambda}^2)U -\psi(E-\tfrac{1}{2}mv^2)U=0. \tag{5}$$

The first term in this equation represents the reaction of the radiation on the electron; its order of magnitude relative to the remaining terms is given by the ratio of the mean recoil momentum to the momentum $mv$ of the electron. In accordance with our program we neglect this term. Such a procedure is quite analogous to what is done in the theory of molecules, where the reaction of the fluctuating motion of the electrons on the nuclei is similarly left out of account. The resulting equation is separable with respect to the various modes of vibration of the radiation field. Thus $U$ is approximately equal to $\prod_{s\lambda}u_{s\lambda}(\mathbf{r}, Q_{s\lambda})$, where

$$(\mathbf{p}\psi/m)(\mathbf{p}-\mathbf{a}_{s\lambda}[P_{s\lambda}\cos(\mathbf{k}_s, \mathbf{r}) +Q_{s\lambda}\sin(\mathbf{k}_s, \mathbf{r})])u_{s\lambda}+(\psi/2)\hbar\omega_s(P_{s\lambda}^2 +Q_{s\lambda}^2)u_{s\lambda}-\psi E_{s\lambda}u_{s\lambda}=0. \tag{6}$$

This approximate separability is an expression of the fact that the behaviors of different components of the radiation field, in particular any changes in the numbers of light quanta present in them, are almost independent. The coupling between different components exists only in virtue of the intermediary action of the electron and is therefore small whenever the reaction of the radiation on the electron is small.

We proceed to the solution of Eq. (6), which is to be carried out in the approximation $\omega\ll 1/T$. Let $R$ be the "radius" of the scattering field, or more precisely, the smallest radius for which $\psi(\mathbf{r})$ is well represented by (3). For $r>R$ we have then, dropping the subscripts $s$, $\lambda$ temporarily,

$$\exp(im(\mathbf{v}, \mathbf{r})/\hbar)\{(\mathbf{v}, \mathbf{p}-\mathbf{a}[P\cos(\mathbf{k}, \mathbf{r}) +Q\sin(\mathbf{k}, \mathbf{r})])+\tfrac{1}{2}\hbar\omega(P^2+Q^2)-E\}u +f(\vartheta, \varphi)/r\cdot\exp(imvr/\hbar)\{(\mathbf{w}, \mathbf{p}-\mathbf{a}[P\cos(\mathbf{k}, \mathbf{r}) +Q\sin(\mathbf{k}, \mathbf{r})]+\tfrac{1}{2}\hbar\omega(P^2+Q^2)-E\}\leqq 0, \tag{7}$$

where $\mathbf{w}$ is the final velocity of the electron, i.e., $\mathbf{w}$ has the magnitude of $\mathbf{v}$ and the direction of $\mathbf{r}$. In the derivation of (7) we have neglected terms of order $1/r^2$ coming from the differentiation of $f(\vartheta, \varphi)/r$.

The solution of (7) which we require is defined by the condition that the incident electron be accompanied by no free light quanta. Hence at $r=\infty$, $u$ must be the function appropriate to the motion of a free electron with velocity $\mathbf{v}$, accompanied only by its proper field. This function $u^{(0)}$ is a solution of $\{F-E\}u^{(0)}=0$, where $\{F-E\}$ is the first bracket in (7), and is, according to I,

$$u^{(0)}=\exp\{i\sigma\cos(\mathbf{k}, \mathbf{r})[Q-\tfrac{1}{2}\sigma \times\sin(\mathbf{k}, \mathbf{r})]\}\cdot h_0(Q-\sigma\sin(\mathbf{k}, \mathbf{r})), \tag{8}$$

$$E=\tfrac{1}{2}\hbar\omega$$

where $\sigma=(\mathbf{v}, \mathbf{a})/h(\omega-(\mathbf{v}, \mathbf{k}))$, and where we have neglected a term of order $v^2/c^2$ in $E$.

Now since the scattering of the electron occurs within a small fraction of a period of the radiation, we should expect the wave function of the field to remain unaltered by the scattering. Hence $u^{(0)}$ should be a solution of the complete Eq. (6) in our approximation. To show that this is true, we must prove first that $\{G-E\}u^{(0)}\sim 0$ where $\{G-E\}$ is the second bracket in (7); and second, that the values of $u^{(0)}$ at different points on the sphere $r=R$ join on to each other correctly according to Eq. (6).

That $u^{(0)}$ is an approximate solution of $\{G-E\}u^{(0)}=0$, and thus of the whole Eq. (7), is best shown by expanding $u^{(0)}$ in terms of the proper functions of $G$. We have according to I

$$u^{(0)}=\sum_{n=0}^{\infty}\alpha_n^{(0)}f_n(Q) \tag{9}$$

where

$$f_n(Q)=\exp\{i\tau\cos(\mathbf{k}, \mathbf{r})[Q-\tfrac{1}{2}\tau\sin(\mathbf{k}, \mathbf{r})]\} \cdot h_n(Q-\tau\sin(\mathbf{k}, \mathbf{r})),$$

$$\alpha_n^{(0)}=\exp\{-in(\mathbf{k}, \mathbf{r})\}\cdot K(\sigma, 0; \tau, n),$$

the quantity $K$ being given by formula (20) in I. Hence

$$\{G-E\}u^{(0)}=\sum_n\alpha_n^{(0)}n\hbar(\omega+(\mathbf{w}, \mathbf{k}))f_n(Q).$$

By an alteration of $u^{(0)}$ which is negligible for $\hbar\omega\ll mv^2$ we may bring $\{G-E\}u^{(0)}$ to vanish: we

need evidently only replace $\alpha_n^{(0)}$ by

$$\alpha_n^{(0)} \exp\{-in(\omega+(\mathbf{w},\mathbf{k}))r/v\}.$$

This involves an alteration of $u^{(0)}$ consisting of inserting factors of the kind $\exp\{-i(mvr/\hbar)\cdot(\hbar\omega/mv^2)\}$. On account of the smallness of $\hbar\omega/mv^2$, such factors vary much less rapidly with $\mathbf{r}$ than $\psi$, the wave function of the electron, and so may be replaced by unity.[2] To be consistent we also replace $\cos(\mathbf{k},\mathbf{r})$ by one and $\sin(\mathbf{k},\mathbf{r})$ by zero, since $k$, the wave number of the radiation, is likewise small compared to $mv/\hbar$. The solution of (7) is then

$$u^{(0)} \sim e^{i\sigma} q_0(Q). \tag{10}$$

It remains to be shown that the values of $u^{(0)}$ at various points on the surface of the sphere $r=R$ are correctly related to each other in virtue of Eq. (6). The argument by which this may be proved is essentially that used for the behavior of a quantum mechanical system under the influence of a sudden external perturbation.[3] Let us write Eq. (6) in the form

$$(\hbar/i)(\mathbf{v}(\mathbf{r}),\operatorname{grad})u = \{(\mathbf{v}(\mathbf{r}),\mathbf{a})P-\tfrac{1}{2}\hbar\omega(P^2+Q^2)+E\}u,$$

where $\mathbf{v}(\mathbf{r})=(\mathbf{p}\psi)/m\psi$. Integrating each side of this equation roughly from a point $\mathbf{r}_1$ on the sphere $r=R$ through the sphere to the point $\mathbf{r}_2$ on the sphere, we find

$$(\hbar R/T)(u(\mathbf{r}_2)-u(\mathbf{r}_1)) \sim \hbar\omega R\bar{u},$$

where $\bar{u}$ is a certain average value of $u$ in the region $r<R$. Hence

$$u(\mathbf{r}_2)-u(\mathbf{r}_1) \sim (\omega T)\bar{u} \sim 0.$$

Thus (10) is the solution of (6) for frequencies such that $\omega T \ll 1$, $\hbar\omega/mv^2 \ll 1$ and $\hbar\omega/mvc \ll 1$.

The whole wave function $\Psi$ may now be written down. For purposes of interpretation we use the expansion (9), which expresses the function $u^{(0)}$ appropriate to the initial motion $\mathbf{v}$ of the electron in terms of the functions $f_n(Q)$ appropriate to the final motion $\mathbf{w}$, in writing the coefficient of the scattered wave:

$$\Psi \sim \exp(im(\mathbf{v},\mathbf{r})/\hbar)\prod_{s\lambda} u_{s\lambda}^{(0)}(Q_{s\lambda}) + f(\vartheta,\varphi)/r\cdot\exp(imvr/\hbar)\prod_{s\lambda}\{\sum_{n_{s\lambda}} K(\sigma_{s\lambda},0;\tau_{s\lambda},n_{s\lambda}) f_{s\lambda,\,n_{s\lambda}}(Q_{s\lambda})\}. \tag{12}$$

From this it follows that the cross section for scattering with the emission of $n_{s\lambda}$ light quanta of the kind $s$, $\lambda$ is

$$|f(\vartheta,\varphi)|^2 \sin\vartheta d\vartheta d\varphi \prod_{s\lambda} |K(\sigma_{s\lambda},0;\tau_{s\lambda},n_{s\lambda})|^2. \tag{13}$$

For the interpretation of this fomula the reader is referred to I, where the equivalent formula (25) is discussed. In particular, it is easily to be seen by using the value of $K$ given in I, that the total probability of scattering of the electron irrespective of what radiation is emitted is just $|f(\vartheta,\varphi)|^2 \sin\vartheta d\vartheta d\varphi$; that the probability of emission of any finite number of quanta is zero; and that the mean number of quanta emitted with definite frequency and direction when the electron is deflected into the solid angle $\sin\vartheta d\vartheta d\varphi$ is

$$(e^2/4\pi^2c^3)(v_\perp - w_\perp)^2(d\omega_s/\hbar\omega_s)d\Sigma, \tag{14}$$

which corresponds exactly to the classical formula (2).

As was shown in I, the method of expanding in powers of the interaction between electron and radiation leads to the same result for the mean radiated energy. This may be understood on the basis that the various modes of vibration of the radiation field behave independently, as we have already mentioned in connection with Eq. (6). Because of this independence, the method of expanding in powers of $e^2/\hbar c$ gives correctly the probability that a definite amount of radiation be emitted in one mode irrespective of the behavior of all other modes. One may therefore calculate the mean radiated energy in each mode separately and then add them together, and this is just the procedure used in the method of expanding in powers of $e^2/\hbar c$.

The author is grateful to Professor J. R. Oppenheimer for very helpful discussions of the questions considered above.

[2] The rigorous justification for neglecting the variation of such factors lies in the possibility of forming a wave packet describing the motion of the electron, with dimensions so large that the energy of the electron is well defined and yet small compared to $(v/c)\lambda$, where $\lambda$ is the wavelength of the radiation. The factors concerned are approximate constants over the region occupied by such a wave packet. Our method is thus valid provided only that an electron with relative uncertainty in energy $\delta(mv^2)/mv^2 \sim \hbar\omega/mv^2$ is scattered in sensibly the same way as one of definite energy.

[3] See e.g. W. Pauli, *Handbuch der Physik*, Vol. 24, pp. 163–4.

# The Absorption of High Energy Electrons, Part I

J. J. Turin and H. R. Crane
*University of Michigan, Ann Arbor, Michigan*

(Received May 21, 1937)

The recoil electrons produced by the 6 Mev gamma-radiation from fluorine bombarded with protons were allowed to pass through 5 mm carbon and 0.5 mm lead absorbers placed across the center of a cloud chamber. The curvatures of the incident and emergent tracks in the magnetic field were measured, the difference giving the loss in passing through the absorber. The losses in carbon are in good agreement with the theoretical losses due to electron collisions alone, and this is satisfactory, since practically no radiative losses are expected in a substance of such low atomic number. In the case of lead, the data show clearly that radiative losses play a large part, and increase with increasing energy of incident particle. The losses in lead are slightly greater than those predicted by theory.

## Introduction

THE abundant gamma-radiation emitted when fluorine is bombarded with protons[1] can be used conveniently to produce recoil electrons with energies extending up to approximately 6 Mev. We have made a study of the energy loss of these particles in passing through carbon and lead absorbers. The results which we propose to report constitute the first data which have been obtained in the region between 3 and 6 Mev, although several authors have reported upon experiments performed with electrons in the region of energy available with natural radioactive substances.

Skobeltzyn and Stepanowa,[2] using the beta-rays from radium in an expansion chamber reported that the stopping of these particles in air took place much too frequently to be accounted for by the present radiation theory. They observed that about 100 times as many particles suffered sudden large losses of energy as theoretically predicted, and they were led to conclude that there must be some other totally independent process by which beta-rays lose energy. Leprince-Ringuet,[3] using the gamma-rays from radio-thorium and its products to produce recoil electrons, studied their passage through thin foils of lead and various gases by means of a cloud chamber. He also came to the conclusion that the average energy loss observed was much too large to be explained on the basis of the present theory. He observed from 5 to 10 times as much energy loss supposedly due to radiation as predicted by theory. Klarmann and Bothe,[4] studied the passage of recoil electrons from the gamma-rays of thorium C″ through xenon and krypton. They observed tracks in the expansion chamber which suffered a sudden deviation and energy loss without the presence of another ionizing particle visibly connected with the process. They assumed that these processes were radiative collisions of the electrons with the nuclei of the atoms in the gas. Their conclusion was that the number of large energy losses observed for the total length of track measured in both xenon and krypton was about 3.5 times as great as that predicted by theory. They also expressed the opinion that there must exist a process by which an electron can lose energy which is not included in the quantum theory of radiation. As a result of observations of cosmic-ray particles in a cloud chamber Anderson and Neddermeyer[5] gave a value for the average energy loss of electrons which seemed to indicate that there was no appreciable departure from the theory at extremely high energies.

Thus for electrons of energies of the order of 2 Mev we are confronted with a radiative loss which seems to be too large, while in the region of cosmic-ray energies the observed radiative loss is in agreement with theory. The suggestion has been made that because the contribution which radiation makes to the total energy loss is small

[1] Crane, Delsasso, Fowler and Lauritsen, Phys. Rev. **46**, 531 (1934); Delsasso, Fowler and Lauritsen, Phys. Rev. **51**, 527 (1937).
[2] Skobeltzyn and Stepanowa, Nature **137**, 234 (1935).
[3] Leprince-Ringuet, Comptes rendus **201**, 712 (1935); Ann. de physique **11**, 5 (1937).
[4] Klarmann and Bothe, Zeits. f. Physik **101**, 489 (1936).
[5] Anderson and Neddermeyer, Phys. Rev. **50**, 263 (1936).

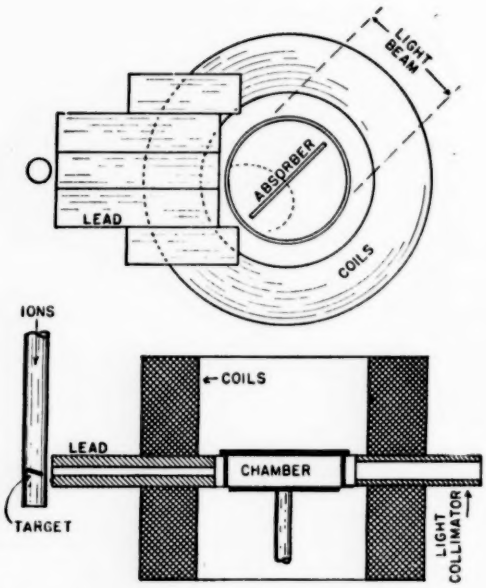


FIG. 1. Experimental arrangement of cloud chamber and gamma-ray collimator.

at energies of 2 Mev and less, the errors in the values obtained for the radiative loss may be quite large. The advantage of the experiments to be reported in this paper over the previous ones is that in the neighborhood of 6 Mev the energy loss in lead due to radiation is comparable to that due to mechanical collisions. A more accurate test of the theory should therefore be possible.

## EXPERIMENTAL ARRANGEMENT

The cloud chamber employed (see Fig. 1) was 15 cm in diameter and 4 cm deep, filled with air and ethyl alcohol vapor at atmospheric pressure. It was equipped with an air core solenoid arranged so as to bend the electron tracks in the plane of the chamber. A collimated beam of parallel light from a carbon arc illuminated a portion of the chamber 1.5 cm in depth, located centrally between the top and bottom. The gamma-rays from the fluorine target were collimated into a beam the same height as the light beam, by means of a lead channel 5 cm wide and 1.5 cm in height. The absorber was placed across the center of the chamber in such a position that most of the recoil electrons ejected from the wall of the chamber were incident normally upon the absorber. By measuring the radii of curvature of the incident and emergent tracks both the primary energy and the energy loss of each electron which passed through the absorber was determined.

## RESULTS

A total of 448 measurable tracks were observed which passed through 5 mm carbon and 0.5 mm lead absorbers. The energies of the incident particles ranged from 2 to 6 Mev, and the data for each absorber were separated into two groups according to incident energy, 2 to 4 Mev and 4 to 6 Mev. Plots of the change in energy against the number of electrons for the two absorbers and the two energy groups are shown in Figs. 2, 3 and 4. The average energy loss, calculated by using the points themselves, rather than the smooth curve, and the most probable energy loss, which is indicated by the highest point of the curve, are given for each of the four groups in Table I.

## DISCUSSION OF POSSIBLE ERRORS

### Measurement of tracks

Because the absorber was placed at the center of the chamber there was a maximum of 7 cm from the absorber to the side wall of the chamber. This placed a limit upon the length of visible track on each side of the absorber. A length of at least 5 cm of sharp and distinct track on each side

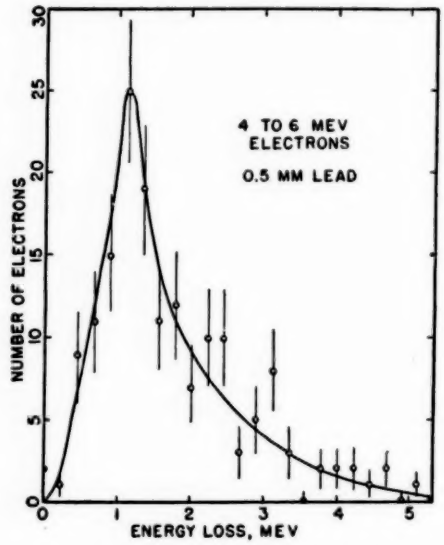


FIG. 2. Energy losses plotted against the number of electrons, for 5 mm carbon and primary energies 4 to 6 Mev.

of the absorber, extending to within ½ cm of the absorber was required before a track was accepted for measurement. A track was not used if other tracks appeared on the picture in such a way as to provide any doubt as to the association of the incident and emergent parts of the track. In addition only those tracks which made angles of less than 15° with the normal to the absorber on the incident side were used. No restriction was made as to angle in the horizontal plane of the emergent tracks. The angle in the vertical plane was, however, limited to approximately 15 degrees on either side of the horizontal direction, because of the requirement that at least 5 cm length of track be included in the light beam.

The strength of the magnetic field was always so chosen that it was never necessary to measure tracks with radii of curvature greater than 15 cm, regardless of the energy in question. The curvatures were measured to half-centimeter intervals by matching the tracks in the full size reprojected image to circles drawn on a celluloid card. Very few tracks showed visible departure from circularity due to scattering in the gas, and it is believed that in the region of energy dealt with here the errors due to this cause are quite small.

Taking into account all the sources of error discussed above a fair estimate for the average error in the determination of the energies of individual

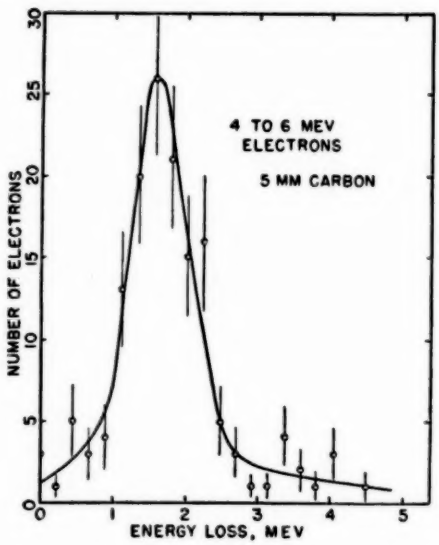


FIG. 3. Energy losses plotted against the number of electrons, for 0.5 mm lead and primary energies 4 to 6 Mev.

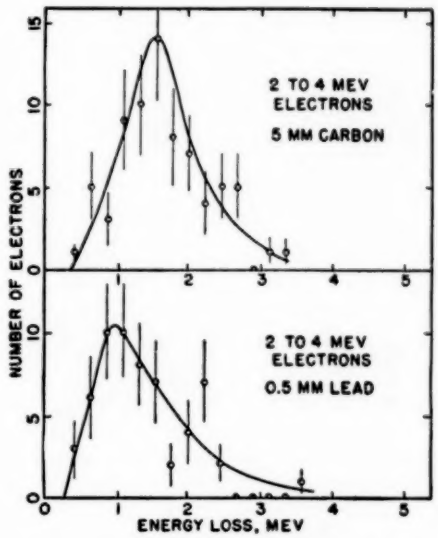


FIG. 4. Energy losses plotted against the number of electrons, for 5 mm carbon and 0.5 mm lead absorbers, primary energies 2 to 4 Mev.

electrons seems to be 0.3 Mev. Since the determination of energy loss depends upon the difference between two measured energies, the average error in these values is expected to be somewhat larger. However, in combining all the data to obtain the values for average energy loss given in the table, the errors in the individual measurements of the tracks balance out to a great extent, so that the error in the values in the table due to measurement is almost certainly less than 0.1 Mev.

### Tracks which end at the absorber

Tracks which are incident upon the absorber but do not appear to emerge from the absorber at all are not included in the data. Cases of this kind are numerous enough to change the value of the average energy loss considerably, if included. The exclusion of this class of tracks from the data can, however, be justified. Unless the present radiation theory is seriously wrong, the energy

TABLE I.

| ABSORBER | INCIDENT ENERGY | AVERAGE LOSS | MOST PROBABLE LOSS |
|---|---|---|---|
| 5 mm carbon | 2 to 4 Mev | 1.70 Mev | 1.5 Mev |
| 5 mm carbon | 4 to 6 Mev | 1.73 Mev | 1.6 Mev |
| 0.5 mm lead | 2 to 4 Mev | 1.41 Mev | 0.9 Mev |
| 0.5 mm lead | 4 to 6 Mev | 1.73 Mev | 1.2 Mev |

loss curves do not rise abruptly at the extreme right sides of the diagrams in Figs. 2, 3 and 4, but continue to fall; i.e., the number of electrons which lose almost their entire energy by means of radiation and electron collisions is relatively small. Our faith in the correctness of this general shape of theoretical energy loss curve is strengthened by the fact that the present data are in agreement with it over the region of low and moderate energy losses. We therefore prefer at present to attribute the apparent complete stopping of this considerable number of electrons to some other cause, such as scattering out of the field of vision or to a separate mechanism by which an electron may be stopped catastrophically. The number of electrons which are expected actually to lose their entire energy by known processes in a length of path equal to the thickness of the absorber used can be estimated and should be applied as a correction to the data obtained. Both from the trend of our experimental curves and from the shapes of the accepted theoretical energy loss curves, the number of such cases should be small and would not be expected to raise the values for the average energy losses by more than a few percent.

**Length of path in the absorber**

If appreciable scattering occurs along the path of the particle inside of the absorber the real length of path traversed will be greater than the thickness of the absorber. Theory predicts that scattering by nuclei is proportional to the atomic number squared, and is therefore very much smaller in carbon than in lead. Actually the electrons emerging from the carbon absorber were found to be well concentrated in the forward direction, with few large deviations apparent. For this reason the thickness of the carbon (5 mm) represents quite closely the actual length of path of the electrons traversing it. In lead, however, the scattering is large. About 50 percent of the emerging electrons were observed to lie within $\pm 30°$ of the forward direction in the horizontal plane, and within $\pm 15°$ of the forward direction in the vertical plane. In consideration of this, we estimate that the real average length of path in the lead may be as large as 1.5 times the thickness of the lead.

**Scattering which accompanies energy loss**

If a large change in direction of an electron takes place in the same event in which it loses a large amount of its energy, this will tend to introduce an angular dependence upon energy loss for the emerging particles. This must be considered in the case of the lead absorber. Head-on electron-electron collisions in which large loss and large deflection occur simultaneously are known both from experiment and from theory to be too rare to influence the present results. In the process of radiation large losses are, on the average, accompanied by large deflections, although there is no exact correspondence for the individual case between loss and deflection. However, because of the circumstance that the electron pursues a tortuous path through the lead absorber, due to multiple nuclear scattering, any correspondence between energy loss and angle of emergence will be largely obliterated. Therefore the sample of electrons which emerges within the solid angle visible in the present experiment may be expected to give a fair representation of the average energy loss by all the particles.

## Discussion

The curves obtained for the energy loss in carbon are in excellent agreement with the theoretical predictions, both as to shape and as to the value of the average energy loss, on the assumption that the loss by radiation is very small compared to the loss by electron collisions. The widths of the curves for carbon are not too great to be attributed mainly to the errors in the measurements of the individual tracks, and it is therefore not feasible to estimate the amount of real straggling which accompanies the energy loss. The curves for lead definitely show a large amount of straggling, which indicates that large losses of energy occur in single events in the absorber. On the basis of present theoretical knowledge these large losses can only be attributed to radiation. The values for the average losses contributed by radiation alone are found to be 0.38 and 0.64 Mev for 2–4 and 4–6 Mev electrons, respectively. In consideration of scattering effects, we have used in this calculation 0.75 mm as the effective thickness of the lead. Using Bethe and Heitler's formulae for radiative loss, we find

values of 0.28 and 0.57 Mev, for the two energy ranges. All the possible sources of error pointed out in the foregoing discussion, however, are in the direction of tending to favor the electrons which have lost the least energy. Therefore it is probable that the real values are somewhat higher than our experimental values, which would make them differ still more from the theoretical values. On the other hand, it has been pointed out to us by Professor H. A. Bethe that the use of the Born approximation for lead may give theoretical values which are as much as 30 percent too low. We believe that the largest uncertainty in our experiment lies in the estimation of the average length of path of the electrons in the absorber. We have had valuable discussions on this point with Dr. M. E. Rose of Cornell University, who is making some calculations[6] on the path length-thickness ratio in this energy region. Dr. Rose suggested that the ratio which would be necessary to bring our results into agreement with theory might be well within the calculated limits.

The large discrepancy between the results reported here and those of Skobeltzyn and Stepanowa, Leprince-Ringuet and of Klarmann and Bothe should not be considered as a direct contradiction, because the methods used are by no means the same. The most important difference in the various experiments lies in the treatment of those electrons which appear to lose their entire energy in the absorbing material. We have excluded tracks of this class on the assumption that the great majority of them do not represent actual energy loss, but scattering out of the field of vision or stopping by a separate process. At the same time, we do not wish to lose sight of the possibility that the theory may be quite wrong in the region in which the electron loses nearly its entire energy in a single event, and that these cases should rightfully be included in the data. If so, the value for the average energy loss will be much higher. There remains also the possibility, as suggested by several authors, that this complete stopping may be a new process which is separate from radiative stopping in the ordinary sense.

Investigations similar to these are now under way on the absorption of the beta-rays from $Li^8$, which will extend the data up to about 11 Mev. These results will follow shortly in a separate publication.

The authors wish to express their gratitude to the Horace H. Rackham Endowment Fund for the support of this work.

[6] M. E. Rose, Abstract, Washington Meeting, 1937.

JULY 15, 1937 PHYSICAL REVIEW VOLUME 52

# Absorption Coefficients for Thermal Neutrons

C. T. ZAHN
*Department of Physics, University of Michigan, Ann Arbor, Michigan*
(Received April 7, 1937)

A discussion is given of several integrals arising in the interpretation of experiments on the absorption of thermal neutrons in a $1/V$ absorber. In order to evaluate these integrals they have been expressed in the form of convenient series. There is also given a table of numerical values, which should be useful in the interpretation of experimental data on slow neutron absorption.

IN studying the absorption of slow (thermal) neutrons one has in general to deal with neutrons having a given angular distribution and approximately a Maxwellian energy distribution, and with absorbers whose coefficient of absorption is a function of the relative energy of the neutrons with respect to the individual absorbing nuclei. If the scattering cross section is of importance, as in the case of neutron-proton collisions, the general problem (of the absorption and back-scattering of the a layer of absorber-scatterer) is complicated by the scattering; but if the scattering cross section is negligible in comparison with the absorption cross section, then the neutrons may be considered as moving in straight lines without deviation until they are

finally absorbed. The latter condition is apparently very nearly valid[1] for the capture of neutrons by the heavier nuclei. If the absolute value of the resonance energy for neutron capture is large compared to the average thermal energy, the absorption coefficient may be regarded as inversely proportional to the square root of the relative energy ($1/V$ absorption); but if, as in the case of cadmium, the thermal and resonance regions overlap appreciably, one must consider the general form of the Breit-Wigner formula for neutron capture. Presumably most cases of neutron capture fall in the class of $1/V$ absorption.

As is well known, in the case of $1/V$ absorption the average absorption cross section for neutrons is quite independent of the angular and energy distributions of the absorbing nuclei, and therefore independent of the temperature of the absorber,—and in fact equal to the value obtained by regarding the absorbing nuclei at rest relative to their center of gravity and replacing the relative velocity in the $1/V$ formula by the actual velocity of the neutrons relative to the absorber as a whole.

Several types of absorption problem have arisen in the interpretation of experimental data on slow neutrons:

I. Absorption of a parallel beam of neutrons from a Maxwellian distribution, in a $1/V$ absorber.[2]

II. Absorption of the same beam by a layer of $1/V$ absorber, and subsequent detection by a $1/V$ detector.[3]

III. Absorption of neutrons having an isotropic angular distribution and a Maxwelliam energy distribution.[4]

IV. Absorption of neutrons emerging from the surface of a scatterer such as paraffin or water.[5]

V. Detection of the latter beam by a $1/V$ detector.

In the interpretation of data obtained in connection with the above types of experiment there have appeared in the literature two definite integrals,[2, 3] which apparently cannot be expressed in closed form, and which have been evaluated presumably by numerical integration. It is proposed here to show that these integrals, together with some other useful related integrals, can be expressed in terms of a single integral, which in turn can be evaluated by means of a convenient series,—and to give for the various integrals a table of values, which it is hoped may be found useful in the interpretation of absorption data.

## Case I

### Parallel beam with Maxwellian distribution

The energy distribution may be expressed as $ye^{-y}dy$, where $y$ is the energy measured in units of $kT$, and $T$ is the "temperature" of the beam. (This distribution gives the relative numbers of neutrons arising from a Maxwellian distribution and falling on a given area per second, in contradistinction to the ordinary Maxwellian distribution for the number in a given volume.) If the absorption coefficient of the $1/V$ absorber is given by $K=A/E^{\frac{1}{2}}=A/(kTy)^{\frac{1}{2}}$, and the thickness of the absorbing layer is $t$, then the fraction of neutrons transmitted is given by:

$$\varphi_1=\int_0^\infty ye^{-y}e^{-At/(kTy)^{\frac{1}{2}}}dy\equiv\int_0^\infty ye^{-y-x/y^{\frac{1}{2}}}dy$$

(where $x\equiv At/(kT)^{\frac{1}{2}}$).

## Case II

If the latter neutrons are detected by a *thin* layer of a $1/V$ detector, the observed activity will be proportional to:

$$\varphi_{\frac{1}{2}}=\int_0^\infty y^{\frac{1}{2}}e^{-y-x/y^{\frac{1}{2}}}dy.$$

## Case III

### Neutrons with an isotropic angular distribution and a Maxwellian energy distribution

For an isotropic angular distribution of neutrons of temperature $T$ the fraction trans

[1] Cf. G. Breit and E. Wigner, Phys. Rev. **49**, 519 (1936).
[2] D. P. Mitchell, J. R. Dunning, E. Segrè, and G. B. Pegram, Phys. Rev. **48**, 774 (1935); D. P. Mitchell, Phys. Rev. **49**, 453 (1936).
[3] H. H. Goldsmith and F. Rasetti, Phys. Rev. **50**, 328 (1936).
[4] E. Amaldi and E. Fermi, Ricerca Scient. II, VII, I, 3 (1936); E. Segrè, Ricerca Scient. II, VII, I, 9–10 (1936); D. S. Bayley, B. R. Curtis, E. R. Gaerttner, and S. Goudsmit, Phys. Rev. **50**, 570 (1936); C. T. Zahn, E. L. Harrington, and S. Goudsmit, Phys. Rev. **50**, 570 (1936).
[5] E. Fermi, Ricerca Scient. II, VII, II, 3 (1936).

mitted through a foil is given by:

$$\varphi_0=\int_{y=0}^{\infty}\int_{\theta=0}^{\pi/2} ye^{-y-x/y^{\frac{1}{2}}\cos\theta}2\sin\theta\cos\theta dyd\theta.$$

By means of the transformation $z=y\cos^2\theta$ it can be shown that:

$$\varphi_0=\int_0^{\infty} e^{-y-x/y^{\frac{1}{2}}}dy.$$

Hence it is seen that all three of the above integrals belong to the class:

$$\varphi_n\equiv\int_0^{\infty} y^n e^{-y-x/y^{\frac{1}{2}}}dy.$$

(The effect of changing from a parallel beam to an isotropic distribution is simply to reduce the exponent $n$ from 1 to 0.)

In order to evaluate these integrals in series it is convenient first to evaluate $\varphi_0$, and then to derive the others from $\varphi_0$ by integration. Integrating by parts it is easily seen that:

$$\varphi_n=n\varphi_{n-1}+\tfrac{1}{2}x\varphi_{n-1\frac{1}{2}}$$

and since $d^m\varphi_n/dx^m=(-1)^m\varphi_{n-\frac{1}{2}m}$, it follows that $\varphi_0$ must satisfy the differential equation:

$$d^3\varphi_0/dx^3=-2\varphi_0/x.$$

The latter equation can be solved in the form:

$$\varphi_0=\sum_{n=0}^{\infty}(a_n\log x+b_n)x^n,$$

where $$a_n=\frac{-2a_{n-2}}{n(n-1)(n-2)};$$

$$b_n=\frac{-2b_{n-2}-(3n^2-6n+2)a_{n-2}}{n(n-1)(n-2)}$$

$$a_0=a_1=0\quad(a_2=-b_0)$$

and $b_0$, $b_1$, and $b_2$ are taken as the three necessary arbitrary constants. The boundary conditions give immediately that $b_0=1$ and $b_1=-\pi^{\frac{1}{2}}$ (by direct integration of the expressions for $\varphi_0$ and $d\varphi_0/dx$ after setting $x=0$). The evaluation of $b_2$ requires special consideration, which for the sake of brevity is not included here. It may be shown that $b_2=\frac{3}{2}(1-C)$, where $C$ is Euler's constant. This value of $b_2$ was checked by numerical integration, for $x=1$, of the expression

$$\varphi_0=\int_0^1 e^{-x/\log^{\frac{1}{2}}(1/z)}dz.$$

In this way one obtains:

$$\varphi_0=1-\pi^{\frac{1}{2}}x+0.6342x^2+0.5908x^3-0.1431x^4$$
$$-0.01968x^5+0.00324x^6+0.000188x^7\cdots$$
$$-x^2\log x(1-0.08333x^2+0.001389x^4$$
$$-0.0000083x^6\cdots)$$

and by direct integration and appropriate choice of integration constants:

$$\varphi_{\frac{1}{2}}=\frac{\pi^{\frac{1}{2}}}{2}-x+\frac{\pi^{\frac{1}{2}}}{2}x^2-0.3225x^3-0.1477x^4$$
$$+0.03195x^5+0.00328x^6$$
$$-0.000491x^7-0.0000235x^8\cdots$$
$$+x^3\log x(\tfrac{1}{3}-0.01667x^2+0.000198x^4\cdots)$$

and

$$\varphi_1=1-\frac{\pi^{\frac{1}{2}}}{2}x+\frac{x^2}{2}-0.2954x^3+0.1014x^4$$
$$+0.02954x^5-0.00578x^6$$
$$-0.00047x^7+0.000064x^8\cdots$$
$$-x^4\log x(0.0833-0.00278x^2+0.000025x^4\cdots).$$

## Case IV

The case of neutrons emerging from the surface of a block of paraffin requires special consideration. For the angular distribution of such neutrons Fermi[5] has given the approximate expression

$$\frac{2\sqrt{3}}{2+\sqrt{3}}(\cos\theta+\sqrt{3}\cos^2\theta)\sin\theta d\theta.$$

If these neutrons also may be assumed to have approximately a Maxwellian energy distribution, the transmission coefficient for a layer of $1/V$ absorber is given by:

$$\psi=\frac{2\sqrt{3}}{2+\sqrt{3}}\int_{y=0}^{\infty}\int_{\theta=0}^{\pi/2} ye^{-y-x/y^{\frac{1}{2}}\cos\theta}$$
$$\times(\cos\theta+\sqrt{3}\cos^2\theta)\sin\theta dyd\theta,$$

TABLE I. *Values of five integrals* $\varphi_0$, $2/\pi^{\frac{1}{2}}\varphi_{\frac{1}{2}}$, $\varphi_1$, $x$, *and* $-\psi'/1.5350$ *normalized to unity for* $x=0$.

| $x$ | $\varphi_0$ | $2\varphi_{\frac{1}{2}}/\pi^{\frac{1}{2}}$ | $\varphi_1$ | $\psi$ | $-\psi'/1.5350$ |
|---|---|---|---|---|---|
| 0.00 | 1.0000 | 1.0000 | 1.0000 | 1.0000 | 1.0000 |
| .01 | .9829 | .9888 | .9912 | .9850 | .9612 |
| .02 | .9664 | .9778 | .9825 | .9705 | .9314 |
| .03 | .9506 | .9670 | .9739 | .9564 | .9050 |
| .04 | .9353 | .9564 | .9653 | .9427 | .8810 |
| .05 | .9205 | .9459 | .9569 | .9293 | .8536 |
| .1 | .8527 | .8959 | .9161 | .8671 | .7652 |
| .2 | .7395 | .8063 | .8408 | .7608 | .6282 |
| .3 | .6476 | .7282 | .7729 | .6724 | .5283 |
| .4 | .5711 | .6611 | .7114 | .5975 | .4507 |
| .5 | .5063 | .5989 | .6557 | .5333 | .3867 |
| .6 | .4510 | .5497 | .6051 | .4768 | .3372 |
| .7 | .4031 | .4968 | .5586 | .4289 | .2947 |
| .8 | .3615 | .4538 | .5169 | .3874 | .2588 |
| .9 | .3252 | .4153 | .4784 | .3508 | .2281 |
| 1.0 | .2932 | .3802 | .4431 | .3166 | .2018 |

the first part of which is proportional to $\varphi_0$; and the second part to

$$\eta=\int_{y=0}^{\infty}\int_{\theta=0}^{\pi/2} ye^{-y-x/y^{\frac{1}{2}}\cos\theta}\cos^2\theta\sin\theta dyd\theta$$

$$\equiv x^3\int_x^{\infty}\frac{\varphi_1(z)}{z^4}dz\equiv x^3\left(B-\int^x\frac{\varphi_1(z)}{z^4}dz\right).$$

It may be shown that $B$, the value of the upper limit of the latter auxiliary integral, is equal to:

$$\frac{\pi^{\frac{1}{2}}}{6}\left(\frac{9C-11}{6}+\log 2\right)\equiv -0.08078.$$

It then follows that

$$\eta=\frac{1}{3}-\frac{\pi^{\frac{1}{2}}}{4}x+\frac{x^2}{2}-0.08078x^3-0.1847x^4$$
$$-0.01477x^5+0.002236x^6-0.000118x^7$$
$$-0.0000138x^8\cdots+x^3\log x(0.2954+0.0833x$$
$$-0.000927x^3+0.000005x^5\cdots)$$

and

$$\psi=\frac{1}{2+\sqrt{3}}(\sqrt{3}\varphi_0+6\eta)\equiv 1-1.5350x$$
$$+1.0982x^2+0.1443x^3-0.3634x^4-0.03288x^5$$
$$-0.005098x^6+0.00277x^7-0.000022x^8\cdots$$
$$-x^2\log x(0.4641-0.4749x-0.1726x^2$$
$$+0.002135x^4-0.0000119x^6\cdots).$$

## CASE V

If the latter neutrons are detected by a thin foil of a $1/V$ absorber, the activity will be proportional to $-d\psi/dx\equiv-\psi'$. Then

$$-\psi'/1.5350=1-1.1285x-0.5915x^2$$
$$+0.8344x^3+0.1071x^4-0.01853x^5-0.001263x^6$$
$$+0.0001079x^7\cdots+x\log x(0.6047-0.9282x$$
$$-0.4497x^2+0.008345x^4-0.0000620x^6\cdots).$$

In Table I are given some values of the five integrals $\varphi_0$, $2\varphi_{\frac{1}{2}}/\pi^{\frac{1}{2}}$, $\varphi_1$, $\psi$, and $-\psi'/1.5350$, all normalized so as to have the value unity for $x=0$.

It may be noted that all of these integrals are functions only of $x$. Hence $x$ plays the role of a characteristic absorption function. $x=At/(kT)^{\frac{1}{2}}$, where $A$ is the constant in the expression for the absorption coefficient for homogeneous neutrons of relative energy $E$, and $t$ is the thickness of the absorber. $A/(kT)^{\frac{1}{2}}$ is then the value of $K$ for $E=kT$ (that is, for an energy equal to the most probable energy, or to one-half the average energy of the incident neutrons). It is of interest to calculate the apparent absorption exponent, $K't$, for $\varphi_0$, defined by:

$$\varphi_0(x)\equiv e^{-K't}\quad\text{or}\quad K't=-\log\varphi_0(x).$$

TABLE II. *Values of the fraction* $p$ *for the five functions of Table I.*

| $x$ | $\left(\frac{x}{\log\varphi_0}\right)^2$ | $\left(\frac{x}{\log(2\varphi_{\frac{1}{2}}/\pi^{\frac{1}{2}})}\right)^2$ | $\left(\frac{x}{\log\varphi_1}\right)^2$ | $\left(\frac{x}{\log\psi}\right)^2$ | $\left(\frac{x}{\log(-x'/1.5350)}\right)^2$ |
|---|---|---|---|---|---|
| 0.00 | 0.318 | 0.785 | 1.273 | 0.425 | 0.000 |
| .01 | .336 | .786 | 1.277 | .437 | .064 |
| .03 | .350 | .799 | 1.286 | .453 | .090 |
| .05 | .364 | .808 | 1.286 | .465 | .100 |
| .1 | .394 | .826 | 1.303 | .492 | .140 |
| .3 | .476 | .892 | 1.355 | .571 | .221 |
| .5 | .540 | .950 | 1.403 | .632 | .277 |
| .7 | .594 | 1.001 | 1.446 | .684 | .328 |
| .9 | .642 | 1.049 | 1.490 | .737 | .371 |
| 1.0 | .664 | 1.069 | 1.510 | .755 | .391 |

One may then calculate the fraction $y=p$ of the energy $kT$ to which this value of $K't$ corresponds:

$$p=(x/\log \varphi_0)^2.$$

In Table II are given some values of the fraction $p$ for the five different functions, and in Fig. 1 are shown the graphs of the functions given in Table I, together with the exponential function $e^{-x}$, for the purpose of comparison. The graphs show, for example, that the functions $e^{-x}$ and $2\varphi_{\frac{1}{2}}/\pi^{\frac{1}{2}}$ lie close to each other and actually coincide for a value of $x$ around 0.6, or for about 45 percent absorption.[3] In the range from 45 percent to 55 percent absorption the latter functions practically coincide.

For thin absorbers one may obtain an idea of the importance of the present considerations by comparing the slopes of the various curves of Fig. 1 for $x=0$. The general behavior of the various functions is the same for all except $-\psi'/1.5350$, which has an infinite slope for $x=0$. This is due to the presence of a term as low as $x \log x$ in the logarithmic part of the expansion for this function. The function $\varphi_{-\frac{1}{2}}$ would show a similar behavior. For these cases the apparent absorption for a thin absorber would not be proportional to the thickness of the absorber.

The expansions given here for the functions $\varphi_n(x)$ are sufficient for the determination of fairly accurate values in the interval $0<x<1$. By adding a few terms to the series it would be easy to extend Table I for values of the argument

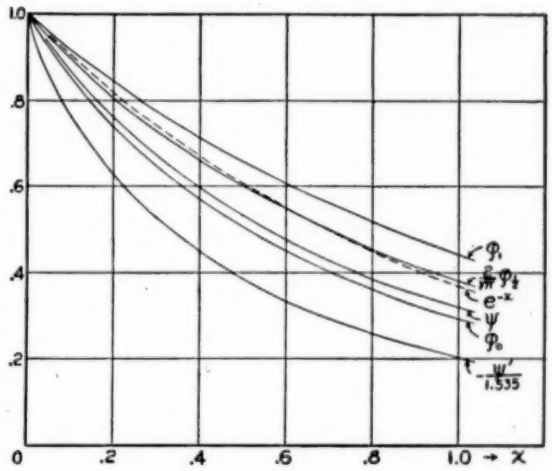


FIG. 1. Graphs of the functions given in Table I. Dashed curve is $e^{-x}$.

considerably greater than unity, since the coefficients $a_n$ and $b_n$ themselves converge fairly rapidly. For large values of $x$, Professor O. Laporte has derived asymptotic expansions. (See a note immediately following.) The two sets of expansions will give the general behavior of the functions in the entire interval $0<x<\infty$.

In conclusion the author wishes to acknowledge his indebtedness to Mr. D. S. Bayley for assistance in the evaluation of the above integrals, and to Mr. W. C. Parkinson for checking the numerical values given here; and finally to acknowledge support from the Horace H. Rackham School of Graduate Studies of the University of Michigan.

# Absorption Coefficients for Thermal Neutrons

## Remarks on the Preceding Paper of C. T. Zahn

OTTO LAPORTE
*University of Michigan, Ann Arbor, Michigan*
(Received April 7, 1937)

The integrals for which developments for small values of the argument were given in the preceding paper, are discussed for larger values of the independent variable. Asymptotic series are derived whose main term is of the form $\exp[3(x/2)^{\frac{1}{3}}]$.

IN the preceding paper Dr. C. T. Zahn showed that several types of absorption coefficients for slow neutrons are reducible to functions defined by the following integral:

$$\varphi_n(x)=\int_0^\infty y^n \exp[-(y+x/y^{\frac{1}{3}})]dy. \quad (1)$$

These functions were shown to be solutions of a third-order linear differential equation and convergent expansions were obtained for small values of $x$. Since these series converge increasingly slowly for large values of $x$, it seemed desirable also to study the function (1) for large values of the argument and thus to gain an asymptotic series. Two methods of obtaining these will be briefly reported upon: the first is the well-known saddle point method of Lord Rayleigh and Debye, which, however, gives only the first term of the expansion; the second method which is fashioned after Hankel's researches on the Bessel function gives the complete expansion. In the course of these developments some exact integral formulae for $\varphi_n(x)$ which are perhaps more convenient and more flexible than (1) will be constructed.

(1)

Introduce in (1) a new integration variable by means of

$$y=x^{\frac{1}{3}}\eta^{-2}; \quad \eta=+x^{\frac{1}{3}}y^{-\frac{1}{3}}; \quad (2)$$

we then have

$$\varphi_n(x)=2x^{\frac{1}{3}(n+1)}\int_0^\infty \eta^{-2n-3}\exp[-x^{\frac{1}{3}}(\eta+1/\eta^2)]d\eta. \quad (3)$$

This substitution causes $x$ to appear as factor only in the exponent. For large values of $x$ the exponential function will have a sharp maximum at the point where

$$f(\eta)=\eta+1/\eta^2 \quad (4)$$

has its minimum. This will be the case for $\eta=2^{\frac{1}{3}}$ (and also for two other points which do not interest us now since the path of integration does not pass through them). Thus at the right and left of $\eta=2^{\frac{1}{3}}$ the integrand of (3) decreases rapidly while above and below it increases. We therefore expand $f(\eta)$ in the vicinity of this saddle point:

$$f(\eta)=3\cdot 2^{-\frac{1}{3}}+3\cdot 2^{-4/3}\omega^2, \quad \omega=\eta-2^{\frac{1}{3}}. \quad (5)$$

The linear term vanishes of course. The rest of the integrand of (3), *viz.* $\eta^{-2n-3}$ being a slowly varying function we put in front of the integral sign and take its value *at* the saddle point. We thus get for (3) using (5):

$$\varphi_n(x)\sim 2^{\frac{1}{3}}(x/2)^{\frac{1}{3}(n+1)}\exp(-3(x/2)^{\frac{1}{3}} \times\int_{-\infty}^{+\infty}\exp(-3\cdot 2^{-4/3}x^{\frac{1}{3}}\omega^2)d\omega. \quad (6)$$

The error committed in taking as the limits of the integral $-\infty$ and $+\infty$ is negligible. The final result is

$$\varphi_n(x)\sim 2(\pi/3)^{\frac{1}{3}}(x/2)^{\frac{1}{3}(2n+1)}\exp(-3(x/2)^{\frac{1}{3}}). \quad (7)$$

This is the first and most essential term of an expansion in descending powers of $x$. To obtain this expansion we might use a process analogous to that used by Debye[1] for the cylinder functions, but the calculations become extremely involved.

[1] Debye, Math. Annalen **67**, 535 (1909).

(2)

The alternative method uses the differential equation satisfied by (1), which was given by Dr. Zahn in the preceding paper for the case $\eta=0$. By means of one partial integration it is readily seen that (1) is a solution of the following differential equation:

$$\frac{d^3\varphi}{dx^3}-\frac{2n}{x}\frac{d^2\varphi}{dx^2}+\frac{2}{x}\varphi=0. \tag{8}$$

The asymptotic formula suggests, however, that the new independent variable

$$3(x/2)^{\frac{1}{3}}=z \tag{9}$$

be introduced, for then $\varphi$ will behave for large values like a simple exponential. It will also be convenient to modify the dependent variable, namely to introduce for $\varphi(x)$ a function $g(z)$, such that

$$\varphi(x)=z^{3(n+1)}g(z). \tag{10}$$

The reason for splitting off just such a power of $z$ is readily understood when examining the roots of the indicial equation of (8). Elementary calculations give as differential equation for $g(z)$:

$$z^2g'''+3(2n+5/2)zg''+(3n+5/2)(3n+4)g'+z^2g=0. \tag{11}$$

This differential equation has still a nonessential singularity at zero and an essential singularity at infinity and represents therefore no immediate improvement over (8). But the advantage of (11) is seen if we apply a Laplace integral transformation to it:

$$g(z)=\int e^{-zt}G(t)dt, \tag{12}$$

where the path and the function $G(t)$ have yet to be determined. (Applying (12) to (8) would lead back to (1) again.) We enter (11) with (12) and remove any explicitly appearing powers of $x$ by partial integration.[2] The resulting differential equation for $G(t)$ is

$$(1-t^3)G_{tt}+3(2n+\tfrac{1}{2})t^2G_t-(3n+2)(3n+\tfrac{1}{2})tG=0. \tag{13}$$

[2] For details of this method see e.g., Courant-Hilbert, *Methoden der Mathematischen Physik*, p. 405.

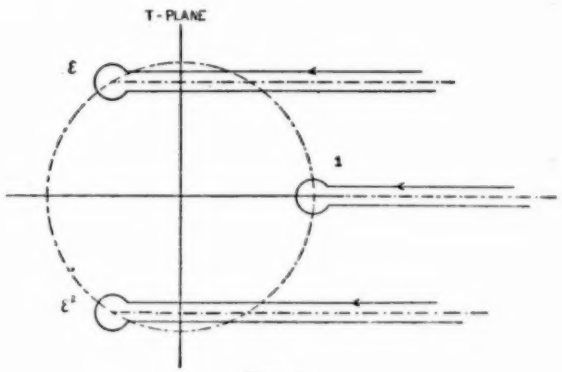


FIG. 1.

One sees readily that this equation has no longer any essential singularities at all, but that it possesses four non-essential singularities at $t=1$, $\epsilon$, $\epsilon^2$ and $t=\infty$.[3] Moreover, since the roots of the indicial equations at 1, $\epsilon$, $\epsilon^2$ agree it must be possible to collapse these three singularities into one. This can indeed be brought about by putting $t^3=\tau$, and (13) turns out to be a hypergeometric differential equation with the parameters

$$\alpha=-n-\tfrac{2}{3},\quad \beta=-n-\tfrac{1}{6};\quad \gamma=\tfrac{2}{3}. \tag{14}$$

For the purpose of writing down an explicit formula we choose an expression for the solution of the hypergeometric equation in the vicinity of the singularity $t^3=1$. This is[4]

$$G=C_1F(-n-\tfrac{2}{3},\ -n-\tfrac{1}{6};\ -2n-\tfrac{1}{2};\ 1-t^3)+C_2(1-t^3)^{2n+\frac{1}{2}}F(n+5/6,\ n+4/3;\ 2n+5/2;\ 1-t^3), \tag{15}$$

where $F$ is the Gaussian series. This we carry into (13) and choose as path of integration a loop which, coming from $+\infty$ encircles one of the three singular points $t^3=1$ and returns to $+\infty$. (See Fig. 1.) Since the first of the above series is unbranched at these points the integral containing it vanishes. We are thus left with

$$g(z)=C_2\int e^{-zt}(1-t^3)^{2n+\frac{1}{2}}\times F(n+5/6,\ n+4/3;\ 2n+5/2;\ 1-t^3)dt. \tag{16}$$

According to the contour we choose, we get different solutions of (11) or of (8). The particular function $\varphi_n(x)$ we are interested in is of

[3] 1, $\epsilon$, $\epsilon^2$ are cube roots of unity.

[4] See for instance Whittaker-Watson, *Modern Analysis*, fourth edition, p. 286.

course obtained by integrating (16) along the loop around $t=+1$. The multiplicative constant may be determined by means of the asymptotic series which we shall derive now.

(3)

For this purpose put

$$t=1+s/z. \tag{17}$$

The path now comes from $+\infty$, encircles $s=0$ and returns to $+\infty$. We write (16) now, absorbing constants into $C_2$

$$g(z)=C_2'z^{-2n-5/2}e^{-z}\int e^{-s}(sS)^{2n+\frac{1}{2}} \cdot F(n+5/6, n+4/3; 2n+5/2; 3(s/z)S)ds \tag{18}$$

with

$$S=1+s/z+s^2/3z.$$

One now has to use for $F$ the familiar Gaussian series and redevelop all powers of $S$ which thus occur in the integrand into powers of $s/z$. All such developments presuppose that $|s|<|z|$, but since this inequality cannot possibly be fulfilled for the distant parts of the path the resulting series will be divergent.[5] One should, therefore, go only so far as the terms of the series decrease.

Let the result of this expansion be

$$S^{2n+\frac{1}{2}}F(\cdots; 3(s/z)S)=1+\sum_{1, 2\cdots}\nu a_\nu(s/z)^\nu.$$

The integrals occurring when exchanging integration and summation are of the type[6]

$$\int e^{-s}s^\nu ds=2\Gamma(\nu+1).$$

Thus (18) becomes

$$g(z)=C_2''z^{-2n-5/2}e^{-z} \times\left[\Gamma(2n+5/2)+\sum_{1, 2\cdots}\nu\Gamma(2n+5/2+\nu)\frac{a_\nu}{z^\nu}\right].$$

Now $\Gamma(2n+5/2)$ is absorbed into $C_2''$, and the functional equation of the gamma-function is used on the further terms of the series. Substituting the result into (10) and using (9), a final asymptotic series for $\varphi_n(x)$ is gained, after the multiplicative constant has been adjusted by comparison with (7).

I have carried out this process up to and including terms proportional to $z^{-2}$ or to $x^{-4/3}$. The result of the very elementary calculation is

$$\varphi_n(x)\sim 2(\pi/3)^{\frac{1}{2}}(x/2)^{\frac{1}{2}(2n+1)}\exp(-3(x/2)^{\frac{1}{2}})\cdot \cdot[1+K_1(2/x)^{\frac{1}{2}}+K_2(2/x)^{4/3}+O(1/x^2)] \tag{19}$$

$$\text{with}\quad K_1=\frac{1}{6}\left(2n^2+3n+\frac{5}{6}\right), \qquad K_2=\frac{1}{6^2}\left(2n^4+\frac{14}{3}n^3+\frac{7}{6}n^2-4n-\frac{35}{72}\right). \tag{20}$$

It is hoped that the above description of the very elementary calculation necessary to compute the $K_i$ will enable anyone desiring higher accuracy to obtain further coefficients.

It should be noted that according to (19) $\varphi_n(x)$ does not even for large values behave like a true decay function.

Dr. Zahn's convergent series can also be obtained by putting in (16) $zt=\sigma$ and expanding the hypergeometric function around the point infinity into series proceeding according to ascending powers of $z/\sigma$.

[5] This situation is of course common to all asymptotic developments.

[6] Compare Whittaker-Watson, p. 245.

# The Range of Protons in Aluminum and in Air

D. B. PARKINSON, R. G. HERB, J. C. BELLAMY AND C. M. HUDSON
*Department of Physics, University of Wisconsin, Madison, Wisconsin*

(Received May 10, 1937)

By the use of the two million volt generator developed at this laboratory the range of protons in air and in aluminum has been measured as a function of proton energy up to about 2 Mev energy. The range in air data are in good agreement with the theoretical values of Mano at high energies but diverge considerably at energies below 0.7 Mev. The ratio of the range in air to the range in aluminum has been found to increase from a value of approximately 1000 at 200 kv to a value of 1550 at 1200 kv. From 1200 kv up to the maximum voltage available the ratio is shown to remain nearly constant.

## INTRODUCTION

THE measurement of the range of protons in aluminum and in air was undertaken at this laboratory both because of the importance of the data in the interpretation of the results of nuclear disintegration experiments and to get reliable information on the energy absorption in the aluminum foil windows used in our proton-proton scattering apparatus. Blackett and Lees[1] have published data obtained from cloud chamber measurements, but these are for only lower energy protons. Blackett[2] gives range values for fast protons in air by using a theoretical expression with empirically determined constants to extrapolate alpha-particle range curves. Mano[3] has published a table giving proton ranges in air as a function of energy up to an energy of 19 Mev. These are theoretical values, obtained by integrating an equation from the work of Bethe and Bloch after making certain approximations and then applying corrections. These values of range are consistently higher than Blackett's by a few percent.

The only direct experimental data obtained under conditions comparable to ours are a curve given by Tuve, Heydenburg and Hafstad[4] showing the visually estimated range of protons in air up to about 1.2 Mev energy. It was therefore thought advisable to make a careful determination of the range curves using protons from the two million volt electrostatic generator for the purpose.

[1] P. M. S. Blackett and D. S. Lees, Proc. Roy. Soc. **134**, 658 (1931).
[2] P. M. S. Blackett, Proc. Roy. Soc. **135**, 132 (1932).
[3] G. Mano, J. de phys. et rad. **5**, 628 (1934).
[4] M. A. Tuve, N. P. Heydenburg and L. R. Hafstad, Phys. Rev. **50**, 806 (1936).

## RANGE OF PROTONS IN ALUMINUM

Fig. 1 shows the apparatus used to determine the range of protons in aluminum. This was a short cylindrical brass box, 9.5 cm in diameter, mounted with an insulating bushing on the magnetic analyzer of the two million volt generator. A brass disk having twelve holes equally spaced near its circumference was mounted inside the box as shown and could be rotated by turning the ground brass plug. In this way the various aluminum foils mounted over the holes in the disk could be brought one after another into the proton beam which was defined by the slits at the front part of the box. A Faraday cage, mounted directly behind the holes in the wheel served to detect the transmitted protons. A magnetic field across the entrance of the Faraday cage eliminated any trouble from secondary electrons at that point and the whole box was put at a negative potential of 45 volts to prevent secondaries from the defining slits from interfering with current measurement.

The aluminum foils, ranging in thickness from $0.979\times10^{-4}$ cm to $37.6\times10^{-4}$ cm were obtained from the Aluminum Company of America and from the American Platinum Works. The foil thickness was determined as follows. With the edge of an accurately ground quartz crystal as a straight edge, triangles about 3 cm on a side were cut from the foils with a razor blade. The lengths of the sides of these triangles were then measured with a micrometer microscope and the areas computed. The triangles were then weighed on a micro balance, the weight of the lightest being of the order of two milligrams, and the thickness computed using 2.699 g per cc as the density

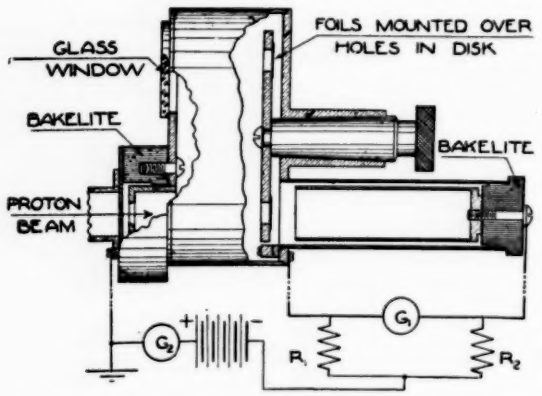


FIG. 1. Apparatus and electrical circuit used to measure the range of protons in aluminum.

of aluminum. In many cases two determinations were made with separate triangles cut from the same sheet of aluminum. The results of these checks will be discussed later.

In order to plot a range curve it was necessary to determine the minimum energy at which protons were able to penetrate each of the various thicknesses of foil. This was done by measuring the current due to protons incident on the foil, and the current to the Faraday cage due to those that penetrated the foil and plotting the ratio of these two currents as a function of proton energy for each of the various thicknesses. Trouble due to continuous small fluctuations of the current was eliminated by using the null method electrical circuit indicated in Fig. 1. When the voltage of the generator and consequently the energy of the protons was such that the galvanometer $G_1$ read zero, the fraction of protons transmitted was equal to the predetermined ratio $R_1/R_1+R_2$. The galvanometer $G_2$ merely served to indicate the order of magnitude of the total current. A series of curves was taken in this way and appear in Fig. 2. Curves III, IV, V, and VI of this group are of particular interest. The circles of curve III are experimental points taken with a foil that was determined to have a thickness of $2.51\times10^{-4}$ cm while the crosses are experimental points taken with another foil measured by a second person to have a thickness of $2.47\times10^{-4}$ cm. The two foils were cut from separate triangles which came from the same sheet of aluminum foil. The same conditions hold for curve IV, the circles representing data taken with a foil determined to be $3.46\times10^{-4}$ cm thick and the crosses representing data taken with a different foil measured to be $3.49\times10^{-4}$ cm thick. Curve V is for a foil which measured $4.67\times10^{-4}$ cm in thickness and curve VI is for a foil taken from a different part of the same sheet and having an apparent thickness of $5.39\times10^{-4}$ cm. This proved to be no error in thickness determinations for the two foils yielded different cut-off curves (Fig. 2) and furnish points that lie very closely on the smooth range curve of Fig. 3. The range curve is constructed by extrapolating the curves of Fig. 2 down to a ratio of zero and plotting the value of energy so obtained against the foil thickness.

## RANGE OF PROTONS IN AIR

The apparatus used to measure the range of protons in air is shown in Fig. 4. An aluminum foil, $A$, $1.44\times10^{-4}$ cm thick was mounted over an aperture 1.0 mm in diameter and served as a window to conduct the protons out of the vacuum system. The proton beam was defined by an aperture 0.8 mm in diameter placed immediately ahead of $A$. After leaving the foil $A$ the protons traversed a predetermined thickness of air and then entered a thin ionization chamber by penetrating the aluminum foil $B$, thickness $0.979\times10^{-4}$ cm. In this work the ratio of ion current to incident proton current at suitable values of proton energy was determined for various thicknesses of air gap between the ionization chamber and the foil $A$, the air gap being measured with a micrometer microscope. Again a balancing method was employed for measuring the current ratios, the circuit being indicated in Fig. 4. As in the arrangement for measuring the range in aluminum it was found most convenient to first adjust the ratio of the resistances $R_1$ and $R_2$ to some con-

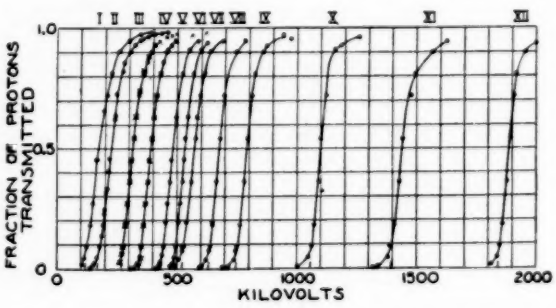


FIG. 2. Curves showing the apparent fraction of incident protons transmitted by various thicknesses of aluminum foil as a function of proton energy.

venient value and then vary the energy of the protons to obtain a balance. Secondary electrons from the slits near $A$ were prevented from interfering with the current measurements by the field of a small electromagnet placed across the ion path.

Curves obtained by this method for various distances traversed in air are shown in Fig. 5. The ionization chamber was kept at a depth of 0.4 mm throughout the experiments. Various clearing potentials were tried but the ratio of ion current to proton current seemed to be independent of clearing potential, provided 180 volts or more were applied, and provided the air path was greater than about 10 mm. All the curves shown were obtained using a potential of 270 volts so that for the majority of them recombination should not have entered in to any great extent. It is probable, however, that the reduced height of the curves taken with the ionization chamber very near $A$ was caused by recombination, since the proton beam was concentrated near $A$ and at high ratios the ion density in the center of the ionization chamber was very great. The curves taken with the longer air paths also show a decrease in the apparent maximum number of ions per proton, probably due to the fact that after having traversed 4 or more cm of air a fair proportion of the protons was scattered through a sufficiently large angle to miss the rather small window in the ionization chamber. The shape of the specific ionization curve at higher energies was determined by continuing curve VI out to the highest obtainable voltage.

The straight sections of the curves of Fig. 5 were extrapolated down to a zero ratio as indicated, thus obtaining values for the energy loss of the protons in the two aluminum foils $A$ and $B$ and the measured thickness of air. The energy loss in the foil $A$ for each of the extrapolated values was easily obtained from the range in aluminum curve. The energy loss in $B$ was a constant, 117 kv, but in order to plot the range in air curve it was necessary to know in addition to this the air equivalent of foil $B$ for incident protons of 117 kv energy. This was determined by placing a duplicate foil in the air path close against $B$, where it proved to be equivalent to $1.0\pm0.1$ mm of air for 215 kv protons. The same foil placed close to $A$ where the protons had an energy of 1550 kv was equivalent to an air path increase of $1.6\pm0.12$ mm. Since the air equivalent of the foil obviously decreased with decreasing proton energy it seemed probable that a value of 0.90 mm would not be greatly in error for protons of 117 kv and consequently this value was used

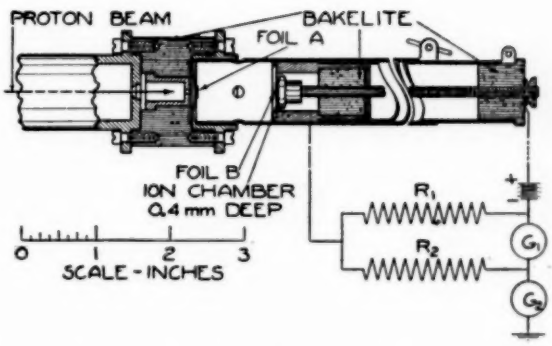


FIG. 4. Apparatus and electrical circuit used to measure the range of protons in air.

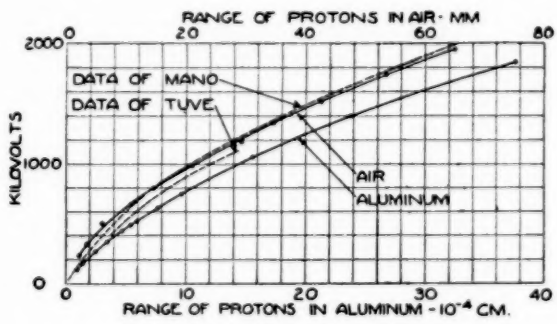


FIG. 3. The range of protons in air and in aluminum. The long dotted line shows Mano's theoretical values for the range in air. The short dotted curve is Tuve's visually estimated range curve.

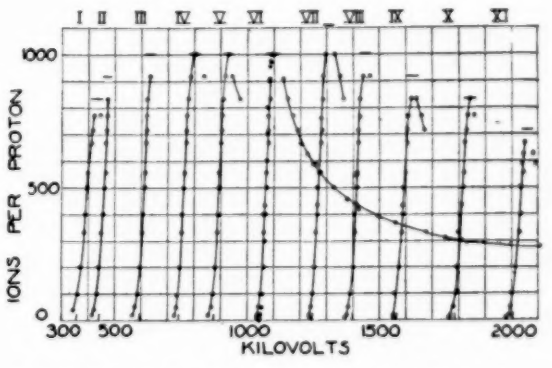


FIG. 5. Curves showing the experimental data taken to determine the range of protons in air. Each curve gives the variation with proton energy of the ratio of current in the ionization chamber to incident proton current for a particular air path. The straggling expected on the basis of Bohr's theory is indicated by the heavy black dots.

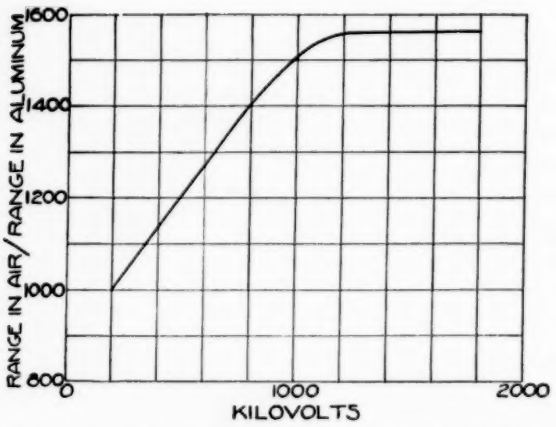


FIG. 6. Ratio of the range of protons in air to the range in aluminum as a function of energy.

in plotting the range in air curve. The curve showing the ratio of the range in air to the range in aluminum as given in Fig. 6 was constructed from values read from this range in air curve and from the range in aluminum curve. A careful study of the shape of the curve of Fig. 6 will show that the value of 0.9 mm as the air equivalent of foil *B* is probably accurate within 3 or 4 percent, which is entirely satisfactory, since even a large error in this correction is of minor importance over the greater part of the range in air curve.

The data on the range of protons in air were taken under laboratory conditions of temperature and pressure and then reduced to corresponding values at 0°C and 760 mm Hg. The temperature of the air through which the protons were passing was taken to be the temperature of the brass tube supporting the ionization chamber, measured to within about 2°C. It is possible however that the effective temperature of the column of air through which the concentrated proton beam was passing may have been considerably higher and that the ranges as given are somewhat greater than would be expected from cloud chamber measurements. The uncertainty of the temperature is probably responsible for most of the spread of the experimental points on the range in air curve.

## DISCUSSION

Several factors contribute to the slope of the curves of Fig. 5, namely: the natural shape of the specific ionization curve of protons, straggling of the protons, inhomogeneity of the proton energies, nonuniformity of the foils and the depth of the ionization chamber. As it would be of interest to know something about the relative magnitudes of some of these contributions the expected straggling of the protons under conditions as of curve VI, Fig. 5, was computed using the theory developed by Bohr[5] for the straggling of alpha-particles. By making the proper substitutions the equations were made to apply to protons, and yielded the points shown by the heavy black dots in Fig. 5. The energy spread of this theoretical curve is about 40 kv. The depth of the ionization chamber, 0.40 mm, could account for about 10 kv, making for these two factors a total of about 50 kv spread which is as nearly as can be determined the spread of the experimental data. Thus if the straggling theory is correct, nonuniformity of the foils, inhomogeneity of the proton beam and slope of the specific ionization curve must be of negligible importance.

The shape of the tops of the curves could not be determined due to a lack of sensitivity of the measuring instruments. The bars over the curves are at ratios of $R_1$ and $R_2$ at which it was either just possible or impossible to obtain a balance and are consequently equal to or greater than the maximum height of the curves.

The comparatively wide spread in energy of the curves taken with the aluminum foils and Faraday cage is a matter of some interest. When a proton is leaving a foil with low energy there is a certain probability that it will capture an electron and leave as a neutral atom, and consequently not register in the Faraday cage. The probability that this will occur is a function of the energy with which the proton emerges, increasing as the proton energy decreases. The difference in slopes of the curves of Figs. 2 and 5 is thought to be due entirely to this effect since the loss due to wide angle scattering was shown experimentally to be negligible. As a result the range curve was plotted using the extrapolated values of energy which would probably be only slightly influenced by the neutralization effect if influenced at all.

That the curve obtained in this way is not greatly in error was checked by modifying the range in air apparatus to accommodate the foils and mountings used in the aluminum range measurements and determining the absorption of

[5] N. Bohr, Phil. Mag. **30**, 581 (1915).

the same foils by means of the ionization chamber, foils being inserted one after another in the air path. The check was not completely satisfactory since the energy losses so determined involved taking the small difference of two large numbers read off the range in air curve, and this small difference could not be determined better than about 8 percent. With this limitation the values determined in the two ways agree. The data taken when testing the air equivalence of foil *B* constitute a better check on this point and indicate that the aluminum values are reliable.

Since the data presented here depend for their accuracy on the calibration of the voltmeter, its reliability, and its linearity over wide ranges it is of interest to note here the checks that were made in these respects. It was found that the cut-off curves for the aluminum foils could be repeated from day to day and would give the same experimental points within less than 2 percent. The absolute value of the voltage was determined as described in an earlier publication[6] and was rechecked shortly before this work was started. An excellent check on the linearity was provided by the range in aluminum apparatus. In energy ranges where it was possible, after a cut-off curve for a given foil had been taken with protons, some of the experimental points were rechecked using the diatomic ion beam. This would necessitate increasing the generator voltage by a factor of exactly two, and it was found that within 1 percent the voltmeter reading would also increase by a factor of two. Additional checks, made from time to time, showed that within less than 1 percent, the voltage indicated was independent of the pressure in the tank.

TABLE I. *Range of protons in air and in aluminum.*

| kv | RANGE IN Al (cm) | kv | RANGE IN AIR (cm) |
|---|---|---|---|
| 117 | $0.979\times10^{-4}$ | 232 | 0.226 |
| 166 | 1.44 | 329 | 0.345 |
| 267 | 2.51 | 500 | 0.600 |
| 342 | 3.46 | 657 | 1.09 |
| 433 | 4.67 | 798 | 1.49 |
| 486 | 5.39 | 983 | 2.11 |
| 520 | 5.93 | 1184 | 2.93 |
| 630 | 7.69 | 1339 | 3.47 |
| 745 | 9.65 | 1514 | 4.26 |
| 1055 | 15.6 | 1739 | 5.34 |
| 1393 | 23.8 | 1950 | 6.50 |
| 1842 | 37.6 | | |

For convenience of comparison, Mano's range in air data, reduced to 0°C, are shown by the long dotted curve of Fig. 3. Mano's values are for mean range, and the two curves would probably agree well at high energies if we had plotted mean values instead of extrapolated values of energy. Disagreement at lower energies is very marked. The short dotted curve is the visual range curve of Tuve, Heydenburg, and Hafstad.

For convenience in using these data the experimental points from which our two range curves are plotted are given in Table I.

We wish to express our appreciation to Professor G. Breit, Professor H. B. Wahlin, and Professor L. R. Ingersoll for their generous support in this research. We are also indebted to D. W. Kerst for valuable help and to the Wisconsin Alumni Research Foundation for generous financial assistance.

[6] R. G. Herb, D. B. Parkinson and D. W. Kerst, Phys. Rev. **51**, 75 (1937).

# The Influence of the Earth's Magnetic Field on Cosmic-Ray Intensities up to the Top of the Atmosphere

I. S. Bowen, R. A. Millikan, and H. V. Neher
*California Institute of Technology, Pasadena, California*

(Received May 8, 1937)

Accurate observations on cosmic-ray intensities as measured by Neher electroscopes were made in the equatorial belt (Madras, India, mag. lat. 3 N) up to more than 98 percent of the way to the top of the atmosphere with the following results: 1. Cosmic rays whatever their nature are so rapidly absorbed in the outer layers of the atmosphere that even in the equatorial belt they get into equilibrium with their secondaries and produce their maximum ionization before they have penetrated through the first tenth of the atmosphere. 2. From that point on they fall off exceedingly rapidly in intensity following an exponential equation, their law of absorption being like that of x-rays and not that of particles that exhibit range phenomena such as low energy $\beta$-rays, proton rays or $\alpha$ rays. 3. The differences between the present curve, the San Antonio curve (mag. lat. 38.5 N) and the curve obtained on the Settle-Fordney flight (mag. lat. 53 N) fix for the first time the complete curves of ionization produced in the atmosphere by incoming charged particles having energies in the $2.5-6.7\times10^3$ Mev and $6.7-17\times10^3$ Mev ranges. These curves are reasonably well in accord with the Bethe Heitler theory as extended by Carlson and Oppenheimer. 4. The exceedingly rapid absorption of this latitude sensitive radiation with a coefficient nearly constant and independent of energy qualitatively justifies the shower theory of the foregoing authors. 5. The latitude sensitive part of the cosmic-ray ionization found in the lower portion of the atmosphere is practically all due to the secondary effects of varied nature resulting from the absorption of the incoming electrons in the upper tenth of the atmosphere. 6. The apparent absorption coefficient of the whole progeny of secondary influences resulting, down to sea level from the absorption of incoming electrons in the very top layers of the atmosphere is approximately the same as that found by Johnson and by Neher for the east-west effect thus proving that the particles causing the latitude and the east-west effects are of the same type. Both absorption coefficients are such as to suggest that these particles are electrons (predominantly positive) and not protons.

## 1. The New Experimental Latitude Findings

IMMEDIATELY after the San Antonio flights[1] we set about obtaining similar data at, or very near, the magnetic equator. Through the exceedingly generous and efficient cooperation of the Indian Meteorological Department represented by Director-General Dr. C. W. B. Normand, Assistant Director Dr. S. K. Banerji, Meteorologist Dr. K. Das and Assistant-in-Charge of the Madras Observatory, Mr. Narayanamurthi, H. Victor Neher, who sailed with our equipment for India on the S. S. President Van Buren on August 12, 1936, succeeded in the month of October 1936 in obtaining in Madras (mag. lat. 3° N) successful flights to nearly the same altitudes (98 percent of the way to the top) reached in San Antonio, 1936. Sample record of two of these flights is shown in Fig. 1. As heretofore explained[1] the barometer and thermometer

[1] R. A. Millikan, H. V. Neher and S. K. Haynes, Phys. Rev. **50**, 992 (1936).

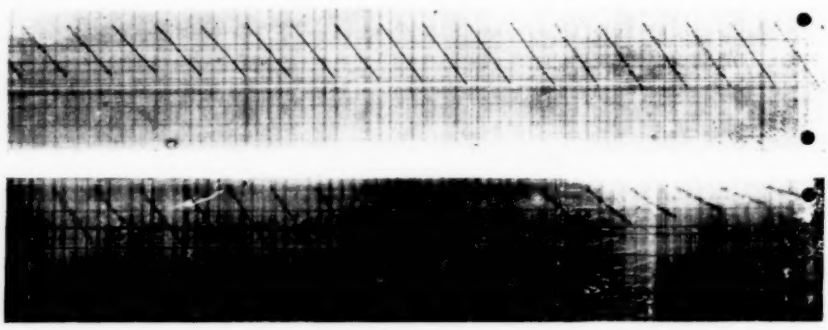

Fig. 1. Sample portions of two electroscope records taken at Madras, India (mag. lat. 3° N) in October 1936.

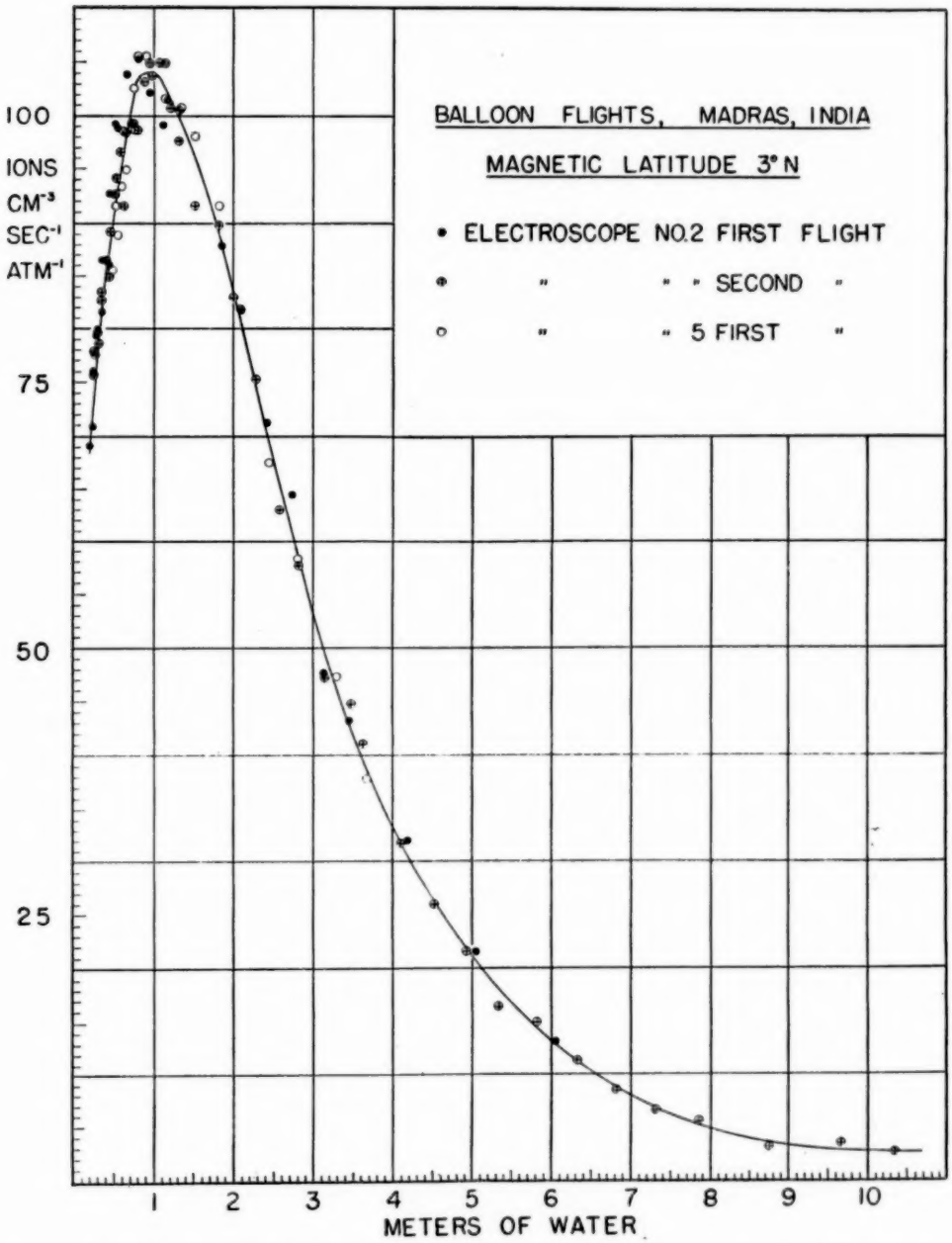


FIG. 2. Ionization as a function of depth, in meters of water equivalent, below the top of the atmosphere at Madras, India (mag. lat. 3° N).

lines and the changing slopes of the fine electroscope-discharge lines enable us to obtain a most satisfactory curve showing the relation of cosmic-ray ionization and altitude at the magnetic equator. Such a curve is shown in Fig. 2.

In order to show the effect of latitude on such curves we give in Fig. 3 the results of all of our high altitude observations. The upper curve combines our data obtained (a) in the Settle-Fordney flight[2] of November 1933, (b) in the Kepner-Stevens-Anderson flight of July 1934 (these latter data not before published) and (c) in the airplane flights[2] made at Spokane in September 1932. All of these flights were made in a magnetic latitude

[2] I. S. Bowen, R. A. Millikan and H. V. Neher, Phys. Rev. **46**, 641 (1934).

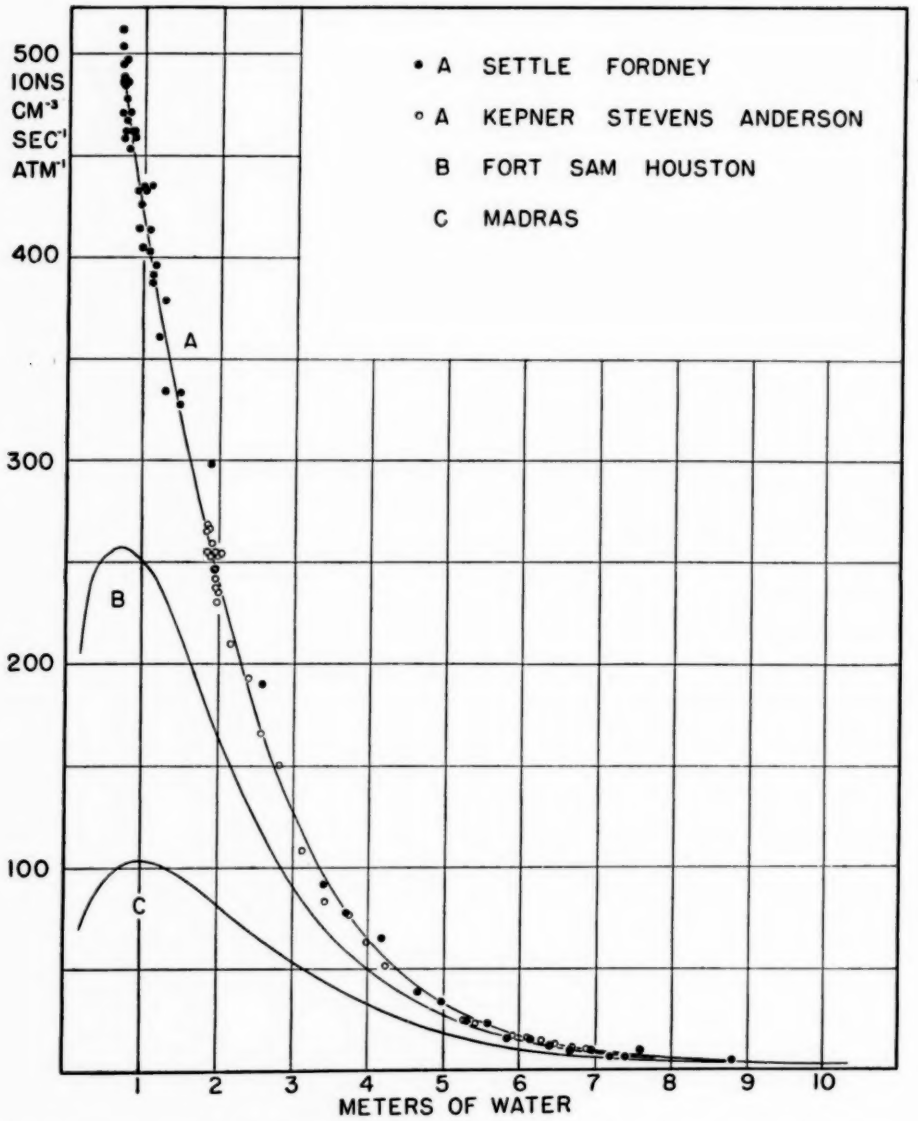


FIG. 3. Comparison of the ionization at Madras, India (mag. lat. 3° N), Fort Sam Houston, San Antonio, Texas (mag. lat. 38.5° N) and on the Settle-Fordney flight (mag. lat. 53° N).

of approximately 53° and between them carry the curve to a pressure of approximately 5 cm of mercury. The second curve gives the results of the Fort Sam Houston balloon flights[1] (San Antonio, Texas, mag. lat. 38.5°) combined with the airplane flights at March Field[2] (corrected for the slight difference in magnetic latitude). The lower curve indicates the ionization at mag. lat. 3° N as given by the balloon flights at Madras and the airplane flights at Manila,[3] made in November 1935. In order to make the data, obtained with the thin walled electroscopes used in the sounding balloon flights at Madras and Fort Sam Houston agree with the results obtained with the thick walled electroscopes used in the airplanes and manned balloons at the same latitude it was found necessary to increase by 10 percent all readings of the thin walled instruments.

The difference between the San Antonio and the Madras flights makes possible for the first time a particularly reliable and unambiguous determination of the absorption of the atmos-

[3] I. S. Bowen, R. A. Millikan, S. A. Korff and H. V. Neher, Phys. Rev. **50**, 579 (1936).

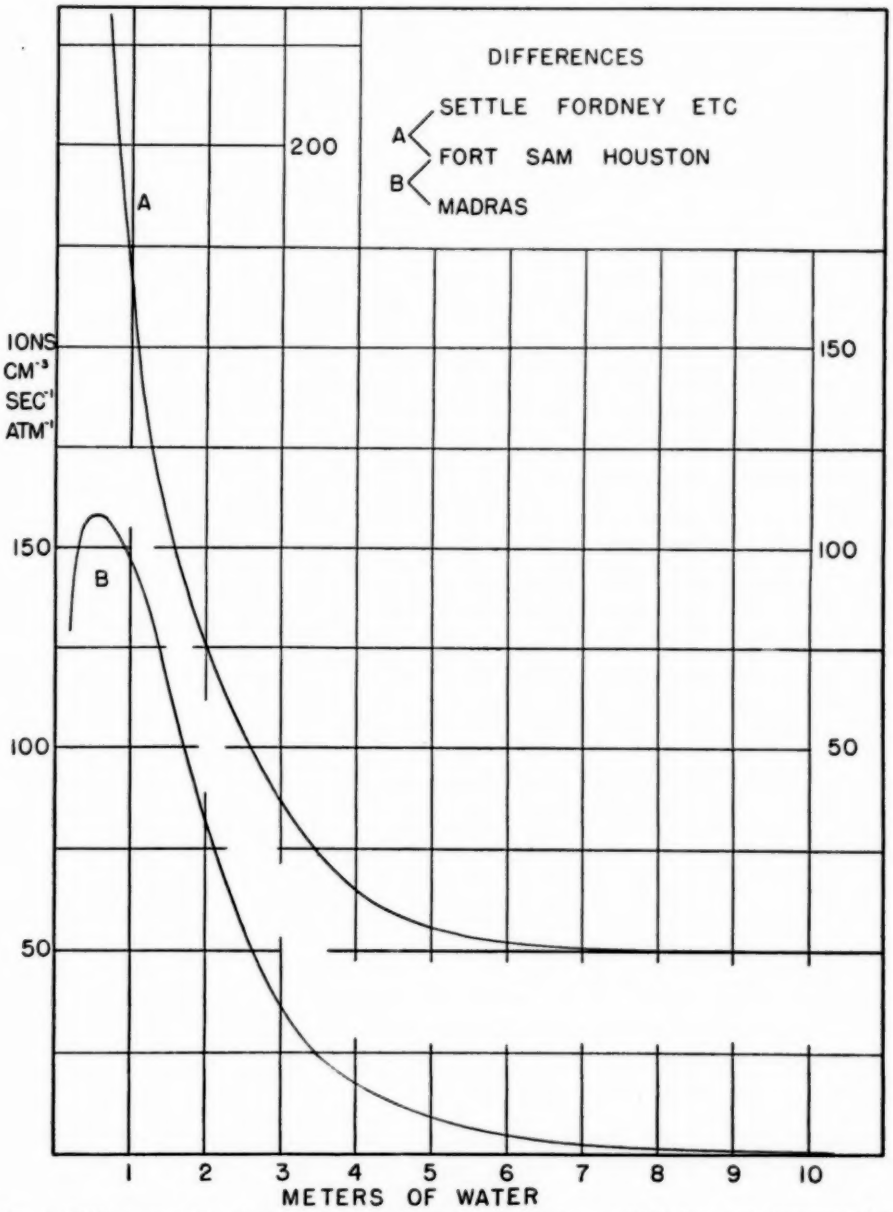


FIG. 4. Differences in ionization between Fort Sam Houston and Madras and between the Settle-Fordney flight and Fort Sam Houston.

phere for electrons having a mean incident energy of about 10,000 million electron volts, this being the weighted mean between the energy of 6700 Mev necessary for electrons (+ or −) to just get through the earth's magnetic field at the zenith in magnetic latitude 38.5° and that of 17,000 Mev necessary to get through at the equator in the longitude of Madras.

Similarly the difference between the curves corresponding to the flights in magnetic latitude 53° and those in magnetic latitude 38.5° gives a fairly reliable determination of such a mean absorption of the atmosphere for electrons having a weighted mean energy of about 4 billion ev. These two difference curves are shown in Fig. 4.

### 2. Qualitative Results from Curves

A first and most significant result obtained from a comparison of these curves is embodied in the statement that cosmic rays of all energies,

even as high as 10,000 Mev coming into the earth from all directions on the average can penetrate not more than one-tenth of the way through the earth's atmosphere before coming into equilibrium with their secondaries. Everyone of the five curves shown save those taken at magnetic latitude 53°, which did not go high enough to reach the turn-over point, shows that the incoming cosmic rays whatever their nature act just like x-rays or gamma-rays in that as greater and greater thicknesses of the absorbing material, in this case air, are introduced between the source and the measuring electroscope the ionization in that electroscope increases to a maximum which is reached when the incoming rays are first in equilibrium with their secondaries and thenceforward falls off at a rate which is rapid if the absorption of the incoming rays is large, slower if that rate of absorption is smaller. This is in general a characteristic of rays, like x-rays, that lose a large fraction of their energy in one act and are therefore absorbed exponentially. It is not a characteristic of rays, like $\alpha$- and $\beta$-rays, which have a range and ionize more or less uniformly along their paths.

Further, since the difference curves can only be due to the effect of the earth's magnetic field on incoming electrons these curves show that the nuclear absorption of electrons is unlike the extranuclear absorption in that it is an exponential absorption as required by the Bethe-Heitler theory and that the absorption coefficient is *very large* and does not vary rapidly with energy, also as required by that theory. Indeed the penetrating power of all the cosmic rays is so small that one meter of water is enough to get the whole group of incoming rays, whatever their nature, to the depth at which they are producing their maximum of ionization and close to the depth at which they are in equilibrium with their secondaries. This is seen from a comparison of the curves in Figs. 2, 3, 4, all of which reveal that the maximum of ionization is reached before the rays have penetrated through the upper tenth of the atmosphere.

In the case of the incoming 10,000 Mev electrons the lower curve of Fig. 4 shows that while these electron rays are intense enough to produce 160 ions per cc per sec. at a distance of but one-fifteenth of the way (0.7 meter of water) through the atmosphere, at a distance halfway through (5 meters of water) their influence has fallen off so rapidly that their total ionizing effect has dropped to 10 ions and at sea level (10 meters of water) it has fallen to three-tenths of an ion per cc per sec.

A further qualitative result of the study of all these curves is to emphasize the conclusion which one of us stressed in 1932[4] and suggested as a possibility in connection with the report on the 1926 expedition[5] from Los Angeles to South America made expressly to test the effects of the earth's magnetic field on the incoming cosmic rays, namely, that practically all of the observed cosmic-ray ionization at or anywhere near the earth's surface is due to the secondary effects of incoming rays which are absorbed in the very top of the atmosphere and through that absorption create secondary radiations of some sort that reach down to sea level and beyond.

TABLE I. *Comparison of differences with Gold formula.*

| Meters of Water | Fort Sam Houston-Madras | | Settle, Fordney-Fort Sam Houston | |
|---|---|---|---|---|
| | Obs. | 580 G(0.54) | Obs. | 1800 G(0.80) |
| 0.2 | 135.5 | | | |
| 0.4 | 156.3 | | | |
| 0.7 | 156.8 | 235.5 | 233 | 532 |
| 1.0 | 147.9 | 177.1 | 167 | 362 |
| 1.5 | 115.8 | 114.7 | 108 | 200 |
| 2 | 83.6 | 76.7 | 74.3 | 115 |
| 2.5 | 56.1 | 52.3 | — | — |
| 3 | 36.2 | 36.1 | — | — |
| 3.5 | 24.4 | 25.2 | 24 | 24.5 |
| 4 | 17.2 | 17.8 | 15.0 | 15.0 |
| 4.5 | 13.0 | 12.6 | 9.3 | 9.3 |
| 5 | 9.6 | 9.0 | 5.4 | 5.8 |
| 5.5 | 6.8 | 6.4 | 3.6 | 3.6 |
| 6 | — | — | 2.2 | 2.27 |
| 7 | 2.14 | 2.41 | 1.0 | 0.90 |
| 8.5 | 0.79 | 0.93 | — | — |
| 10.33 | 0.30 | 0.30 | 0.046 | 0.046 |

[4] R. A. Millikan, Phys. Rev. **43**, 661 (1933).

[5] R. A. Millikan and G. H. Cameron, Nature **121**, 21 (1928). In this first report made at the meeting of the B.A.A.S. at Leeds in Sept. '27 on the purpose and results of this voyage from Los Angeles (mag. lat. 41° N) to Peru (mag. lat. 1° S) to look for the effect of the earth's magnetic field on incoming electrons, the authors state that "if the northern hemisphere and southern hemisphere curves (of ionization with altitudes) coincide it would go a long way toward eliminating the possibility the rays are generated by the incidence of high speed beta-rays on the outer layers of our atmosphere . . . for such beta-rays would be expected to be influenced by the earth's magnetic field so as to generate stronger radiation over the poles than over the equator."

### 3. Quantitative Treatment of Field Sensitive Rays

As in our report to the London Conference[6] we find it essential to divide all incoming rays into field-sensitive and non-field-sensitive rays. We leave the nature of the non-field-sensitive rays for the present undetermined and attempt to see what can be done in the way of an understanding of the field sensitive rays, i.e., the rays which are the cause of the ionization represented by the difference curves of Fig. 4. These rays can only be due to incoming charged particles.

One way of analyzing the results of the direct measurement of the absorption of 4 and 10 billion volt electrons, without calling in any theory at all, is by building up the observed ionization curves from Gold integrals following the method already used by us in the study of the total cosmic-ray ionization curve.[7] This analysis is made in Table I for both of the difference curves. It is at once seen that unlike the total cosmic-ray ionization curve discussed in the previous article the whole difference curve (from 1.5 meters of water from the top of the atmosphere down to sea level (10 m)) representing the ionization produced in our electroscopes by 10 billion volt incoming electrons, with the progeny of secondaries of all kinds, may be approximately represented by one single absorption coefficient, namely 0.54 per meter of water, over a range in the ionization of a factor of 400. Similarly the ionization produced by 4.0 billion volt incoming electrons is fairly closely reproduced by an apparent absorption coefficient of 0.80 per meter of water. Of course the numerical values of the coefficients thus obtained have no simple relationship to the absorption coefficients of the primary particles involved since the observed ionization curve, which these values describe is produced by a complex mixture of primaries, secondaries, tertiaries, etc. The coefficients are here given merely as a convenient method of describing quantitatively the observed variation of ionization with depth which can then be compared with similar results obtained with counters (see Section 4) or with measurements on the total ionization (see above).

These observed absorption coefficients are of the order of magnitude given by theory for the apparent absorption of electrons after coming into equilibrium with their secondaries as determined primarily by the formation of "impulse radiation" or bremsstrahlung (see below). This absorption is on the other hand much greater than that of heavy charged particles such as protons since neither according to theory nor to experiment can *heavy* charged particles lose energy in appreciable amount by exciting x-radiation of the bremsstrahlung type. We know this experimentally because neither protons nor alpha-rays have ever been observed to give rise to appreciable amounts of such radiation and we know it theoretically because this radiation is due to rapid deceleration of the charged particle as it approaches or passes by a nucleus, but the mass of a heavy particle precludes the possibility of such rapid deceleration while the electron (+ or −) must, because of its lightness and its charge, experience such decelerations exceedingly easily and suddenly. This therefore rules out incoming protons as a significant source of the latitude sensitive part of cosmic radiation. Furthermore the constancy of the absorption coefficient of the latitude sensitive rays is perhaps another indication that the ionization produced by them may be explained without the introduction of incoming particles as penetrating as protons. Of course this last argument would no longer be valid if heavy particles should be found to have another mechanism of absorption such as nuclear transmutations with a coefficient comparable to the observed values discussed above.

The present experiments seem therefore to give the first direct measurements on the nuclear absorption by air of up to 10 billion volt electrons over a wide range of depths in the atmosphere. They show conclusively that incoming electrons of such stupendous energy are absorbed exceedingly rapidly in the first tenth of the earth's atmosphere. *They transmit, not themselves, but only their secondary influence to the lower regions of the atmosphere.* According to the Oppenheimer-Bethe-Heitler theory these secondary influences are limited to the following. The impulse rays, or scattered x-rays, into which the energy of the 10 billion volt incoming electrons (+ and −) are at first partially transformed, produce in turn by

[6] I. S. Bowen, R. A. Millikan and H. V. Neher, *Papers of the International Conference of Physics* (London, 1934), p. 206.

[7] I. S. Bowen, R. A. Millikan and H. V. Neher, Phys. Rev. **44**, 246 (1933).

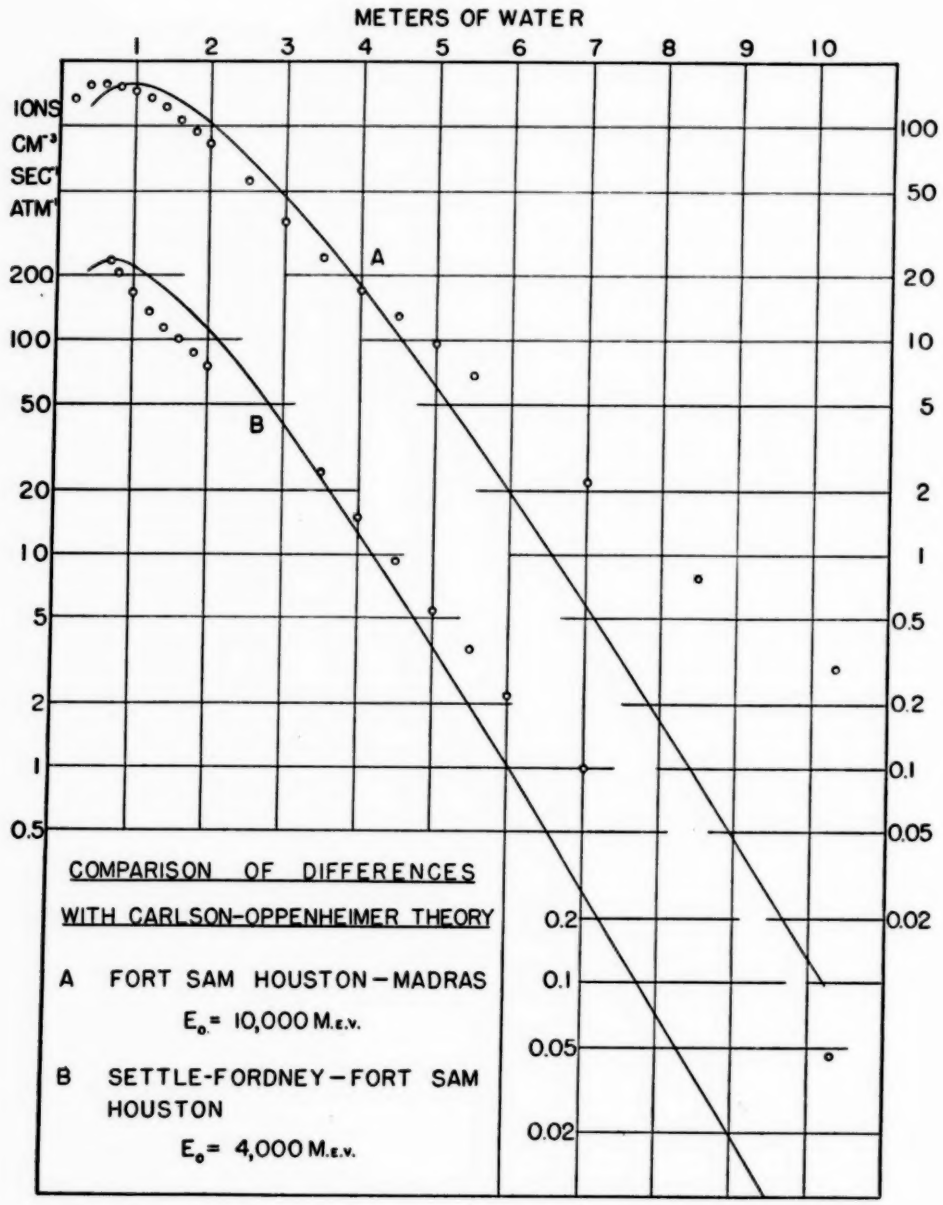


FIG. 5. Comparison of the difference curves with the Carlson-Oppenheimer theory.

their absorption by the nuclei of the molecules of the air, electron pairs, the energy of which is in turn quickly again transformed into lower energy impulse radiation and so on until the whole energy of the incoming electron has been frittered away by the summed ionizing power of the very large progeny of beta-rays of all energies which are ultimately formed. Carlson and Oppenheimer[8] have recently carefully followed through this whole process, and without introducing further mechanisms of absorption have so extended the Bethe-Heitler theory as to make it possible to compare the full curve of variation of 10 billion volt cosmic-ray ionization as a function of altitude with our observed variation. Similar calculations have also been made by Bhabha and Heitler[9] with results in substantial agreement with those of Carlson and Oppenheimer. To make

[8] J. F. Carlson and J. R. Oppenheimer, Phys. Rev. **51**, 220 (1937).

[9] H. J. Bhabha and W. Heitler, Proc. Roy. Soc. **159**, 432 (1937).

possible this comparison Carlson and Oppenheimer's equations which were worked out for radiation coming in vertically, were transformed so as to make them applicable to rays coming in from all directions such as those to which our electroscopes actually respond. This is a purely geometrical transformation which is essentially the inverse of the Gross analysis.

The comparison of this transformed Carlson-Oppenheimer formula with the observed difference curves, plotted on a log scale, is shown in Fig. 5. In both cases the general form of the calculated and observed curves are in agreement thus indicating that the mechanisms discussed above play a major role in the production of ions by these high energy particles. In detail however it is evident that certain systematic differences occur between observation and theory, namely, (a) the maxima are observed at about $\frac{2}{3}$ of the predicted distance from the top of the atmosphere and (b) the apparent absorption coefficient near sea level is from $\frac{1}{2}$ to $\frac{2}{3}$ of the value predicted by theory. Both Carlson and Oppenheimer and Bhabha and Heitler emphasized the second discrepancy but did not find the first type of difference in comparing their curves with the observations of Pfotzer[10] who used vertical coincidence counters at mag. lat. 50° N. However, in making the comparison both groups of authors used the theoretical curve for an energy of the incident electrons of $2.5\times10^3$ Mev, this being the minimum energy that can enter at this latitude. Our own Fig. 2, however, indicates unambiguously that at this latitude over half of the ionization is due to incoming particles of energy greater than $6.7\times10^3$ Mev. If one compares Pfotzer's observed curve with the theoretical curve for the correct mean energy, say 6 to $8\times10^3$ Mev, the observed maximum occurs at a depth about $\frac{2}{3}$ as great as that given by the theoretical curve in agreement with our own findings. As pointed out to us privately by Dr. Oppenheimer the theoretical calculations are more uncertain in the initial part of the curves than at greater depths and consequently the first type of discrepancy (position of maximum) is probably less serious than the second (absorption coefficient near sea level). Since in our curves the ionization is produced by particles in a definite range of energy the discrepancy in the apparent absorption coefficient at sea level cannot be explained by the presence of a few primary particles of very high energy.

It is interesting to observe too as our data (see Table I) have already shown that at a depth of 3 or 4 meters of water equivalent where the theory fits best, the apparent coefficient of absorption is essentially the same as at 6 or 7 meters where the present theory explains less than half of the observed ionization. This is in line with the fact which we have earlier reported that there seems to be a constancy at these elevations in the fraction of the radiation removed by 6.5 cm of lead.[11] Similarly some observers report constancy in the ratio of number of showers to total ionization over this range.[12] The last two observations were made on total radiation which, however, is made up largely of the radiation of the type under consideration at depths of 6 or 7 meters of water or less. In these cases the constancy breaks down at depths greater than 6 or 7 meters where the penetrating non-field-sensitive component of the cosmic rays becomes an important factor of the total ionization. This similarity in the behavior of the radiation at 3 or 4 meters and 6 or 7 meters seems to indicate that the discrepancy near sea level cannot be explained by the addition of a small penetrating component whose influence extends to sea level but that a rather more fundamental modification or extension of the interpretation must be made.

## 4. The East-West Effect and the Longitude Effect

Both of these effects are best observable at the magnetic equator and both must be considered as a part of the field sensitive subdivision of cosmic-ray phenomena. They are here treated together because the understanding of the former should carry with it that of the latter also.

Johnson[13] has measured with very great care the east-west effect in Peru, in Mexico and in the United States both at sea level and at altitudes up to 4300 meters. By comparing the excess of west over east counts as the amount of at-

[10] G. Pfotzer, Zeits. f. Physik **102**, 41 (1936).

[11] I. S. Bowen, R. A. Millikan and H. V. Neher, Phys. Rev. **46**, 646 (1934).

[12] R. H. Woodward, Phys. Rev. **49**, 711 (1936) and H. J. Braddock and C. W. Gilbert, Proc. Roy. Soc. **156**, 570 (1936).

[13] T. H. Johnson, Phys. Rev. **48**, 287 (1935).

mosphere through which the particles have passed is varied by changing the zenith angle and also by changing the elevation of the observing station, he has computed the absorption of the atmosphere for the particles producing the east-west effect. He found this coefficient to vary between 0.33 and 0.53 per meter of water. These observations are also in substantial agreement with a fairly extended series of measurements on the east-west effect made by Neher in India in October 1936. The point upon which we would here lay emphasis is the approximate agreement between this coefficient of absorption of the particles which give rise to the east-west effect and the apparent coefficient of absorption of the $10^4$ Mev electrons which give rise to the lower curve of Fig. 4, namely 0.54 per meter of water. This general agreement seems to require that the east-west effect like the latitude effect be due to incoming particles of the electronic type, in this case positrons rather than protons. The net result then of this whole study of the east-west effect in its relation to the latitude effect is to indicate that the particles responsible for this east-west effect are positive electrons. Further as observed above it does not even require accurate analysis to show that they cannot be protons for if protons or any other similarly penetrating particles were found in appreciable numbers in the incoming swarm of charged particles, these penetrating particles would be found in abundance at zenith angles between, say, 75° and 90°, where in fact the number of incoming cosmic rays at sea level is very small.

We reach the conclusion then that for the understanding of latitude effects, east-west effects and longitude effects, or in a word for the interpretation of all field sensitive phenomena we require only incoming electrons (+ or −) and if protons or other penetrating particles are present at all they have a negligible influence upon measuring instruments of either the electroscope or the counter types.

In conclusion the authors wish to express their indebtedness to Dr. S. K. Haynes for preparing the condensers used in these electroscopes and otherwise assisting in the preparation for the flights. We also wish to make grateful acknowledgement to the Carnegie Corporation of New York and the Carnegie Institution of Washington for providing the funds which made this investigation possible.

---

JULY 15, 1937 PHYSICAL REVIEW VOLUME 52

# The Near Infrared Absorption Band of Liquid Water at 1.79$\mu$

J. R. COLLINS
*Cornell University, Ithaca, New York*

(Received May 20, 1937)

The near infrared absorption band of liquid water at 1.79$\mu$ has been studied at various temperatures. No apparent changes in the band were detected in the temperature range from 4°C to 137°C.

## INTRODUCTION

RECENTLY, Kellner[1] has raised a doubt concerning the existence of the weak absorption band of liquid water at 1.79$\mu$ which was discovered and reported by Ellis.[2] The presence of this band is of considerable interest in connection with the classification of the near infrared absorption bands of liquid water. If this band really exists, it is the second band to be found in the absorption spectrum of liquid water which has not been found in the spectrum of the vapor phase. The other such band is the well-known one at 4.7$\mu$.

To classify all the bands except the three fundamental vibrational bands of the water molecule it is customary to regard them as harmonic or combination bands of the fundamental bands. Since these fundamental bands are located at 2.8$\mu$, 2.9$\mu$, and 6.1$\mu$, respectively, it is evident

[1] Kellner, Proc. Roy. Soc. **159**, 410 (1937).
[2] Ellis, Phys. Rev. **38**, 693 (1931).

that this method of classification will not serve for the bands at 1.79$\mu$ and 4.7$\mu$. For their classification Ellis assumed the existence of a band of liquid water (a band due to either hindered rotation or to vibration of one water molecule against another) whose frequency was the difference between the frequency of the lowest vibrational band and that of the 4.7$\mu$ band. Then the 1.79$\mu$ band was ascribed to a combination of the two vibrational bands at 6.1$\mu$ and 2.9$\mu$ together with this newly assumed band at about 20$\mu$.

Ellis pointed out that the band at 1.79$\mu$ was very weak and situated near a very strong absorption band with a maximum at 1.96$\mu$. Hence a spectrometer with fairly good resolving power is needed to observe the weak band. The present author has just assembled a mirror spectrometer with a Pellin-Broca prism of dense flint glass which permits observations from the visible part of the spectrum to about 2.2$\mu$. The slit width is small enough to reveal the weak band at 1.79$\mu$ and it was thought worth while to study the band quantitatively at various temperatures to find out if any information could be obtained which would aid in establishing its classification.

## Experimental Procedure

The slit width of the spectrometer was such that about 100 angstroms was included in it at a wave-length of 1.80$\mu$. Thus the practical resolving power is determined by the width of the slit. To test this resolving power the shape of the curve was studied when the thermopile readings were plotted against wave-length for several single emission lines from the mercury arc. Also the absorption spectrum of an organic liquid was compared with the results obtained with a grating spectrometer of much greater resolving power. In both cases it was found that the resolving power of the present instrument was that determined by the slit width.

The absorption cells were made by clamping plates of plane parallel glass on either face of annular rings made from plane parallel plates of glass. The cells were so mounted that they could be moved into or out of a beam of collimated radiation from a straight filament incandescent lamp. The image of this filament was then focused on the entrance slit of the spectrometer. A linear thermopile connected to a galvanometer served to measure the intensity of the radiation reaching the exit slit of the spectrometer. For each setting of the spectrometer throughout the spectrum readings were taken with the specimen in the beam and with it out of the beam. The ratio of the first reading to the second is the fractional transmission of the cell.

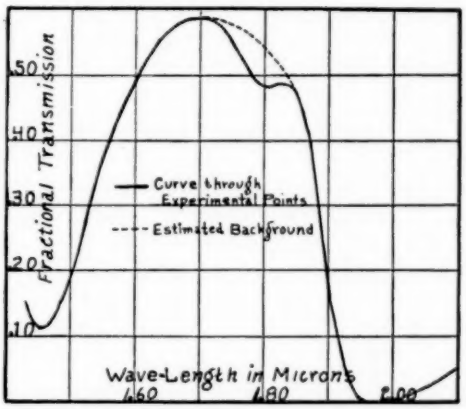


Fig. 1. The fractional transmission of liquid water at 4°C. Thickness of the water was 0.068 cm.

The temperature of the cell was varied by placing it in a double walled metal tube which could be heated electrically or cooled by ice water. Transmission data were taken for several thicknesses of cell ranging from 0.0060 cm to 0.400 cm. It was found that a thickness of somewhat less than a tenth of a centimeter gave the best results, so that two different cells of thicknesses 0.068 cm and 0.069 cm, respectively, were used at various temperatures ranging from 4°C to 137°C. Unfortunately, the intense absorption band on the long wave-length side of the band being studied shifts toward shorter wave-lengths as the temperature rises, so that only at the lowest temperatures is the weak band at all well resolved. However, even at the highest temperature there is no question as to the presence of the band.

In Fig. 1 a curve is drawn between the fractional transmission of the water and wave-length. No attempt is made to show the individual points as they lie too close together. It will be noticed that, at this temperature (4°C), the band is nearly resolved. Fig 1 indicates also the relative intensities of the weak band and the intense bands on either side of it.

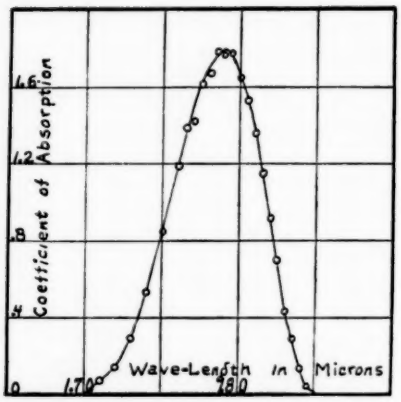


FIG. 2. The absorption band of liquid water at 1.79$\mu$ corrected for background absorption.

In order to compare the results at various temperatures an attempt was made to obtain the absorption curve due to this band alone. Accordingly a curve was drawn to a large scale and a curve drawn which was estimated to be the background due to the intense band on the long wave-length side. The dotted curve in Fig. 1 indicates such a curve. Then the ratio of the ordinate of the experimental curve to that of the dotted curve was taken as the transmission curve of the water corresponding to the weak absorption band. The absorption coefficient was calculated according to the usual formula

$$k = (1/td) \log_e (I_1/I_2),$$

where $t$ is the thickness of the water, $d$ is the density of the water, $I_1$ is the ordinate of the dotted curve and $I_2$ is the ordinate of the experimental curve. This procedure corrects for reflection at the cell surfaces.

When curves were plotted with $k$ as ordinates and wave-length as abscissae it was found that, within the accuracy of the experimental determination, there was no difference between the curves taken at different temperatures. Fig. 2 is accordingly plotted with ordinates taken as the average values of $k$ for all temperatures. Results obtained at room temperature through the use of cell thicknesses of 0.0060 cm and 0.400 cm were also in agreement within the accuracy of the experiment. The intensity of this band as compared with that on the long wave-length side of it is indicated by the comparison of the maximum absorption coefficients, namely, 1.8 and 120.

## CONCLUSIONS

The results of the present paper confirm the existence of the weak absorption band of liquid water at 1.79$\mu$ as reported by Ellis. The classification of this band as made by Ellis is further strengthened by the fact that Hibben[3] has found a low frequency Raman line for liquid water which would correspond to the assumed band near 20$\mu$. The fact that the band at 1.79$\mu$ does not show any marked change with temperature is in agreement with the small changes found[4] for the two bands on either side of it. Small changes due to temperature variation would probably be beyond the accuracy of the present measurements.

The fact that Kellner did not find this weak band in his experiments can apparently be explained only by the fact that his spectrometer had excessive stray radiation or that his resolving power was not as great as would be expected from his reported slit width.

[3] Hibben, J. Chem. Phys. **5**, 166 (1937).
[4] Collins, Phys. Rev. **26**, 771 (1925).

# Band Spectra and Energy of Dissociation of the Rubidium Molecule

NY TSI-ZÉ AND TSIEN SAN-TSIANG
*Institute of Physics, National Academy of Peiping, Peiping, China*
(Received March 18, 1937)

Measurements and vibrational analysis of the violet and blue band systems of $Rb_2$ have been made in absorption. Quantum numbers have been assigned to 118 and 160 bands in the two systems, respectively. The upper vibrational frequency of the violet system is 40.42 $cm^{-1}$ and that of the blue one, 36.46 $cm^{-1}$. The lower level, common to the two systems, is $^1\Sigma$ ground state, and its vibrational frequency is found to be 57.45 $cm^{-1}$. The energies of dissociation of the three states of the molecule have been determined by means of extrapolation, and the value for the ground state is $0.49 \pm 0.02$ volt. A green edge of the blue system at 5032A has been observed.

## INTRODUCTION

THE band spectra of $Rb_2$ have been observed by Carter,[1] Bevan,[2] Dunoyer,[3] McLennan and Ainslie,[4] and Walter and Barratt[5] with instruments of low dispersion. Matuyama[6] has studied the bands in absorption and classified them into four systems. Two systems in the red and infrared regions, associated with the doublet of the first member of the principal series, have been found to be due to the transitions of $^1\Pi \leftarrow {}^1\Sigma$ and $^1\Sigma \leftarrow {}^1\Sigma$, respectively. The other two systems in the blue and violet regions, on the longer wave-length side of the second member of the principal series, appeared only in a denser vapor. Matuyama has reported an analysis of these systems but has not found a value of the energy of dissociation.

Recently Kusch[7] measured and analyzed the magnetic rotation spectrum and absorption spectrum in the region 6500–7100A with instrument of high dispersion, but the data were still not extensive enough for the determination of an accurate value of energy of dissociation.

The purpose of this investigation is to obtain a complete analysis of the violet and blue systems of $Rb_2$ and to extend the band systems to high quantum numbers in order to yield a reliable value of the energy of dissociation.

[1] Carter, Physik. Zeits. **11**, 632 (1910).
[2] Bevan, Proc. Roy. Soc. London **85**, 61 (1911).
[3] Dunoyer, Le Rad. **9**, 218 (1912).
[4] McLennan and Ainslie, Proc. Roy. Soc. London **103**, 304 (1923).
[5] Walter and Barratt, Proc. Roy. Soc. London **119**, 257 (1928).
[6] Matuyama, Tohoku Imp. Univ. Sci. Rep. **23**, 308 (1934).
[7] Kusch, Phys. Rev. **49**, 218 (1936).

## EXPERIMENTAL

A steel absorption tube, 120 cm long, 3 cm internal diameter, was used with quartz windows at the ends. The tube was electrically heated on the main part and cooled near the ends by a circulation of water. In order to prevent quick distillation of the metallic vapor, the tube was filled with nitrogen at 4 cm Hg pressure at room temperature. The introduction of the gas had not affected the absorption spectra materially. The metal was prepared by reducing rubidium chloride with metallic calcium. The temperature of the absorbing vapor in our experiments varied from 350°C to 400°C, as measured by a steel-constantan thermocouple. An incandescent lamp was used as a source of continuous spectrum. The spectrograms were taken in the second-order spectrum with a 3 m concave grating of Eagle mounting, the dispersion of which was about 2.8A/mm. An iron arc was taken as the comparison spectrum.

## RESULTS

### A. The violet system

At about 350°C, the band system begins to appear, having its maximum intensity at 4300A. With increasing temperature, this system spreads out in both directions. On the short wave-length side it approaches rapidly to the 4202 and 4216A doublet. On the long wave-length side it terminates, gradually with decreasing intensity, at the doublet 4555 and 4593A of caesium which appeared as impurity. All band heads are rather sharp, and the bands are degraded to the red. The rotational structure can be seen on the plate

but it is not sufficiently resolved to be measured. We have measured 118 band heads in the system and assigned vibrational quantum numbers to all of them.

The frequencies of the bands can be represented by the following equation found by the method of least squares

$$\nu = 22777.5 + [40.42(v'+\tfrac{1}{2}) - 0.0745(v'+\tfrac{1}{2})^2 - 0.00144(v'+\tfrac{1}{2})^3] - [57.45(v''+\tfrac{1}{2}) - 0.104(v''+\tfrac{1}{2})^2]. \quad (1)$$

Since the values of $\omega_e$ and $x_e\omega_e$ in the lower state are approximately the same as those of the ground state of the red system (57.31 and 0.105) obtained by Kusch,[7] the lower state of the system is therefore the $^1\Sigma$ ground state.

The measured frequencies ($\nu_{obs.}$), the estimated intensities ($I$), the assigned quantum numbers ($v'$, $v''$) and the differences ($\Delta\nu$) between the measured frequencies and those calculated from the Eq. (1) are given in Table I. The average value of $|\Delta\nu|$ is 0.68 cm$^{-1}$.

An improved Franck-Condon[8] diagram for the system is shown in Fig. 1. The diagram appears to be normal.

## B. The blue system

This band system begins to appear at 360°C, a temperature a little higher than that for the violet system, having its maximum intensity at 4750A. With increasing temperature the system extends out in both directions, slowly toward the red and rapidly toward the violet. On the short wave-length side it approaches to 4700A with apparently decreasing intensity. On the long

[8] Loomis and Nusbaum, Phys. Rev. **38**, 1447 (1931).

TABLE I. *Band heads in the violet system of $Rb_2$.*

| $\nu$ observed | $I$ | $v'$ | $v''$ | $\Delta\nu$ $\nu_{obs.}-\nu_{cal.}$ | $\nu$ observed | $I$ | $v'$ | $v''$ | $\Delta\nu$ $\nu_{obs.}-\nu_{cal.}$ | $\nu$ observed | $I$ | $v'$ | $v''$ | $\Delta\nu$ $\nu_{obs.}-\nu_{cal.}$ |
|---|---|---|---|---|---|---|---|---|---|---|---|---|---|---|
| 23673.3 | 3 | 24 | 0 | +0.1 | 23008.7 | 6 | 6 | 0 | +0.7 | 22565.7 | 5 | 2 | 5 | +0.4 |
| 23649.3 | 3 | 25 | 1 | −0.6 | 22989.9 | 6 | 7 | 1 | 0.0 | 22549.8 | 3 | 3 | 6 | +0.8 |
| 23638.9 | 4 | 23 | 0 | +0.1 | 22972.1 | 8 | 8 | 2 | +0.3 | 22533.2 | 2 | 4 | 7 | +0.5 |
| 23615.9 | 4 | 24 | 1 | −0.1 | 22969.3 | 4 | 5 | 0 | +0.7 | 22525.6 | 2 | 1 | 5 | +0.4 |
| 23604.2 | 5 | 22 | 0 | +0.1 | 22953.9 | 3 | 9 | 3 | +0.2 | 22509.2 | 4 | 2 | 6 | +0.1 |
| 23581.9 | 5 | 23 | 1 | +0.3 | 22950.9 | 4 | 6 | 1 | +0.1 | 22501.7 | 3 | 6 | 9 | +1.4 |
| 23569.0 | 5 | 21 | 0 | 0.0 | 22934.6 | 4 | 10 | 4 | −1.0 | 22494.4 | 2 | 3 | 7 | +1.4 |
| 23547.5 | 5 | 22 | 1 | +0.6 | 22933.0 | 8 | 7 | 2 | +0.2 | 22484.9 | 1 | 0 | 5 | 0.0 |
| 23533.4 | 6 | 20 | 0 | −0.3 | 22929.3 | 5 | 4 | 0 | +0.3 | 22468.9 | 4 | 1 | 6 | −0.1 |
| 23512.3 | 5 | 21 | 1 | +0.5 | 22915.3 | 3 | 8 | 3 | +0.3 | 22453.7 | 3 | 2 | 7 | +0.6 |
| 23497.4 | 7 | 19 | 0 | −0.6 | 22893.7 | 7 | 6 | 2 | 0.0 | 22446.6 | 2 | 6 | 10 | +1.7 |
| 23476.4 | 5 | 20 | 1 | −0.1 | 22876.2 | 4 | 7 | 3 | +0.3 | 22437.3 | 2 | 3 | 8 | +0.1 |
| 23461.4 | 7 | 18 | 0 | −0.5 | 22872.1 | 3 | 4 | 1 | +0.3 | 22428.5 | 1 | 0 | 6 | −0.2 |
| 23440.2 | 5 | 19 | 1 | −0.6 | 22854.9 | 5 | 5 | 2 | +0.6 | 22412.8 | 3 | 1 | 7 | −0.2 |
| 23425.0 | 7 | 17 | 0 | −0.6 | 22837.0 | 7 | 6 | 3 | +0.1 | 22397.7 | 2 | 2 | 8 | +0.4 |
| 23403.8 | 5 | 18 | 1 | −0.9 | 22815.0 | 3 | 4 | 2 | +0.3 | 22380.9 | 2 | 3 | 9 | −0.7 |
| 23388.3 | 8 | 16 | 0 | −0.7 | 22802.3 | 3 | 8 | 5 | +0.3 | 22371.8 | 2 | 0 | 7 | −0.9 |
| 23367.3 | 6 | 17 | 1 | −1.1 | 22797.9 | 6 | 5 | 3 | +0.4 | 22357.1 | 3 | 1 | 8 | −0.1 |
| 23363.8 | 3 | 20 | 3 | +1.2 | 22792.7 | 4 | 2 | 1 | +0.5 | 22342.2 | 2 | 2 | 9 | +0.5 |
| 23351.1 | 9 | 15 | 0 | −0.9 | 22783.6 | 2 | 9 | 6 | −0.9 | 22326.5 | 1 | 3 | 10 | +0.3 |
| 23330.3 | 6 | 16 | 1 | −1.5 | 22775.7 | 3 | 3 | 2 | +0.7 | 22316.0 | 2 | 0 | 8 | −0.9 |
| 23313.5 | 10 | 14 | 0 | −1.3 | 22769.6 | 3 | 0 | 0 | +0.6 | 22302.1 | 3 | 1 | 9 | +0.5 |
| 23293.2 | 6 | 15 | 1 | −1.6 | 22758.6 | 6 | 4 | 3 | +0.7 | 22286.3 | 2 | 2 | 10 | 0.0 |
| 23275.5 | 9 | 13 | 0 | −1.8 | 22735.6 | 4 | 2 | 2 | +0.5 | 22261.2 | 2 | 0 | 9 | −0.1 |
| 23255.7 | 6 | 14 | 1 | −1.9 | 22719.0 | 3 | 3 | 3 | +0.8 | 22246.3 | 2 | 1 | 10 | +0.1 |
| 23255.1 | 4 | 17 | 3 | +0.6 | 22712.1 | 2 | 0 | 1 | +0.3 | 22231.3 | 1 | 2 | 11 | +0.1 |
| 23237.7 | 9 | 12 | 0 | −1.9 | 22702.4 | 5 | 4 | 4 | +1.1 | 22215.8 | 1 | 3 | 12 | −1.3 |
| 23218.4 | 6 | 13 | 1 | −1.7 | 22695.8 | 4 | 1 | 2 | +0.8 | 22206.1 | 2 | 0 | 10 | +0.2 |
| 23199.9 | 9 | 11 | 0 | −1.7 | 22678.6 | 3 | 2 | 3 | +0.3 | 22191.3 | 1 | 1 | 11 | +0.2 |
| 23181.1 | 7 | 12 | 1 | −1.3 | 22670.0 | 2 | 6 | 6 | +2.3 | 22176.2 | 1 | 2 | 12 | −1.0 |
| 23161.9 | 6 | 10 | 0 | −1.4 | 22662.6 | 5 | 3 | 4 | +1.0 | 22150.8 | 2 | 0 | 11 | 0.0 |
| 23145.6 | 4 | 14 | 3 | +1.9 | 22652.7 | 4 | 7 | 7 | +1.9 | 22136.0 | 1 | 1 | 12 | −1.1 |
| 23143.5 | 9 | 11 | 1 | −0.9 | 22646.2 | 3 | 4 | 5 | +1.3 | 22121.1 | 1 | 2 | 13 | −1.3 |
| 23123.5 | 6 | 9 | 0 | −1.3 | 22638.9 | 3 | 1 | 3 | +0.7 | 22095.8 | 2 | 0 | 12 | −1.0 |
| 23105.5 | 10 | 10 | 1 | −0.6 | 22633.8 | 2 | 8 | 8 | −0.2 | 22081.4 | 1 | 1 | 13 | −0.9 |
| 23085.0 | 6 | 8 | 0 | −1.1 | 22622.3 | 2 | 2 | 4 | +0.6 | 22067.1 | 1 | 2 | 14 | −0.8 |
| 23067.6 | 9 | 9 | 1 | 0.0 | 22613.2 | 2 | 6 | 7 | +1.5 | 22040.9 | 1 | 0 | 13 | −1.1 |
| 23047.2 | 6 | 7 | 0 | +0.1 | 22605.4 | 5 | 3 | 5 | +0.2 | 22026.9 | 1 | 1 | 14 | −0.9 |
| 23029.0 | 9 | 8 | 1 | +0.1 | 22590.2 | 3 | 4 | 6 | +1.5 | | | | | |
| 23010.6 | 4 | 9 | 2 | +0.1 | 22581.8 | 2 | 1 | 4 | +0.2 | | | | | |

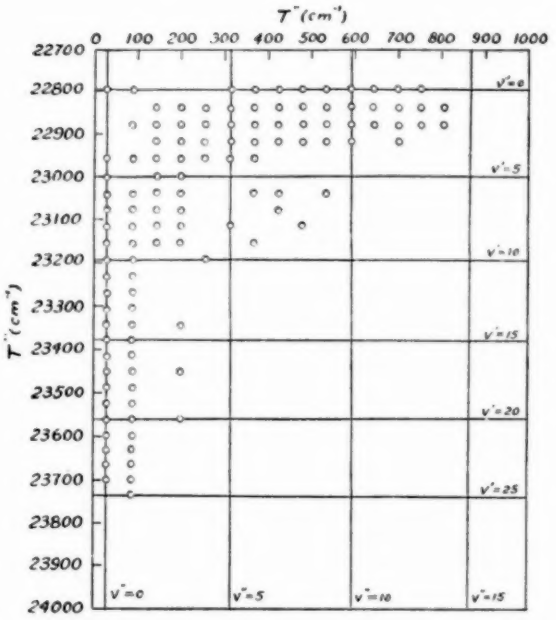


FIG. 1. Improved Franck-Condon diagram for the violet system.

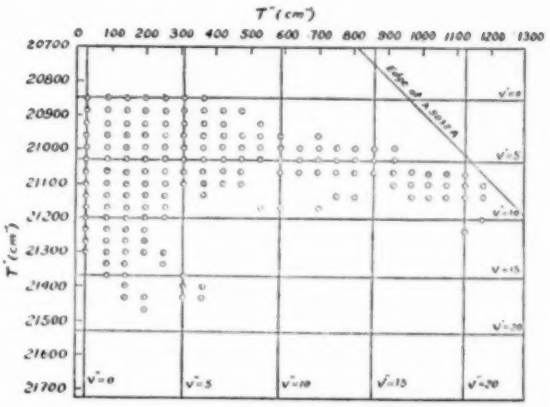


FIG. 2. Improved Franck-Condon diagram for the blue system.

wave-length side it terminates abruptly at higher temperatures (>380°C) in an edge at 5032A, just in the same manner as the 5223A edge of the blue-green band system of $Cs_2$ reported by Loomis and Kusch.[9]

All band heads in the system, except those in the region of longer wave-length appearing at higher temperatures, are sharp. The bands are degraded to the red. We have measured 167 heads and assigned vibrational quantum numbers to 160 of them.

The frequencies of all assigned bands can be represented by the following equation found by the method of least squares

$$\nu = 20835.1 + [36.46(v'+\tfrac{1}{2}) - 0.124(v'+\tfrac{1}{2})^2] - [56.78(v''+\tfrac{1}{2}) - 0.0785(v''+\tfrac{1}{2})^2 - 0.00083(v''+\tfrac{1}{2})^3]. \quad (2)$$

In the blue system the lower vibrational quantum numbers extends far to 21. It is hard to represent the lower vibrational terms satisfactorily by a polynomial of second degree as in the case of the violet system. As the vibrational frequencies in Eqs. (1) and (2) are approximately equal, we may therefore conclude that the lower state in the blue system as well as that in the violet system is the $^1\Sigma$ ground state. In the case of $K_2$, Loomis and Nusbaum[10] have pointed out that the polynomial of low degree could be considered as the best available representation of the constants of the molecule near the equilibrum point, whereas the extrapolation to dissociation could be based on the equation of higher orders. According to this idea, we regard 57.45 $cm^{-1}$ as the lower vibrational frequency and use the constants in Eq. (2) for the determination of energy of dissociation of the ground state.

The measured frequencies ($\nu_{obs.}$), the estimated intensities ($I$), the assigned quantum numbers ($v'$, $v''$) and the difference ($\Delta\nu$) between the measured frequencies and those calculated from Eq. (2) are given in Table II. The unidentified bands are also included. The mean value of $|\Delta\nu|$ is 0.66 $cm^{-1}$.

The upper and lower vibrational terms of the bands are plotted in Fig. 2, with the green edge at 5032A represented by a straight line on the upright corner. The diagram is also normal. It will be noted that in this case the right arm of the locus is more extensive, while in the violet system, on the contrary, the left is more extensive. The blue system extends the lower vibrational quantum numbers to 21 while the violet system extends the upper vibrational quantum numbers to 25. These two extensions of the vibrational quantum numbers are all favorable for the determination of energy of dissociation.

[9] Loomis and Kusch, Phys. Rev. **46** 292 (1934).

[10] Loomis and Nusbaum, Phys. Rev. **39**, 89 (1932).

TABLE II. *Band heads in the violet system of $Rb_2$.*

| $\nu$ observed | $I$ | $v'$ | $v''$ | $\Delta\nu$ $\nu_{obs.}-\nu_{cal.}$ | $\nu$ observed | $I$ | $v'$ | $v''$ | $\Delta\nu$ $\nu_{obs.}-\nu_{cal.}$ | $\nu$ observed | $I$ | $v'$ | $v''$ | $\Delta\nu$ $\nu_{obs.}-\nu_{cal.}$ |
|---|---|---|---|---|---|---|---|---|---|---|---|---|---|---|
| 21293.0 | 0 | 17 | 2 | −0.6 | 20890.1 | 6 | 5 | 2 | −0.3 | 20504.9 | 5 | 2 | 7 | +0.5 |
| 21284.1 | 0 | 15 | 1 | −1.3 | 20882.2 | 5 | 8 | 4 | +0.1 | 20501.1 | 4 | 5 | 9 | +0.8 |
| 21275.1 | 0 | 13 | 0 | −1.0 | 20876.8 | 5 | 3 | 1 | +0.6 | 20487.3 | 3 | 0 | 6 | −0.4 |
| 21268.7 | 0 | 18 | 3 | −0.6 | 20868.7 | 5 | 6 | 3 | −0.3 | 20486.1 | 6 | 3 | 8 | +1.4 |
| 21260.6 | 1 | 16 | 2 | −0.7 | 20861.4 | 7 | 1 | 0 | +0.3 | 20481.5 | 5 | 6 | 10 | +1.3 |
| 21250.9 | 1 | 14 | 1 | −1.7 | 20854.7 | 6 | 4 | 2 | −0.4 | 20474.9 | 5 | 9 | 12 | −0.4 |
| 21242.1 | 1 | 12 | 0 | −0.9 | 20847.6 | 6 | 7 | 4 | −0.1 | 20468.3 | 4 | 1 | 7 | −0.1 |
| 21236.5 | 1 | 17 | 3 | −0.8 | 20844.6 | 4 | | | | 20466.3 | 6 | 4 | 9 | +1.3 |
| 21227.8 | 2 | 15 | 2 | −1.1 | 20840.0 | 9 | 2 | 1 | −0.5 | 20446.3 | 5 | 5 | 10 | +1.0 |
| 21218.1 | 2 | 13 | 1 | −1.4 | 20833.7 | 6 | 5 | 3 | −0.4 | 20431.1 | 5 | 3 | 9 | +1.5 |
| 21208.6 | 2 | 11 | 0 | −0.9 | 20825.2 | 7 | 0 | 0 | +0.3 | 20426.5 | 4 | 6 | 11 | +1.1 |
| 21195.1 | 2 | 14 | 2 | −1.0 | 20819.2 | 5 | 3 | 2 | −0.5 | 20412.8 | 3 | 1 | 8 | −0.2 |
| 21185.1 | 2 | 12 | 1 | −1.3 | 20812.6 | 5 | 6 | 4 | −0.3 | 20411.3 | 6 | 4 | 10 | +1.3 |
| 21175.1 | 2 | 10 | 0 | −0.7 | 20804.3 | 8 | 1 | 1 | −0.2 | 20395.1 | 4 | 2 | 9 | +1.2 |
| 21162.1 | 3 | 13 | 2 | −0.9 | 20798.5 | 7 | 4 | 3 | −0.3 | 20391.5 | 5 | 5 | 11 | +1.0 |
| 21152.1 | 3 | 11 | 1 | −0.8 | 20791.7 | 4 | 7 | 5 | −0.1 | 20385.3 | 4 | 8 | 13 | −0.5 |
| 21141.3 | 4 | 9 | 0 | −0.5 | 20783.2 | 5 | 2 | 2 | −0.8 | 20376.3 | 5 | 3 | 10 | +1.7 |
| 21128.5 | 5 | 12 | 2 | −1.4 | 20777.6 | 4 | 5 | 4 | −0.4 | 20371.9 | 3 | 6 | 12 | +1.0 |
| 21124.1 | 4 | 17 | 5 | −1.2 | 20770.2 | 4 | 8 | 6 | −0.2 | 20356.3 | 5 | 4 | 11 | +1.1 |
| 21118.6 | 5 | 10 | 1 | −0.6 | 20767.8 | 5 | 0 | 1 | −0.5 | 20336.7 | 5 | 5 | 12 | +0.7 |
| 21107.6 | 6 | 8 | 0 | 0.0 | 20763.0 | 6 | 3 | 3 | −0.4 | 20330.7 | 4 | 8 | 14 | −1.0 |
| 21105.6 | 4 | 13 | 3 | −1.1 | 20756.5 | 5 | 6 | 5 | −0.5 | 20317.6 | 4 | 6 | 13 | +1.0 |
| 21095.1 | 8 | 11 | 2 | −1.3 | 20747.3 | 8 | 1 | 2 | −0.7 | 20301.6 | 4 | 4 | 12 | +0.9 |
| 21091.9 | 5 | 16 | 5 | −1.1 | 20742.6 | 6 | 4 | 4 | −0.1 | 20282.4 | 4 | 5 | 13 | +0.7 |
| 21084.6 | 6 | 9 | 1 | −0.6 | 20736.2 | 5 | 7 | 6 | +0.2 | 20266.4 | 4 | 3 | 12 | +1.1 |
| 21082.0 | 5 | 14 | 4 | −1.7 | 20727.5 | 6 | 2 | 3 | −0.2 | 20263.2 | 4 | 6 | 14 | +0.7 |
| 21073.6 | 7 | 7 | 0 | +0.4 | 20721.3 | 5 | 5 | 5 | −0.8 | 20247.1 | 4 | 4 | 13 | +0.7 |
| 21072.0 | 5 | 12 | 3 | −1.6 | 20711.3 | 7 | 0 | 2 | −0.5 | 20228.1 | 4 | 5 | 14 | +0.5 |
| 21068.6 | 5 | 17 | 6 | −0.9 | 20707.4 | 6 | 3 | 4 | +0.1 | 20209.0 | 4 | 6 | 15 | +0.4 |
| 21062.1 | 10 | 10 | 2 | −0.6 | 20701.3 | 5 | 6 | 6 | +0.1 | 20192.8 | 4 | 4 | 14 | +0.5 |
| 21059.3 | 5 | 15 | 5 | −1.3 | 20691.3 | 6 | 1 | 3 | −0.4 | 20190.7 | 4 | 7 | 16 | +0.9 |
| 21051.2 | 9 | 8 | 1 | +0.2 | 20686.4 | 5 | 4 | 5 | −0.4 | 20182.4 | | | | |
| 21039.3 | 7 | 6 | 0 | +0.9 | 20680.4 | 4 | 7 | 7 | −0.1 | 20173.9 | 4 | 5 | 15 | +0.2 |
| 21038.8 | 6 | 11 | 3 | −1.3 | 20671.6 | 6 | 2 | 4 | 0.0 | 20172.3 | 3 | 8 | 17 | +1.5 |
| 21036.2 | 4 | 16 | 6 | −1.0 | 20666.2 | 5 | 5 | 6 | −0.1 | 20155.4 | 4 | 6 | 16 | +0.4 |
| 21028.7 | 8 | 9 | 2 | 0.0 | 20654.8 | 7 | 0 | 3 | −0.7 | 20138.8 | 3 | 4 | 15 | +0.4 |
| 21017.1 | 7 | 7 | 1 | +0.5 | 20651.3 | 6 | 3 | 5 | −0.1 | 20137.3 | 4 | 7 | 17 | +0.9 |
| 21005.4 | 6 | 10 | 3 | −1.0 | 20645.6 | 5 | 6 | 7 | −0.1 | 20120.2 | 4 | 5 | 16 | +0.1 |
| 21004.2 | 6 | 5 | 0 | +0.7 | 20639.4 | 5 | 9 | 9 | −0.6 | 20119.2 | 3 | 8 | 18 | +1.5 |
| 20994.6 | 7 | 8 | 2 | +0.1 | 20635.2 | 6 | 1 | 4 | −0.4 | 20113.3 | 3 | 11 | 20 | −0.7 |
| 20982.1 | 8 | 6 | 1 | +0.3 | 20631.4 | 5 | 4 | 6 | +0.4 | 20109.8 | | | | |
| 20972.1 | 6 | 9 | 3 | −0.3 | 20625.1 | 4 | 7 | 8 | 0.0 | 20102.0 | 4 | 6 | 17 | +0.4 |
| 20968.8 | 8 | 4 | 0 | +0.6 | 20616.3 | 6 | 2 | 5 | +0.6 | 20085.0 | 3 | 4 | 16 | +0.2 |
| 20960.1 | 6 | 7 | 2 | 0.0 | 20610.9 | 5 | 5 | 7 | +0.1 | 20084.2 | 4 | 7 | 18 | +0.9 |
| 20955.4 | 6 | | | | 20598.8 | 7 | 0 | 4 | −0.6 | 20066.3 | 4 | 8 | 19 | +1.5 |
| 20949.6 | 6 | 10 | 4 | −0.7 | 20596.3 | 5 | 3 | 6 | +0.7 | 20049.0 | 4 | 6 | 18 | +0.5 |
| 20947.1 | 7 | 5 | 1 | +0.2 | 20590.1 | 4 | 6 | 8 | −0.2 | 20031.3 | 4 | 7 | 19 | +0.9 |
| 20942.1 | 5 | | | | 20584.5 | 4 | 9 | 10 | +0.9 | 20026.2 | 4 | 10 | 21 | −1.7 |
| 20938.5 | 5 | 8 | 3 | +0.3 | 20579.8 | 6 | 1 | 5 | +0.1 | 20013.8 | 4 | 8 | 20 | +1.7 |
| 20933.2 | 8 | 3 | 0 | +0.4 | 20576.1 | 5 | 4 | 7 | +0.6 | 20009.6 | | | | |
| 20925.2 | 6 | 6 | 2 | −0.1 | 20560.4 | 6 | 2 | 6 | +0.5 | 19996.2 | 4 | 6 | 19 | +0.6 |
| 20920.7 | 5 | | | | 20555.7 | 5 | 5 | 8 | +0.3 | 19978.7 | 4 | 7 | 20 | +0.8 |
| 20916.2 | 6 | 9 | 4 | −0.1 | 20543.1 | 6 | 0 | 5 | −0.4 | 19961.4 | 4 | 8 | 21 | +1.8 |
| 20911.9 | 5 | 4 | 1 | +0.3 | 20541.1 | 6 | 3 | 7 | +1.0 | 19943.8 | 4 | 6 | 20 | +0.9 |
| 20903.7 | 5 | 7 | 3 | −0.1 | 20523.8 | 4 | 1 | 6 | −0.1 | 19926.7 | 4 | 7 | 21 | +1.5 |
| 20897.3 | 7 | 2 | 0 | +0.2 | 20521.1 | 5 | 4 | 8 | +1.0 | | | | | |

### C. The products and energies of dissociation

It is well known that the energy of dissociation of molecules may be obtained by means of extrapolation. The vibrational intervals $\Delta T$ are plotted against the upper vibrational terms for the violet system in Fig. 3, and against the upper and lower vibrational terms for the blue system in Figs. 4 and 5, respectively. The circles represent the experimental points, the full curves correspond to the intervals as well as terms calculated from Eqs. (1) and (2). As usually in cases of alkali molecules NaK, $Cs_2$[9, 11] etc., the

[11] Loomis and Arvin, Phys. Rev. **46**, 286 (1934).

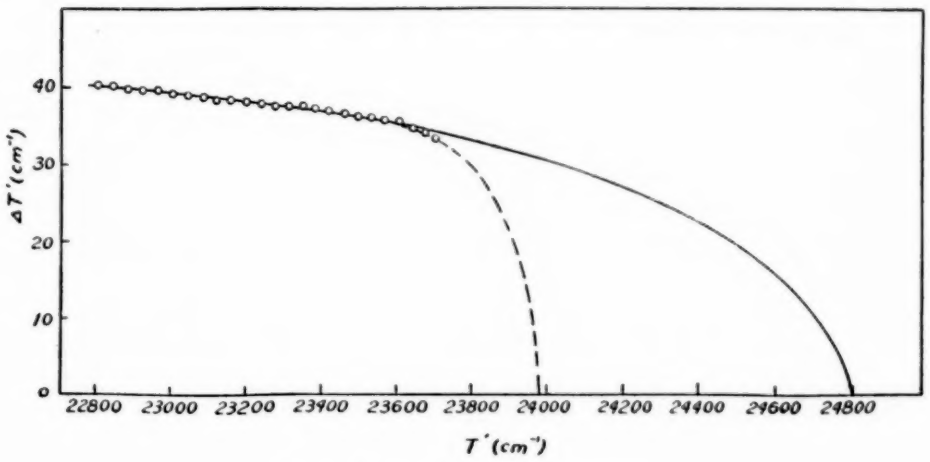


FIG. 3. $\Delta T'$ *vs.* $T'$ for the violet system.

last experimental points begin to drop below the curves so that the values of $T$ at which the curves strike the axes can be taken as the maximum values of the energies of dissociation. That is, $T_v' < 24800\,\text{cm}^{-1}$ for the violet system, $T_b' < 23520$ $\text{cm}^{-1}$ for the blue system and $T'' < 4250\ \text{cm}^{-1}$. On the other hand, since the experimental values of $T$ are far from converging, it seems probable that the minimum values of the energies of dissociation are given by the dashed curves, which yield $T_v' > 23980\ \text{cm}^{-1}$, $T_b' > 22270\ \text{cm}^{-1}$ and $T'' > 3500$ $\text{cm}^{-1}$.

Let us first take temporarily the mean value of $T'' = 3880\ \text{cm}^{-1}$ as the energy of dissociation of the lower state, $D_e''$, and see what will be the products of dissociation of the two upper states. The difference of $T'$ and $T''$ is the atomic energy $T_a$, so we have $20920\ \text{cm}^{-1} > T_a > 20100\ \text{cm}^{-1}$ for the violet system and $19640\ \text{cm}^{-1} > T_a > 18390$ $\text{cm}^{-1}$ for the blue system. The products of dissociation of the ground state of the molecule are two normal $(5s, {}^2S)$ rubidium atoms. From the limiting values of atomic energies, we may conclude that the upper state of the violet system dissociates into one atom in the normal state $(5s, {}^2S)$ and one atom in the excited state $(6s, {}^2S)$, while that of the blue system into one in the normal state and one in the excited state $(4d, {}^2D)$, though such transitions are forbidden in the atomic spectra.

Now we come to determine accurately the value of energy of dissociation of the ground state by using the known values of the atomic energies and the experimental data. From the lower state, we have $3500\ \text{cm}^{-1} < D_e'' < 4250\ \text{cm}^{-1}$, and from the upper states of the violet and blue systems we get $3850\ \text{cm}^{-1} < D_e'' < 4670\ \text{cm}^{-1}$ and $2920\ \text{cm}^{-1} < D_e'' < 4170\ \text{cm}^{-1}$, respectively. According to the three pairs of the limiting values of $D_e''$, we may conclude that

$$3850\ \text{cm}^{-1} < D_e'' < 4170\ \text{cm}^{-1}.$$

The actual energy of dissociation $D_0$ is thus given by

$$3820\ \text{cm}^{-1} < D_0'' < 4140\ \text{cm}^{-1},$$

or in the unit of electron volt,

$$0.47\ \text{volt} < D_0'' < 0.51\ \text{volt}.$$

We take the mean value $D_0'' = 0.49$ volt and feel confident that it is not in error by more than 0.02 volt.

From this value for the ground state, the

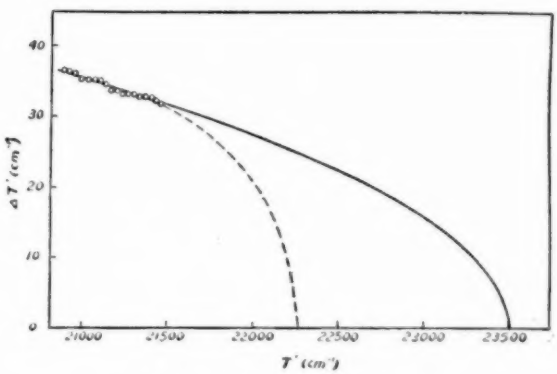


FIG. 4. $\Delta T'$ *vs.* $T'$ for the blue system.

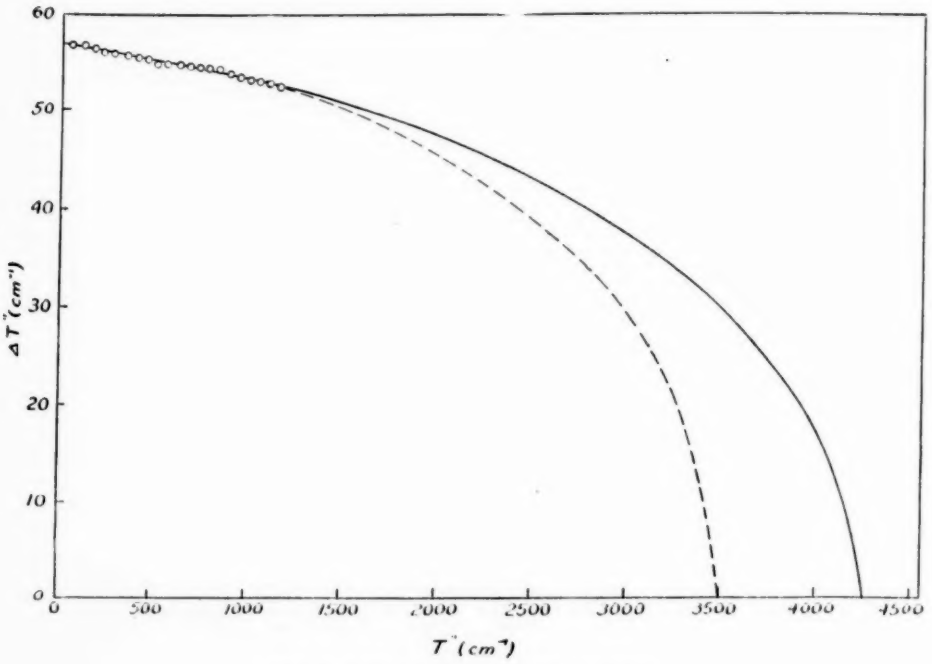


FIG. 5. $\Delta T''$ *vs.* $T''$ for the blue system.

energy of dissociation of the upper state of the violet system is calculated to be 0.17 volt and that of the blue system to be 0.31 volt.

## DISCUSSION

The value of energy of dissociation of the ground state of $Rb_2$ thus determined agrees, within experimental errors, with that obtained by interpolation from the energies of other alkali molecules (0.47 volt). Although the products and energies of dissociation of the upper states of the two systems are determined in this investigation, we still cannot draw any conclusion about the molecular states of the two levels.

The blue and violet systems of $Rb_2$ are similar to the blue band system of $K_2$ reported by Yamamoto[12] and the blue-green system of $Cs_2$ reported by Loomis and Kusch,[9] of which neither the energy of dissociation nor the molecular state was definitely determined. Owing to the similarity between the edge at 5223A of $Cs_2$ and the edges of $^1\Sigma \leftarrow {}^1\Sigma$ systems of $Li_2$, $Na_2$ and $K_2$, Loomis and Kusch thought that the blue-green system of $Cs_2$ was very likely a $^1\Sigma \leftarrow {}^1\Sigma$ system associated with the second doublet of the principal series of caesium. But this argument cannot hold, at least in the present case, because the necessary conditions for the existence of an edge explained by Loomis and Nile[13] namely, $\omega_e'' > \omega_e'$ and $D'' < D'$ are only half fulfilled. So the question about the molecular states of the systems is still open. We write arbitrarily $D \leftarrow {}^1\Sigma$ for the blue system and $E \leftarrow {}^1\Sigma$ for the violet system.

Finally let us compare our results with the work of Matuyama.[6] All band heads in his data coincide approximately with our strong heads, but none of the weaker bands in our data, especially those with high quantum numbers, has been observed by him. The analysis made by him appears to be erroneous partly due to the incompleteness of his data and partly due to the mistake in the arrangement of the square array.

[12] Yamamoto, Nat. Research Council Japan **5**, 146 (1929).

[13] Loomis and Nile, Phys. Rev. **32**, 873 (1932).

# Deep Terms in the Spectra of Sc VIII and Sc IX

P. GERALD KRUGER AND L. W. PHILLIPS
*Department of Physics, University of Illinois, Urbana, Illinois*

(Received May 18, 1937)

Twenty-three lines in the scandium spectrum have been identified as radiations connecting higher terms with the ground states of Sc VIII and Sc IX.

IN a previous paper[1] it was reported that the spectrum of scandium had been photographed with a twenty-one foot grazing incidence vacuum spectrograph, and a classification was given for lines arising from transitions to the ground state of Sc V. On the same spectrograms lines are found which have been identified as due to radiations from Sc VIII and Sc IX.

The ground state configuration of Sc VIII (isoelectronic with Si I) is $3s^23p^2$, yielding $^3P$, $^1D$, and $^1S$ terms. Above this are the configurations $3s3p^3$, $3s^23p3d$, and $3s^23p4s$ in the order named, each giving rise to several odd singlet and triplet terms. The transitions $3s^23p^2\,^3P-3s3p^3\,^3S^0$, $3s^23p^2\,^3P-3s^23p3d\,^3P^0$, and $3s^23p^2\,^3P-3s^23p4s\,^3P^0$ have been identified. These data are shown in Table I.

TABLE I. *Scandium VIII.*

| CONFIGURATION | $3s^23p^2\,^3P_0$ | | $3s^23p^2\,^3P_1$ | $3s^23p^2\,^3P_2$ |
|---|---|---|---|---|
| | TERM VALUES | 0 | 2273 | 5509 |
| | | $I=$ (5) | (15) | (25) |
| | | $\lambda=367.083$ | 370.174 | 374.658 |
| $3s3p^3\,^3S_1^0$ | 272,418 | $\nu=272,418$ | 270,143 | 266,910 |
| | | | (15) | (20) |
| | | | 315.163 | 318.408 |
| $3s^23p3d\,^3P_2^0$ | 319,570 | | 317,296 | 314,062 |
| | | (20) | (8) | (12) |
| | | 310.042 | 312.239 | 315.420 |
| $^3P_1^0$ | 322,541 | 322,536 | 320,268 | 317,038 |
| | | | (8) | |
| | | | 311.138 | |
| $^3P_0^0$ | 323,674 | | 321,401 | |
| | | | (4) | |
| | | | 166.323 | |
| $3s^23p4s\,^3P_0^0$ | 603,512 | | 601,239 | |
| | | (2) | (3) | (3) |
| | | 165.396 | 166.021 | 166.920 |
| $^3P_1^0$ | 604,605 | 604,610 | 602,333 | 599,089 |
| | | | (2) | (9) |
| | | | 164.771 | 165.655 |
| $^3P_2^0$ | 609,175 | | 606,903 | 603,664 |

In Sc IX, isoelectronic with Al I, the ground state configuration is $3s^23p$. Radiations involving transitions to the $^2P^0$ term of this configuration

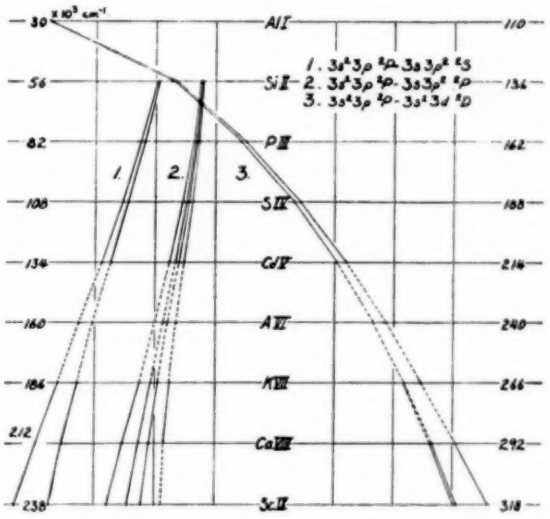


FIG. 1. Isoelectronic sequence Si I–Sc VIII.

TABLE II. *Scandium IX.*

| CONFIGURATION | | $3s^23p\,^2P_{1/2}^0$ | $3s^23p\,^2P_{3/2}^0$ |
|---|---|---|---|
| | TERM VALUES | 0 | 5758 |
| | | $I=$ (8) | (1) |
| | | $\lambda=318.615$ | 324.570 |
| $3s^23d\,^2P_{3/2}$ | 313,858 | $\nu=313,858$ | 308,100 |
| | | | (12) |
| | | | 324.199 |
| $^2D_{5/2}$ | 314,211 | | 308,453 |
| | | (2) | (3) |
| | | 416.036 | 426.250 |
| $3s3p^2\,^2S_{1/2}$ | 240,363 | 240,364 | 234,604 |
| | | (8) | (4) |
| | | 390.888 | 399.890 |
| $3s3p^2\,^2P_{1/2}$ | 255,828 | 255,828 | 250,069 |
| | | | (12) |
| | | (385.883) | 394.652 |
| $^2P_{3/2}$ | 259,146 | (259,146) | 253,388 |

[1] Kruger and Phillips, Phys. Rev. **51**, 1087 (1937).

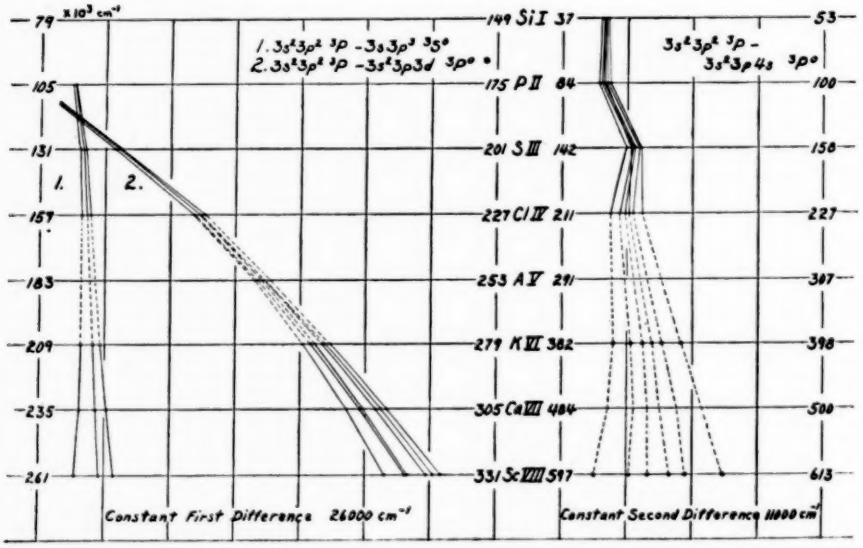


FIG. 2. Isoelectronic sequence Al I–Sc IX. Constant first difference 26,000 $cm^{-1}$.

from $3s3p^2\ ^2P$, $^2S$ and from $3s^23d\ ^2D$ have been identified. These data are given in Table II. The transition $3s^23p\ ^2P_{1/2}{}^0 - 3s3p^2\ ^2P_{3/2}$ has not been observed, the predicted position 385.883A being too close to the second order position of the strong oxygen line 192.906A. Since the only satisfactory method so far found for the excitation of Sc spectra in the vacuum region involves the use of electrodes made of a mixture of scandium and boron oxides, observation of this line has been impossible.

Displaced frequency diagrams for the isoelectronic sequences Si I to Sc VIII and Al I to Sc IX are shown in Fig. 1 and Fig. 2, respectively. The only marked irregularity appears in the case of the $3s^23p^2\ ^3P - 3s^23p4s\ ^3P^0$ transitions in S III.

JULY 15, 1937 PHYSICAL REVIEW VOLUME 52

# Interferometer Wave-Lengths in the Secondary Spectrum of Hydrogen

REGINALD G. LACOUNT AND ROBERT E. HODGDON
*Boston University, Boston, Massachusetts*

(Received April 22, 1937)

Interferometer determinations of the wave-lengths of thirty-four lines in the spectrum of $H_2$ have been made, using an etalon crossed with a Littrow spectrograph. The average probable error of these measurements is 0.0003A.

## INTRODUCTION

THE complexity of the many-lined spectra of hydrogen and its isotopes, makes it important that some sort of tertiary standards be determined to facilitate the work in analysis of these spectra. Interferometer wave-lengths serve this purpose. No such wave-lengths of hydrogen have been published below λ4171.[1] The present paper deals with the region between λ3750 and λ4200.

## APPARATUS

With the exception of the discharge tube the apparatus used was the same as that described by one of the present writers in a previous paper.[2]

The quartz capillary of the discharge tube was 8 mm in diameter and 60 cm long. The front elec-

[1] Gale, Monk and Lee, Ap. J. **67**, 89 (1928).

[2] Kent and Lacount, Phys. Rev. **51**, 241 (1937).

trode chamber was coaxial with the capillary, and the radiation emerged along this axis through the electrode. Both electrodes were cylindrical in shape and made of aluminum, the front electrode and the capillary were of quartz, and the rear chamber of Pyrex glass attached by a conical joint. The entire tube was water cooled.

The secondary spectrum of the 30-foot Littrow spectrograph was used, giving an auxiliary dispersion of 0.88A per mm. The etalon had a separation of about 10 mm.

## Procedure

The standard Pfund arc was used as a source for the iron lines, the wave-lengths being those recommended by the International Astronomical Union.[3] The arc was exposed for 45 sec. every hour during the 12 hour exposures.

A continuous flow of hydrogen was used in order to wash out impurities. This flow was controlled by stopcocks at each end of the tube, and a capillary between the tube and the electrolytic generator. A long rod attached to the needle valve of the Bunsen burner under the mercury diffusion pump also facilitated control. A pressure of about 0.2 mm of mercury appeared to give the best spectrum.

Eastman spectroscopic plates I-O were used throughout.

Table I. *Wave-lengths of thirty-four lines in the spectrum of $H_2$.*

| Wave-length | Intensity | Vacuum Wave Number |
|---|---|---|
| 3771.505 | $0^4$ | 2650711 |
| 3796.596 | $0^2$ | 2633193 |
| 3803.033 | $0^3$ | 2628737 |
| 3861.508 | $0^3$ | 2588931 |
| 3863.210 | $0^3$ | 2587790 |
| 3869.940 | $0^3$ | 2583290 |
| 3871.598 | $0^1$ | 2582183 |
| 3879.533 | $0^4$ | 2576902 |
| 3924.414 | $0^4$ | 2547432 |
| 3962.336 | $0^4$ | 2523052 |
| 3982.567 | $0^4$ | 2510236 |
| 3986.931 | $0^4$ | 2507488 |
| 3990.039 | 0 | 2505535 |
| 4028.341 | $0^1$ | 2481713 |
| 4043.568 | $0^3$ | 2472367 |
| 4069.632 | 1 | 2456533 |
| 4072.963 | $0^3$ | 2454525 |
| 4078.838 | 0 | 2450990 |
| 4082.383 | $0^2$ | 2448861 |
| 4087.749 | 1 | 2445646 |
| 4133.998 | $0^4$ | 2418286 |
| 4159.313 | $0^4$ | 2403568 |
| *4171.307 | 0 | 2396657 |
| 4175.161 | $0^1$ | 2394445 |
| 4177.112 | 2 | 2393326 |
| 4179.588 | $0^3$ | 2391909 |
| 4180.107 | 0 | 2391612 |
| 4182.169 | 0 | 2390432 |
| *4195.670 | 1 | 2382741 |
| 4199.790 | 0 | 2380403 |
| 4209.169 | $0^4$ | 2375099 |
| *4212.500 | 1 | 2373221 |
| 4222.522 | 1 | 2367588 |
| 4223.942 | 0 | 2366792 |

[3] Transactions of International Astronomical Union **3**, 86 (1928).

## Results

The reduction of wave-lengths was made following the method used at Mount Wilson, and employed by one of the present writers in a previous paper.[2]

The preliminary values of wave-lengths were obtained from the then unpublished grating measurements made by Dr. Kent. These were accurate to a few thousandths of an angstrom.

Table I lists the wave-lengths as computed from the means of three plates. The maximum probable error of the thirty-four lines measured is 0.0006A, for only two of them is it greater than 0.0004A, and the average is 0.0003A.

Three of these lines marked with an asterisk in the table were measured interferometrically by Gale, Monk, and Lee. Our values compare with their values, preceded by the letter $G$, as follows: $\lambda$4171.307, $G=0.308$; $\lambda$4195.670, $G=0.674$; $\lambda$4212.500, $G=0.498$.

The intensities listed were determined visually, $0^4$ being the intensity of the weakest lines on the plate, 0 the average intensity, and 4 that of the strongest line.

The wave numbers in vacuum, were calculated from Kayser's table.

The work was done in the Rumford Committee Room of the Massachusetts Institute of Technology.

The writers are indebted to the institute for the splendid facilities placed at their disposal and especially to Drs. Harrison, Boyce and Stockbarger for their valuable suggestions.

The writers also wish to acknowledge their indebtedness to Professor Wood and Dr. Dieke for the loan of the grating used and to Dr. Kent for his valuable aid and inspiration.

A grant from the Rumford Committee of the American Academy of Arts and Sciences to Dr. Kent, made this research possible.

# Bands of HD and $D_2$ Ending on the $2p^1\Sigma$ State

G. H. DIEKE AND MARGARET N. LEWIS
*Johns Hopkins University, Baltimore, Maryland*

(Received May 10, 1937)

Two extensive band systems of HD and $D_2$, $3d^1\Sigma \rightarrow 2p^1\Sigma$ and $3d^1\Pi \rightarrow 2p^1\Sigma$ are given and described and a few weaker and less complete systems ending on the same state. The rotational constants of $2p^1\Sigma$ can be corrected with the help of the isotopic relations and satisfactory values obtained. There is at present, however, no way to obtain very accurate values of the vibrational constants for any state of the hydrogen molecule. The $H_2$ constants of all the states concerned have been recalculated and from the comparison of the three isotopic molecules much can be learned about the reliability of the constants and other properties of the states. $3d^1\Pi^-$ is strongly decoupled but free from prominent perturbations, whereas $3d^1\Sigma$ and $3d^1\Pi^+$ are strongly perturbed.

PROBABLY the most extensive band system in the spectrum of the hydrogen molecule is that which originates from a transition of the $3d^1\Sigma$ and $3d^1\Pi$ states to the $2p^1\Sigma$ level. These regularities were discovered for $H_2$ by Richardson and Davidson[1] and simultaneously by Mecke and Finkelnburg[2] who gave, however, an interpretation since abandoned. The upper state of the bands, the singlet $3d$ complex, shows several unusual features which make an investigation of the corresponding HD and $D_2$ bands very desirable, and the results of this investigation are given in the present paper.

## §1

The manner in which the necessary plate material was obtained has been described before.[3] The bands lie chiefly in the violet and blue region of the spectrum. Most of the wave-length measurements were done in the usual way under the comparator. About 100,000 readings were taken with the measuring machine of Professor Harrison of the Massachusetts Institute of Technology. The readings obtained in this way were afterward corrected so that they show no systematic errors. The relative accuracy of these measurements is only slightly less than those made under the comparator (this refers to our particular kind of plates only) and we were helped considerably by them to obtain a fairly complete list of wave-lengths in a reasonable time. We wish to express our thanks to Professor Harrison for his cooperation and to Mr. W. Bartlett, who operated the machine.

The intensities given in the tables are again visual estimates only and, as they are obtained from plates taken under very different conditions, they can be relied upon only as rough guides.[4]

The wave numbers and intensities of the bands are listed in Tables I–VI. As in previous cases the analysis of the $D_2$ bands is, in general, more complete than that of the HD bands. The reason for this is that the HD spectrum is best developed in a mixture which contains approximately equal parts $H_2$ and $D_2$. But only 50 percent of this mixture consists of HD molecules, and therefore it is impossible to obtain the HD spectrum without having at the same time the $H_2$ and $D_2$ spectra on the plates. The $D_2$ spectrum, on the other hand, can be obtained pure, and therefore the conditions in this case are much more favorable for observing faint lines.

## §2. THE $2p^1\Sigma$ LEVEL

The $2p^1\Sigma$ state, the final level of all the bands under discussion is also the final state of the infrared $2s^1\Sigma \rightarrow 2p^1\Sigma$ bands described previously.[5] It is the upper level for the so-called "$B$" bands $2p^1\Sigma \rightarrow 1s^1\Sigma$ in the far ultraviolet. The analysis of these latter bands has been given by Mie[6] and Fujioka and Wada[7] for HD and by Jeppesen[8]

[1] O. W. Richardson and P. M. Davidson, Proc. Roy. Soc. **A123**, 54 (1929); **A123**, 466 (1929); **A124**, 50 (1929); **A124**, 69 (1929); **A125**, 23 (1929). O. W. Richardson, *Molecular Hydrogen and its Spectrum* (Yale University Press, 1934), Chapter 5.

[2] W. Finkelnburg and R. Mecke, Zeits. f. Physik **54**, 597 (1929).

[3] G. H. Dieke and R. W. Blue, Phys. Rev. **47**, 261 (1935).

[4] Quantitative intensity measurements are now being made in this laboratory.

[5] G. H. Dieke, Phys. Rev. **50**, 979 (1936).

[6] K. Mie, Zeits. f. Physik **91**, 475 (1934).

[7] Y. Fujioka and T. Wada, Sc. Papers, Inst. Phys. Chem. Res. **27**, 210 (1935).

[8] C. R. Jeppesen, Phys. Rev. **49**, 797 (1936).

TABLE I. *The $3d^1\Sigma \rightarrow 2p^1\Sigma$ system of HD.*

| $J$ | $P$ BRANCH | | | $R$ BRANCH | | |
|---|---|---|---|---|---|---|
| | | | 0→0 | | | |
| 0 | — | — | | 21502.24 | 3 | |
| 1 | 21463.02 | 4 | | 21499.59 | 5 | |
| 2 | 414.47 | 3 | | 492.98 | 4 | |
| 3 | 353.89 | 4 | blend | 524.93 | 4 | |
| 4 | 290.62 | 1 | | 536.07 | 5 | |
| 5 | 267.18 | 1 | | 562.95 | 5 | |
| 6 | | | | 602.98 | 6 | |
| 7 | | | | 654.44 | 3 | |
| 8 | | | | 717.17 | 2 | $+D_2$ |
| | | | 0→1 | | | |
| 0 | — | — | | 20354.88 | 4 | |
| 1 | 20316.90 | 2 | | 353.51 | 6 | |
| 2 | 270.95 | 0 | | 349.52 | 5 | |
| 3 | 214.28 | 3 | | 385.24 | 8 | |
| 4 | 155.76 | 1 | | 401.19 | 8*r* | |
| 5 | 138.35 | 2 | | 434.12 | 5 | |
| 6 | | | | 481.05 | 4 | |
| 7 | | | | 540.25 | 3 | |
| 8 | | | | 610.77 | 5 | blend |
| | | | 0→2 | | | |
| 0 | — | — | | 19235.68 | 5 | blend |
| 1 | 19198.98 | 2 | | 19235.68 | 5 | blend |
| 2 | 155.14 | 3 | | 233.75 | 4 | |
| 3 | 101.74 | 3 | | 272.72 | 6*v* | |
| 4 | 047.58 | 2 | blend | 293.01 | 6 | |
| 5 | 035.20 | 00*dd* | | 331.01 | 4 | |
| 6 | | | | 383.98 | 3 | |
| 7 | | | | 449.88 | 2 | |
| 8 | | | | 527.19 | 00 | |
| | | | 0→3 | | | |
| 0 | — | — | | | | |
| 1 | | | | 18144.14 | 1 | blend |
| 2 | 18065.63 | 0 | $+D_2$ | 18144.14 | 1 | blend |
| 3 | | | | 186.13 | 1 | $+D_2$ |
| 4 | | | | 210.16 | 2 | |
| 5 | | | | 252.81 | 2 | |
| 6 | | | | 311.27 | 3 | $+H_2$ |
| 7 | | | | 383.28 | 0 | |
| 8 | | | | 466.55 | 0 | |
| | | | 1→0 | | | |
| 0 | — | — | | 23383.34 | 8 | blend |
| 1 | 23342.96 | 00 | $+H_2$ | 23383.34 | 8 | blend |
| 2 | 295.61 | 3 | | 380.47 | 7 | |
| 3 | 237.63 | 2 | | 378.28 | 9*b* | blend |
| 4 | 178.02 | 1 | blend | 378.28 | 9*b* | blend |
| 5 | 120.47 | 0 | | 378.28 | 9*b* | blend |

| $J$ | $P$ BRANCH | | | $R$ BRANCH | | |
|---|---|---|---|---|---|---|
| | | | 1→1 | | | |
| 0 | — | — | | 22236.13 | 0 | |
| 1 | 22196.93 | 0 | $+H_2$ | 237.40 | 2 | blend |
| 2 | | | | 237.40 | 2 | blend |
| 3 | | | | 238.81 | 3 | |
| 4 | | | | 243.22 | 0 | |
| 5 | | | | 249.66 | 1 | |
| | | | 1→2 | | | |
| 0 | — | — | | 21117.09 | 5 | |
| 1 | 21078.81 | 3 | $+H_2$ | 119.38 | 6 | |
| 2 | | | | 121.28 | 6 | |
| 3 | 20985.57 | 4 | $+H_2$ | 126.11 | 6 | |
| 4 | 935.06 | 2 | | 135.14 | 6 | |
| 5 | 888.61 | 2 | $+H_2$ | 146.65 | 5 | |
| 6 | | | | | | |
| | | | 1→3 | | | |
| 0 | — | — | | 20024.63 | 4 | |
| 1 | | | | 027.87 | 8 | |
| 2 | 19946.90 | 3 | | 031.76 | 9 | |
| 3 | 19898.88 | 3 | blend | 039.46 | 7 | |
| 4 | 852.20 | 3 | | 052.31 | 6 | |
| 5 | 810.45 | 3 | | 068.48 | 3*v* | |
| | | | 1→4 | | | |
| 0 | — | — | | 18957.87 | 2*d* | |
| 1 | | | | 962.35 | 1 | $+D_2$ |
| 2 | | | | 967.66 | 4 | $+D_2$ |
| 3 | 18837.44 | 1 | $+D_2$ | 978.00 | 3 | |
| 4 | | | | 994.26 | 3 | |
| 5 | | | | 19014.70 | 3 | |
| | | | 2→0 | | | |
| 0 | — | — | | 25266.49 | 1 | |
| 1 | 25239.32 | 00 | | 250.49 | 3 | |
| 2 | | | | 230.72 | 4 | $+H_2$ |
| 3 | | | | 210.95 | 1 | |
| 4 | | | | 184.36 | 0 | |
| 5 | | | | 151.51 | 0 | $+H_2$ |
| | | | 2→1 | | | |
| 0 | — | — | | 24118.98 | 3*b* | |
| 1 | 24093.26 | 00 | | 104.45 | 4 | |
| 2 | | | | 087.20 | 3 | |
| 3 | | | | 071.23 | 3 | |
| 4 | | | | 049.61 | 4 | |
| 5 | | | | 022.40 | 0*d* | |

TABLE I.—*Continued.*

| J | P BRANCH | | | R BRANCH | | |
|---|---|---|---|---|---|---|
| | | | 2→2 | | | |
| 0 | — | — | | 23000.08 | 1 | |
| 1 | | | | 22986.51 | 3 | |
| 2 | | | | 971.44 | 2 | |
| 3 | | | | 958.74 | 2 | |
| 4 | 22785.36 | 00 | | 941.30 | 3 | |
| 5 | | | | 919.19 | 1*d* | |
| | | | 2→3 | | | |
| 0 | — | — | | 21907.61 | 2 | $+D_2$ |
| 1 | 21883.80 | 1 | | 895.04 | 1 | |
| 2 | | | | 882.06 | 1*ha* | |
| 3 | | | | 871.96 | 3 | |
| 4 | | | | 858.57 | 0 | |
| 5 | | | | 841.17 | 0*ha* | |
| | | | 2→4 | | | |
| 0 | — | — | | 20840.77 | 3 | |
| 1 | 20817.81 | 4*b* | blend | 829.18 | 4 | |
| 2 | | | | 817.81 | 4*b* | blend |
| 3 | | | | 810.69 | 5 | $+D_2$ |
| 4 | | | | 800.52 | 3 | |
| 5 | | | | | | |
| | | | 2→5 | | | |
| 0 | — | — | | 19799.16 | 3 | |
| 1 | | | | 788.39 | 5 | |
| 2 | | | | 778.72 | 5 | |
| 3 | | | | 773.93 | 3 | |
| 4 | | | | 767.05 | 5 | |
| 5 | | | | | | |
| | | | 3→0 | | | |
| 0 | — | — | | 27140.34 | 1 | |
| 1 | 27138.31 | 0 | | 115.23 | 3 | blend |
| 2 | | | | 101.21 | 3 | blend |
| 3 | | | | 101.21 | 3 | blend |
| 4 | | | | 115.23 | 3 | blend |
| 5 | | | | 143.71 | 1 | |
| | | | 3→1 | | | |
| 0 | — | — | | 25993.00 | 1 | |
| 1 | 25992.23 | 1 | $+H_2$ | 969.27 | 1 | |
| 2 | | | | 957.90 | 2 | |
| 3 | | | | 961.47 | 1 | |
| 4 | | | | 980.35 | 1 | |
| 5 | | | | 26014.76 | 1 | |

| J | P BRANCH | | | R BRANCH | | |
|---|---|---|---|---|---|---|
| | | | 3→2 | | | |
| 0 | — | — | | 24873.90 | 0 | |
| 1 | | | | 851.30 | 1 | |
| 2 | | | | 842.05 | 1 | |
| 3 | 24717.40 | 0 | | 848.89 | 2 | $+D_2$ |
| 4 | 656.05 | 0 | | 872.07 | 1 | |
| 5 | | | | 911.74 | 0 | |
| | | | 3→3 | | | |
| 0 | — | — | | 23781.42 | 00*b* | |
| 1 | | | | 760.10 | 0*b* | |
| 2 | | | | 752.51 | 1 | |
| 3 | | | | 762.26 | 0 | |
| 4 | 23573.07 | 00 | | 789.00 | 0*b* | |
| 5 | | | | 833.47 | 1 | |
| | | | 3→4 | | | |
| 0 | — | — | | | | |
| 1 | 22717.16 | 0*b* | $+H_2$ | 22694.05 | 00 | |
| 2 | | | | 688.43 | 0*d* | |
| 3 | | | | 700.78 | 00 | |
| 4 | | | | 730.77 | 0*v* | |
| 5 | | | | 779.72 | 00 | |
| | | | 3→5 | | | |
| 0 | — | — | | | | |
| 1 | | | | 21653.61 | 1 | |
| | | | 3→6 | | | |
| 0 | — | — | | | | |
| 1 | | | | 20637.13 | 7 | blend |
| 2 | | | | 634.77 | 0 | $+D_2$ |
| | | | 3→7 | | | |
| 0 | — | — | | | | |
| 1 | | | | 19645.20 | 00 | $+D_2$ |
| 2 | | | | 644.38 | 00 | $+H_2$ |

TABLE II. *The $3d^1\Sigma \rightarrow 2p^1\Sigma$ system of $D_2$.*

| J | P BRANCH | | | R BRANCH | | |
|---|---|---|---|---|---|---|
| | | | 0→0 | | | |
| 0 | — | — | | 21442.05 | 1 | |
| 1 | 21413.48 | 2 | | 445.95 | 4 | |
| 2 | 382.98 | 2*c* | | 450.64 | 3 | |
| 3 | 347.83 | 3 | | 459.57 | 4 | |
| 4 | 313.94 | 1 | | 474.58 | 4 | |
| 5 | 284.96 | 4 | | 496.66 | 4 | |
| 6 | 262.90 | 1 | | 526.34 | 3 | |
| 7 | 248.93 | 2 | | 564.07 | 4 | |
| 8 | 243.50 | 0*d* | | 609.69 | 3 | |
| 9 | 247.72 | 0 | | 663.24 | 2 | |
| 10 | 261.11 | 00 | | 724.42 | 1 | |
| | | | 0→1 | | | |
| 0 | — | — | | 20499.68 | 2 | |
| 1 | 20471.87 | 2 | | 504.30 | 5 | |
| 2 | 442.80 | 1 | | 510.44 | 4 | |
| 3 | 409.78 | 3 | | 521.51 | 6 | |
| 4 | 378.70 | 1 | | 529.31 | 5 | |
| 5 | 353.17 | 1 | | 564.85 | | *Hβ* ghost |
| 6 | 335.09 | 0 | | 598.57 | 5 | |
| 7 | 325.70 | 0 | | 640.84 | 5 | |
| 8 | | | | 691.51 | 3 | |
| 9 | | | | 750.53 | 3 | |
| 10 | | | | 817.55 | 1 | |
| | | | 0→2 | | | |
| 0 | — | — | | 19576.73 | 1*b* | |
| 1 | 19549.66 | 1 | | 582.07 | 4 | |
| 2 | 521.84 | 0 | | 589.45 | 2 | |
| 3 | 490.65 | 0 | | 602.36 | 5 | |
| 4 | 462.06 | 0 | | 622.66 | 3 | |
| 5 | 439.54 | 0 | | 651.22 | 5 | |
| 6 | 424.97 | 00 | | 688.47 | 1 | |
| 7 | 419.57 | 00 | | 734.81 | 6 | |
| 8 | | | | | | |
| 9 | | | | | | |
| 10 | | | | | | |
| | | | 0→3 | | | |
| 0 | — | — | | 18672.20 | 00 | |
| 1 | 18645.56 | 00 | | 677.99 | 1 | |
| 2 | 618.96 | 00 | | 686.50 | 0 | |
| 3 | 589.41 | 00 | | 701.11 | 2 | |
| 4 | 562.89 | 1 | | 723.61 | 1 | |
| 5 | 543.25 | 00 | | 754.87 | 2 | |
| 6 | | | | 795.34 | 0 | |
| 7 | | | | 845.28 | 1 | |

| J | P BRANCH | | | R BRANCH | | |
|---|---|---|---|---|---|---|
| | | | 0→4 | | | |
| 0 | — | — | | | | |
| 1 | | | | 17791.44 | 00 | |
| 2 | | | | | | |
| 3 | | | | 817.14 | 0 | |
| 4 | | | | | | |
| 5 | | | | 875.36 | 0 | |
| | | | 1→0 | | | |
| 0 | — | — | | 22886.24 | 2 | |
| 1 | 22854.31 | 3 | | 892.93 | 4 | |
| 2 | 827.18 | 2 | | 896.91 | 3 | |
| 3 | 794.83 | 3*c* | | 901.14 | 4*d* | |
| 4 | 760.24 | 1 | | 915.28 | 1 | |
| 5 | 703.65 | 00 | | | | |
| | | | 1→1 | | | |
| | Too weak for observation | | | | | |
| | | | 1→2 | | | |
| 0 | — | — | | 21020.99 | 1 | |
| 1 | 20990.40 | 2 | | 029.06 | 4 | |
| 2 | 996.03 | 4 | blend | 035.74 | 3 | |
| 3 | 937.65 | 3 | | 043.98 | 4 | |
| 4 | 906.84 | 1 | | 063.28 | 0*d* | |
| 5 | 881.10 | 2 | | 095.08 | 3 | |
| | | | 1→3 | | | |
| 0 | — | — | | 20116.33 | 1 | |
| 1 | 20086.34 | 2*c* | | 125.03 | 4 | |
| 2 | 063.07 | 1 | | 132.78 | 3 | |
| 3 | 036.39 | 2 | | 142.71 | 4 | |
| 4 | | | | 164.19 | 0*d* | |
| 5 | 19984.77 | 1 | | 198.73 | 2 | |
| | | | 1→4 | | | |
| 0 | — | — | | 19229.34 | 1 | |
| 1 | 19199.72 | 00 | | 238.41 | 1 | |
| 2 | 177.43 | 1 | | 247.27 | 0 | |
| 3 | 152.45 | 3 | +HD | 258.71 | 1 | |
| 4 | | | | 282.35 | 00 | |
| | | | 1→5 | | | |
| 0 | — | — | | 18359.35 | 0*dd* | |
| 1 | | | | 368.93 | 1 | |
| 2 | | | | 378.71 | 1 | |
| 3 | | | | 391.59 | 1 | |
| | | | 1→6 | | | |
| 0 | — | — | | | | |
| 1 | | | | 17516.30 | 1 | |

TABLE III. *The $3d^1\Pi \rightarrow 2p^1\Sigma$ system of HD.*

| J | P BRANCH | | | R BRANCH | | |
|---|---|---|---|---|---|---|
| | | | 0→0 | | | |
| 0 | — | — | | 21824.15 | 2 | |
| 1 | — | — | | 913.02 | 5 | $+H_2$ |
| 2 | 21736.36 | 5 | | | | |
| 3 | 767.46 | 6 | | | | |
| 4 | 808.14 | 6 | | | | |
| 5 | 853.68 | 7 | | | | |
| 6 | 906.35 | 4 | | | | |
| 7 | 965.41 | 3 | | | | |
| 8 | 22047.07 | 0 | | | | |
| | | | 0→1 | | | |
| 0 | — | — | | 20676.82 | 2 | |
| 1 | — | — | | 767.11 | 1 | |
| 2 | 20592.87 | 5 | | | | |
| 3 | 627.77 | 7 | | | | |
| 4 | 673.33 | 6 | | | | |
| 5 | 724.83 | 5 | | | | |
| 6 | 784.40 | 5 | | | | |
| 7 | 851.17 | 4 | | | | |
| 8 | 940.84 | 3 | | | | |
| | | | 0→2 | | | |
| 0 | — | — | | 19557.80 | 4 | blend |
| 1 | — | — | | 649.17 | 0 | |
| 2 | 19477.08 | 1 | | | | |
| 3 | 515.27 | 3 | | | | |
| 4 | 565.10 | 4 | | | | |
| 5 | 621.80 | 2 | | | | |
| 6 | 687.34 | 2 | | | | |
| 7 | 760.92 | 1 | | | | |
| 8 | | | | | | |
| | | | 0→3 | | | |
| 0 | — | — | | 18465.28 | 1 | |
| 1 | — | — | | 557.73 | 3 | |
| 2 | 18387.62 | 2 | | | | |
| 3 | 428.81 | 2 | | | | |
| 4 | 482.27 | 4 | | | | |
| 5 | 543.59 | 3 | | | | |
| 6 | 614.47 | 2 | | | | |
| 7 | 694.29 | 3 | | | | |
| | | | 0→4 | | | |
| 0 | — | — | | | | |
| 1 | — | — | | | | |
| 2 | | | | | | |
| 3 | 17367.44 | 00 | $+D_2$ | | | |
| 4 | 424.40 | 1*d* | $+D_2$ | | | |
| 5 | 489.87 | 3 | $+H_2$ | | | |
| | | | 1→0 | | | |
| 0 | — | — | | 23653.58 | 4 | |
| 1 | — | — | | 723.89 | 2 | |
| 2 | 23565.74 | 4 | | 799.20 | 3 | |
| 3 | 578.27 | 7 | | 871.37 | 2 | |
| 4 | 596.80 | 5 | | | | |
| 5 | 613.64 | 4 | | | | |

| J | P BRANCH | | | R BRANCH | | |
|---|---|---|---|---|---|---|
| | | | 1→1 | | | |
| 0 | — | — | | | | |
| 1 | — | — | | | | |
| 2 | 22421.64 | 1*bb* | $+H_2$ | | | |
| 3 | 438.71 | 2 | | | | |
| 4 | 462.11 | 3 | | | | |
| 5 | 484.77 | 1 | | | | |
| | | | 1→2 | | | |
| 0 | — | — | | 21387.17 | 1 | |
| 1 | — | — | | 459.97 | 0 | |
| 2 | 21306.63 | 2 | $+H_2$ | 540.02 | 0 | |
| 3 | 326.07 | 3 | | 619.17 | 0 | |
| 4 | 353.89 | 4 | blend | | | |
| 5 | 381.72 | 2 | $+D_2$ | | | |
| | | | 1→3 | | | |
| 0 | — | — | | 20294.70 | 2 | |
| 1 | — | — | | 368.44 | 0 | |
| 2 | 20217.00 | 3 | blend | | | |
| 3 | 239.62 | 4*b* | blend | | | |
| 4 | 270.95 | 0 | blend+$H_2$ | | | |
| 5 | 303.48 | 4 | $+H_2$ | | | |
| | | | 1→4 | | | |
| 0 | — | — | | 19227.97 | 2 | |
| 1 | — | — | | 302.62 | 3 | |
| 2 | 19152.95 | 3 | | | | |
| 3 | 177.99 | 3 | | | | |
| 4 | 212.99 | 3 | | | | |
| 5 | 249.79 | 1 | | | | |
| | | | 1→5 | | | |
| 0 | — | — | | | | |
| 1 | — | — | | | | |
| 2 | — | — | | | | |
| 3 | 18141.24 | 0*bd* | | | | |
| | | | 2→0 | | | |
| 0 | — | — | | 25387.43 | 0*D* | |
| 1 | — | — | | 448.92 | 00 | $+D_2$ |
| 2 | 25299.73 | 1 | | | | |
| 3 | 303.37 | 1 | | | | |
| 4 | 356.80 | 0 | | | | |
| | | | 2→1 | | | |
| 0 | — | — | | 24240.16 | 2 | |
| 1 | — | — | | 303.04 | 2 | |
| 2 | 24156.21 | 3 | | 415.92 | 1 | |
| 3 | 163.63 | 3 | | | | |
| 4 | 222.12 | 2 | | | | |
| 5 | 281.03 | 00 | | | | |

TABLE III.—*Continued.*

| J | P BRANCH | | | R BRANCH | | |
|---|---|---|---|---|---|---|
| | 2→2 | | | | | |
| 0 | — | — | | 23121.10 | 00 | |
| 1 | — | — | | | | |
| 2 | 23040.47 | 0 | | | | |
| 3 | 051.09 | 0 | | | | |
| 4 | 114.06 | 2 | $+D_2$ | | | |
| 5 | 178.02 | 1 | blend | | | |
| | 2→3 | | | | | |
| 0 | — | — | | | | |
| 1 | — | — | | | | |
| 2 | 21950.97 | 1 | | | | |
| 3 | 964.56 | 1 | | | | |
| 4 | 22031.23 | 3 | $+H_2$ | | | |
| 5 | 099.89 | 0 | | | | |
| | 2→4 | | | | | |
| 0 | — | — | | 20961.95 | 0 | |
| 1 | — | — | | 21027.69 | 0 | |
| 2 | 20886.87 | 3 | | | | |
| 3 | 903.10 | 3 | | | | |
| 4 | 973.13 | 4 | | | | |
| 5 | 21046.23 | 1*d* | | | | |
| | 2→5 | | | | | |
| 0 | — | — | | 19920.57 | 0 | |
| 1 | — | — | | | | |
| 2 | 19847.55 | 3*D* | | | | |
| 3 | 866.51 | 2*b* | | | | |
| 4 | 939.55 | 3 | | | | |
| 5 | 20016.55 | 00 | $+D_2$ | | | |
| | 2→6 | | | | | |
| 0 | — | — | | | | |
| 1 | — | — | | | | |
| 2 | 18833.06 | 0 | | | | |
| 3 | 854.03 | 0 | | | | |
| 4 | 930.31 | 00 | | | | |
| 5 | 19011.03 | 00*d* | | | | |
| | 2→7 | | | | | |
| 0 | — | — | | | | |
| 1 | — | — | | | | |
| | 3→0 | | | | | |
| 0 | — | — | | | | |
| 1 | — | — | | | | |
| 2 | — | — | | | | |
| 3 | 26881.53 | 00 | | | | |
| | 3→1 | | | | | |
| 0 | — | — | | 25836.49 | 0 | |
| 1 | — | — | | 881.11 | 1 | |
| 2 | 25752.45 | 0 | | | | |
| 3 | 741.84 | 1 | | | | |
| 4 | 811.78 | 00 | | | | |
| 5 | 875.97 | 0 | | | | |

| J | P BRANCH | | | R BRANCH | | |
|---|---|---|---|---|---|---|
| | 3→2 | | | | | |
| 0 | — | — | | | | |
| 1 | — | — | | 24763.18 | 0 | |
| 2 | 24636.77 | 1 | | 889.84 | 00 | $+H_2$ |
| 3 | 629.33 | 1 | | | | |
| 4 | 703.52 | 0 | | | | |
| 5 | 772.70 | 0 | $+H_2$ | | | |
| | 3→3 | | | | | |
| 0 | — | — | | | | |
| 1 | — | — | | | | |
| 2 | 23547.24 | 2 | | | | |
| 3 | 542.72 | 2 | | | | |
| 4 | 620.70 | 0 | | | | |
| 5 | 694.55 | 3 | $+D_2$ | | | |
| | 3→4 | | | | | |
| 0 | — | — | | | | |
| 1 | — | — | | | | |
| 2 | 22483.10 | 2 | | | | |
| 3 | 481.61 | 1 | | | | |
| 4 | 562.83 | 1 | | | | |
| 5 | 640.82 | 2 | $+D_2$ | | | |
| | 3→5 | | | | | |
| 0 | — | — | | | | |
| 1 | — | — | | | | |
| 2 | 21444.02 | 0 | | | | |
| 3 | 444.53 | 0 | | | | |
| 4 | 529.32 | 00 | | | | |
| 5 | 611.03 | 00 | | | | |
| | 3→6 | | | | | |
| 0 | — | — | | | | |
| 1 | — | — | | | | |
| 2 | 20429.39 | 2 | $+D_2$ | | | |
| 3 | 432.23 | 2 | | | | |
| 4 | 520.00 | 00 | | | | |
| | 3→7 | | | | | |
| 0 | — | — | | | | |
| 1 | — | — | | | | |
| 2 | 19439.01 | 1 | | | | |
| 3 | 444.06 | 2 | | | | |
| 4 | 534.63 | 1 | | | | |
| 5 | | | | | | |
| | 3→8 | | | | | |
| 0 | — | — | | | | |
| 1 | — | — | | | | |
| 2 | 18472.62 | 2 | | | | |
| 3 | 479.51 | 3 | | | | |
| 4 | 573.26 | 0 | | | | |

TABLE III.—*Continued.*

| J | Q BRANCH | | | Q BRANCH | | | Q BRANCH | | |
|---|---|---|---|---|---|---|---|---|---|
| | 0→0 | | | 0→1 | | | 0→2 | | |
| 1 | 21756.78 | 5 | | 20610.77 | 5 | blend | 19492.82 | 4 | |
| 2 | 763.03 | 6 | | 619.54 | 7 | $+H_2$ | 503.77 | 5 | |
| 3 | 776.87 | 6 | | 637.13 | 7 | | 524.59 | 5 | |
| 4 | 800.84 | 5 | | 666.03 | 6 | | 557.80 | 4 | blend |
| 5 | 836.55 | 6 | | 707.71 | 6 | | 604.67 | 2 | |
| 6 | 884.80 | 7*d* | $+H_2$ | 763.06 | 5 | | 665.94 | 2*b* | |
| 7 | 964.68 | 3 | | 832.45 | 4 | | 742.21 | 4 | $+H_2$ |
| 8 | 22023.66 | 0 | | 917.37 | 1 | | 834.02 | 00 | |
| | 0→3 | | | 0→4 | | | 1→0 | | |
| 1 | 18401.32 | 4 | | | | | 23595.22 | 4 | blend |
| 2 | 414.29 | 5 | | 17350.26 | 2 | $+D_2$ | 603.23 | 6 | |
| 3 | 437.97 | 8*b* | | 376.53 | 00 | | 617.26 | 7 | |
| 4 | 474.99 | 7 | | 417.13 | 0 | $+D_2$ | 639.27 | 6 | |
| 5 | 526.48 | 4 | | 472.88 | 0 | | 670.42 | 5 | $+D_2$ |
| 6 | 593.18 | 3 | | | | | 711.82 | 3 | |
| 7 | 675.56 | 2 | | | | | 766.75 | 3 | $+D_2$ |
| 8 | 773.25 | 0 | | | | | | | |
| | 1→1 | | | 1→2 | | | 1→3 | | |
| 1 | 22449.23 | 4 | $+D_2$ | 21331.23 | 3 | | 20239.62 | 4*b* | blend |
| 2 | 459.67 | 1 | | 344.06 | 6 | $+H_2$ | 254.40 | 4 | |
| 3 | 477.60 | 1 | | 365.10 | 3 | | 278.46 | 5 | |
| 4 | 504.38 | 0 | | 396.24 | 3 | | 313.38 | 5 | |
| 5 | 541.69 | 1 | | 438.59 | 2 | | 360.37 | 2 | |
| 6 | 590.09 | 1 | $+D_2$ | 492.98 | 4 | blend | 420.29 | 2*r* | |
| 7 | 652.46 | 1 | | | | | 495.71 | 00 | |
| | 1→4 | | | 1→5 | | | 2→0 | | |
| 1 | 19173.90 | 5 | | 18133.29 | 0 | | 25317.38 | 2 | |
| 2 | 190.33 | 6 | | 151.09 | 2 | | 325.62 | 3 | |
| 3 | 217.02 | 4 | | 180.29 | 1 | | 339.03 | 3 | |
| 4 | 255.40 | 3 | | 221.91 | 1 | | 358.57 | 3 | |
| 5 | 306.64 | 3 | | 277.10 | 1 | | 385.28 | 1 | |
| | 2→1 | | | 2→2 | | | 2→3 | | |
| 1 | 24171.40 | 4 | | 23053.40 | 1 | | 21961.98 | 2 | |
| 2 | 182.14 | 4 | | 066.39 | 2 | | 976.90 | 2 | |
| 3 | 199.28 | 4 | | 086.78 | 2 | | 22000.17 | 4 | |
| 4 | 223.75 | 3 | | 115.52 | 1 | | 032.70 | 2 | $+D_2$ |
| 5 | 256.41 | 3 | | 153.31 | 0 | | 075.08 | 0 | |
| | 2→4 | | | 2→5 | | | 2→6 | | |
| 1 | 20896.14 | 4 | | 19855.32 | 3 | | 18839.07 | 4 | $+D_2$ |
| 2 | 912.80 | 5 | | 873.72 | 6 | $+H_2$ | 859.01 | 4 | |
| 3 | 938.74 | 5 | | 902.04 | 3 | | 889.68 | 3 | |
| 4 | 974.72 | 4 | | 941.21 | 3 | | 931.93 | 4 | |
| 5 | 21021.42 | 3 | | 991.84 | 2 | | 986.30 | 2 | |

TABLE III.—*Continued.*

| *J* | *Q* BRANCH | | | *Q* BRANCH | | | *Q* BRANCH | | |
|---|---|---|---|---|---|---|---|---|---|
| | 2→7 | | | 3→0 | | | 3→1 | | |
| 1 | 17848.00 | 4 | | 26915.02 | 0 | | 25769.04 | 3 | $+H_2$ |
| 2 | 868.70 | 0 | | 922.28 | 0 | | 778.85 | 2 | |
| 3 | 901.59 | 0 | | 933.70 | 0 | | 793.99 | 2 | |
| 4 | 946.69 | 0 | | 949.91 | 0 | | 815.15 | 3 | |
| 5 | 18004.86 | 7 | $+H_2$ | | | | 842.54 | 2 | $+D_2$ |
| | 3→2 | | | 3→3 | | | 3→4 | | |
| 1 | 24651.11 | 2 | | 23559.59 | 2 | | | | |
| 2 | 663.06 | 3 | | 573.55 | 3 | | | | |
| 3 | 681.50 | 3 | | 595.22 | 4 | blend | 22533.82 | 00 | $+D_2$ |
| 4 | 706.71 | 1 | $+D_2$ | 623.98 | 3 | | | | |
| 5 | 739.50 | 1 | | 661.28 | 3 | | | | |
| | 3→5 | | | 3→6 | | | 3→7 | | |
| 1 | 21452.80 | 1 | | 20436.76 | 1*D* | | 19444.92 | 2 | |
| 2 | 470.30 | 2 | | 455.74 | 3 | | 465.31 | 3 | |
| 3 | 496.65 | 3 | $+D_2$ | 484.35 | 3 | | 496.25 | 4 | |
| 4 | 532.49 | 1 | | 523.13 | 2 | | 537.82 | 3*b* | |
| 5 | 578.06 | 1 | | 572.41 | 2*d* | | 590.82 | 1 | |
| | 3→8 | | | 4→3 | | | 4→4 | | |
| 1 | 18477.20 | 3 | | 25020.50 | 00 | | | | |
| 2 | 499.04 | 4 | | 032.56 | 00 | | | | |
| 3 | 532.06 | 4 | | 049.93 | 00 | | | | |
| 4 | 576.51 | 2 | | 074.91 | 0 | | | | |
| | 4→5 | | | 4→6 | | | 4→7 | | |
| 1 | | | | | | | | | |
| 2 | 22929.30 | 1 | | 21914.65 | 00 | | 20924.27 | 0 | |
| 3 | 951.75 | 00 | | 939.38 | 1 | $+D_2$ | | | |
| 4 | | | | 974.37 | 1 | $+D_2$ | | | |
| | 4→8 | | | | | | | | |
| 1 | | | | | | | | | |
| 2 | 19958.13 | 00 | | | | | | | |

TABLE IV. *The $3d^1\Pi \rightarrow 2p^1\Sigma$ system of $D_2$.*

| J | P BRANCH | | | R BRANCH | | |
|---|---|---|---|---|---|---|
| | | | 0→0 | | | |
| 0 | — | — | | 21710.15 | 1 | |
| 1 | — | — | | 769.65 | 1 | |
| 2 | 21651.09 | 2 | | 839.94 | 00 | |
| 3 | 671.69 | 5*b* | blend | 917.18 | 0 | |
| 4 | 703.22 | 2 | | | | |
| 5 | 742.49 | 3 | | | | |
| 6 | 787.52 | 2 | | | | |
| 7 | 839.02 | 3 | | | | |
| 8 | 893.72 | 1 | | | | |
| 9 | 948.10 | 1 | | | | |
| | | | 0→1 | | | |
| 0 | — | — | | 20767.97 | 4 | blend |
| 1 | — | — | | 828.07 | 1 | |
| 2 | 20710.92 | 1 | | | | |
| 3 | 733.54 | 5 | | 979.03 | 00 | |
| 4 | 767.97 | 4 | blend | | | |
| 5 | 810.68 | 5 | | | | |
| 6 | 859.77 | 4 | | | | |
| 7 | 915.81 | 5 | | | | |
| 8 | 975.54 | 2 | | | | |
| 9 | 21035.39 | 2 | | | | |
| | | | 0→2 | | | |
| 0 | — | — | | | | |
| 1 | — | — | | 19905.86 | 0 | |
| 2 | 19789.97 | 2 | | | | |
| 3 | 814.44 | 2 | | | | |
| 4 | 851.33 | 1 | | | | |
| 5 | 897.12 | 4*c* | | | | |
| 6 | 949.64 | 1 | | | | |
| 7 | 20009.77 | 2 | | | | |
| 8 | 073.96 | 0 | | | | |
| 9 | 138.55 | 0*d* | | | | |
| | | | 0→3 | | | |
| 0 | — | — | | | | |
| 1 | — | — | | | | |
| 2 | | | | | | |
| 3 | 913.15 | 0 | | | | |
| 4 | 952.23 | 0 | | | | |
| 5 | 19000.70 | 0 | | | | |
| 6 | 056.52 | 0 | | | | |
| 7 | 120.25 | 0 | | | | |
| | | | 1→0 | | | |
| 0 | — | — | | 23221.67 | 2 | |
| 1 | — | — | | 266.82 | 2 | |
| 2 | 23162.66 | 2*r* | | 319.24 | 1 | |
| 3 | 168.68 | 3 | | 371.26 | 1 | |
| 4 | 182.55 | 3 | | | | |
| 5 | 196.70 | 3 | | | | |
| 6 | 228.37 | 2 | | | | |

| J | P BRANCH | | | R BRANCH | | |
|---|---|---|---|---|---|---|
| | | | 1→2 | | | |
| 0 | — | — | | 21356.46 | 0 | |
| 1 | — | — | | 402.95 | 0 | |
| 2 | 21301.48 | 0 | | 457.87 | 0*d* | |
| 3 | 311.56 | 1 | | 514.13 | 0 | |
| 4 | 330.61 | 1 | blend | | | |
| 5 | 351.23 | 2 | | | | |
| 6 | 390.45 | 1 | | | | |
| 7 | | | | | | |
| | | | 1→3 | | | |
| 0 | — | — | | 20451.82 | 1 | |
| 1 | — | — | | 498.85 | 2 | |
| 2 | 20398.49 | 1 | | 555.13 | 0 | |
| 3 | 410.26 | 3 | | 612.83 | 0 | |
| 4 | 431.59 | 2 | | | | |
| 5 | 454.91 | 2 | | | | |
| 6 | 497.34 | 1 | | | | |
| | | | 1→4 | | | |
| 0 | — | — | | | | |
| 1 | — | — | | | | |
| 2 | 19512.95 | 0 | | | | |
| 3 | 526.28 | 1 | | | | |
| 4 | 549.66 | 1 | blend | | | |
| 5 | 575.42 | 1 | | | | |
| 6 | 620.83 | | | | | |
| | | | 1→5 | | | |
| 0 | — | — | | | | |
| 1 | — | — | | | | |
| 2 | 18644.41 | 00 | | | | |
| 3 | 659.14 | 0 | | | | |
| 4 | 684.38 | 00 | | | | |
| 5 | 712.53 | 0 | | | | |
| | | | 2→0 | | | |
| 0 | — | — | | 24665.27 | 2 | |
| 1 | — | — | | 706.71 | 3 | |
| 2 | 24606.13 | 2 | | 752.24 | 2 | |
| 3 | 608.46 | 4 | | 798.33 | 3 | |
| 4 | 615.60 | 3 | | | | |
| 5 | 623.71 | 3 | | | | |
| | | | 2→1 | | | |
| 0 | — | — | | 23723.01 | 2 | |
| 1 | — | — | | 764.89 | 2 | |
| 2 | 23666.07 | 1 | | 812.11 | 1 | |
| 3 | 670.29 | 3 | | 860.27 | 2 | |
| 4 | 680.34 | 2 | | | | |
| 5 | 691.92 | 3 | | | | |

TABLE IV.—*Continued.*

| J | P BRANCH | | | R BRANCH | | |
|---|---|---|---|---|---|---|
| | 2→2 | | | | | |
| 0 | — | — | | | | |
| 1 | — | — | | 22842.70 | 1 | |
| 2 | 22745.23 | 1 | | 891.11 | 0 | |
| 3 | 751.31 | 1 | | 941.18 | 0 | |
| 4 | 763.74 | 1 | | | | |
| 5 | 778.31 | 1 | | | | |
| | 2→3 | | | | | |
| 0 | — | — | | | | |
| 1 | — | — | | | | |
| 2 | | | | | | |
| 3 | 21849.97 | 0 | | | | |
| 4 | 864.61 | 1 | | | | |
| 5 | 881.96 | 0 | | | | |
| | 2→4 | | | | | |
| 0 | — | — | | | | |
| 1 | — | — | | | | |
| 2 | 20956.64 | 0 | | | | |
| 3 | 966.03 | 4 | blend | | | |
| 4 | 982.71 | 1 | | | | |
| 5 | 21002.49 | 0 | | | | |

| J | P BRANCH | | | R BRANCH | | |
|---|---|---|---|---|---|---|
| | 2→5 | | | | | |
| 2 | 20088.12 | 0 | | | | |
| 3 | 098.92 | 2 | | | | |
| 4 | 117.46 | 1 | | | | |
| 5 | 139.58 | 3 | | | | |
| | 2→6 | | | | | |
| 2 | 19236.25 | 00 | | | | |
| 3 | 248.41 | 0 | | | | |
| 4 | 268.71 | 00 | | | | |
| 5 | 293.02 | 1 | | | | |
| | 2→7 | | | | | |
| 2 | | | | | | |
| 3 | 18414.31 | 0 | | | | |
| 4 | 436.32 | 0 | | | | |
| 5 | 462.75 | 1 | | | | |

| J | Q BRANCH | | | Q BRANCH | | | Q BRANCH | | |
|---|---|---|---|---|---|---|---|---|---|
| | 0→0 | | | 0→1 | | | 0→2 | | |
| 1 | 21671.69 | 6 | blend | 20730.10 | 5 | | 19807.88 | 3 | |
| 2 | 681.05 | 3 | | 740.86 | 4 | | 819.89 | 1 | |
| 3 | 695.92 | 4 | | 757.88 | 5 | | 838.76 | 4 | |
| 4 | 717.17 | 3 | | 781.93 | 4 | | 865.29 | 1 | |
| 5 | 745.60 | 3 | | 813.72 | 6 | | 900.09 | 3 | |
| 6 | 781.56 | 2 | | 853.81 | 5 | | 943.69 | 1 | |
| 7 | 825.72 | 3 | | 902.47 | 5 | | 996.43 | 1 | |
| | 0→3 | | | 0→4 | | | | | |
| 1 | 18903.79 | 1 | | 18017.26 | 00 | | | | |
| 2 | 916.92 | 0 | | | | | | | |
| 3 | 937.48 | 2 | | 053.46 | 00 | | | | |
| 4 | 966.24 | 0 | | | | | | | |
| 5 | 19003.75 | 1 | | | | | | | |
| 6 | 050.54 | 0 | | | | | | | |
| 7 | 106.93 | 0 | | | | | | | |
| | 1→0 | | | 1→1* | | | 1→2 | | |
| 1 | 23192.22 | 4 | | Too weak for observation | | | 21328.33 | 2 | |
| 2 | 201.26 | 3 | | | | | 340.13 | 2 | |
| 3 | 215.46 | 4 | | | | | 358.29 | 3 | |
| 4 | 235.19 | 3 | | | | | 383.28 | 2c | |
| 5 | 261.04 | 4 | | | | | 415.56 | 2 | |
| 6 | 293.36 | 2 | | | | | 455.47 | 1 | |
| 7 | 332.58 | 2 | | | | | 503.29 | 1 | |

TABLE IV.—*Continued.*

| $J$ | $Q$ BRANCH | | | $Q$ BRANCH | | | $Q$ BRANCH | | |
|---|---|---|---|---|---|---|---|---|---|
| | 1→3 | | | 1→4 | | | 1→5 | | |
| 1 | 20424.29 | 4 | | 19537.73 | 3 | | 18668.21 | 1 | |
| 2 | 437.20 | 2 | | 551.67 | 1 | | 683.14 | 1 | |
| 3 | 457.04 | 4 | | 573.03 | 4 | | 705.91 | 2 | |
| 4 | 484.23 | 4 | | 602.36 | 5 | blend | 737.04 | 0 | |
| 5 | 519.19 | 4 | | 639.75 | 2 | | | | |
| 6 | 562.34 | 1 | | 685.80 | 0 | | | | |
| 7 | 613.60 | 5*b* | blend | 740.63 | 1 | | | | |
| | 2→0 | | | 2→1 | | | 2→2 | | |
| 1 | 24636.15 | 4 | | 23694.54 | 3 | | 22772.33 | 2 | |
| 2 | 644.65 | 3 | | 704.44 | 2 | | 783.50 | 1 | |
| 3 | 657.47 | 5 | | 719.57 | 3 | | 800.50 | 2 | |
| 4 | 675.47 | 4 | | 740.25 | 3 | | 823.55 | 1*d* | |
| 5 | 698.53 | 4 | | 766.75 | 3 | | 853.14 | 2 | |
| 6 | 727.10 | 3 | | 799.35 | 2 | | 889.27 | 0*v* | |
| 7 | 761.60 | 4 | | 838.35 | 2 | | 932.28 | 1 | |
| 8 | 802.09 | 1 | | 884.00 | 1 | | | | |
| 9 | | | | 936.24 | 1 | | | | |
| | 2→3 | | | 2→4 | | | 2→5 | | |
| 1 | 21868.14 | 0 | | 20981.69 | 3 | | 20112.18 | 3 | |
| 2 | 880.48 | 00 | | 995.00 | 2 | | 126.46 | 1 | |
| 3 | 899.15 | 0 | | 015.23 | 5 | | 148.12 | 4 | |
| 4 | | | | 042.60 | 2 | | 177.36 | 2 | |
| 5 | 956.69 | 00 | | 077.33 | 3 | | 214.42 | 3 | |
| 6 | | | | 119.63 | 2*b* | | 259.53 | 2 | |
| 7 | | | | 169.66 | 1 | | | | |
| 8 | | | | 227.57 | 0 | | | | |
| | 2→6 | | | 2→7 | | | | | |
| 1 | 19259.44 | 2 | | 18423.22 | 1 | | | | |
| 2 | 274.61 | 1 | | 439.30 | 0 | | | | |
| 3 | 297.61 | 3 | | 463.51 | 2 | | | | |
| 4 | 328.65 | 1 | | 496.25 | 0 | | | | |
| 5 | 367.90 | 2 | | 537.57 | 0 | | | | |
| 6 | 415.57 | 0 | | 587.80 | 00 | | | | |
| 7 | 471.75 | 0 | | 646.76 | 1 | | | | |
| | 3→0 | | | 3→1 | | | 3→2 | | |
| 1 | 26000.46 | 00 | | 25058.84 | 2 | | 24136.59 | 4 | |
| 2 | 008.03 | 2 | | 067.80 | 4 | | 146.81 | 4 | |
| 3 | 019.41 | 3 | | 081.41 | 6 | | 162.26 | 5 | |
| 4 | 035.08 | 2 | | 099.86 | 6 | | 183.21 | 3 | |
| 5 | 055.09 | 2 | | 123.31 | 6 | | 209.66 | 4 | |
| 6 | 079.66 | 0 | | 152.06 | 4 | | 241.91 | 00 | |
| 7 | 109.29 | 0 | | 186.16 | 4 | | | | |
| 8 | | | | 225.96 | 1 | | | | |
| 9 | | | | 271.28 | 00 | | | | |

TABLE IV.—*Continued.*

| $J$ | Q BRANCH | | | Q BRANCH | | | Q BRANCH | | |
|---|---|---|---|---|---|---|---|---|---|
| | 3→3 | | | 3→4 | | | 3→5 | | |
| 1 | 23232.54 | 2 | | 22345.99 | 00*dc* | | 21476.45 | 0 | |
| 2 | 243.86 | 2 | | 358.10 | 0*v* | | 489.67 | 0*db* | |
| 3 | 261.04 | 4 | blend | 377.09 | 00 | | 509.93 | 1 | |
| 4 | 284.23 | 2*b* | | 402.14 | 0 | | 536.99 | 1 | |
| 5 | 313.34 | 2 | | 433.90 | 0 | | 571.01 | 1 | |
| 6 | 348.78 | 1 | | 472.31 | 1 | | | | |
| 7 | 390.61 | 1 | | | | | | | |
| 8 | | | | | | | | | |
| 9 | | | | | | | | | |
| | 3→6 | | | 3→7 | | | 3→8 | | |
| 1 | 20623.72 | 2 | | 19787.54 | 2 | | 18967.66 | 1 | |
| 2 | 637.96 | 1 | | 802.63 | 1 | | 983.55 | 1 | |
| 3 | 659.42 | 4 | | 825.36 | 3 | | 19007.52 | 2 | |
| 4 | 688.21 | 1 | | 855.81 | 1 | | 039.58 | 1 | |
| 5 | 724.42 | 2 | | 894.14 | 2 | | 079.88 | 2 | |
| 6 | 767.97 | 4 | blend | 940.38 | 0 | | | | |
| 7 | 819.53 | 1 | | 994.58 | 0*d* | | | | |
| | 3→9 | | | | | | | | |
| 1 | 18163.97 | 0 | | | | | | | |
| 2 | 180.66 | 0 | | | | | | | |
| 3 | 205.79 | 1 | | | | | | | |
| | 4→1 | | | 4→2 | | | 4→3 | | |
| 1 | 26336.94 | 3 | | 25414.68 | 5 | | 24510.68 | 00 | |
| 2 | 344.79 | 2 | | 423.84 | 5*D* | | | | |
| 3 | 356.46 | 3 | | 437.34 | 6 | | 536.17 | 1 | |
| 4 | 372.38 | 1 | | 455.66 | 4 | | 556.56 | 00 | |
| 5 | 392.35 | 2 | | 478.78 | 5 | | 582.52 | 0 | |
| 6 | 417.03 | 0 | | 506.98 | 3 | | | | |
| 7 | 446.30 | 0 | | 540.22 | 3 | | | | |
| | 4→4 | | | 4→5 | | | 4→6 | | |
| 1 | 23624.03 | 3 | | 22754.59 | 0 | | Too weak for observation. | | |
| 2 | 635.22 | 2 | | 766.67 | 1 | | | | |
| 3 | 652.03 | 3 | | 784.96 | 1 | | | | |
| 4 | 674.59 | 1 | | 809.43 | 2 | | | | |
| 5 | 702.95 | 2 | | 840.08 | 1 | | | | |
| 6 | 737.24 | 0 | | | | | | | |
| 7 | 777.56 | 1 | | | | | | | |
| | 4→7 | | | 4→8. | | | 4→9 | | |
| 1 | 21065.65 | 1 | | 20245.79 | 1 | | 19442.11 | 1*d* | |
| 2 | 079.52 | 1*d* | | 260.48 | 1 | | 457.61 | 0 | |
| 3 | 100.40 | 2 | | 282.52 | 3 | | 480.85 | 1 | |
| 4 | 128.30 | 0 | | 312.08 | 0 | | 511.82 | 0*d* | |
| 5 | 163.25 | 1 | | 349.01 | 1 | | 550.74 | 0 | |
| 6 | 205.32 | 00 | | 393.47 | 00 | | | | |
| 7 | 254.57 | 00 | | 445.37 | 0 | | | | |

TABLE V.

*The $3d^1\Delta \rightarrow 2p^1\Sigma$ system of HD.*

| J | P BRANCH | | | R BRANCH | | |
|---|---|---|---|---|---|---|
| | 0→0 | | | | | |
| 1 | — | — | | 22128.78 | 00 | |
| 2 | — | — | | 267.85 | 00 | |
| 3 | 21983.20 | 0 | | | | |
| 4 | 22065.47 | 00 | | | | |
| | 0→1 | | | | | |
| 1 | — | — | | 20982.69 | 2 | |
| 2 | — | — | | 21124.55 | 1 | |
| 3 | 20843.26 | 1*d* | | | | |
| 4 | 930.68 | 00 | blend | | | |
| | 0→2 | | | | | |
| 1 | — | — | | | | |
| 2 | — | — | | | | |
| 3 | | | | | | |
| 4 | 19822.64 | 00 | | | | |
| | 0→3 | | | | | |
| 1 | — | — | | | | |
| 2 | — | — | | | | |
| 3 | 18644.41 | 0 | $+D_2$ | | | |
| 4 | 739.71 | 1 | | | | |

| J | P BRANCH | | | R BRANCH | | |
|---|---|---|---|---|---|---|
| | 1→0 | | | | | |
| 1 | — | — | | | | |
| 2 | — | — | | | | |
| 3 | | | | | | |
| 4 | 23896.46 | 00 | | | | |
| | 1→1 | | | | | |
| 1 | — | — | | | | |
| 2 | — | — | | | | |
| 3 | | | | | | |
| 4 | 22761.76 | 1 | $+H_2$ $+D_2$ | | | |
| | 1→2 | | | | | |
| 1 | — | — | | | | |
| 2 | — | — | | | | |
| 3 | | | | | | |
| 4 | 21653.61 | 1 | blend | | | |
| | 1→3 | | | | | |
| 1 | — | — | | | | |
| 2 | — | — | | | | |
| 3 | | | | | | |
| 4 | 20570.51 | 0 | | | | |
| | 1→4 | | | | | |

| J | Q BRANCH | | | Q BRANCH | | | Q BRANCH | | |
|---|---|---|---|---|---|---|---|---|---|
| | 0→0 | | | 0→1 | | | 0→2 | | |
| 0 | — | — | | — | — | | — | — | |
| 1 | — | — | | — | — | | — | — | |
| 2 | 22074.23 | 0 | $+D^2$ | 20930.68 | 00 | blend | | | |
| 3 | 151.28 | 2 | | 21011.68 | 0 | | | | |
| 4 | 200.74 | 1 | | 066.10 | 00 | | 19958.13 | 00 | blend |
| | 0→3 | | | 1→0 | | | 1→1 | | |
| 1 | — | — | | — | — | | — | — | |
| 2 | 18725.47 | 0 | | 23907.06 | 00 | | 22763.64 | 2 | $+D_2$ |
| 3 | 812.59 | 0 | | 982.17 | 0*d* | | 842.50 | 2 | |
| 4 | 875.25 | 00 | | 24023.22 | 0 | | 888.68 | 0 | |
| | 1→2 | | | 1→3 | | | 1→4 | | |
| 0 | — | — | | — | — | | | | |
| 1 | — | — | | — | — | | | | |
| 2 | 21647.76 | 0 | | 20558.34 | 0 | | | | |
| 3 | 729.91 | 0 | | | | | | | |
| 4 | 780.23 | 0 | | | | | | | |

TABLE V.—*Continued.*

*The $3^1K \rightarrow 2p^1\Sigma$ system of HD.*

| J | P BRANCH | | | R BRANCH | | |
|---|---|---|---|---|---|---|
| | | | 0→0 | | | |
| 0 | — | — | | 21363.21 | 1 | blend |
| 1 | | | | 21363.21 | 1 | blend |
| 2 | | | | | | |
| 3 | | | | 21339.56 | 1 | |
| | | | 0→1 | | | |
| 0 | — | — | | 20215.90 | 1*b* | blend |
| 1 | | | | 217.00 | 3 | blend |
| 2 | 20132.18 | 0 | | 215.90 | 1*b* | blend |
| 3 | | | | 199.90 | 2 | |
| | | | 0→2 | | | |
| 0 | — | — | | 19096.55 | 2 | |
| 1 | | | | 099.01 | 2 | |
| 2 | | | | 19100.03 | 3*b* | |
| 3 | 18965.11 | 00 | | 087.39 | 2 | |
| | | | 1→0 | | | |
| 0 | — | — | | | | |
| 1 | | | | 23344.28 | 3 | |
| 2 | | | | | | |
| 3 | | | | 23304.97 | 0 | |
| | | | 1→1 | | | |
| 0 | — | — | | | | |
| 1 | | | | 22198.34 | 00*b* | |
| 2 | | | | | | |
| 3 | | | | 22165.23 | 3 | $+D_2$ |
| 4 | | | | 090.16 | 00 | |
| | | | 1→2 | | | |
| 0 | — | — | | 21076.12 | 2 | $+H_2$ |
| 1 | | | | 080.30 | 3 | |
| 2 | | | | 081.78 | 3 | $+H_2$ |
| 3 | | | | 052.58 | 3 | |
| 4 | | | | 20981.70 | 3 | $+D_2$ |

| J | P BRANCH | | | R BRANCH | | |
|---|---|---|---|---|---|---|
| | | | 1→3 | | | |
| 0 | — | — | | 19983.60 | 0 | |
| 1 | | | | 988.80 | 3 | |
| 2 | | | | 992.44 | 2 | |
| 3 | | | | 965.95 | 3 | |
| 4 | | | | 898.88 | 3 | blend |

*The $3^1M \rightarrow 2p^1\Sigma$ system of HD.*

| J | P BRANCH | | | R BRANCH | | |
|---|---|---|---|---|---|---|
| | | | α→0 | | | |
| 0 | — | — | | | | |
| 1 | 22753.13 | 1 | | 22815.64 | 2 | |
| 2 | | | | 22798.89 | 3 | |
| 3 | 22670.06 | 1 | $+D_2$ | 809.39 | 2 | $+D_2$ |
| 4 | 596.26 | 0 | | | | |
| | | | α→1 | | | |
| 0 | — | — | | | | |
| 1 | 21607.14 | 0 | | 21669.66 | 0 | blend |
| 2 | | | | 21655.41 | 0 | |
| 3 | 530.33 | 0 | $+D_2$ | 669.66 | 0 | blend |
| | | | α→2 | | | |
| 0 | — | — | | | | |
| 1 | 20489.42 | 0 | $+D_2$ | 20551.79 | 0 | |
| 2 | | | | 20539.33 | 3 | $+D_2$ |
| 3 | 418.08 | 00 | | 557.06 | 00 | |
| | | | α→3 | | | |
| 0 | — | — | | | | |
| 1 | | | | | | |
| 2 | | | | 19449.88 | 2 | blend |
| 3 | | | | 470.47 | 00 | |

TABLE VI.

*The $3^1K \rightarrow 2p^1\Sigma$ system of $D_2$.*

| $J$ | P BRANCH | | | R BRANCH | | |
|---|---|---|---|---|---|---|
| | | | 0→0 | | | |
| 0 | — | — | | | | |
| 1 | | | | 21279.94 | 1 | |
| 2 | 21199.71 | 00 | | 21265.61 | 0 | |
| 3 | | | | 21250.55 | 2 | |
| 4 | | | | | | |
| | | | 0→1 | | | |
| 0 | — | — | | | | |
| 1 | | | | 20338.15 | 0 | |
| 2 | 20259.53 | 1*b* | | 20325.70 | 0 | +HD |
| 3 | | | | 20312.70 | 1 | |
| | | | 0→2 | | | |
| 0 | — | — | | | | |
| 1 | | | | 19416.04 | 00 | |
| 2 | 19338.61 | 00 | | | | |
| 3 | | | | 19393.61 | 00 | |
| | | | 1→0 | | | |
| 0 | — | — | | | | |
| 1 | | | | 22943.14 | 00 | |
| | | | 1→1 | | | |
| 0 | — | — | | | | |
| 1 | | | | 22001.62 | 00 | blend |
| 2 | | | | 22001.62 | 00 | blend |
| 3 | 21900.50 | 0 | | 21988.24 | 00 | |
| 4 | | | | | | |
| 5 | 21820.31 | 00 | | | | |
| | | | 1→2 | | | |
| 0 | — | — | | | | |
| 1 | | | | 21079.52 | 1*d* | blend |
| 2 | | | | 21080.51 | 00 | |
| 3 | 20981.70 | 3 | +HD | 21069.43 | 0 | |
| 4 | | | | 21040.27 | 00 | |
| 5 | 20894.50 | 2 | +HD | | | |

| $J$ | P BRANCH | | | R BRANCH | | |
|---|---|---|---|---|---|---|
| | | | 1→3 | | | |
| 0 | — | — | | | | |
| 1 | | | | | | |
| 2 | | | | | | |
| 3 | | | | 20168.27 | 00 | |
| 4 | | | | 20141.04 | 00 | |

*$3^1M \rightarrow 2p^1\Sigma$ system of $D_2$.*

| $J$ | P BRANCH | | | R BRANCH | | |
|---|---|---|---|---|---|---|
| | | | *a*→0 | | | |
| 0 | — | — | | 22339.38 | 0 | |
| 1 | 22304.49 | 1 | | 328.24 | 1 | |
| 2 | 280.48 | 0 | +HD | 317.12 | 0 | |
| 3 | 230.24 | 1 | | 298.77 | 2 | |
| 4 | 180.40 | 0 | | | | |
| 5 | 124.25 | 1 | | | | |
| | | | *a*→1 | | | |
| 0 | — | — | | 21396.97 | 0 | |
| 1 | 21362.99 | 0 | | 386.46 | 00 | |
| 2 | 340.13 | 2 | blend | | | |
| 3 | 292.25 | 0 | | 360.53 | 00 | |
| | | | *a*→2 | | | |
| 0 | — | — | | | | |
| 1 | | | | | | |
| 2 | 20420.29 | 00*dd* | +HD | | | |
| 3 | | | | | | |
| 4 | 20328.76 | 00 | | | | |
| | | | *a*→3 | | | |
| 0 | — | — | | | | |
| 1 | 19536.34 | 00*d* | | | | |
| 2 | | | | | | |
| 3 | 19471.75 | 0 | | | | |
| 4 | 429.58 | 0 | | | | |
| | | | *a*→4 | | | |
| 3 | 18587.80 | 00 | | | | |

for $D_2$. We shall see that the results of our analysis agree well with the data obtained from the far ultraviolet bands, except that our results must be expected to have about a 50-fold accuracy.

Table VII gives the averages of the rotational differences obtained directly from the differences $R(J-1)-P(J+1)$ except those marked with an asterisk which are obtained in a more indirect way. It is a characteristic of the bands in question that usually, if the $R$ branch is well developed, the $P$ branch is extremely weak and partly absent in the less intensive bands, and *vice versa*. This means that especially for the higher vibrational levels the $R(J-1)-P(J+1)$ differences cannot be obtained. They can, however, be calculated if those of some other vibrational level are known with the help of the vibrational differences for any branch, e.g. the $Q$ branches. For

instance, if we know the rotational differences $F_0(J+1)-F_0(J-1)$ of the $V=0$ state, we can find the corresponding differences for the $V=1$ state in the following way.

$$F_1(J+1)-F_1(J-1)=F_0(J+1)-F_0(J-1)+Q_{a\to 0}(J+1)-Q_{a\to 1}(J+1)-Q_{a\to 0}(J-1)+Q_{a\to 1}(J-1),$$

in which $a$ is any value of the initial vibrational quantum number. Atlhough there are now more lines involved in the calculation of a single difference which would increase the magnitude of the probable error, this is counteracted by the fact that the vibrational differences $Q_{a\to 0}(J)-Q_{a\to 1}(J)$ etc., can be obtained as averages of many independent values from strong lines. The rotational HD differences for $J\geq 5$ and $V=0$ were extrapolated with formula (1), as they could not be determined directly for any value of $V$.

If the rotational energy is represented by the usual formula

$$E_V(J)=B_VJ(J+1)-D_VJ^2(J+1)^2+\cdots \quad (1)$$

the constants $B_V$ and $D_V$ can be calculated in the customary way from the differences of Table VII. They are collected in Table VIII which contains also the corresponding constants for $H_2$ which were recalculated from Richardson and Davidson's data[1] and the vibrational differences $\omega_{n+1,\,n}$. We give two sets of these differences. The first set contains the differences between successive vibrational levels with $J=0$. This is the usually adopted procedure. There is, however for a $p\Sigma$ state, a term $2B_V$ which should properly be counted as belonging also to the rotational energy. If this term is first subtracted and then the vibrational differences taken, we obtain the second set which contains the correction $\Delta_b$ discussed in the next paragraph.

The lower part of Table VIII contains the constants occurring in the expression[9]

$$B_V=\sum_l Y_l(V+\tfrac{1}{2})^l \quad (2)$$

and the formula for the vibrational energy

$$W_V=\sum_n Y_{n0}(V+\tfrac{1}{2})^n. \quad (3)$$

[9] In what follows the more systematic expressions $Y_{lm}$ occurring in the formula

$$W=\sum_{l,\,m} Y_{lm}(V+\tfrac{1}{2})^lJ^m(J+1)^m$$

for the vibration-rotation energy are used rather than the conventional symbols $B_e$, $\omega$, $x$ etc. In Table VIII, both designations are given for comparison. We make, however, a distinction between $Y_{01}$ and $B_e$. $Y_{01}$ is the constant obtained by extrapolating according to (2) the empirical $B_V$ values to $V=0$ whereas $B_e=h/8\pi^2c\mu r_e^2$ in which $r_e$ is the equilibrium distance for the molecule with nonrotating and nonvibrating nuclei. $B_e$ can be obtained from $Y_{01}$ by applying the corrections discussed in the next paragraph. A similar distinction is observed for $Y_{10}$ and $\omega_e$.

TABLE VII. *Rotational differences $F(J+1)-F(J-1)$ for $2p^1\Sigma$.*

| $J$ | $V=0$ | 1 | 2 | 3 | 4 | 5 | 6 | 7 | 8 | 9 |
|---|---|---|---|---|---|---|---|---|---|---|
| | | | | | HD | | | | | |
| 1 | 87.80 | 83.97 | 80.63 | 77.70 | 75.05 | 72.80* | 70.37* | 68.11* | 66.23* | |
| 2 | 145.62 | 139.31 | 133.88 | 128.90 | 124.61 | 120.73* | 116.81* | 112.99* | 109.82* | |
| 3 | 202.38 | 193.78 | 186.11 | 179.50 | 173.29* | 167.64* | 162.38* | 157.29* | 152.33* | |
| 4 | 257.74 | 246.91* | 237.45* | 229.09* | 221.33* | 214.22* | 207.43* | 200.90* | | |
| 5 | 311.19* | 298.33* | 287.22* | 277.21* | | | | | | |
| 6 | 362.35* | 347.69* | 334.95* | 323.35* | | | | | | |
| 7 | 410.81* | 395.13* | 381.40* | 369.36* | | | | | | |
| | | | | | $D_2$ | | | | | |
| 1 | 59.06 | 56.90 | 54.93 | 53.29 | 51.81* | 50.37* | 49.04* | 47.75* | 46.53* | 45.37* |
| 2 | 98.13 | 94.53 | 91.41 | 88.59 | 86.11* | 83.73* | 81.51* | 79.40* | 75.39* | 75.41* |
| 3 | 136.67 | 131.75 | 127.40 | 123.53 | 119.88* | 116.55* | 113.45* | 110.53* | 107.69* | 105.07* |
| 4 | 174.62 | 168.35 | 162.86 | 157.93 | 153.43* | 149.21* | 145.26* | 141.46* | 137.85* | 134.42* |
| 5 | 211.68 | 204.22 | 197.69 | 191.70* | 186.33* | 181.22* | 176.43* | 171.80 | 167.43* | |
| 6 | 247.73 | 239.16* | 231.65 | 224.78* | | | | | | |
| 7 | 282.84 | 273.22* | 264.70* | | | | | | | |
| 8 | 316.35 | 305.83* | 296.62* | | | | | | | |
| 9 | 348.58 | 337.31* | | | | | | | | |

TABLE VIII. *Constants of the $2p^1\Sigma$-level.*

| | $H_2$ | | HD | $D_2$ | |
|---|---|---|---|---|---|
| $B_0$ | 19.434 | 19.457* | 14.685 | 9.866 | 9.827* |
| $B_1$ | 18.460 | 18.482 | 14.041 | 9.503 | 9.495 |
| $B_2$ | 17.641 | 17.652 | 13.482 | 9.187 | 9.196 |
| $B_3$ | 16.913 | 16.933 | 12.982 | 8.903 | 8.898 |
| $B_4$ | 16.246 | 16.265 | 12.544 | 8.642 | 8.582 |
| $B_5$ | 15.637 | 15.626 | 12.146 | 8.400 | 8.390 |
| $B_6$ | 15.055 | 15.004 | 11.75 | 8.177 | 8.178 |
| $B_7$ | 14.477 | 14.410 | 11.37 | 7.966 | 7.966 |
| $B_8$ | | | 11.10 | 7.762 | |
| $B_9$ | | | | 7.571 | |
| $D_0$ | 0.0147 | | 0.00874 | 0.00395 | |
| $D_1$ | 126 | | 779 | 357 | |
| $D_2$ | 114 | | 714 | 323 | |
| $D_3$ | 102 | | 623 | 304 | |
| $D_4$ | 093 | | 613 | 280 | |
| $D_5$ | 086 | | 603 | 261 | |
| $D_6$ | 078 | | 557 | 253 | |
| $D_7$ | 069 | | 529 | 252 | |
| $D_8$ | | | | 241 | |
| $D_9$ | | | | 244 | |

Vibrational differences

| | For $J=0$ | corrected | for $J=0$ | corrected | for $J=0$ | corrected |
|---|---|---|---|---|---|---|
| $\omega_{10}$ | 1318.349 | 1320.299 | 1147.30 | 1148.59 | 942.344 | 943.071 |
| $\omega_{21}$ | 1281.472 | 1283.109 | 1119.105 | 1120.223 | 922.861 | 923.473 |
| $\omega_{32}$ | 1246.71 | 1248.146 | 1092.46 | 1093.46 | 904.631 | 905.198 |
| $\omega_{43}$ | 1213.04 | 1214.373 | 1066.65 | 1067.52 | 887.061 | 887.583 |
| $\omega_{54}$ | 1179.97 | 1181.191 | 1042.30 | 1042.30 | 869.986 | 870.470 |
| $\omega_{65}$ | 1147.47 | 1148.63 | 1016.99 | 1017.78 | 853.179 | 853.625 |
| $\omega_{76}$ | 1115.47 | 1116.626 | 992.66 | 993.42 | 836.608 | 837.029 |
| $\omega_{87}$ | | | 968.214 | 968.75 | 820.283 | 820.692 |
| $\omega_{98}$ | | | | | 804.041 | 804.423 |
| | $Y_{01}$ | 20.0109 | | 15.0549 | | 10.0716 |
| $\alpha$ | $-Y_{11}$ | 1.227 | | 0.781 | | 0.429 |
| $\beta$ | $Y_{21}$ | 0.160 | | 0.0890 | | 0.0391 |
| $\gamma$ | $-Y_{31}$ | 0.0231 | | 0.0145 | | 0.00408 |
| $\delta$ | $Y_{41}$ | 0.0015 | | 0.0013 | | 0.00020 |
| $D_e$ | $Y_{02}$ | 0.0156 | | 0.00949 | | 0.00410 |
| | $-Y_{12}$ | 0.0020 | | 0.0013 | | 0.00040 |
| | $Y_{22}$ | 0.00014 | | 0.00012 | | 0.000024 |
| | $Y_{10}$ | 1360.634 | | 1179.218 | | 964.403 |
| $x$ | $-Y_{20}$ | 21.253 | | 16.091 | | 11.269 |
| $y$ | $Y_{30}$ | 0.738 | | 0.528 | | 0.410 |
| $z$ | $-Y_{40}$ | 0.045 | | 0.032 | | 0.025 |
| | $B_e$ | 20.2758 | | 15.2050 | | 10.1387 |
| | $\bar{B}_e$ | 20.2485 | | 15.1896 | | 10.1319 |
| | $I\cdot10^{40}$ | 1.3659 | | 1.8211 | | 2.7298 |
| | $r_e\cdot10^8$ | 1.2819 | | 1.2821 | | 1.2819 |
| | $\omega_e$ | 1363.03 | | 1180.77 | | 965.249 |

* From the ultraviolet $2p^1\Sigma \rightarrow 1s^1\Sigma$ bands.

TABLE IX. *Comparison of the constants of $2p^1\Sigma$ for (1) $H_2$, (2) HD and (3) $D_2$.*

| | | HD : $H_2$ | $D_2$ : $H_2$ | $D_2$ : HD | $n$ |
|---|---|---|---|---|---|
| | | Theoretical values | | | |
| | $\rho$ | 0.86613 | 0.70737 | 0.81670 | 1 |
| | $\rho^2$ | 0.75019 | 0.50038 | 0.66700 | 2 |
| | $\rho^3$ | 0.6498 | 0.3540 | 0.5447 | 3 |
| | $\rho^4$ | 0.5628 | 0.2504 | 0.4449 | 4 |
| | $\rho^5$ | 0.4874 | 0.1771 | 0.3633 | 5 |
| | | Observed ratios | | | |
| | $Y_{01}$ | 0.75233 | 0.50331 | 0.66899 | 3 |
| $\alpha$ | $-Y_{11}$ | 0.6365 | 0.3498 | 0.5500 | 2 |
| $\beta$ | $Y_{21}$ | 0.557 | 0.245 | 0.439 | 4 |
| $\gamma$ | $-Y_{31}$ | 0.628 | 0.177 | 0.281 | 5 |
| $\delta$ | $Y_{41}$ | 0.867 | 0.133 | 0.154 | 6 |
| $D_e$ | $Y_{02}$ | 0.6083 | 0.2628 | 0.4320 | 4 |
| | $-Y_{12}$ | 0.650 | 0.200 | 0.308 | 5 |
| | $Y_{22}$ | 0.857 | 0.171 | 0.200 | 6 |
| | $Y_{10}$ | 0.86667 | 0.70879 | 0.81783 | 1 |
| $x$ | $-Y_{20}$ | 0.75712 | 0.53023 | 0.70633 | 2 |
| $y$ | $Y_{30}$ | 0.71545 | 0.55556 | 0.77652 | 3 |
| $z$ | $-Y_{40}$ | 0.711 | 0.556 | 0.781 | 4 |
| | $B_e$ | 0.74991 | 0.50004 | 0.66680 | 2 |
| | $\overline{B}_e$ | 0.75016 | 0.50038 | 0.66703 | 2 |
| | $\omega_e$ | 0.86629 | 0.70816 | 0.81747 | 1 |

In Table VIII are also listed (in small print) the $B_V$ values of $H_2$ [10] and $D_2$ [8] obtained from the far ultraviolet bands for which $2p^1\Sigma$ is the upper level. (Those for HD are not given by the authors.) A comparison of these with our values shows that the agreement is as good as can be expected.

## §3. Comparison of the Constants of the $2p^1\Sigma$ State for $H_2$, HD and $D_2$

The formulae used for the calculation of the constants are only approximations and the reliability of the values obtained for these constants depends on how well these approximations represent the actual data. By comparing corresponding constants for the three molecules $H_2$, HD and $D_2$ we can get an idea of their reliability. In Table IX the ratios of the constants are given. These ratios should be equal, according to the elementary theory, to powers of the isotopic mass factor $\rho_{ij}=(\mu_i/\mu_j)^{\frac{1}{2}}$. The exponent $n$ and the theoretical values of $\rho_{ij}^n$ calculated from the known masses of the H and D atoms are also given in the table.[11] From the table it appears that the agreement between the observed ratios of the constants and their theoretical values is not very good, in most cases much less than would be warranted by the errors of the measurements. The reasons for this discrepancy lie in the nature of the $2p^1\Sigma$ state.

The elementary relations between the vibrational and rotational constants of isotopic molecules hold only if the various interactions between electronic motion and rotation and vibration can be neglected and not even then, as Dunham has shown that even for the ordinary rotating oscillator there are small corrections which will change the isotopic ratios.

The various corrections which have to be applied to obtain the constants of the nonrotating, nonvibrating molecule free from interactions have been given by various investigators.[12] More recently, Van Vleck[13] has discussed systematically

[10] C. R. Jeppesen, Phys. Rev. **44**, 165 (1933).

[11] Jordan and Bainbridge, Phys. Rev. **51**, 385 (1937).

[12] Dunham, Phys. Rev. **41**, 721 (1932); R. de L. Kronig, Physica **1**, 617 (1934); G. H. Dieke, Phys. Rev. **47**, 661 (1935).

[13] J. H. Van Vleck, J. Chem. Phys. **4**, 327 (1936).

all these corrections and their interrelations and limitations. The constants, after the corrections have been applied, should satisfy the elementary isotope relations.

Let us consider $Y_{01}$ first and designate by $B_e$ the corrected value. If we call the various corrections $\Gamma_a$, $\Gamma_b$ etc. we have[12, 13]

$$Y_{01}=B_e+\Gamma_a+\Gamma_b+\Gamma_c=B_e+\Gamma$$

with

$$\Gamma_a=\frac{B_e^3}{2\omega_e^2}[15-23a_1a_2+14a_1-9a_2+15a_3+10.5(a_1^2+a_1^3)], \quad (4)$$

$$\Gamma_b=\frac{-16B_e^3}{\omega_e^2},$$

$$\Gamma_c=\frac{-4B_e^2}{\delta}.$$

$\Gamma_c$ is due to the interaction with the $2p^1\Pi$ state which lies about $\delta=8890$ cm$^{-1}$ above the $2p^1\Sigma$ state.

$\Gamma_a$ requires the knowledge of the constants which occur in the expression

$$V=ha_0\xi^2(1+a_1\xi+a^2\xi^2+\cdots)$$

for the potential energy. They can be obtained from the approximate relations

$$Y_{11}=\frac{6B_e^2}{\omega_e}(1+a_1),$$

$$Y_{20}=1.5B_e(a_2-5/4a_1^2),$$

$$Y_{21}=\frac{6B_e^3}{\omega_e^2}[5+10a_1-3a_2+5a_3-13a_1a_2+7.5(a_1^2+a_1^3)], \quad (5)$$

$$Y_{30}=\frac{B_e^2}{2\omega_e}[10a_4-35a_1a_3-8.5a_2^2+225a_1^2a_2/4-705a_1^4/32],$$

and are found to be

$$a_1=-1.680,$$
$$a_2=\ \ 2.781,$$
$$a_3=-4.055,$$
$$a_4=\ \ 4.59.$$

They are calculated from the constants of $D_2$ as the relations (5) hold best for that molecule. $a_3$ and especially $a_4$ are not very reliable as they come out as differences between rather big numbers which all have a considerable possible error.

The values of these constants can now be substituted into (4) and the corrections calculated. They turn out to be all negative and have the values

| | $H_2$ | HD | $D_2$ |
|---|---|---|---|
| $-\Gamma_a$ | 0.0155 | 0.0087 | 0.0039 |
| $-\Gamma_b$ | 0.0692 | 0.0394 | 0.0176 |
| $-\Gamma_c$ | 0.1802 | 0.1020 | 0.0456 |
| $-\Gamma$ | 0.2649 | 0.1501 | 0.0671 |

If the total correction $\Gamma$ is applied to $Y_{01}$ we get the values $B_e$ given in Table VIII, and the isotopic ratios in Table IX. We note that the discrepancy between the observed and theoretical ratios is much smaller but still too big to be accounted for entirely by experimental errors.

There are several possible explanations for this remaining discrepancy. In the first place the corrections (4) are derived under certain simplifying assumptions. E.g. $\Gamma_c$ is derived under the assumption that the orbital angular momentum $L=1$ is constant in magnitude and precesses about the internuclear axis, and further that the $2p^1\Pi$ state is the only state by which $2p^1\Sigma$ is affected. That is certainly not rigorously the case, but a calculation of the exact nature of the other influences would presuppose a knowledge of the structure of the wave functions of the states which we do not yet possess. But in first approximation these additional corrections should have the same isotopic factor $\rho^4$ as those given in (4). If we grant this, it is possible to find the magnitude of the correction and therefore the true value of $B_e$ and the internuclear distance by a comparison of the three isotopic molecules in the following manner. Let us call $\bar{B}_e$ the true value of $B_e$ while $B_e$ is the observed value (with the corrections (4) applied) and $q$ as yet the unknown magnitude of the correction for $H_2$ so that

$$B_e=\bar{B}_e+q.$$

Then for the two other molecules the value of $B_e$ becomes $\rho^2\bar{B}_e+\rho^4q$ so that the observed ratio $\rho'^2$ is

$$\frac{\rho^2\bar{B}_e+\rho^4q}{\bar{B}_e+q}=\rho^2\frac{B_e-(1-\rho^2)q}{Be}=\rho'^2,$$

from which follows

$$q=-\frac{B_e}{1-\rho^2}\left(\frac{\rho'^2}{\rho^2}-1\right). \tag{6}$$

In this expression $\rho=\rho_{12}$, if we compare $H_2$ with HD and we obtain $q=-0.0300$. If we compare $H_2$ with $D_2$ ($\rho=\rho_{13}$) we find $q=-0.0276$. The good agreement of these two entirely independent values is a good argument in favor of our assumption. We can now find the values of $\bar{B}_e$ by adding to $B_e$ $q$ for $H_2$, $\rho_{12}{}^4q$ for HD, and $\rho_{13}{}^4q$ for $D_2$. Those values are also given in Table VIII. They are believed to be as near to the true values of $B_e$ as it is possible to get at present. The values of the moment of inertia I and the equilibrium distance $r_e$ derived from them are listed as well. Table IX shows that the agreement of the $\bar{B}_e$ ratios with the theoretical values is now within the limits of experimental errors. The influence of the mass of an electron on the moments of inertia would now be considerably bigger than the discrepancy between the theoretical values of $\rho^2$ and the observed ratios of $\bar{B}_e$.

There is, however, another source of errors which is only partly compensated for by the above calculations. We recognize it best if we realize how the values of $B_e$ are originally obtained, by fitting the formula (2) to the values of $B_V$ and then extrapolate to $V=0$. This formula converges well only for small values of $V$ and by neglecting the higher terms we may get an appreciable error in all the constants. It is difficult to estimate the magnitude of this error, but very likely it is not very prominent for $B_e$, as the convergence of the series is relatively good for the values of $V$ used for the calculation of the constants.

The other rotational constants $Y_{11}$, $Y_{21}$, $Y_{02}$, $Y_{12}$, etc. are affected by the interactions discussed above in a way similar to $Y_{01}$ but less easily amenable to an exact numerical evaluation. We shall omit, therefore, a discussion of these corrections now, but hope to return to them in a subsequent paper when we shall discuss the structure of the $2p^1\Pi$ state. It is obvious though from Table IX that the values of $Y_{31}$ and $Y_{41}$ can have no significance at all, which is not surprising, as they are very strongly influenced by small errors in the measurements.

Before we are able to judge the agreement between the theoretical values of $\rho_{ij}$ and the ratios of the values of $\omega_e$, we must apply corrections similar to those given in (4) for $B_e$. If we call these corrections $\Delta_a$, $\Delta_b$ etc. we have

$$\Delta_a=\frac{B_e^2}{32\omega_e}(200a_4-380a_1a_3-134a_2{}^2+459a_1{}^2a_2-1155a_1{}^4/8), \tag{7}$$

$$\Delta_b=-2Y_{11}.$$

There is a third correction $\Delta_d$ due to the interaction of $2p^1\Sigma$ with other $^1\Sigma$ levels of the proper symmetry type. However, for the evaluation of this correction a more detailed knowledge of the energy states and wavefunctions is necessary than is available now. We do not think that the omission of this term accounts for the big discrepancies which will remain.

The corrections $\Delta_a$ and $\Delta_b$ are found to be

| | $H_2$ | HD | $D_2$ |
|---|---|---|---|
| $\Delta_a$ | −2.396 | −1.556 | −0.846 |
| $\Delta_b$ | −2.454 | −1.562 | −0.858 |

The correction $\Delta_b$ is implied in the $Y_{10}$ values given in the Table VIII, as the extra term $2B_V$ in the energy which is responsible for the correction was regarded as belonging to the rotational energy and subtracted before the vibrational differences were evaluated. The application of (7) will make the agreement between the isotopic ratios and the theoretical values better, but the discrepancies are still considerable.

A large part of this discrepancy will be due to the fact that the expression (3) used for the calculation of the constants converges so badly that the neglected higher terms may be important enough to falsify the results. If that were the only source of errors we might try to obtain better values of the vibrational constants by making use only of the levels with $V=0$ and 1 for which (3) converges best and the influence of the higher terms is negligible, and make use at the same time of the isotopic relations between the constants. We would have then

$$\begin{aligned}
\omega-2x+3.25y-5z&=1322.694,\\
\rho_{12}\omega-2\rho_{12}{}^2x+3.25\rho_{12}{}^3y-5\rho_{12}{}^4z&=1150.15,\\
\rho_{13}\omega-2\rho_{13}{}^2x+3.25\rho_{13}{}^3y-5\rho_{13}{}^4z&=943.917,\\
\rho_{13}\omega-4\rho_{13}{}^2x+12.25\rho_{13}{}^3y-34\rho_{13}{}^4z&=924.319,
\end{aligned} \tag{8}$$

in which the right sides are the first vibrational differences with the $\Delta_a$ and $\Delta_b$ corrections applied.

Unfortunately the solution of these equations gives values for the constants which seem quite impossible, from which we can conclude that the neglected interaction terms are sufficiently big to make themselves felt. Although, therefore, Eqs. (8) cannot be used in this case to obtain better values for the vibrational constants, they serve as a test for the reliability of these constants. In our case this test must be considered negative, showing that the true vibrational constants may be considerably different from those obtained by the conventional methods.

The ratios of the other vibrational constants deviate even more from their theoretical values than those of $Y_{10}$. The discrepancy is more than 5 percent for $Y_{20}$ and more than 60 percent for $Y_{30}$ and $Y_{40}$. Various corrections should be applied, but most of these corrections are even more uncertain than those for $Y_{10}$ and therefore it seems futile to try to apply tham at the present stage.

## §4. The $3d^1\Pi^-$ State

The $3d^1\Sigma$ and $3d^1\Pi$ levels show the phenomenon of $L$ decoupling to such a degree that the quadratic formula (1) for the rotational energy is no more a good first approximation. The formulae for the rotational energy if the $L$ decoupling is taken into account are much more complicated,[14] and very disagreeable to handle for the computation of the constants. Furthermore we must expect that there are perturbations, which it would be difficult to recognize as we do not have a simple expression for the unperturbed levels. The reason for expecting the perturbations is that Richardson and Davidson[1] discovered in the vicinity of the $3d$ state a number of other electronic levels the origin of which is not completely cleared up yet, but which in all probability must have both electrons excited.[15] All these levels give rise to $P$ and $R$ branches when they combine with the $2p\Sigma_u^+$ state which proves that they must be even and plus levels[16] and they must be able to perturb the $3d^1\Sigma^+$ and $3d^1\Pi^+$ states but not the $3d^1\Pi^-$ levels. Whereas this fact makes it very likely that the $3d^1\Sigma$ and $3d^1\Pi^+$ states will show perturbations, it proves by no means that $3d^1\Pi^-$ is free of them. There may be minus levels which can perturb $3d^1\Pi^-$ but as long as they have not been discovered it seems worth while to go out from the assumption that $3d^1\Pi^-$ is free from perturbations and try to calculate the constants.

If we start out with Van Vleck and Hill's model of an atom with rigidly connected nuclei and an orbital angular momentum $L=2$ which is loosely coupled to the internuclear axis[14, 17] the rotational energy turns out to be the root of a quadratic secular equation

$$W(J)=B[J(J+1)+1]+5A/2 \\ -[(2J+1)^2B^2-9AB+9A^2/4]^{\frac{1}{2}}. \quad (9)$$

When we apply this formula to the empirical data we must realize that it applies to rigidly connected nuclei only. For the vibrating molecule because of the much higher frequency of the vibrations compared with the rotational frequency, a similar formula will hold; only the constants are now certain averages over all the positions of the nuclei during a vibration and therefore functions of the vibrational quantum number $V$.

If (9) is to be applied to the empirical data it is necessary to take into account the effect of the distortion of the molecule due to the centrifugal

[14] G. H. Dieke, Zeits. f. Physik **57**, 71 (1929).

[15] W. Weizel, Zeits. f. Physik **65**, 456 (1930); O. W. Richardson, *Molecular Hydrogen and Its Spectrum*.

[16] It is very unfortunate that the nomenclature of the symmetry properties is in a rather confused state. The wave functions which are multiplied by a factor $+1$ or $-1$, respectively, with a reflection of the electrons at the origin are called even ($g$) and odd ($u$), but positive and negative if all the particles are reflected (Wigner and Witmer, Weizel, Mulliken). Others (Kronig, Pauling and Wilson) call them even and odd in both cases, and that seems preferable to us, as it is the same property and the designation positive and negative becomes available to characterize the behavior if the sign of the azimuth $\varphi$ about the internuclear axis is changed (reflection at the $\xi$ $\zeta$plane). It seems unnatural to have to avoid the words positive and negative in connection with symbols like $\Sigma^+$ and $\Sigma^-$ which are universally used to express this property. Therefore it seems only natural to express the same property for the sublevels of a $\Pi$ state by $\Pi^+$ and $\Pi^-$. These levels are now often called $\Pi_c$ and $\Pi_d$ but there seems to be little need for this rather arbitrary designation and we believe that all confusion can be avoided if we call $\Sigma^+$, $\Pi^+$ etc. states plus states and the $\Sigma^-$, $\Pi^-$ etc. minus states and avoid the words positive and negative, the use of which seems not yet to be generally agreed upon. We may remind the reader of the fact that for a plus state the rotational levels with even values of $J$ are even and those with odd values of $J$ odd. This applies to all diatomic molecules whether the nuclei are identical or not.

[17] E. L. Hill and J. H. Van Vleck, Phys. Rev. **32**, 250 (1928).

TABLE X. *Constants of* $3d^1\Pi^-$.

| | $H_2$ | HD | $D_2$ | | $H_2$ | HD | $D_2$ |
|---|---|---|---|---|---|---|---|
| $B_0$ | 29.03 | 21.75 | 14.475 | $A_0$ | 153.8 | 150.3 | 148.0 |
| $B_1$ | 27.52 | 20.52 | 13.95 | $A_1$ | 184.6 | 181.0 | 168.3 |
| $B_2$ | 26.00 | 19.34 | 13.42 | $A_2$ | 220.5 | 224.0 | 191.8 |
| $B_3$ | | 18.11 | 12.90 | $A_3$ | | 299.7 | 217.7 |
| $B_4$ | | 18.00 | 12.51 | $A_4$ | | 240.1 | 219.5 |
| $D_0$ | 0.013 | 0.007 | 0.0025 | $\omega_{10}$ | 2108.29 | 1845.72 | 1523.64 |
| $D_1$ | 0.14 | .0045 | .0030 | $\omega_{21}$ | 1951.36 | 1729.30 | 1447.14 |
| $D_2$ | 0.14 | .004 | .0033 | $\omega_{32}$ | 1781.68 | 1605.04 | 1367.41 |
| $D_3$ | | .004 | .0035 | $\omega_{43}$ | | 1461.59* | 1280.45 |
| $D_4$ | | .005 | .0037 | | | | |
| $Ae$ | 136.3 | 127.3 | 136.5 | | | | |
| $Be$ | 29.790 | 22.36 | 14.739 | $Y_{10}$ | 2265.22 | 1962.14 | 1600.14 |
| $Y_{11}$ | 1.515 | 1.21 | 0.526 | $Y_{20}$ | 78.47 | 58.21 | 39.42 |

forces of the rotation. If the decoupling can be neglected the effect on the energy is

$$-DJ^2(J+1)^2.$$

If on the other hand the decoupling is practically complete this term becomes

$$-D(J-1)^2J^2.$$

For intermediate decouplings it will lie between these two values. But as we are here dealing only with a small correction term and because of the approximate character of the calculations it is sufficiently accurate to take the first expression throughout.

The evaluation of the constants can be done most conveniently in the following way. We note that $W(1)=A+6B$. The differences $W(J)-W(1)$ can be obtained from the frequencies of the lines of the $Q$ branches and the known values for the corresponding differences of the $2p^1\Sigma$ state. It is now necessary to find such values for the constants $A$, $B$ and $D$ that

$$W(J)-W(1)=3A/2+B[J(J+1)-5]-[(2J+1)^2B^2-9AB+9A^2/4]^{\frac{1}{2}}-D[J^2(J+1)^2-4] \quad (10)$$

for all values of $J$ except the higher ones for which other terms neglected here might become important. As the expression (10) is too complicated for any of the standard methods of evaluating constants, the best way is a systematic method of trial and error. Table X gives the results of these calculations. The first question is whether (9) or (10) represent the actual energies with sufficient approximation. This can be answered by a study of Table XI in which the empirical values for $W(J)-W(1)$ are given and their differences with the calculated values. It can be seen that the agreement is quite good except for a few of the highest $J$ values. For $D_2$ the agreement is within the limits of experimental errors for all values of $J$ up to 6. For HD the agreement is less good and that is probably due to the fact mentioned and explained previously that on the whole the data for HD are not as accurate and reliable as those for $H_2$ and $D_2$.

While it is thus established that a formula of the type (10) represents well the empirical energy levels, we must not expect that it will be able to give account of all the fine details, as the interaction between vibration and rotation and electronic motion is inadequately taken care of.[18] We shall see, however, that even with the approximate treatment the main features of all the constants are as they must be expected for a level of this type.

The constant $A$ expresses the degree of coupling of the orbital angular momentum to the internuclear axis. If the angle between internuclear axis and orbital momentum is $\alpha$ the coupling energy for a $d$ electron is

$$4A\cos^2\alpha.$$

$A$ is a measure for the departure from central

[18] At the symposium on molecular structure of the Physical Chemistry Section of the American Chemical Society in Princeton on January 1, 1937 an account was given in which this interaction was properly treated. As however not all the details of these calculations are completely finished, we reserve the application of these formulae to the energy levels under discussion to a future paper.

symmetry. It would be zero if the two nuclei coincide and increases with increasing internuclear distance. If the molecule vibrates, the average internuclear distance is larger than for the nonvibrating molecule, which means that the value of $A$ should increase with increasing vibrational quantum numbers. That is exactly what happens, as Table X shows. Also in agreement with the expectations is the fact that $A$ increases less rapidly for $D_2$ than for $H_2$, as for a given quantum number $V$ the amplitudes are biggest for $H_2$ and smallest for $D_2$. The variation of $A$ with $V$ is roughly linear.[19]

We can extrapolate to the vibrationless molecule and find the values listed under $A_e$ in Table X. They should be the same for the three molecules as the coupling is not influenced by the masses of the nuclei. The agreement is very good for $H_2$ and $D_2$. The value for HD is not unreasonably off, as the possible error in the determination of the $A_V$ values is considerable.

The values of $B_V$ decrease approximately linearly with $V$, as is the case in general for diatomic molecules. The agreement of the ratios of $B_e$ for the three molecules 0.7506, 0.4948 and 0.6592 with the theoretical values 0.7502, 0.5004 and 0.6670 is not very good, which shows the limitations of expression (9).[20]

Not much reliance can be put on the values of $D_V$ in Table XI, although they seem fairly consistent.

[19] The value $A_4$ for $D_2$ seems to be abnormal. The reason for this is not clear. There may possibly be a small perturbation.

[20] Corrections similar to those in §3 should be applied to $B_e$, $\omega_e$ etc. but their influence will be small compared with the much larger discrepancies observed and therefore it would be futile to apply them.

TABLE XI. *Observed rotational levels of $3d^1\Pi^-$ and the differences between the observed and calculated levels.*

| | $V=0$ | | 1 | | 2 | | 3 | | 4 | |
|---|---|---|---|---|---|---|---|---|---|---|
| $J$ | | diff. | | diff. | | diff. | | diff. | | diff. |
| | | | | | $H_2$ | | | | | |
| 1 | 0 | | 0 | | 0 | | 0 | | | |
| 2 | 74.71 | 0.00 | 80.73 | 0.00 | 83.10 | 0.00 | 77.19 | | | |
| 3 | 199.19 | −.02 | 206.98 | .00 | 209.59 | 0.05 | 201.39 | | | |
| 4 | 376.22 | −.01 | 380.83 | −.04 | 380.30 | .07 | 367.08 | | | |
| 5 | 606.20 | .01 | 602.96 | −.06 | 595.31 | −.07 | 573.99 | | | |
| 6 | 888.31 | .01 | 873.16 | −.20 | 854.46 | −.01 | | | | |
| 7 | | | 1189.45 | .08 | 1156.17 | −.11 | | | | |
| | | | | | HD | | | | | |
| 1 | 0 | | 0 | | 0 | | 0 | | 0 | |
| 2 | 64.73 | 0.00 | 66.52 | 0.02 | 66.76 | 0.01 | 65.78 | 0.02 | 63.85* | 0.32 |
| 3 | 165.68 | −.03 | 167.78 | −.01 | 167.26 | −.06 | 164.30 | −.06 | 158.39* | −.54 |
| 4 | 304.90 | .10 | 304.94 | .00 | 302.03 | −.02 | 295.67 | −.05 | 285.76* | −.46 |
| 5 | 483.18 | .10 | 478.75 | .07 | 471.29 | .07 | 459.81 | .07 | | |
| 6 | 700.27 | .18 | 688.94 | −.42 | | | | | | |
| 7 | 955.62 | −.36 | 937.27 | .30 | | | | | | |
| 8 | 1249.72 | −.06 | | | | | | | | |
| | | | | | $D_2$ | | | | | |
| 1 | 0 | | 0 | | 0 | | 0 | | 0 | |
| 2 | 48.69 | 0.00 | 48.46 | 0.00 | 47.85 | 0.01 | 46.95 | 0.02 | 45.74 | 0.05 |
| 3 | 122.35 | .00 | 121.40 | .01 | 119.62 | −.03 | 117.20 | .04 | 114.12 | .00 |
| 4 | 221.49 | .01 | 219.02 | −.02 | 215.33 | −.10 | 210.68 | −.05 | 205.02 | −.11 |
| 5 | 346.56 | .07 | 341.54 | .05 | 335.14 | .01 | 327.46 | −.07 | 318.45 | −.08 |
| 6 | 497.55 | −.06 | 488.84 | .03 | 478.68 | .05 | 467.06 | −.03 | 453.91 | −.11 |
| 7 | 674.49 | −.42 | 660.87 | −.05 | 645.92 | .21 | | | 611.50* | .27 |
| 8 | | | | | 836.51 | .45 | | | | |
| 9 | | | | | 1049.64* | −.40 | | | | |

* Uncertain.

## §5. The Vibrational Constants of $3d^1\Pi^-$

The vibrational differences can be best obtained from the $Q(1)$ lines. By subtracting e.g., $Q(1)$ of $1\rightarrow V''$ and $0\rightarrow V''$ the $E_1-E_0$ differences are obtained. They still contain a part of the rotational energy as from (9) it follows that $W(J)=A+6B$ for $J=1$. The differences $6(B_0-B_1)$, $6(B_1-B_2)$ etc. must be added therefore to the differences in the table to obtain the real vibrational differences from which the constants occurring in (3) can be evaluated. The average values of all these differences are listed in Table X.

The data are sufficient only for $D_2$ to calculate the four constants $Y_{10}$, $Y_{20}$, $Y_{30}$, $Y_{40}$. They are

$$Y_{10}=1600.73, \qquad Y_{20}=-39.42,$$
$$Y_{30}=0.796, \qquad Y_{40}=-0.167.$$

In order to obtain the constants for $H_2$ and HD for which only three differences are known, we might take $Y_{40}$ of $D_2$ divide it by $\rho_{13}^4$ and $\rho_{23}^4$ respectively, and then calculate the three other constants from the observed differences. Such a procedure is, however, not very advisable on account of the poor convergence of the series (3) to which attention has already been drawn in §3.

For $H_2$ the series would be for $V=3$ and $V=4$ if the constants given above for $D_2$ are correct

$$W_3=7928.27-961.26+96.43-100.05,$$
$$W_4=10193.49-1589.02+204.94-272.47.$$

From the behavior of the successive terms we see that we cannot expect the omitted higher terms to be so small that they are negligible. Any attempt to calculate the constants from a series with such poor convergence would be liable to very considerable errors and some of the constants would probably be entirely meaningless.

For this reason it is better to give up entirely the attempt to find the values of $Y_{30}$ and $Y_{40}$ and to restrict ourselves to finding the values of $Y_{10}$ and $Y_{20}$ from the first two differences only. Those values are listed in Table X.

The values of the isotopic ratios of these constants with their theoretical values in brackets are

| | | | | | | |
|---|---|---|---|---|---|---|
| $Y_{10}$ | 0.86620 | (0.86613) | 0.70640 | (0.70737) | 0.81551 | (0.81670) |
| $Y_{20}$ | 0.7418 | (0.7502) | 0.5024 | (0.5004) | 0.6772 | (0.6670). |

There are big deviations which show that the values of $Y_{10}$ and $Y_{20}$ must have considerable errors.

One can adopt a procedure similar to the one proposed in §3 by making use of the first differences of HD and $D_2$ only which will have the smallest errors.

From

$$Y_{10}+2Y_{20}=1845.72$$
$$\rho_{23}Y_{10}+2\rho_{23}^2Y_{20}=1523.64$$

we obtain the constants $Y_{10}$ and $Y_{20}$ for HD. By multiplying them with the appropriate isotopic factors those for the two other molecules are found. They are

Table XII. *Origins of bands* $3d^1\Pi\rightarrow 2p^1\Sigma$.

| $V'$ \ $V''$ | 0 | 1 | 2 | 3 | 4 | 5 | 6 | 7 | 8 | 9 |
|---|---|---|---|---|---|---|---|---|---|---|
| | | | | | HD | | | | | |
| 0 | 21684.97 | 20536.38 | 19416.16 | 18322.70 | 17255.18 | | | | | |
| 1 | 23530.69 | 22382.10 | 21261.88 | 20168.42 | 19100.90 | 18058.69 | | | | |
| 2 | 25259.99 | 24111.40 | 22991.18 | 21897.72 | 20830.20 | 19787.90 | 18770.12 | 17776.70 | | |
| 3 | 26865.03 | 25716.44 | 24596.22 | 23502.76 | 22435.24 | 21392.96 | 20375.18 | 19381.76 | 18413.01 | |
| 4 | | | | 24964.36 | | 22854.54 | 21836.76 | 20843.34 | 19874.59 | |
| | | | | | $D_2$ | | | | | |
| 0 | 21624.30 | 20681.26 | 19757.78 | 18852.65 | 17964.98 | 17094.54 | | | | |
| 1 | 23147.98 | | 21281.38 | 20376.20 | 19488.60 | 18618.11 | | | | |
| 2 | 24595.09 | 23652.03 | 22728.56 | 21823.23 | 20935.51 | 20065.26 | 19211.63 | 18374.56 | | |
| 3 | 25962.52 | 25019.45 | 24095.94 | 23190.75 | 22303.16 | 21432.65 | 20579.03 | 19742.00 | 18921.31 | 18116.85 |
| 4 | | 26299.89 | 25376.37 | 24471.23 | 23583.54 | 22712.63 | | 21022.45 | 20201.78 | 19397.33 |

| | $H_2$ | HD | $D_2$ |
|---|---|---|---|
| $Y_{10}$ | 2256.28 | 1954.23 | 1596.02 |
| $-Y_{20}$ | 72.32 | 54.26 | 36.73 |

and differ considerably from the values in Table X. We are inclined to believe that these values are better but as we saw in §3 that this method is not free from objections, we cannot be sure. We see here again that we cannot expect to obtain very accurate values for the vibrational constants of the hydrogen molecule which have the theoretical significance they are supposed to have.

Table XII gives the zero lines of all the observed bands. The contribution

$$[L(L+1)-\Lambda^2]B_V$$

to the energy[17, 13, 21] has been regarded as belonging to the rotational energy, and the zero lines are defined as transitions between the rotationless molecule.

By adding and subtracting respectively the vibrational energies of the final and initial states we obtain as the origins of the band systems

| $H_2$ | HD | $D_2$ |
|---|---|---|
| 21295.22 | 21304.06 | 21312.68 |

These three values should be identical except for some small interaction terms. The term

$$[L(L+1)-\Lambda^2]B_V$$

discussed previously[21] has been taken into account so that the remaining discrepancy must be due to the other more uncertain terms.[13]

## §6. The $3d^1\Sigma$ and $3d^1\Pi^+$ States

In the preceding paragraphs it was shown that the regular $L$ decoupling is sufficient to account for the structure of the $3d^1\Pi^-$ level, and that there is no positive evidence for perturbations. For the $3d^1\Sigma$ and $3d^1\Pi^+$ states, however, the situation is different. We know[14] that the rotational energy of $d^1\Sigma$ should be for $J=0$ equal to $6B$, whereas the rotational energy of $d^1\Pi^-$ for $J=1$ is equal to $A+6B$. The difference between these two levels should, therefore, be equal to the constant $A$. Whereas for the actual molecule we cannot expect this relation to hold exactly, it should be right at least approximately even for the nonrigid molecule. We find this difference empirically to be 260.25 for $H_2$, 293.76 for HD, and 258.21 for $D_2$, whereas $A_0$ was found above to be about 150. If we accept the assumption that the $3d^1\Pi^-$ level is free from perturbations we are led to the conclusion that the $3d^1\Sigma$ levels are shifted more than 100 $cm^{-1}$ from their expected positions. That this shift is due at least partly to perturbations is supported by the fact that the difference for HD is more than 33 $cm^{-1}$ bigger than that for $H_2$ and $D_2$. If a more systematic cause were responsible for it we would expect the value for HD to lie between that of $H_2$ and $D_2$. Moreover, we can calculate the rotational levels of $3d^1\Sigma$ and $3d^1\Pi^+$ by solving the cubic secular equation with the values of $A$ and $B$ obtained from the $3d^1\Pi^-$ level. If we do so, we find that the rotational levels obtained in this way do not agree at all with those empirically found. This proves again that both the $3d^1\Sigma$ and $3d^1\Pi^+$ states are abnormal.

It was mentioned before that the source of the perturbations is probably one or more of the numerous extra levels found by Richardson and Davidson in this region. The nature of the perturbations is in agreement with this. All the extra levels identified with any dgree of certainty are $^1\Sigma_g^+$ levels. Their interaction with the $3d^1\Sigma_g^+$ states would give rise to type $B$ perturbations[22] which are due to vibrational coupling, and for which also the rotationless levels, i.e., the vibrational levels are perturbed. That is exactly what is observed, for the shift of the whole $V=0$ level by more than 100 $cm^{-1}$ from its expected position can only be explained by class $B$ perturbations. Class $B$ perturbations give rise for the same reason to irregular vibrational intervals. This is shown by the following table which gives the vibrational differences for $J=0$, or $J=1$ when the $J=0$ level is not known. In the latter case the value is marked by an asterisk.

| | $H_2$ | HD | $D_2$ |
|---|---|---|---|
| $\omega_{10}$ | 2232.02 | 1879.93 | 1440.83 |
| $\omega_{21}$ | 2120.21 | 1896.39 | |
| $\omega_{32}$ | 1744.68* | 1899.02 | |

[21] G. H. Dieke, Phys. Rev. **47**, 661 (1935).

[22] G. H. Dieke, Phys. Rev. **47**, 870 (1935).

We see that for $H_2$ and HD the first two differences are larger than the corresponding differences of the $3d^1\Pi^-$ level, whereas for $D_2$ just the opposite is true. For $H_2$ the differences decrease rapidly with increasing $V$ for HD they increase. This can happen only when there are marked anomalies of the vibrational levels. For the $D_2$ molecule the vibrational levels with $V>1$ could not be found, and certainly are not in or near the expected position with anything like the expected intensity. Very likely a strong perturbation is the cause for that.

While the perturbations of the $3d^1\Sigma$ state are found to be of class $B$, those of $3d^1\Pi^+$ should be of type $A$, because the values of $\Lambda$ of the perturbing and perturbed states differ by one. Class $A$ perturbations are due to the interaction of rotation and electronic motion and therefore should be absent for the rotationless molecule. That is found to be the case, for if one extrapolates the $3d^1\Pi^+$ levels to the rotationless state they coincide with the rotationless $3d^1\Pi^-$ levels with the accuracy to which such an extrapolation is possible. (See Table XIII.) However, the actual differences between $3d^1\Pi^+$ and $3d^1\Pi^-$ rotational levels ($\Lambda$ doubling) vary quite irregularly with the vibrational quantum number which shows again that if $3d^1\Pi^-$ is normal $3d^1\Pi^+$ must have irregularities.

With the presence of perturbations thus established, there is no point in trying to calculate the rotational and vibrational constants of $3d^1\Sigma$ and $3d^1\Pi^+$. An accurate evaluation of the rotational constants would be even much more cumbersome than for the $3d^1\Pi^-$ state as no workable formula for the rotational energy can be given. The rotational levels can only be found as the roots of a fairly complicated secular equation.

TABLE XIII. $\Lambda$ *doubling of* $3d^1\Pi$.

| $J$ | $V=0$ | 1 | 2 | 3 |
|---|---|---|---|---|
| | | $H_2$ | | |
| 1 | 62.33 | 51.82 | 39.34 | 53.22 |
| 2 | 134.63 | 100.89 | 151.62 | 63.15 |
| 3 | 198.95 | 123.38 | 171.04 | 50.97 |
| 4 | 254.58 | 124.69 | 180.20 | 3.57 |
| | | HD | | |
| 1 | 38.05 | 29.11 | 40.84 | 39.45 |
| 2 | 91.61 | 62.24 | 64.94 | 46.34 |
| 3 | 146.51 | 94.80 | 133.13 | 128.11 |
| 4 | 195.40 | 116.94 | 193.98 | 197.40 |
| 5 | 238.42 | | | |
| 6 | 274.08 | | | |
| 7 | 317.54 | | | |
| | | $D_2$ | | |
| 1 | 18.75 | 9.77 | 9.49 | |
| 2 | 49.30 | 26.16 | 22.55 | |
| 3 | 85.18 | 45.00 | 35.85 | |
| 4 | 122.06 | 58.21 | 44.99 | |
| 5 | 156.95 | 82.32 | | |
| 6 | 190.27 | | | |
| 7 | 218.06 | | | |

## §7. Other Band Systems

Tables V and VI give bands ending on the $2p^1\Sigma$ level which originate from unclassified upper states. They are analogous to the extra levels which Richardson and Davidson found for $H_2$ and to which we have referred previously. However we have not yet been able to find these extra levels for HD and $D_2$ with nearly the same completeness as they were found in $H_2$. Also the identification of these lines is not of the same degree of reliability as for the bands in Tables I–IV. Therefore we restrict ourselves to merely listing these bands without trying to find an interpretation for them. For their ultimate classification the facts of the preceding paragraph seem to be significant, namely that from the perturbations of the $3d^1\Sigma$ and $3d^1\Pi$ levels there is no evidence that there are in this region other than $\Sigma^+$ levels,[23] which is very curious as almost any electron arrangement should also give other types of states.

There are also some HD bands originating from $3d^1\Delta$. These bands are also weak and incomplete as the $\Delta\rightarrow\Sigma$ transition is ordinarily forbidden and made possible only by the $\Lambda$ decoupling in the $d\Delta$ state.

We wish to thank Mr. W. Durding for his help with some of the calculations.

[23] Richardson's $\lambda$4142.8 progression seems to be an exception, as it seems to consist of $Q$ branches only. However, whether these branches are actually $Q$ branches or perhaps disguised $R$ branches is difficult to decide without more knowledge about the bands.

# Breakdown of Vacuum Spark Gaps

R. C. MASON
*Research Laboratories, Westinghouse Electric and Manufacturing Company, East Pittsburgh, Pennsylvania*
(Received May 18, 1937)

Experiments with vacuum spark gaps show that the critical cathode field required for breakdown is not reduced by considerable thermionic emission from the cathode. It is concluded that positive ion emission from the anode under electron bombardment, which apparently enters at higher voltages, is not a factor up to 50 kv.

THE initiation of a self-maintained discharge in the region where the starting voltage is independent of the small density of residual gas present is usually referred to as the "breakdown of a vacuum spark gap." For the (comparatively) large current and low voltage which result on breakdown, gas must be present in far larger quantity than exists before breakdown. By the accepted theory[1] of the breakdown of vacuum spark gaps the gas results from vaporization of the anode, which is heated by electrons freed from the cold cathode by high fields. Experiments of Beams and his students,[2–4] however, with Hg cathodes to which very short time impulses were applied show breakdown occurring at fields far lower than the current theories[5] of high field emission would predict emission of electrons in amount sufficient to vaporize the anode. Either the theory of the breakdown of vacuum spark gaps, or the theory of high field emission, is incomplete.

It occurred to me that the breakdown of these spark gaps might occur through electrons freeing positive ions from the anode, as has been suggested in other connections.[6] The condition for breakdown would then be $\gamma\delta \geqq 1$, where $\gamma$ represents the number of electrons liberated per positive ion striking the cathode, and $\delta$ is the number of positive ions set free from the anode by one electron; $\gamma$ and $\delta$ would be expected to be functions of the total voltage but not of the field. For the discharge to start, however, at least one electron must be liberated somehow from the cathode. In some cases, a high field at the cathode might still be needed just to provide an initiatory electron, but not nearly as large a field as would be necessary to furnish enough electrons to heat the anode. If another source of electrons, ample for initiatory purposes, but not large enough to cause any appreciable heating of the anode, were present and if the breakdown voltage for different electrode separations were found, then it should be possible to test the hypothesis of positive ion emission from anodes in vacuum breakdown. The experiments described below were designed for that purpose.

## EXPERIMENTAL

A 28 mil tungsten wire, bent in an approximate semi-circle of one inch diameter, was welded to two nickel leads to serve as cathode. The anode was a two inch diameter copper disk perpendicular to the plane of the cathode semi-circle, mounted on a threaded shaft so that the electrode separation could be varied by an external magnet. The tube was baked for several hours at 500°C, but no further outgassing of the metal parts was undertaken. The pressure during the experiments was always less than $10^{-4}$ mm.

The tungsten filament was heated by an insulated transformer. The emission current here recorded was measured with 200 volts applied to the anode; calculations show the Schottky effect increased the emission by not more than a factor of 10 at the highest fields used.

Voltage was applied to the tube from a 1/16 microfarad condenser bank through a 6000 ohm resistance. The condensers were charged by a full wave rectifier. Starting from a low value, the

[1] Hull and Burger, Phys. Rev. **31**, 1121 (1928); Snoddy, Phys. Rev. **37**, 1678 (1931).
[2] Beams, Phys. Rev. **44**, 803 (1934).
[3] Quarles, Phys. Rev. **48**, 260 (1935).
[4] Moore, Phys. Rev. **50**, 344 (1936).
[5] Fowler and Nordheim, Proc. Roy. Soc. **A119**, 173 (1928); Stern, Gossling and Fowler, Proc. Roy. Soc. **A124**, 699 (1929).
[6] Van Atta, Van de Graaf and Barton, Phys. Rev. **43**, 158 (1933).

voltage between the electrodes was raised slowly, over several seconds, by means of a regulator in the primary of the supply transformer, until breakdown occurred. The breakdown voltage was obtained by reading the primary voltage, which in turn was calibrated directly against a standard spark gap in air in the rectified output. Breakdown was obtained for cathode cold and for 0.04 microamp. and 7.0 microamp. emission, with separations from 0.013 to 0.12 cm between the anode and the closest point of the cathode filament.

## Results

The breakdown voltages are plotted against electrode separation in Fig. 1. At each point, the vertical line connects the highest and lowest voltages obtained in that particular series of tests, while the horizontal dash marks the average breakdown voltage of the series. The breakdown voltage gradually increased with testing; the higher points shown for certain separations were gotten after the lower points, with some intervening breakdowns.

The curve in Fig. 1 shows the voltage necessary to give a constant field at the cathode of 600 kv per cm (calculated on the assumption that the electrodes consisted of an infinite plane and infinite parallel cylinder).

Most of the points for cathode cold fall very well along the curve. Even with ample initiatory electrons, the breakdown voltage certainly increases with increasing separation, in such a way as to maintain approximately constant cathode field. When the cathode is heated, actually somewhat higher voltage seems to be required than when no electron emission occurs. The experiments, then, fail to show any evidence for emission of positive ions by electron bombardment up to 50 kv. Anderson[7] found for very large electrode separation, requiring up to 500 kv for breakdown, the breakdown voltage increased less rapidly than the electrode separation, so the cathode field required continually decreased from 800 kv per cm at 80 kv to less than 50 kv per cm at 500 kv. He attributed the reduction of gradient to positive ion emission from the anode, but his experiments are not conclusive enough to show that the effect on breakdown is simply that postulated above.

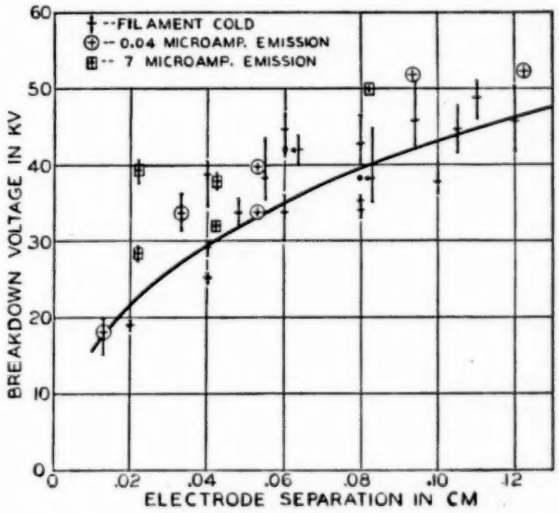


FIG. 1. Breakdown voltage *vs.* electrode separation, with cathode cold and with cathode heated to give different electron emission (measured at 200 volts). Solid curve shows voltage necessary to produce a constant field of 600 kv per cm at the cathode.

Some experiments with aluminum electrodes, which had a breakdown gradient of about 300 kv per cm for steady applied voltage, were performed with an impulse voltage which rose to 60 kv crest in 1.5 microseconds. For a given separation, the breakdown voltage, measured by cathode-ray oscillograms, was much higher for the impulse than for the steady voltage. A probable explanation is that no electrons were emitted until a critical field was reached; then, the supply voltage continued to rise above this d.c. breakdown voltage during the time required for vapor from the anode to reach the cathode. A few tests for separations from 0.02 to 0.07 cm may be explained in this way if the vapor velocity is about $10^5$ cm per sec.

[7] Anderson, Trans. A. I. E. E. **54**, 1315 (1935).

# Magnetic Focusing of Ion Beams

H. A. STRAUS
*Ryerson Physical Laboratory, University of Chicago, Chicago, Illinois*
(Received April 28, 1937)

In the mass spectrographs constructed hitherto, the ion beam enters the magnetic field at right angles. Herzog has shown in his treatment of ion optics that focusing can also be attained when the ion beam enters the field along a line other than the field normal. An experiment is described which affords a test of the predictions as to the effect of the angle of incidence on the position of the focus. Satisfactory agreement between the observations and the theory is found.

THE possibility of focusing a divergent ion beam by passing it through a homogeneous magnetic field has long been recognized. This property of the magnetic field has, in fact, been utilized in the design of the mass spectrograph. In each mass spectrograph described to date, the geometry is such that the mean ray enters the magnetic field at normal incidence.[1] Aston's first[2] and, apparently, his latest instrument,[3] as well as Costa's,[4] use a circular field which the ion beam enters along a radius.

Herzog has shown[5] that the methods of ordinary geometrical optics can be applied to the calculation of the performance of a mass spectrograph. He shows that a radial electric field, as well as a homogeneous magnetic field, acts on the rays as a combination of a cylindrical lens and a prism. The method of calculating the cardinal points of the system is developed in the same paper. It follows from this work that focusing of ion beams can be attained in a more general case. The path of entrance and exit of the ion beam need not lie along the normal to the magnetic field at the point of intersection of the orbit with the field boundary. The following is a report of an experimental investigation of this aspect of the theory of focusing in magnetic fields.

The accompanying diagram, Fig. 1, will serve to indicate the nomenclature to be adopted. $-X'$ is the direction of the incident ion beam. $X''$ is the direction of the beam after passing through the field. The source and image slits are indicated. $\epsilon'$ is taken positive if $n'$ lies between the positive directions of $X'$ and $Y'$.

The position of the image can be found from the relation $(l'-g')(l''-g'')=f^2$. Here $l'$ and $l''$ are, respectively, the distances, measured along the corresponding $X$ axes, of the object and

[1] Smythe, Rumbaugh, and West, Phys. Rev. **45**, 724 (1934) describe an instrument for the high intensity separation of isotopes which uses an extended source, so that a large range of angles of incidence is used. The theory here mentioned does not apply to their instrument.
[2] Aston, Phil. Mag. **38**, 707 (1919). Aston's second instrument is described in: Aston and Fowler, Phil. Mag. **43**, 514 (1922).
[3] Sawyer, Proc. Camb. Phil. Soc. **32**, 453 (1936).
[4] Costa, Ann. de physique **4**, 425 (1925).
[5] Herzog, Zeits. f. Physik **89**, 447 (1934).

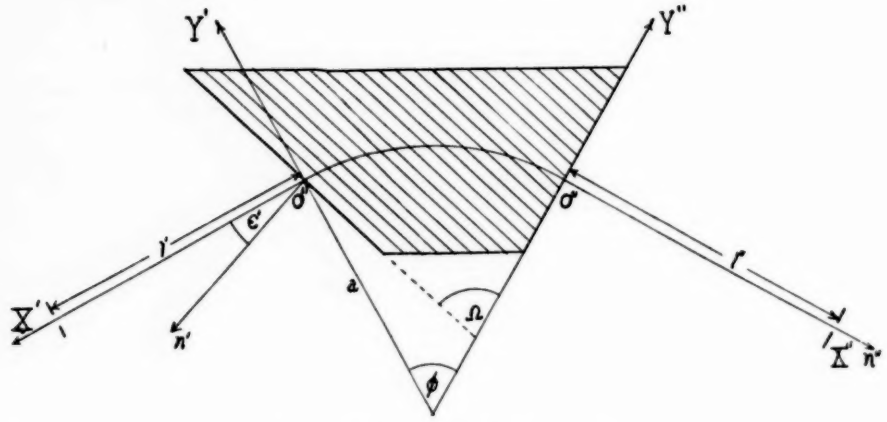


FIG. 1. Diagram showing ion path.

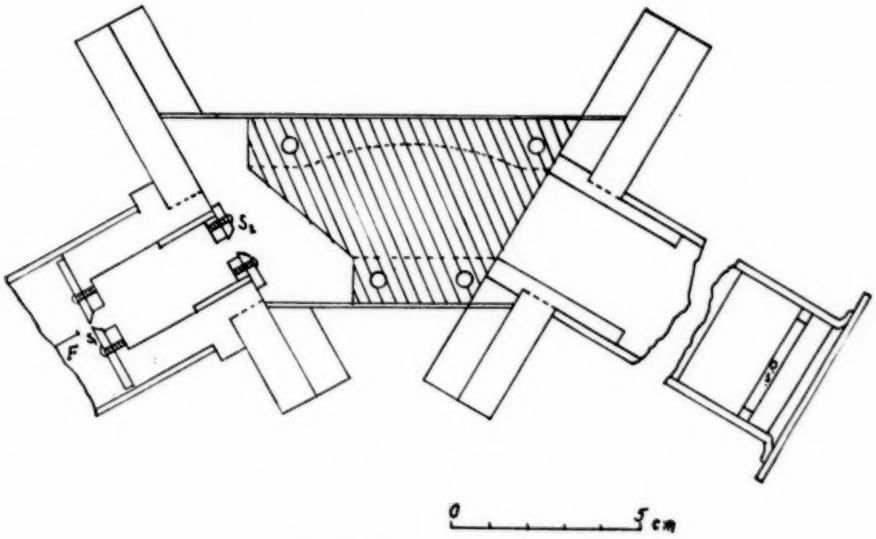


FIG. 2. Diagram of apparatus.

image slits from the field boundary. In the special case that the normal to the field at the point of exit coincides with the direction of the ion beam, the expressions for the other quantities take the form:

$$g'=\frac{a\cos\epsilon'\cos\phi}{\sin(\phi-\epsilon')};\quad g''=\frac{a\cos(\phi-\epsilon')}{\sin(\phi-\epsilon')};$$

$$f=\frac{a\cos\epsilon'}{\sin(\phi-\epsilon')}.$$

The apparatus used is indicated in horizontal section in Fig. 2. The ion source, $F$, was a hot platinum filament coated with spodumene. Both isotopes of lithium could be observed on the fluorescent screen, $O.S.$ The isotope at 7 was used rather than the one at 6 because of its greater intensity. The source was maintained at a positive potential of 8400 volts, and the slits, $S_1$ and $S_2$, were at ground potential with the deflection chamber. The magnetic field intensity was maintained at 5630 oersteds. Four magnets, one of which is shown shaded in the figure, were used. The magnets were machined so that the angles of incidence were respectively approximately 0°, −10°, −20°, −30°. The gap between pole faces was 0.32 cm. Outside the deflection chamber the cross section of the core of the magnet continues approximately the same as that of the pole pieces. Thus the flux distribution was not disturbed by the spreading of the lines within the iron. The images were observed on a willemite screen which could be moved by a magnet outside the glass tube in which it was mounted. The position of the screen was read on a scale fixed to the apparatus.

The ion beam was limited by a first slit $S_1$ of $\frac{1}{2}$ mm width at a distance of 4 mm from the source and 6.20 cm from the field boundary. The second slit, $S_2$, was about 5 mm wide. From the discolored spot on the face of the magnet, it was found that the angle between the extreme rays was about 6.5°.

Observations were made in a darkened room. The images were observed on the front of the screen where the intensity is greatest and the true cross section of the beam could be seen without any effects due to scattering or secondary radiation in the screen. Observing from the front also avoided the background illumination from the filament. The screen was moved back and forth along the tube until an optimum focus was at-

TABLE I. *Comparison of observed and calculated image distances. See Fig. 1 for notation.*

| $\epsilon'$ | $l'$ cm | $l''$ cm (calculated) | $l''$ cm (observed) |
|---|---|---|---|
| 0° | 6.20 | 25.21 | 22.7±.5 |
| − 8.75° | 6.20 | 15.98 | 15.5±.5 |
| −18.75° | 6.20 | 13.44 | 13.4±.4 |
| −28.20° | 6.20 | 9.65 | 9.6±.4 |

tained. The spread in the velocity of the ions was very small compared to the average velocity of the ion beam so that the image width was due almost entirely to the width of the first slit. The final observations were made at a pressure of $1\text{–}3\times10^{-5}$ mm Hg. It was found that if the pressure were allowed to rise as high as $10^{-4}$ mm the focus was not sharp. At times the ions would be deflected to such an extent that the focusing of the ion beam was destroyed.

It was found that, if the stray field at the edges of the magnetic field were neglected, considerable discrepancies between the theory and observations resulted. By applying a correction for the stray field it was found that satisfactory agreement could be obtained for all four series of observations with the same correction. The correction amounted to assuming that the deflection in the stray field was the same as if the field between the poles extended 2 mm beyond the pole faces.

In Table I the observations are compared with the calculated positions of the image corrected for the stray field.

The discrepancy in the first row of the table is probably due to the fact that in this series the ion beam converged so slowly that the position of optimum focus is more difficult to estimate. In general these observations serve to confirm the theory of magnetic focusing for oblique incidence as given by Herzog.

In conclusion, the author wishes to express his deep appreciation to Dr. A. J. Dempster, who suggested this problem, for his continued interest in the work and the many valuable suggestions he has made during the investigation. He also wishes to acknowledge the kind assistance of Dr. A. E. Shaw.

---

JULY 15, 1937 PHYSICAL REVIEW VOLUME 52

# The Coexistence of Dia- and Paramagnetism in Single Crystals of Antimony-Tin Alloys

HAROLD M. HART
*Sloane Physics Laboratory, Yale University, New Haven, Connecticut*
(Received May 20, 1937)

IN recent years the application of quantum mechanics in explaining magnetic properties of metals has met with considerable success. In particular, Jones,[1] using Bloch's description of the metallic state, has succeeded in calculating approximate values of the diamagnetic susceptibility of bismuth and other metals. Further, Jones' treatment makes it possible to predict how particular foreign atoms will affect the susceptibility of an element.

In the present work the effect of adding small amounts of tin to antimony has been investigated by studying the magnetic anisotropy at room temperature. (The anisotropy is here measured by the ratio of the magnetic mass susceptibility parallel to the principal crystal axis, $\chi_{\parallel}$, to that perpendicular thereto, $\chi_{\perp}$.)

The alloys were synthesized from the elements by the usual method of melting under hydrogen. The antimony was of high purity, supplied by Eimer and Amend. The tin was from stock used in previous magnetic experiments in this laboratory[2] and was known to be very pure. Castings made from these melts were converted to single crystals under hydrogen (horizontal traveling furnace method). Furnace speeds varied from 4.5 mm·min.$^{-1}$ down to 2 mm·min.$^{-1}$ for the higher tin percentages. In their final form the crystals were roughly cylindrical rods 3–8 cm long and about 3 mm in diameter. Minor irregularities in cross section are ascribed to the high surface tension of molten antimony. Check analyses are being undertaken.

Measurements were made by the Gouy method using a Sartorius microbalance and a Weiss electromagnet. Comparison at various field strengths made it certain that the crystals were iron-free. The crystals were adjusted in the mag-

[1] H. Jones, Proc. Roy. Soc. **A147**, 396–417 (1934).

[2] H. J. Hoge, Phys. Rev. **48**, 615–619 (1935).

netic field to azimuths for maximum and minimum force, and vertical forces were measured. They were then removed, cleaved, and the inclination of the cylinder axis to the (111) plane thus found. The formula

$$\chi_{\theta,\alpha}=\chi_\perp \sin^2\theta+(\chi_\perp \cos^2\alpha+\chi_\parallel \sin^2\alpha)\cos^2\theta,$$

where $\theta$ = angle between trigonal axis and magnetic field, and $\alpha$ = angle between trigonal axis and the vertical, then sufficed to determine the ratio $\chi_\parallel/\chi_\perp$. Fig. 1 shows $\chi_\parallel/\chi_\perp$ *versus* weight percent tin.

The anisotropy ratio without added tin was found to be 2.52, which agrees well with the value 2.56 calculated from Shoenberg and Uddin's[3] data for highly purified antimony.

The course of the curve suggests that the absolute value of $\chi_\parallel$ (originally negative) decreases as tin is added and that finally $\chi_\parallel$ changes sign so that the crystals become paramagnetic parallel to the trigonal axis. Due to the irregularities in cross section only crude measurements of the principal susceptibilities could be made. Comparison of the crystal containing 3.5 percent tin with a bismuth rod of known susceptibility gave $\chi_\parallel=(1.5\pm0.3)\times10^{-6}$ and $\chi_\perp=(-0.77\pm0.15)\times10^{-6}$. These values show that most of the change in $\chi_\parallel/\chi_\perp$ is due to change in $\chi_\parallel$, $\chi_\perp$ remaining comparatively constant. (Shoenberg and Uddin[3] give $\chi_\perp=-0.55\times10^{-6}$ for antimony.)

Goetz and Focke[4] have noted the same reversal in sign of $\chi_\parallel$ in bismuth-tin alloys. Extending the argument of Mott and Jones,[5] this may be explained by assuming $\chi_\parallel$ to be largely due to electrons overlapping into the next Brillouin zone, $\chi_\perp$ being attributed to "positive holes." (The term "positive holes" is used for unoccupied, but possible, electronic energy states.) Substituting tin is then supposed to decrease the number of overlapping electrons since tin has one less valence electron than bismuth. Thus the diamagnetic part of $\chi_\parallel$ is decreased until finally, as shown experimentally, $\chi_\parallel$ becomes positive.

Now antimony is isomorphous with bismuth and has the same number of valence electrons.

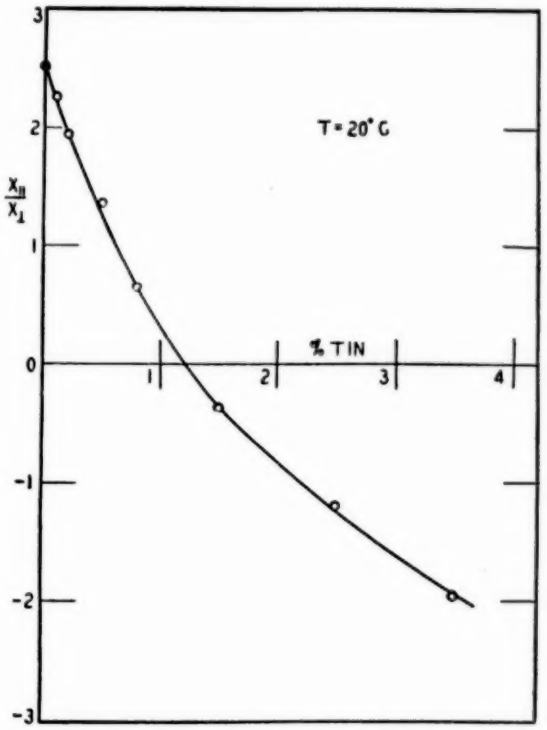


FIG. 1. Magnetic anisotropy in antimony-tin single crystals $\chi_\parallel/\chi_\perp$ *vs.* weight percent tin (by synthesis).

However, in antimony, $|\chi_\parallel|$ is greater than $|\chi_\perp|$ and is more temperature sensitive,[3] whereas in bismuth $|\chi_\parallel|$ is less than $|\chi_\perp|$ and is less temperature sensitive.[6] Furthermore, the Hall coefficient (which is closely allied with magnetic properties) is positive for antimony but negative for bismuth.[7] But the present data show that in antimony, as in bismuth, it is $\chi_\parallel$ which changes in sign when the number of overlapping electrons is presumably decreased by adding an element with one less valence electron, namely, tin. Thus structures, valences and magnetic effects of tin addition suggest similarity in electron configuration (Brillouin zones) between Sb and Bi; Hall effect, magnetic anisotropy in the pure metals and its change with temperature suggest dissimilarity.

In conclusion the writer wishes to express his thanks to Cecil T. Lane of this laboratory, who suggested and encouraged the investigation, and to L. W. McKeehan for aid in the preparation of this report.

[3] D. Shoenberg and M. Z. Uddin, Proc. Camb. Phil. Soc. **32**, 499–502 (1936).
[4] A. Goetz and A. B. Focke, Phys. Rev. **38**, 1569–1572 (1931).
[5] N. F. Mott and H. Jones, *Properties of Metals and Alloys* (Oxford University Press, 1936), pp. 212–213.
[6] D. Shoenberg and M. Z. Uddin, Proc. Roy. Soc. **A156**, 687–701 (1936), esp. p. 691.
[7] N. F. Mott and H. Jones, reference 5, p. 284.

# LETTERS TO THE EDITOR

*Prompt publication of brief reports of important discoveries in physics may be secured by addressing them to this department. Closing dates for this department are, for the first issue of the month, the eighteenth of the preceding month, for the second issue, the third of the month. Because of the late closing dates for the section no proof can be shown to authors. The Board of Editors does not hold itself responsible for the opinions expressed by the correspondents.*

**Communications should not in general exceed 600 words in length.**

## Space and Surface Waves in Radio Propagation

In his 1909 solution of the problem of the propagation of radio waves Sommerfeld[1] showed that the radiation field of a vertical electric dipole over a plane earth consisted of a space and a surface wave. In 1935 the author[2] pointed out a discrepancy in sign between Sommerfeld's original solution and the later solutions obtained by Weyl,[3] Sommerfeld,[4] and van der Pol and Niessen;[5] and the author showed that this difference in sign was responsible for the anomalies in transmission ("negative attenuation" and zero field intensity on the ground at finite distances) which had been predicted by the original solution. Recently this correction in sign was verified experimentally by Burrows[6] and theoretically by Wise.[7] Since this correction in sign affects the term which Sommerfeld had identified with a surface wave in such a manner that it does not appear in the asymptotic radiation field of a vertical electric dipole (as is evident in the asymptotic expansion of the vertical dipole wave function which was recently obtained by the author[8]), one might be led to believe that no surface wave exists in the asymptotic field of a vertical electric dipole. However, recent theoretical studies by the author[9] indicate that the radiation from a vertical electric dipole over a plane earth consists of a space and a surface wave component and that the surface wave is just the "ground wave" which is the medium for most low and medium frequency radio communication. The total radiation field (determined by Eqs. (55) and (70)[9]) may be separated into two components $\mathbf{E}_{sp}$ and $\mathbf{E}_{su}$ which will be identified as space and surface waves:

$$\mathbf{E}_{sp}=ik\cos\psi(1+R_v)\frac{e^{i(kR-\omega t)}}{R}\boldsymbol{\psi}, \tag{1}$$

$$\mathbf{E}_{su}=ik(1-R_v)F\frac{e^{i(kR-\omega t)}}{R}\left[\mathbf{k}+\mathbf{r}\frac{\cos\psi}{n}\left(1+\frac{\sin^2\psi}{2}\right)(1-\cos^2\psi/n^2)^{\frac{1}{2}}\right], \tag{2}$$

where

$$F=[1+i(\pi w)^{\frac{1}{2}}e^{-w}\operatorname{erfc}(-i\sqrt{w})], \tag{3}$$

$$w=\frac{ikR}{2n^2}[(1-\cos^2\psi/n^2)^{\frac{1}{2}}+n\sin\psi]^2, \tag{4}$$

$$\operatorname{erfc}(x)=\frac{2}{\pi^{\frac{1}{2}}}\int_x^\infty e^{-u^2}du. \tag{5}$$

The sum of (1) and (2) represents the total radiation field of a vertical electric dipole; these equations apply at any point in space above the surface of a (plane) earth such that $R\gg\lambda$ and may be used for any frequency or set of ground constants found in practice. $\mathbf{k}$ and $\mathbf{r}$ are unit vectors, respectively parallel and perpendicular to the vertical dipole. $R_v$ is the Fresnel reflection coefficient of a plane wave with its electric vector parallel to the plane of incidence and with angle of incidence $(\pi/2-\psi)$, $k=2\pi/\lambda$ and $n$ is the complex index of refraction of the earth. The other symbols, not defined in Fig. 1, have their usual meanings. The Poynting vectors for the space and surface waves may be determined from (115) and (117) in the above paper[9]

$$\mathbf{S}_{sp}=\left[ik\cos\psi(1+R_v)\frac{e^{i(kR-\omega t)}}{R}\right]^2\boldsymbol{\psi}, \tag{6}$$

$$\mathbf{S}_{su}=\cos\psi\left(1+\frac{\sin^2\psi}{2}\right)\left[ik(1-R_v)F\frac{e^{i(kR-\omega t)}}{R}\right]^2\times\left[\mathbf{r}-\mathbf{k}\frac{\cos\psi}{n}\left(1+\frac{\sin^2\psi}{2}\right)(1-\cos^2\psi/n^2)^{\frac{1}{2}}\right]. \tag{7}$$

(1) and (6) clearly determine a plane polarized space wave since the energy flows radially and $\mathbf{E}_{sp}$ lies in the surface of a hemisphere centered on the base of the radiating dipole. (2) and (7) determine a surface wave with a forward tilt and polarization (determined by the quantity in the square brackets in (2)) the same as the surface wave discussed by Sommerfeld. It is of interest to note that the surface wave exists only over an imperfectly conducting earth; over a perfectly conducting earth (since $R_v=1$) our surface wave disappears and our space wave reduces to the well-known Abraham solution for this case. An evaluation of the intensities of the two waves shows that the space wave represents most of the field for large values of the angle $\psi$ while near the surface, when $\psi$ is small, the surface wave predominates (on the surface $R_v=-1$ so that the surface wave exists alone). Due to the error in sign in his original paper, Sommerfeld supposed that the surface wave was attenuated exponentially as it travels along the ground while our surface wave contains an "attenuation factor" $|F|$. To those familiar with ground wave attenuation theory, this $|F|$ will be readily identified with the "ground wave attenuation factor" which varies first exponentially with the "numerical

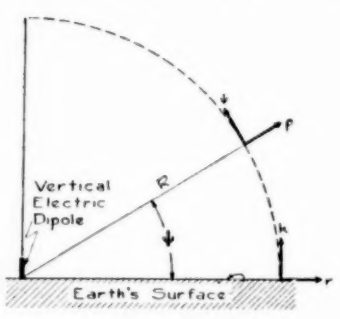


FIG. 1. Geometry for radiation formulas.

distance" and finally, at large distances, inversely as the "numerical distance." At the surface of the ground the "numerical distance," which played such a prominent part in Sommerfeld's original discussion, is given by $|w|$. A more complete discussion of the function $F$ is contained in a recent paper by the author.[8] Eq. (7) shows that a part of the energy in the surface wave flows downward into the ground and is thus the seat of the energy of the ground current set up by a radiating vertical electric dipole. Finally we may note a similarity of our surface wave to a guided wave on a wire when we remember that "ground waves" (with which we have identified our surface wave) are not affected by diffraction in traveling around the curvature of the earth until they have passed far beyond the line of sight.[9]

K. A. NORTON

Federal Communications Commission,
Washington, D. C.,
June 26, 1937.

[1] A. Sommerfeld, Ann. d. Physik **28**, 665–736 (1909).
[2] K. A. Norton, Nature **135**, 954–955 (1935).
[3] H. Weyl, Ann. d. Physik **60**, 481–500 (1919).
[4] A. Sommerfeld, Ann. d. Physik **81**, 1135–1153 (1926).
[5] B. van der Pol and K. F. Niessen, Ann. d. Physik **6**, 273–294 (1930).
[6] C. R. Burrows, Nature **138**, 284 (1936) and Proc. I. R. E. **25**, 219–229 (1937).
[7] W. H. Wise, Bell Sys. Tech. J. **16**, 35–44 (1937).
[8] K. A. Norton, Proc. I. R. E. **24**, 1367–1387 (1936).
[9] K. A. Norton, Proc. I. R. E. **25**, To be published in August (1937).

## Pressure Shift of Spectral Lines

The author has shown[1] that the purely statistical calculation of the pressure shift of spectral lines, neglecting the motion of atoms and assuming London's potential law $C/r^6$ of the van der Waals forces, gives the shift of the maximum proportional to the square of the density of the gas. In the formula given[1]

$$\delta\nu = 6.8 \times C \times N^2$$

($C$ = constant of van der Waals potential, $N$ = number of perturbing atoms per cc) the numerical factor was an estimated lower limit. Later, Margenau[2] who at first predicted proportionality of the shift with $N$, revised his original results and arrived at the same conclusion. He was able to replace the above value 6.8 of the constant by the more accurate value 9.2.

A quantitative theory of pressure broadened lines, including both the statistical and the kinetic effect, does not exist. Neither the abstract theory of Lenz[3] nor the more qualitative method of London and the author,[4] which was mathematically extended by Margenau[2] can claim to be satisfactory solutions of the problem. It is therefore of interest to test the statistical theory in cases where the influence of the atomic motion is small.

In general, the intensity near the maximum of the broadened line is influenced to a considerable extent by the motion of the atoms. Accordingly, the shift of the maximum has always been found to increase only little more than linearly with $N$. In view of this situation it seems worth pointing out that a case has recently been investigated where the low speed of the atoms (low temperature and high atomic weight) together with another condition mentioned below give an exceptionally good opportunity for applying the statistical theory even to the maximum of intensity.

TABLE I. *Term shifts at various pressures and van der Waals constants.*

| Term | Shift at 4 mm | Shift at 10 mm | Shift at 20 mm | $C$ in sec.$^{-1}$ × cm$^6$ |
|---|---|---|---|---|
| $4p^5\,5p$ | | | 0.003 cm$^{-1}$ | $2.4\times10^{-29}$ |
| $4p^5\,6p$ | 0.0003 cm$^{-1}$ | 0.003 cm$^{-1}$ | 0.011 cm$^{-1}$ | $8.7\times10^{-29}$ |
| $4p^5\,7p$ | 0.006 cm$^{-1}$ | | | $120\times10^{-29}$ |
| $4p^5\,6d$ | | | 0.015 cm$^{-1}$ | $12\times10^{-29}$ |

The pressure shifts of krypton lines were measured interferometrically with great accuracy by C. V. Jackson.[5] Thirty lines in the visible spectrum were investigated, involving the levels of the configurations $4p^5\,5s$, $4p^5\,5p$, $4p^5\,6p$, $4p^5\,7p$ and $4p^5\,6d$. In the range of pressures used (0.1 to 20 mm Hg) the shifts of all the lines were found to be proportional to the square of the pressure. The shift is always to the red. As several of the lines have the lowest level $4p^5\,5s$ in common, definite statements could even be made on the shifts of the terms involved, only a small additive constant common to all of them being unknown. Terms belonging to the same configuration were found to have equal shifts, and the shifts increased with increasing principal quantum number. Applying the above-mentioned theory, the van der Waals constants are found in Table I.

The good agreement of the statistical calculation with the observed shifts must be ascribed to two causes. The first is the small relative speed of the atoms mentioned before; the second and probably more important one is the very great value of $C$, characteristic of these high terms (it is about 1000 times greater than the known $C$ values for lower terms). This makes, for a given value of $\delta\nu$, the gradient of the potential very small, which causes the velocity correction to be small.[4]

That the perturbing and the perturbed atom are of the same kind is no objection to the interpretation given here, as according to Weisskopf[6] the influence of the resonance forces is negligible. It must be emphasized that the theory of the polarization forces can, for higher levels, be applied only if the density of the gas is very small. For the opposite limiting case of the distances between the atoms being small compared with the size of the orbitals, a theory of the shifts has been given by Fermi.[7]

The first experimental method of testing the sixth power potential law of the polarization forces was based on the calculation of the intensity in the wings of pressure broadened lines; the theoretical prediction[1] was completely verified.[8, 9] A second method of testing this law and determining $C$ values seems to be given by the pressure shift of lines under conditions similar to those described above for krypton.

H. KUHN

Clarendon Laboratory,
Oxford, England,
June 19, 1937.

[1] H. Kuhn, Phil. Mag. **18**, 987 (1934).
[2] H. Margenau, Phys. Rev. **48**, 755 (1935).
[3] W. Lenz, Zeits. f. Physik **80**, 423 (1933).
[4] H. Kuhn and F. London, Phil. Mag. **18**, 983 (1934).
[5] C. V. Jackson, Phil. Trans. Roy. Soc. **A236**, 1 (1936).
[6] V. Weisskopf, Physik. Zeits. **34**, 1 (1933).
[7] E. Fermi, Nuovo Cimento **11**, 157 (1934).
[8] R. Minkowski, Zeits. f. Physik **93**, 731 (1935).
[9] H. Kuhn, Proc. Roy. Soc. **A158**, 212 and 230 (1937).

### Nuclear *K* Electron Capture

As has frequently been pointed out, one of the simple consequences of Fermi's theory of $\beta$-decay,[1,2] taken together with the Dirac theory of the positron, is that positron-active nuclei may capture atomic electrons instead of emitting positrons. Since the nuclei in this case emit no observable particles, the decay must be detected in some unusual manner, as for example, (1), by comparing the rate of growth of the daughter substance with that calculated from the activity of the parent, (2) by counting the number of radioactive atoms formed, and later the number of positrons ejected, or (3) by detecting the x-rays which would result from the refilling of the *K* shell. Jacobsen[3] has recently attempted to observe the latter in a cloud chamber, using $Sc^{43}$; he found no evidence in support of the electron capture hypothesis. Walke[4] has recently found that a strong positron activity of 16 days' half-life may be induced in Ti, by deuteron bombardment. Chemical separation indicates that a vanadium isotope is responsible for the activity, whose positrons have an upper limit of 1.05 MV. Since this activity fits the second Sargent curve (instead of the first, as does $Sc^{43}$), it seemed likely that its ratio of *K* quanta to positrons would be greater. The results of an experimental attempt to observe the x-radiation are reported below.

A source of radio-vanadium was placed in a magnetic field of about 2000 oersteds, and was surrounded on five sides by 2 mm of aluminum. The gamma-rays passed through 20 cm of He, and 16 cm of air before reaching a Cellophane-walled counter filled with argon at atmospheric pressure.[5] The cathode was of 0.00025 cm Cu, curved to form three-fourths of a cylinder; the radiation had to pass through only 0.0025 cm of Cellophane to reach the active volume of the counter. When thin sheets of Al were introduced between the source and counter, the counting rate fell from 21.3 to 15.4 per second. The soft component responsible for this decrease was all absorbed in 0.0025 cm of Al; the interposition of more Al (up to 0.0075 cm) had no detectable effect upon the counting rate. Fig. 1 is an absorption curve of the soft component; the constant gamma-ray background has been subtracted from all the actual readings. The line has been drawn to fit the highest point, with a slope calculated from the known absorption coefficient of Ti $K\alpha$. 15,000 counts were taken for each point on the curve, and the background and linearity of the counter were frequently checked. The ratio of x-ray counts to gamma-ray counts, after correction had been made for the absorption in the air path and in the Ti, was 1.9. The last correction involved the plotting of an excitation function for the reaction. The source was then replaced by a weaker sample, and the magnetic field removed. The ratio of gamma-ray counts to positron counts was determined by measuring the relative counting rates when the source was bare, and when it was covered with 2 mm of Al. This ratio (corrected for the absorption of the positrons in the air, He and Cellophane) was 0.082. 0.75 of the x-ray quanta should produce photoelectrons in the argon, so it will be assumed that the efficiencies for positron and quantum detection were 100 percent and 75 percent, respectively. The ratio of the numbers of *K* quanta and positrons is then $1.9\times0.082/0.75=0.21$. This ratio must be divided by the fluorescence yield[6] of the *K* shell in Ti, to give the relative probability for capture and emission. This yield is 0.21 from data given by Compton and Allison. Therefore, the ratio of the probabilities of *K* electron capture and positron emission is

$$1.0\pm0.4.$$

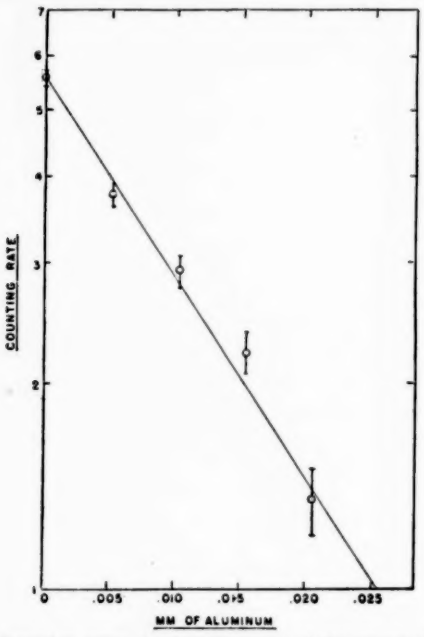


FIG. 1. Absorption curve of soft component of the gamma-radiation.

This observed ratio of *K* electron capture to positron emission is of the order of magnitude suggested by the Konopinski-Uhlenbeck modification of the theory proposed by Fermi. To exclude the possibility that the radiation was due to the impact of positrons on Ti, the sample was covered with 0.0025 cm of chromium. This would be sufficient to absorb all the observed Ti *K*-radiation, and if the effect were of a secondary nature, Cr *K*-radiation should be produced in almost equal numbers. No such effect could be detected.

*Note added June 28:*

Sizoo[7] has recently shown that if the first and last of three isobaric nuclei with consecutive charge numbers are stable, the second will in most cases be capture-unstable as well as $\beta^-$-radioactive. The 2.5 day radioactive antimony isotope formed by deuteron bombardment is the second of three isobars, and emits only negative electrons. A search was made for Sn *K*-radiation from active Sb, but without success. The electrons were stopped with a magnetic field, and the gamma-rays were absorbed in aluminum. No soft component was found which produced as much as 2 percent of the total gamma-ray ionization in a Lauritsen type electroscope. If Sizoo's theory is correct, this must be one of the rare cases where the two lightest isobars are both stable with respect to each other.

In conclusion, the author wishes to express his gratitude to Professor E. O. Lawrence for the privilege of working

in the Radiation Laboratory and to Professor J. R. Oppenheimer for discussions of the theoretical aspects of the problem. The work was made possible by grants to the laboratory from the Chemical Foundation, the Research Corporation, and the Josiah Macy, Jr. Foundation.

LUIS W. ALVAREZ

Radiation Laboratory,
University of California,
Berkeley, California,
June 21, 1937.

[1] E. Fermi, Zeits. f. Physik **88**, 161 (1934).
[2] E. J. Konopinski and G. E. Uhlenbeck, Phys. Rev. **48**, 7 (1935).
[3] J. C. Jacobsen, Nature **139**, 879 (1937).
[4] H. Walke, Phys. Rev. **51**, 1011 (1937).
[5] J. S. Allen and L. W. Alvarez, R. S. I. **6**, 329 (1935).
[6] A. H. Compton and S. K. Allison, *X-Rays in Theory and Experiment* (1935), p. 488.
[7] G. J. Sizoo, Physica **4**, 467 (1937).

## Radioactive Isotopes of Manganese, Iron and Cobalt

We wish to make a preliminary report on the radioactive isotopes of Mn, Fe, and Co produced when Fe is bombarded with 5.5 Mev deuterons (20–60 microampere hours) and when Co is bombarded with neutrons. The decay curves of the chemically separated fractions have been measured with a Lauritsen type electroscope.

**Fe:** A negative electron activity of approximately 40 days half-life is found in the Fe fraction of the Fe plus deuteron bombardment, either after precipitation (and repeated reprecipitation) as $Fe(OH)_3$ from a solution containing an excess of ammonium salts or after extraction as $FeCl_3$ by shaking with ether. An Fe activity of the same period (~40 days) has been chemically separated from a sample of CoO that was bombarded intermittently for three months with neutrons ($Be+H^2$) produced in the cyclotron. The conditions of this latter experiment did not allow the detection of the three day Fe isotope reported by Andersen from Co plus neutrons;[1] this isotope definitely was not produced when Fe was bombarded with deuterons.

**Co:** This fraction of the Fe, after deuteron bombardment, contains an 18.0 hour positron emitter, in agreement with the 18.2 hour period reported by Darling, Curtis and Cork[2] for the same reaction. In addition, there is a complex of longer periods of apparent present half-life between 100 and 200 days. Both electrons and positrons are emitted. Undoubtedly this contains the Co isotope with half-life of a year or more (reported by Sampson, Ridenour and Bleakney[3] from Co plus neutrons), and also a positron emitter of shorter period. Our work also gives support to that of Sampson and co-workers in that Co chemically separated from CoO bombarded with neutrons gives an activity which thus far is consistent with a half-life of over a year. We also find that CoO plus neutrons (without chemical separation) yields a negative electron activity with 11 minutes half-life. This period is in disagreement with the 20-minute value reported by Rotblat[4] for the same reaction but supports the values found by Heyn[5] and by Kikuchi, Takeda and Ito.[6]

**Mn:** The Fe plus deuteron bombardments show two new periods in the Mn precipitate; a positron emitter of about 5 days half-life and a negative electron emitter of several months period. This fraction also shows a 21-minute activity (of undetermined sign), in agreement with the 21-minute figure given by Darling, Curtis and Cork[2] for the same reaction. In disagreement with the work of Darling and co-workers the well-known 2.5-hour negative electron activity of $Mn^{56}$ is strongly evident in this same fraction, even when very pure Fe is used for the deuteron bombardment. This is due to the reaction $Fe^{56}(n, p)\ Mn^{56}$, at least partially, for there is a large yield of neutrons (as observed in the cloud chamber) accompanying the transmutation of Fe to Co. This supposition is confirmed by the fact that the 2.5-hour activity also appears in a second piece of Fe placed out of the deuteron beam close to the target Fe.

A Mn positron emitter of 46 minutes half-life is produced when Cr is bombarded with deuterons.

A complete description of the work, including the decay curves and a discussion of the probable reactions involved, will be published at a later date.

We wish to express our appreciation of the continued assistance of the Chemical Foundation, the Josiah Macy, Jr. Foundation and the Research Corporation.

J. J. LIVINGOOD

Radiation Laboratory,
Department of Physics,
and

F. FAIRBROTHER

G. T. SEABORG

Department of Chemistry, University of California,
Berkeley, California,
June 30, 1937.

[1] Andersen, Nature **138**, 76 (1936).
[2] Darling, Curtis and Cork, Phys. Rev. **51**, 110 (1937).
[3] Sampson, Ridenour and Bleakney, Phys. Rev. **50**, 382 (1936).
[4] Rotblat, Nature **136**, 515 (1935).
[5] Heyn, Physica **4**, 160 (1937).
[6] Kikuchi, Takeda and Ito, Proc. Phys.-Math. Soc. Jap. **19**, 43 (1937).

## Radioactive Antimony Isotopes

Bothe and Gentner[1] have obtained a 13 minute activity by irradiating Sb with the 17 Mev gamma-rays from $Li+H^1$. Heyn[2] has produced a radioactive isotope of 17 minutes half-life and Chang, Goldhaber and Sagane[3] have obtained a 13 minute period by bombarding Sb with the fast neutrons from the $Li+H^2$ reaction. Although Sb has two stable isotopes, $Sb^{121}$ and $Sb^{123}$, and only one previously known slow neutron activity (2.5 days[4]), all of these workers have concluded that this new activity is due to $Sb^{120}$ because it is not produced by slow neutrons.

We wish to add confirmatory evidence to their supposition. Upon bombarding Sb both with slow neutrons ($Be+H^2$) and 5.5 Mev deuterons from the cyclotron we have produced, and chemically identified as Sb, a new activity of approximately 60 days half-life, in addition to the 2.5 day period. Both of these are found to be negative electron emitters. It is certain that the 2.5 day and 60 day activities must be associated with $Sb^{122}$ and $Sb^{124}$ or *vice versa*, and therefore the 13 to 17 minute period must be assigned to $Sb^{120}$.

We have confirmed the production of $Sb^{120}$ by bombarding Sb with fast neutrons ($Li+H^2$), and have observed that positrons are emitted. Our value for the half-life is 16 minutes. A chemically identified Sb isotope of the same half-life has also been produced when Sn was bombarded with deuterons. This activity presumably is due also to $Sb^{120}$, the reaction being $Sn^{119}\ (d, n)\ Sb^{120}$.

This research has been made possible through the generous cooperation of the Research Corporation, the Chemical Foundation, and the Josiah Macy, Jr. Foundation.

J. J. LIVINGOOD

Radiation Laboratory,
Department of Physics,
and

G. T. SEABORG

Department of Chemistry,
University of California,
Berkeley, California,
June 30, 1937.

[1] Bothe and Gentner, Naturwiss. **25**, 126 (1937).
[2] Heyn, Nature **139**, 842 (1937).
[3] Chang, Goldhaber and Sagane, Nature **139**, 962 (1937).
[4] Amaldi, D'Agostino, Fermi, Pontecorvo, Rasetti and Segrè, Proc. Roy. Soc. **A149**, 522 (1935).

## Interpretation of High Pressure Arc Data

In the high pressure arc the dependence of electric gradient $E$ (volts cm$^{-1}$) and current density $I$ (amp. cm$^{-2}$) on the nature of the gas and its pressure $p$ has now been studied for A, $N_2$, He, and $H_2$ over a portion of the pressure range up to 1200 atmospheres.[1] We find that the body of experimental results can be correlated by means of convective heat loss from solid cylinders, leading to an explanation of the variation of $E$ and $I$ with $i$ and $p$ which is in good agreement with the experiments.

For this purpose, we neglect radiation and use an equation of the Nusselt[2] type

$$y=f(x) \tag{1}$$

between the dimensionless variables $y$ and $x$ where

$$y=W/k\Delta T\pi, \quad x=D^3\rho^2 g\Delta T\beta/\eta^2, \tag{2}$$

$W$ = loss (in calories) per unit length of axis; $k$ = conductivity; $D$ = diameter; $\rho$ = density; $\beta$ = coefficient of expansion; $\eta$ = viscosity. In the range of interest in arcs,

$$f(x)=\text{const } x^n \tag{1'}$$

with $n=0.1$ provides a satisfactory approximation.

In the usual applications of (1) $\Delta T$ is not large, and the fluid constants $\rho$, $\beta$, $\eta$, $k$ are evaluated at the mean temperature. For this case a large body of experimental data confirms the essential correctness of the relationships. An indication of how to evaluate them for large $\Delta T$ was obtained by studying ways of bringing Langmuir's data on heat losses from wires in air at high temperatures into agreement with (1). This is done by taking $k$, $\rho$, $\eta$ at the arc temperature and $\beta$ at the ambient temperature.

When the method is applied to arcs, we find that the calculated thermal loss agrees satisfactorily with the observed energy input in A and He. In arcs in air, the calculated heat loss is approximately one-third of the observed. This discrepancy we ascribe to dissociation, and when $k$ is increased by Langmuir's diffusion term, good agreement is obtained.

As an application of (1) one can account correctly for the arc characteristics. Assuming constant $T$ and applying Saha's equation, one finds

$$E\sim i^{-a}, \quad \text{where} \quad a=\frac{2-3n}{2+3n}, \tag{3}$$

where $n$ is as in (1'). Thus the Steinmetz equation of the arc is obtained from thermal data. The exponent $a$ has the value 0.74 from the above theory and lies between 0.45 and 1 in experiments.

When pressure $p$ varies, it is necessary to take account of the variation of $T$ with $p$. From arc data which yield the dependence of $T$ on $p$,[1] and Saha's equation, we find the variation of the electron density with $p$. Using this and the previous relations, we find that $E$ varies as $p^{0.3}$ and $D$ as $p^{-0.33}$. At $p=100$ atmospheres, $E_{\text{calc}}/E_{\text{obs}}=1.32$, while $D_{\text{calc}}/D_{\text{obs}}=1.14$.

Measurements of $D$, $E$, $I$, and $i$ for several gases up to 100 atmospheres pressure are being made by a new method of improved accuracy. The new measurements, it is believed, will not change the trends in the variation of these quantities, which are well enough established by data already in hand, but only serve to define the approximations involved.

Thus, by applying conduction and convection heat transfer data to the arc column, and determining the temperature variation experimentally, a simple formulation of the electrical characteristics of the arc and their variation with pressure is obtained.

C. G. SUITS
H. PORITSKY

Research Laboratory and Engineering General Dept.,
General Electric Company,
Schenectady, New York,
June 16, 1937.

[1] Paper presented at Madison meeting of the American Physical Society, June 22, 1937.
[2] Nusselt, Gesundheits-Ingenieur **38**, 477 (1915); Rice, Trans. A. I. E. E. **42**, 653 (1923); **43**, 131 (1924); McAdams, *Heat Transmission* (McGraw-Hill, 1933).

## Ionic Recombination in the Ionosphere—A Correction

In my recent letter to the Editor, Phys. Rev. **51**, 1110 (1937), I gave a value for the coefficient of recombination $\alpha$ for $(O_2)_2$ ions in the $E$ layer of the ionosphere computed from the Thomson theory as $\alpha=1.61\times10^{-8}$. Professor N. E. Bradbury in a letter wrote me that he was unable to check this value. Calculation shows that the value of the coefficient $\epsilon$ in Thomson's equation is critically dependent on the value of $e^{-x}$ for small values of $x$. In my computation I had used only two members of the series expansion. Using three terms I now check Bradbury's value and wish to correct my previous value. The value of $\alpha$ on this calculation is $\alpha=1.68\times10^{-10}$. This is of the same order of magnitude as $\alpha_r$, the value given for a recombination process in which recombination takes place for *all* impacts where the distance of ionic approach $r_0$ is $4\times10^{-8}$ cm or less. These calculations thus show that the Thomson mechanism already ceases to be dominant in the $E$ layer of the ionosphere. Professor Bradbury also points out that the auroral spectrum shows no $O_2$ or $O_2+$ lines so that the oxygen must be atomic. It is doubtful whether this will change the conclusions in the previous letter since O certainly has an electron affinity so that free electrons will probably not exist for any length of time in the $E$ layer.

LEONARD B. LOEB

University of California,
Berkeley, California,
June 25, 1937.

## Energy of the Gamma-Rays of Radioindium and Radiomanganese

We have measured the energies of the gamma-rays from RdIn (54 min.) and RdMn by recording the coincidences produced by Compton electrons ejected from a 0.45 cm aluminum plate placed in front of two counters.[1] Insertion of aluminum foils between the two counters causes a decrease in the number of coincidences. If $D_{\frac{1}{2}}$ is the thickness of aluminum in g/cm² which cuts the number of coincidences to one-half, the energy, $E$, of the gamma-ray is given by the relation

$$D_{\frac{1}{2}}=C_{\frac{1}{2}}\frac{(E/mc^2)^2}{(E/mc^2)+1},$$

where $C_{\frac{1}{2}}$ is a constant, practically independent of energy, which must be determined with the help of some gamma-ray of known energy. A similar formula with a different constant $C$ can be used for the quarter value thickness. The formula assumes that the gamma-ray is monochromatic.

The apparatus was calibrated using the gamma-rays of radiothorium filtered through 6 cm of lead (energy 2.65 Mev), and also those of radium filtered through 4 cm of lead (energy 1.8 Mev). After correcting for the absorption by the counter walls, the values of the constant $C$ shown in Table I were obtained using both standards. They agree to 3 percent.

The curves obtained for RdMn and RdIn are shown in Fig. 1. The initial number of coincidences in 5 minutes were for RdMn 125, for RdIn 266; the background was 8 in 5 minutes. The half-value and quarter-value thicknesses are shown in the table together with the value for the energy of the gamma-rays calculated therefrom. The average energies of the gamma-rays are for RdMn 1.65 Mev, RdIn 1.39 Mev. We also tried to measure the gamma-rays from RdAs but these, while present, were too weak to admit of measurement.

Using a single counter, surrounded by enough lead to stop all beta-rays from the source, we measured the absorption of the gamma-rays of RdMn, RdIn, and Th C″ in lead and copper. Because of the weak intensity of the sources, the geometrical arrangement for these measurements was not good enough to allow one to use the absorption coefficients thus obtained to calculate the energy without applying large corrections. This was apparent from the work on Th C″. The results did show, however, that the gamma-rays were *monochromatic* and that their energy was considerably less than that of the gamma-ray from Th C″. The period of the gamma-ray from each substance was measured and found to be the same as that for the beta-activity.

TABLE I. *Gamma-ray energies from In and Mn.*

| Element | Half-Value cm | Quarter-Value cm | Calibration Energy Mev | $C_{1/2}$ g/cm² | $C_{1/4}$ g/cm² | Energy Mev |
|---|---|---|---|---|---|---|
| Th C″ | 0.110 | 0.178 | 2.65 | 0.0630 | 0.107 | — |
| Ra | 0.070 | 0.118 | 1.8 | 0.0670 | 0.113 | — |
| Mn | 0.059 | 0.106 | — | 0.0650 | 0.110 | 1.61, 1.69 \| 1.65 |
| In | 0.051 | 0.091 | — | 0.0650 | 0.110 | 1.28, 1.49 \| 1.39 |

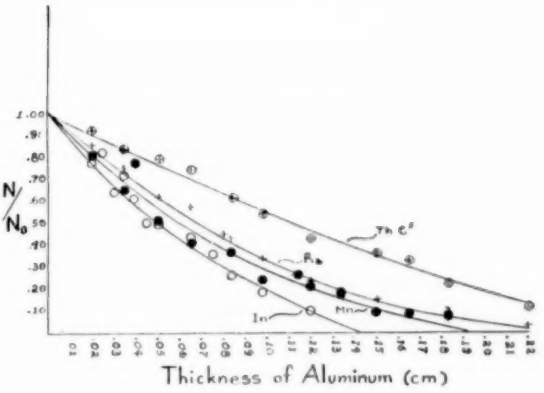


FIG. 1.

The beta-ray spectrum of RdMn has been measured by Brown and Mitchell[2] who found that the distribution curve could be decomposed into two curves with end-points at 2.9 and 1.2 Mev. It was supposed that the difference in energy between these two end-points should correspond to a gamma-ray of this energy, namely 1.7 Mev. The fact that we have found a monochromatic gamma-ray from RdMn of energy 1.65 Mev lends strong support to this view. We hope to extend this work to the study of other elements to see if this relationship holds in general.

The authors wish to express their thanks to the Penrose Fund of the American Philosophical Society for a grant.

ALLAN C. G. MITCHELL
LAWRENCE M. LANGER

Physics Department,
New York University,
University Heights,
June 28, 1937.

[1] F. Rasetti, Zeits. f. Physik **97**, 64 (1935).
[2] M. V. Brown and A. C. G. Mitchell, Phys. Rev. **50**, 593 (1936).

## Sharp Absorption Lines for Use as a Comparison Spectra in Stellar Photography

For a number of years astronomers have been looking for a better substance than thin layers of Nd solution to use as a reference spectra for measuring Doppler shift in connection with an objective prism. It occurred to the author that Eu salt, theoretically, should be a much better substance than Nd for this purpose. The basic state of $Eu^{+++}$ in the solid is a $^7F_0$ and a number of transitions should occur to upper states which have $J$ values of 0 or 1. Sueh states do not split in the electric field of the crystal and therefore should not be much affected in the fluctuating fields caused by temperature vibration. One would then expect that absorption lines arising from such transitions would be sharp in a glass even at room temperatures.

Eu has now become available in appreciable quantities through the brilliant researches of Dr. H. N. McCoy.[1] He very generously gave the author 20 grams to further research on the absorption spectra of solids.

Photographs were made of the absorption spectra of solid $Eu_2(SO_4)_38H_2O$ and of $Eu_2O_3$ suspended and dis-

FIG. 1. $Eu_2(SO_4)_3 8H_2O$ crystal room temperatures 5780A region.

solved in $B_2O_3$ glass. A number of the lines in both solids were extremely sharp even at room temperatures. (See Figs. 1 and 2.) $Eu_2O_3$ does not seem to be very soluble in

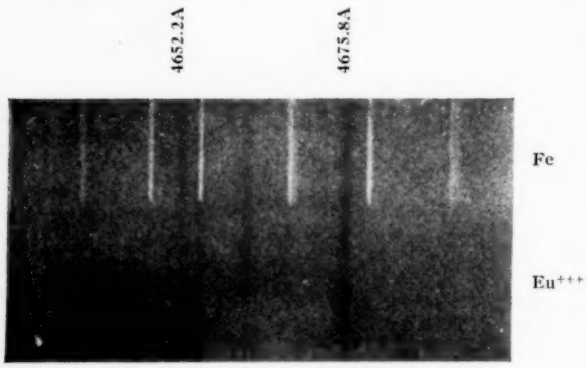


FIG. 2. $Eu_2O_3$ in $B_2O_3$ glass, room temperatures.

$B_2O_3$ as the clear beads of $B_2O_3$ did not show sufficient absorption to register on the plate. Opalescent beads containing suspended $Eu_2O_3$ were therefore used. The absorption multiplets are well suited for measuring Doppler shifts of other lines as the multiplets are simple and well placed, e.g. 4600A, 5200A and 5700A. The lines in solution are also fairly sharp (much better than Nd) and could be used instead of Nd. However, it should be possible to prepare a clear glass similar to Didinium glass in which the lines would still remain sharp and which would be much more convenient for astronomers.

FRANK H. SPEDDING*

Cornell University,
Ithaca, New York,
June 19, 1937.

* George Fisher Baker Research Fellow, Cornell University.

[1] H. N. McCoy, J. Am. Chem. Soc. **58**, 1577 (1936).

## The Proton's Magnetic Moment

A disagreement seems to exist between the values for the proton's magnetic moment, obtained by Stern and by Rabi and their co-workers. The former was the first to measure this fundamental quantity and to discover that the proton did not possess the expected magnetic moment, one nuclear magneton, but a moment 2.5 times this value.[1] An error of approximately 10 percent could be allowed in these earliest measurements. Rabi, using an entirely different method, made a new determination of $\mu_\pi$ and obtained the value 2.85 nm[2] with an accuracy $\pm 0.15$ nm. Stern and his colleagues, have continued their experiments, refining the method and checking carefully all things involved in the calculation of $\mu_\pi$ from the directly measured quantities. Their result. personally communicated,[3] is that $\mu_\pi$ equals $2.46 \pm 0.08$ nm. Thus, it seems that two different methods lead to different values for the same quantity. This, of course, makes it important that both experiments be scrutinized carefully to see that no systematic error is involved in either or whether some factor has been overlooked. At present, it seems improbable that any correction or revision can bring the two experiments into agreement. Let us assume that this is the situation.

We must then look for a fundamental difference in the two experiments. Stern's experiment measures the deflection of hydrogen molecules in an inhomogeneous macroscopic magnetic field; and it is assumed in calculating $\mu_\pi$, first, that the protons possess a magnetic moment, and secondly, that the energy of such a moment in a magnetic field is that given by classical electrodynamics. Rabi's experiment, on the other hand, deals with hydrogen atoms, and measures essentially the strength of external magnetic field necessary to produce a definite degree of uncoupling of the *spins* of the electron and proton, assuming that the spins are coupled only through the interaction of their associated magnetic dipoles. If, in reality, an extra spin-spin interaction between electron and proton existed, the exterternal magnetic field in Rabi's experiment would have to be strong enough to break down the coupling effect of this interaction plus the magnetic dipole interaction. Determination of nuclear magnetic moments from hyperfine structure involves the same assumption as Rabi's experiment and, in case the hypothesis of an extra electron-proton spin-spin interaction should prove tenable, all magnetic moments determined in this way would be necessarily in error. The accuracy with which the h.f.s. interval rule is obeyed practically requires that the extra interaction be represented in the form of a scalar product of the electron and proton spins multiplied by a function of the electron-proton separation

$$U = -(\boldsymbol{\sigma}_\epsilon \cdot \boldsymbol{\sigma}_\pi) V(r_{\epsilon\pi}).$$

In exactly the same way that we introduce the characteristic electron size $\epsilon^2/mc^2$ from a consideration of the electrostatic self-energy, we may establish another such quantity, $r_\mu = (\mu_\epsilon^2/mc^2)^{\frac{1}{3}}$ from a consideration of the magnetic self-energy ($r_\mu \sim 5 \times 10^{-12}$ cm). If the quantity $V(r_{\epsilon\pi})$ were assumed to have an appreciable value only within distances of the order $r_\mu$, then it would have to have an average value of the order of only $10^3$ electron volts to explain the discrepancy between Stern's and Rabi's results.

Breit[4] has shown that a spin dependent interaction of this type satisfies all relativistic requirements which we may reasonably impose. Although he was mainly interested in the possibility of learning something about specifically nuclear interactions between heavy particles, his treatment applies to all elementary particles and hence allows the possibility of such an interaction between electrons and protons.

L. A. YOUNG

Carnegie Institute of Technology,
Pittsburgh, Pennsylvania,
June 28, 1937.

[1] Frisch and Stern, Zeits. f. Physik **85**, 4 (1933); Estermann and Stern, Zeits. f. Physik **85**, 17 (1933).
[2] Kellogg, Rabi and Zacharias, Phys. Rev. **50**, 472 (1936).
[3] Estermann, Simpson and Stern, to be published soon.
[4] Breit, Phys. Rev. **51**, 248 (1937).

**Hyperfine Structure of the Resonance Lines of Rubidium**

The resonance lines λ7800 and λ7947 of rubidium have been photographed with Fabry-Perot etalons of spacing 1.5 and 1.8 cm. Two experimental arrangements were used: (1) The light from a helium-filled Geissler tube containing a small quantity of rubidium was focused directly on the slit of the hyperfine structure spectrograph. The tube was cooled below the point of appreciable self-reversal. (2) Light from the same source was passed through a Jackson-Kuhn atomic beam tube before entering the slit.

Patterns shown in Figs. 1 and 2 were observed for the two lines. Relative positions of the components were measured within 0.003 $cm^{-1}$. The measured values of the separations agree with those of Kopfermann and Krüger[1] within the error of these measurements. The values of the separations are compared in Table I.

TABLE I. *Comparison of measurements on Rb resonance lines.*

| Separation ($cm^{-1} \times 10^{-3}$) | *A–B* | *a–b* | *B–b* | *C–D* | *c–f* | *D–f* |
|---|---|---|---|---|---|---|
| Kopfermann and Krüger | 96 | 220 | 82 | 107 | 255 | 93 |
| Author | 97 | 217 | 79 | 107 | 252 | 91 |

The components *A*, *B*, *C*, and *D* are ascribed to isotope 85 and *a*, *b*, *c*, and *f* to isotope 87, the isotopes being present in the ratio 3 : 1. Values of $\Delta^2S_{\frac{1}{2}}$, $\Delta^2P_{\frac{1}{2}}$, and $\Delta^2P_{\frac{3}{2}}$, the hyperfine structure separations of the levels, obtained from the above data, were 0.102 $cm^{-1}$, 0.016 $cm^{-1}$, and 0.009 $cm^{-1}$ for isotope 85, and 0.225 $cm^{-1}$, 0.027 $cm^{-1}$, and 0.015 $cm^{-1}$ for isotope 87. $\Delta^2P_{\frac{3}{2}}$ represents a total separation of extreme levels; $S_{\frac{1}{2}}$ and $P_{\frac{1}{2}}$ being double only.

In addition to the above measurements, experimental arrangement (2) made it possible to resolve components *C* and *D* each into two components whose separation is due to $\Delta^2P_{\frac{1}{2}}$. The separation of components *C* was measured and a value of 0.015 $cm^{-1}$ obtained for $\Delta^2P_{\frac{1}{2}}$, in agreement with the above value. This experimental value in conjunction with the separation *C–D* of the unresolved components leads to a value of 0.102 $cm^{-1}$ for $\Delta^2S_{\frac{1}{2}}$. Millman and Fox[2] obtained 0.1018 $cm^{-1}$ for this separation by the atomic beam method of "zero moments."

The value of $\Delta^2S_{\frac{1}{2}}$ for isotope 85 gives, from Goudsmit's formula for *s* electrons $g(I)=0.55$. $\mu=1.4$ nuclear magnetons on the basis of the value $I=5/2$ of Millman and Fox. The experimental value of $\Delta^2P_{\frac{1}{2}}$ obtained from experimental arrangement (2) makes it possible to calculate $g(I)$ from Goudsmit's formula for *p* electrons, giving $g(I)=0.68$ and $\mu=1.7$ nuclear magnetons. The percent difference between the two values for $\mu$ is the same as the percent error in the measurement of $\Delta^2P_{\frac{1}{2}}$.

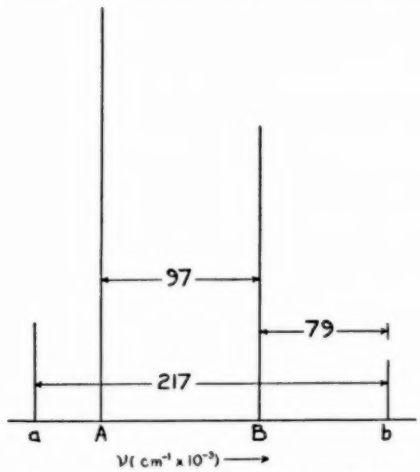


FIG. 1. Hyperfine structure pattern for λ7800.

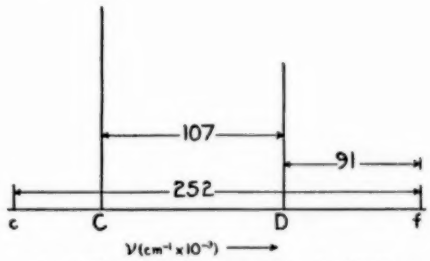


FIG. 2. Hyperfine structure pattern for λ7947.

A. V. HOLLENBERG

New York University,
Washington Square College,
New York, New York,
June 18, 1937.

[1] H. Kopfermann and H. Krüger, Zeits. f. Physik **103**, 485 (1936).
[2] S. Millman and M. Fox, Phys. Rev. **50**, 220 (1936).

**Artificial Radioactivity Produced by Alpha-Particles**

Bothe and Gentner[1] have reported the production of a radioelement of 38 minutes half-life in zinc bombarded with 16 Mev gamma-radiation; this activity they have attributed to $Zn^{63}$, produced in the reaction $Zn^{64}$ $(\gamma, n)Zn^{63}$. In an earlier communication,[2] we stated that this activity did not appear in the case of Ni bombarded with 7 Mev alpha-particles, although it might have been expected according to the reaction $Ni^{60}$ $(\alpha, n)Zn^{63}$. We did find a new radioactive isotope of copper, $Cu^{61}$, formed in the reaction $Ni^{58}$ $(\alpha, p)Cu^{61}$. The same activity has been reported by Thornton[3] in nickel bombarded with deuterons.

We have now removed the thin platinum foil which served as an exit window for the alpha-particles, so that targets can be bombarded directly in the main vacuum chamber of the cyclotron. The additional 1 Mev of particle energy gained thereby has enhanced greatly the total activity in Ni bombarded with alpha-particles, and the presence of a radioelement of half-life about 37 minutes is now evident. The short-period activity is chemically separable from the much stronger $Cu^{61}$, and is doubtless due to $Zn^{63}$. The relative initial intensities, corrected to infinite bombarding time, are in the ratio $Cu^{61} : Zn^{63} = 1.9 : 10$. We believe that a small amount of $Zn^{63}$ was present in Ni bombarded with the 7 Mev alpha-particles, accounting for the fact that the period given by us[2] for $Cu^{61}$ (3.25 hours) was too low, the correct value being that reported by Thornton:[3] 3.4 hours.

A paper dealing in detail with our experiments is in preparation.

LOUIS N. RIDENOUR
W. J. HENDERSON

Palmer Physical Laboratory,
Princeton University,
Princeton, N. J.,
July 1, 1937.

[1] Bothe and Gentner, Naturwiss. **25**, 191 (1937).
[2] Ridenour and W. J. Henderson, Phys. Rev. **51**, 1102 (1937).
[3] Thornton, Phys. Rev. **51**, 893 (1937).

## Contact Potentials for Metals Immersed in a Dielectric and Conduction of Electricity by Liquid Dielectrics

Recent papers by Baker and Boltz[1, 2] and by K. H. Reiss[3, 4] have focused attention on the old problem of the origin of the electrical conductivity of pure nonpolar dielectric liquids. The problem falls naturally into two parts. The first involves the explanation of the "saturation," or field-independent current which is observed under fields up to 25 to 100 kv per cm, depending upon the liquid. The second is concerned with the explanation of the current at higher field strengths, which is approximately an exponential function of the applied stress.

At the present time, there are three theories which purport to explain the high field phenomena. These are (1) the ionization by collision theory of A. Nikuradse,[5] (2) the potential-dissociation theory of K. H. Reiss,[3] and (3) the thermionic emission theory of Edler and Zeier[6] and Baker and Boltz.[1] It is the purpose of this note to describe experiments which are entirely inconsistent with this third theory of dielectric conduction.

According to Baker and Boltz, the current flowing in a liquid dielectric is governed by Schottky's modification of Richardson's equation, the dielectric constant $D$ of the liquid being introduced as a correction:

$$I = AT^2 e^{-\epsilon\phi/kT} e^{\epsilon(\epsilon FD)^{\frac{1}{2}}/kT}.$$

In this equation, $\phi$ represents the work function of the metal when immersed in the dielectric. This is an unknown quantity. Now if two dissimilar metals with metal-dielectric work functions of $\phi_1$ and $\phi_2$ are used as electrodes, we obtain at once from this theory the ratio of the currents $I_1/I_2$ with the first and the second metal respectively serving as cathode:

$$I_1/I_2 = e^{-\epsilon(\phi_1-\phi_2)/kT}.$$

The quantity $\phi_1-\phi_2$ is simply the contact potential between the two metals when immersed in the dielectric. In order to check this prediction of the theory, an experiment was conducted in which the contact potential between gold and brass electrodes immersed in highly purified iso-octane was determined by a modified Kelvin method and subsequently the ratio of the high field currents in the liquid in the two directions.

The electrodes were ground optically flat so that it was possible to bring them into very close proximity (of the order of thousandths of a millimeter). Under these conditions contact potentials could be very accurately determined with a very slight displacement of one electrode. The experiment was conducted in vacuum and an FP-54 amplifier was used to detect the potential changes as well as to measure the currents in the second part of the experiment.

The contact potential between gold and brass was found to be 0.255 volt in vacuum and 0.265 volt in iso-octane. With the value of 300°K for the temperature, the predicted value of $I_1/I_2$ was calculated to be 30,100 where $I_1$ and $I_2$ are the currents with the brass and gold electrodes respectively acting as cathodes.

The results of an actual experiment are given in Table I. The field strength $F$ is given in volts per cm and the currents in amperes per square cm.

TABLE I. *Currents between brass and gold electrodes in iso-octane. F is the field strength in volts per cm. $I_1$ and $I_2$ are the currents with the brass and gold electrodes respectively as cathodes.*

| $F$ (v/cm) | $I_1$ | $I_2$ | $I_1/I_2$ |
|---|---|---|---|
| 10,000 | $1.2\times10^{-13}$ | $1.2\times10^{-13}$ | 1.00 |
| 75,000 | $4.0\times10^{-13}$ | $4.2\times10^{-13}$ | .95 |
| 130,000 | $2.1\times10^{-10}$ | $2.0\times10^{-10}$ | 1.05 |
| 175,000 | $1.5\times10^{-9}$ | $1.3\times10^{-9}$ | 1.15 |

It is evident that the current ratio is unity within experimental error. It is definitely not of the order of magnitude of 30,000 as required by the thermionic emission theory. This same sequence of experiments was carried out with several highly purified mineral oils and the same results were always obtained, i.e., the current ratio was always very near unity. It must be concluded that the thermionic emission theory is inadequate to explain the conductivity of the dielectrics used in these experiments.[7]

It should be noted that there also exist very serious objections to the other two previously mentioned theories of liquid dielectric conduction. It would seem that up to the present time, no satisfactory explanation of the phenomena has been found.

The contact potential difference between gold and brass immersed in several other liquids was determined and in every case its value was very near the value as measured in vacuum. If the liquid be conducting in the slightest degree, one should no longer speak of the contact potential between two metal surfaces immersed in the liquid except in the sense that the liquid itself in this case will assume a contact potential with reference to each metal surface.

This will be true with even the most perfectly insulating liquids if sufficient time in contact is allowed for the attainment of equilibrium. A complication in the case of nonpolar liquids with slight traces of impurities is the presence of an electrochemical e.m.f.

HAROLD J. PLUMLEY

Ryerson Physical Laboratory,
University of Chicago,
June 26, 1937.

[1] E. B. Baker and H. A. Boltz, Phys. Rev. **51**, 275 (1937).
[2] E. B. Baker and H. A. Boltz, Phys. Rev. **51**, 989 (1937).
[3] K. H. Reiss, Zeits f. physik. Chemie **178**, 37 (1936).
[4] K. H. Reiss, Phys. Rev. **51**, 781 (1937).
[5] A. Nikuradse, Physik. Zeits. **34**, 97 (1933).
[6] H. Edler and O. Zeier, Zeits. f. Physik **84**, 356 (1933).
[7] The conductivities observed by Baker and Boltz seem rather high. A possible explanation is that they distilled their toluene over sodium. This is known to be a dangerous practice since sodium phenyl, a relatively good conductor, may be produced. We were unable to measure contact potentials in toluene, which had been purified in this manner, due to the presence of electrochemical e.m.f.'s.

## Solar Diurnal Variation of Cosmic-Ray Intensity as a Function of Latitude

Exceptional opportunity for the study of the solar diurnal variation of cosmic-ray intensity at various latitudes is offered by data obtained by A. H. Compton and R. N. Turner on eleven trips between Vancouver, B. C., and Sydney, Australia on the Canadian-Australasian motorship Aorangi from March 1936 to January 1937. There are presented here the results of a preliminary survey of these data and an outline of the method used in obtaining them.

From the hourly ionization values given on the original record, six-hour means were calculated for the G. M. T. intervals 0–6 hr., 6–12 hr., 12–18 hr., and 18–24 hr. These six-hour means were corrected to a barometric pressure of 30 inches of mercury, and converted to mean solar time. They were then grouped according to geomagnetic latitude, zones of 2.5° being taken. Individual means for different latitude zones included from 1 to 73 data, the average being about 5.

With the data thus arranged, separate latitude curves were drawn for each of the four intervals into which the day was divided, the points being weighted according to the number of data included in each. These are given in Fig. 1, the upper curve being for the interval 0–6 A.M. and the others in order. To separate clearly the various curves, they have each been displaced $5I_{30}$ units lower than the one next earlier. The smooth curves obtained in this way were assumed to give average values at any latitude which best utilized the available data. Average values for the ionization for each six-hour period of the day have been read for 10° intervals and smooth curves drawn through them for a two-day period as shown in Fig. 2. North latitudes are represented by full curves, south latitudes by dashed curves. That amplitudes obtained in this manner should rather be too small than too large follows from the fact that the points represent arithmetic averages over six-hour periods. An arithmetic average assumes a straight line as a line of best fit, so that points obtained in this way will always lie on the concave side of the true curve.

The main points brought out are presented in Table I. Some variation in the times of maxima and minima will

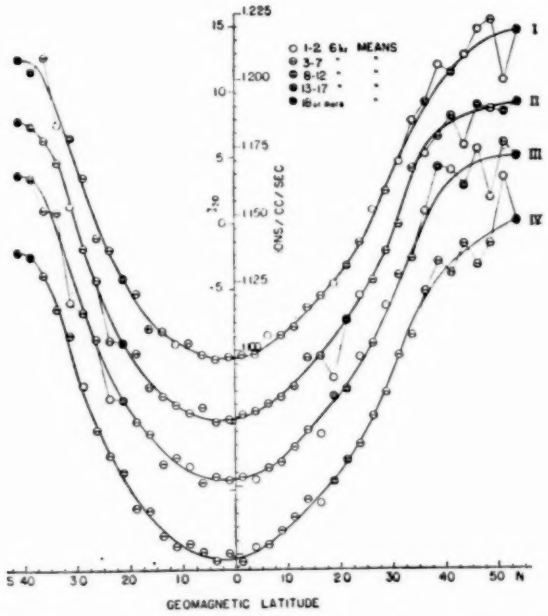


FIG. 1. Latitude effect between Vancouver and Sydney, mean of 11 trips, expressed in $I_{30}$ units (from model $C$ meter) and ions/cc/sec. in standard air, for mean solar time intervals (I) 0–6 hr. (II) 6–12 hr. (III) 12–18 hr. (IV) 18–24 hr. Ionization scale is for upper curve, each curve being displaced $5I_{30}$ units (0.0245 ions/cc/sec.) lower than the next earlier to avoid confusion. (Data, Compton-Turner, 1936–1937.)

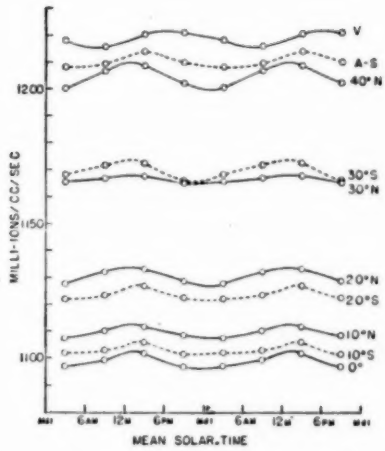


FIG. 2. Intercepts from Fig. 1 plotted against time for various geomagnetic latitudes. Solid curves, north latitudes, dashed curves, south latitudes. *V*—zone including Vancouver; *A–S*—zone including Auckland and Sydney.

be noted, although the daytime averages are all greater than the nighttime averages. Because of the greater number of data included, the results for the zone including Vancouver and also for the latitude of Auckland and Sydney should be most reliable, however individual readings fluctuate much more widely at these latitudes than at the equator. Stops made on each trip at Honolulu, Hawaii and at Suva, Fiji, also result in there being more data represented in the curves for 20° N and 20° S than in the others. The results from the intercepts at the equator agree closely with an average of data from the 10° equatorial zone in which the latitude variation is small. Such an average represents from 16 to 21 six-hour means for each point. Considering these latitudes for which the most data are available the most significant result would appear to be the substantially constant variation of the order of 0.5–0.6 percent over the range from 55° N to 42° S geomagnetic latitude.

TABLE I. *1000 "ml" units = 1 ion per cc per second in air at S. T. P. Times given are mean solar time.*

| GEOMAGNETIC LATITUDE | MEAN IONIZATION *ml* | DAILY VARIATION *ml* | DAILY VARIATION percent | TIME OF MAXIMUM | TIME OF MINIMUM |
|---|---|---|---|---|---|
| 52.6°–55.0° N | 1220 | 6.4 | 0.5 | 6 P.M. | 8 A.M. |
| 40° | 1205 | 10.3 | 0.9 | 1 P.M. | 1 A.M. |
| 30° | 1165 | 2.9 | 0.3 | 1 P.M. | 11 P.M. |
| 20° | 1130 | 6.9 | 0.6 | 1 P.M. | 1 A.M. |
| 10° | 1110 | 5.4 | 0.5 | 1 P.M. | 2 A.M. |
| 0° | 1095 | 6.9 | 0.6 | 2 P.M. | 12 Mdt |
| 10° S | 1105 | 4.9 | 0.4 | 2 P.M. | 10 P.M. |
| 20° | 1110 | 5.9 | 0.5 | 2 P.M. | 12 Mdt |
| 30° | 1170 | 8.8 | 0.8 | 1 P.M. | 11 P.M. |
| 40.1°–42.5° | 1210 | 6.4 | 0.5 | 3 P.M. | 3 A.M. |

Thanks are due to Professor A. H. Compton for his courtesy in making these data available, and for his helpful discussions.

JULIAN L. THOMPSON

Ryerson Physical Laboratory,
Chicago, Illinois,
University of Chicago,
June 23, 1937.

## The Scattering of Slow Neutrons by Liquid Ortho- and Parahydrogen

We have measured the scattering of slow neutrons (90°K) by liquid hydrogen varying in *ortho* and *para* content, and have found that orthohydrogen scatters decidedly more than parahydrogen, as predicted by the theory.[1]

The slow neutrons were produced by a 200 mg (Ra-Be source and were cooled down with liquid methane. A beam of these neutrons was allowed to pass through a quartz Dewar vessel (3 cm diameter, 1 cm thickness) filled with liquid hydrogen, and was detected by the radioactivity induced in rhodium sheets. Measurements with and without cadmium absorbers allowed the detection of the slow neutrons. The ratios of the activities with the vessel filled with water, with 61 percent orthohydrogen, and with 46 percent orthohydrogen, to the activity with the vessel empty were 0.07, 0.3, and 0.5, respectively. With the use of these data, a rough calculation shows that the mean free path of the neutrons in orthohydrogen is about the same as in water (taking into account the proton densities), but much larger in parahydrogen.

J. HALPERN
I. ESTERMANN
O. C. SIMPSON
O. STERN

Research Laboratory of Molecular Physics,
Carnegie Institute of Technology,
Pittsburgh, Pennsylvania,
July 1, 1937.

[1] E. Teller, Phys. Rev. **49**, 420 (1936); Julian Schwinger and E. Teller, Phys. Rev. **51**, 775 (1937).